

INAUGURAL – DISSERTATION
zur
Erlangung der Doktorwürde
der
Naturwissenschaftlich–Mathematischen Gesamtfakultät
der
RUPRECHT – KARLS – UNIVERSITÄT
HEIDELBERG

vorgelegt von
Fabrizio Savarino, M.Sc.
aus Selb, Bayern

Tag der mündlichen Prüfung
18. Juni 2020

VARIATIONAL APPROACHES FOR IMAGE LABELING ON
THE ASSIGNMENT MANIFOLD

Advisor

PROF. DR. CHRISTOPH SCHNÖRR

PROF. DR. PETER ALBERS

Zusammenfassung

Das Kennzeichnungsproblem von Bildern bezeichnet die Aufgabe, jedem Pixel eines Bildes genau ein Element einer vordefinierten Menge an Kennzeichnungen zuzuweisen. Klassische Ansätze dieses Kennzeichnungsproblems sind als Minimierungsprobleme speziell strukturierter Funktionen formuliert. Zuweisungsflüsse für kontextbasiertes Kennzeichnen von Bildern sind eine neuartige, alternative dynamische Formulierung durch räumlich gekoppelte Replikatorgleichungen. In dieser Arbeit werden die klassische und dynamische Sichtweise in einer variationellen Formulierung kombiniert. Dies wird dadurch erreicht, dass das System dem induzierten Riemannschen Gradientenfluss auf einer elementaren statistischen Mannigfaltigkeit bezüglich der Informationsgeometrie folgt. Konvergenz und Stabilität dieses Ansatzes werden mithilfe der logarithmischen Barrierefunktion untersucht. Eine neue Parametrisierung des Zuweisungsflusses durch seine dominante Komponente deckt die enthaltene Struktur eines Riemannschen Gradientenflusses auf, wodurch die beiden beherrschenden Prozesse des Flusses identifiziert werden: räumliche Regularisierung von Zuweisungen und allmähliches Erzwingen eindeutiger Entscheidungen. Des Weiteren wird eine räumlich kontinuierliche Formulierung des zugehörigen Potentials vorgestellt und nachgewiesen, dass das entsprechende Optimierungsproblem gut gestellt ist. Darüber hinaus wird ein alternativer variationeller Ansatz für Maximum-a-posteriori Inferenz hergeleitet, basierend auf diskreten graphischen Modellen unter Verwendung lokaler Wassersteindistanzen. Im resultierenden Inferenzprozess, basierend auf dem Riemannschen Gradientenfluss, sind die lokalen Marginalisierungsbedingungen immer erfüllt und eindeutige Entscheidungen werden asymptotisch erreicht.

Abstract

The image labeling problem refers to the task of assigning to each pixel a single element from a finite predefined set of labels. In classical approaches the labeling task is formulated as a minimization problem of specifically structured objective functions. Assignment flows for contextual image labeling are a recently proposed alternative formulation via spatially coupled replicator equations. In this work, the classical and dynamical viewpoint of image labeling are combined into a variational formulation. This is accomplished by following the induced Riemannian gradient descent flow on an elementary statistical manifold with respect to the underlying information geometry. Convergence and stability behavior of this approach are investigated using the log-barrier method. A novel parameterization of the assignment flow by its dominant component is derived, revealing a Riemannian gradient flow structure that clearly identifies the two governing processes of the flow: spatial regularization of assignments and gradual enforcement of unambiguous label decisions. Also, a continuous-domain formulation of the corresponding potential is presented and well-posedness of the related optimization problem is established. Furthermore, an alternative smooth variational approach to maximum a-posteriori inference based on discrete graphical models is derived by utilizing local Wasserstein distances. Following the resulting Riemannian gradient flow leads to an inference process which always satisfies the local marginalization constraints and incorporates a smooth rounding mechanism towards unambiguous assignments.

Acknowledgements

Many people have contributed to this thesis in one way or another. First of all, I would like to thank my advisor, Prof. Christoph Schnörr, who guided me into the field of mathematical image analysis. He always offered his valuable advice and gave me the necessary freedom and support I needed to complete this thesis. In addition, he also created a very pleasant and family friendly work atmosphere, for which I am deeply grateful.

I also wish to thank my present and former colleagues from the Image & Pattern Analysis Group, the Mathematical Imaging Group and the Research Training Group on Graphical Models. In particular, Dr. Freddie Åström, Jan Plier, Alexander Zeilmann, Artjom Zern and Matthias Zisler for their support as well as many interesting and fruitful discussions. Special thanks also go to my close colleague Ruben Hühnerbein, with whom I shared an office and traveled to many conferences across the world. I had great pleasure of doing mathematics with you. I also warmly thank Evelyn Wilhelm and Barbara Werner for their valuable administrative help, as well as the Dean's Office of the Department of Mathematics and Computer Science. Many thanks also to Anika Schwind, Michael Seufert and my sister, Marina, for their helpful comments and proof-reading.

Finally, I am extremely grateful to my family, especially to my life companion Janina and our daughter Mila, for all their love, encouragement and unconditional support during this time.

Financial support by the German Science Foundation (DFG), grant GRK 1653, is gratefully acknowledged. This work has also been stimulated by the Heidelberg Excellence Cluster STRUCTURES, funded by the DFG under Germany's Excellent Strategy EXC-2181/1 - 390900948.

Contents

List of Publications	1
1. Introduction and Overview	3
1.1. Motivation	3
1.2. Related Work	4
1.2.1. Image Labeling	4
1.2.2. Assignment Flow	5
1.2.3. Replicator Dynamics	5
1.3. Contribution and Organization	6
2. Preliminaries	9
2.1. Basic Notation	9
2.2. Information Geometry	11
2.2.1. Dually Flat Manifolds	11
2.2.2. Discrete Probability Distributions with Full Support	13
2.3. Image Labeling by Geometric Assignment	15
2.3.1. The Labeling Problem on Graphs	16
2.3.2. Assignment Manifold	17
2.3.3. Assignment Flow	26
2.3.4. Geometric Numerical Integration of the Assignment Flow	29
3. General Variational Models on the Assignment Manifold	31
3.1. Log-Barrier Perturbation of the Variational Model	32
3.2. Mathematical Preparations	38
3.2.1. Euclidean Isometric m -Affine Coordinates	38
3.2.2. Analytic Functions and the Łojasiewicz Inequality	43
3.3. Perturbed Riemannian Gradient Descent Flows for Optimization	44
3.3.1. Basic Estimates	44
3.3.2. General Properties of Perturbed Riemannian Gradient Flows	46
3.3.3. Convergence Analysis for Analytic Variational Models	48
3.4. Numerical Integration of the Perturbed Riemannian Gradient Descent Flow	56
3.4.1. Geometric Euler Integration	56
3.4.2. L -smooth Adaptability	58
3.4.3. Geometric Euler with Armijo Step-Size	60
3.4.4. Convergence Analysis for Analytic Variational Models	65

4. Variational Formulation of the Assignment Flow	75
4.1. Discrete-Domain Variational Model	76
4.1.1. Nonexistence of a Potential	76
4.1.2. S-Parameterization and Variational Model	80
4.1.3. Experiments	84
4.2. Continuous-Domain Variational Model	91
4.2.1. Background on Functional Analysis	92
4.2.2. Well-Posedness	94
4.2.3. Fixed Boundary Conditions	95
4.2.4. Numerical Algorithm and Example	96
4.2.5. A PDE Characterizing Optimal Assignment Flows	98
5. A Variational Approach Based on Graphical Models	101
5.1. Background on Graphical Models for Image Labeling	102
5.1.1. Local Polytope Relaxation of Graphical Models	103
5.1.2. Smoothed LP Relaxation and Belief Propagation	105
5.2. Variational Formulation of Graphical Models using local Wasserstein Distances	107
5.2.1. A Reformulation of the Smoothed LP Relaxation	107
5.2.2. General Smoothed Wasserstein Distances	110
5.2.3. Entropy Regularized Wasserstein Distance	117
5.2.4. Variational Formulation on the Assignment Manifold	123
5.3. Experiments	129
5.3.1. Influence of the Integrality Parameter	130
5.3.2. Comparison to Other Methods	133
6. Conclusion and Outlook	135
A. Differential Geometry	137
A.1. General Manifolds and Submanifolds of \mathbb{R}^d	137
A.2. Flows on Manifolds	138
A.3. Connections	139
A.3.1. Parallel Transport	140
A.3.2. Geodesics and Exponential Maps	141
A.3.3. Flat Connections	141
A.4. Riemannian Manifolds	142
A.4.1. Riemannian Gradients	143
A.4.2. Levi-Civita Connection	144
A.4.3. Riemannian Distance and Mean	144
A.4.4. Riemannian Hessian	145
B. Convex Analysis	147
B.1. Affine and Convex Sets	147
B.2. Convex Functions	147

B.3. Bregman Divergences	149
B.4. Lagrange Duality and KKT Conditions	150
Bibliography	153

List of Publications

The following publications were created during the work on this thesis.

- (1) R. Hühnerbein, F. Savarino, F. Åström and C. Schnörr, *Image Labeling Based on Graphical Models Using Wasserstein Messages and Geometric Assignment*, SIAM Journal on Imaging Sciences 11 (2018), no. 2, 1317–1362.
- (2) R. Hühnerbein, F. Savarino, S. Petra and C. Schnörr, *Learning Adaptive Regularization for Image Labeling Using Geometric Assignment*, Proc. SSVM, Springer, 2019.
- (3) F. Savarino, R. Hühnerbein, F. Åström, J. Recknagel and C. Schnörr, *Numerical Integration of Riemannian Gradient Flows for Image Labeling*, Proc. SSVM, Springer, 2017.
- (4) F. Savarino and C. Schnörr, *A Variational Perspective on the Assignment Flow*, Proc. SSVM, Springer, 2019.
- (5) F. Savarino and C. Schnörr, *Continuous-Domain Assignment Flows*, <https://arxiv.org/abs/1910.07287>, European Journal of Applied Mathematics (2019): conditionally accepted subject to revisions.
- (6) A. Zeilmann, F. Savarino, S. Petra and C. Schnörr, *Geometric Numerical Integration of the Assignment Flow*, Inverse Problems 36 (2020).

Chapter 1

Introduction and Overview

1.1. Motivation

The image labeling problem refers to the task of assigning to each pixel a single element from a finite predefined set of labels. This problem formulation can be applied in many different fields, including image compression and denoising, calculating optical flow, object segmentation, and many more. The individual labels in these cases might represent color information, vectors of the velocity field, or fore- and background information in the image, respectively.

The classical approach for image labeling is to devise a quality measure of label assignments, called *objective function*, whose global optima represent desired label configurations depending on the domain of application. A large class of models is given by discrete objective functions related to probabilistic graphical models. These functions are composed of a *data term*, measuring the deviation of labels from the given data, and a *regularizer*, compensating for noise in the data and representing prior knowledge of the problem. In this case, image labeling then corresponds to the task of finding global minimizers for the discrete objective function, resulting in a hard combinatorial problem. Thus, various relaxations are used in practice to arrive at a computationally feasible formulation. Usually, convex relaxations are favored to obtain global optimal solutions of the approximate problem.

There is a recent alternative formulation of image labeling via a *smooth dynamical selection process* using *information geometry*. For this, label decisions at each pixel are relaxed to probabilistic assignments and viewed as points on the manifold of discrete probability distributions with full support on the set of labels, called *assignment manifold*. The resulting dynamical system, called *assignment flow*, is given by *spatially coupled replicator equations* and is mainly driven by two distinct processes: *spatial regularization* of assignments through geometric averages and *gradual enforcement* of unambiguous label decisions.

The goal of this thesis is to combine the classical and recent dynamical viewpoint of the image labeling task into a variational formulation: minimize a given objective function through the dynamics of the induced *Riemannian gradient descent flow* with respect to the underlying information geometry on the assignment manifold. Due to the Riemannian structure, the resulting dynamical system again has the form of a spatially coupled replicator equation. However, in contrast to the classical approach of ‘solely’ finding global minimizers, the focus is on following the dynamics of the system, generally

resulting in local optima. A good analogy might be dropping a ball in a room of a building. The resulting dynamic of the falling ball is adequately described by the equation of motion induced by the corresponding gravitational potential, leading to a local optimum somewhere in the room, rather than by the global minimizer of the potential, lying somewhere in the basement of the building. Similarly, non-convexity of objective functions and local optima in the proposed variational image labeling approach are not an issue, as label decisions are determined through the selection process of the corresponding Riemannian gradient flow, driven by the dynamical flow of information.

1.2. Related Work

1.2.1. Image Labeling

Discrete graphical models are a well established approach for image labeling and dominated the field in the past [GG84, Lau96, WJ08]. The special *binary case* of only two labels can efficiently and optimally be solved [KZ04]. If the regularizer is induced by a metric, then the image labeling problem is referred to as *metric labeling problem* [KT02].

A widely used convex relaxation for the corresponding combinatorial problem is based on the *local polytope relaxation* [Wer07], a special linear programming (LP) relaxation for adequately representing the specific structure of maximum a-posteriori (MAP) inference problems underlying discrete graphical models. As a consequence of the relaxation, however, optimal solutions of the LP do not necessarily correspond to valid labelings of the original problem. To remedy this shortcoming, various *rounding schemes* for converting a relaxed solution into a valid labeling in a post-processing step are available [CKNZ05, KT02]. Due to the large problem size of typical applications, standard methods for solving the LP relaxation are infeasible in practice. For example, the use of *interior point methods* [NN87] is prohibitively expensive because of the dense linear algebra steps required to find update directions. An iterative algorithm for tackling these LPs is given by *belief propagation* and variations thereof [YFW05]. Even though convergence guarantees are only available in special cases, the numerical update can efficiently be implemented via ‘*message passing*’ and the overall method achieves good performance in practice [YMW06]. For further references and experimental evaluations, the reader is referred to the recent survey [KAH⁺15] on the image labeling problem and on algorithms for solving it either approximately or exactly.

In addition, continuous models for image labeling together with various relaxations are investigated in the literature [CCP12, LS11]. Similar to the discrete case, the special binary case of two labels can be solved optimally by convex programming [CEN06].

In recent years, deep convolutional neural networks (CNNs) achieved outstanding performance in different tasks of machine learning and pattern recognition, including image classification and image labeling [KSH12]. However, there are instabilities and systematic failures associated with these approaches, showing that further research for a deeper mathematical understanding of CNNs is needed [ARP⁺19].

1.2.2. Assignment Flow

The assignment flow for smooth geometric image labeling was first proposed in [ÅPSS17]. It was in part motivated by seminal work on relaxation labeling [HZ83, RHZ76] and has connections to other fields, including nonlinear diffusion filters [Wei98], nonlocal means filter [BCM05], and replicator dynamics [HS03]. The assignment flow also fits into a recent development of mathematically interpreting deep residual networks, a network architecture introduced in [HZRS16], as discretized realizations of dynamical systems [E17, HR17]. For a recent overview of the assignment filter in general and additional remarks see [Sch20].

Over the past few years, several extensions of the original assignment flow have been proposed. In [ZSPS20], the *linear assignment flow* together with *geometric numerical integration methods* for integrating flows on the assignment manifold are considered. Incorporating additional prior knowledge as *global constraints* on label assignments via linear filters is explored in [ZRS18]. Initial work on parameter learning is reported in [HSPS19], where the proposed approach is successfully applied to learn regularization parameters for the linearized assignment flow. However, this general framework is not limited to the linear model and can also be used for learning parameters of the fully nonlinear flow. The work of [ZZPS20] introduces an *unsupervised assignment flow*, where specified labels simultaneously evolve on a separate feature manifold coupled with the underlying assignment process, allowing to *adapt* the given label dictionaries. A further extension to a *completely unsupervised* scenario, where no labels are prespecified at all, is presented in [ZZPS19]. There, the emergence of labels together with their assignments is induced by a *low-rank* data representation evolving through dynamically assigning the data to *itself*, resulting in the so-called *self-assignment flow*.

1.2.3. Replicator Dynamics

Replicator equations are a widely used dynamical model in various fields, including evolutionary biology, game theory and economics, see [HS03, San10] and references therein. Even though the replicator dynamic seems to be a simple ordinary differential equation at first glance, it possesses a rich mathematical structure [AE05] and is even capable of chaotic behavior [SC03]. Since the literature on replicator dynamics is vast, only a few related works on models involving spatial interaction in physics [dB13, TC04] and applied mathematics [BPN14, NPB11] are pointed out, as well as extensions to an infinite number of strategies (i.e. infinite labels in the case of image labeling) [AFMS18]. There are also applications for finding good local optima for combinatorial problems, such as the graph isomorphism problem [Pel99].

Regarding the connection to information geometry, it is well known that if the fitness function corresponds to the gradient of a potential, then the replicator equation is nothing else than the Riemannian gradient flow with respect to the Fisher-Rao metric [AJVLS17, HS03].

1.3. Contribution and Organization

In [ÅPSS17], the assignment flow originally started out as a variational model containing Riemannian means on the assignment manifold. Using a simplifying assumption and approximating the Riemannian mean to first order by the geometric mean, the corresponding Riemannian gradient descent flow resulted in the assignment flow formulation. Unfortunately, this approximation is unavoidable for obtaining efficient numerical update schemes, as there is no explicit formula for the Riemannian mean. Even though the mean itself can be computed numerically (cf. [ÅPSS17, Sec. 3.3.2]), the derivation of a numerical scheme for the corresponding derivative, contained in the Riemannian gradient, is rather involved. This motivated the investigation of variational approaches for image labeling on the assignment manifold in this thesis. Among other things, the convergence of general variational models will be investigated together with the question to which extend the assignment flow is still variational.

The main contributions of this thesis include:

- Transferring established convergence and stability results for gradient flows of analytic functions on Euclidean space to Riemannian gradient flows of log-barrier perturbed analytic objective functions on the assignment manifold.
- Proving that the assignment flow is not a Riemannian gradient flow. Introducing a suitable parameterization of the assignment flow by its dominant component and showing that this in turn is a Riemannian gradient flow with an explicitly given potential. Also, generalizing this potential to the continuous-domain case, which reveals connections to harmonic maps and corresponding partial differential equations (PDEs).
- Deriving a relaxed geometric variational formulation of discrete energies corresponding to discrete graphical models on the assignment manifold. This is done by reformulating the smoothed local polytope relaxation in terms of entropy regularized local Wasserstein distances. The resulting inference process through the Riemannian gradient flow always satisfies the local marginalization constraints and incorporates a smooth rounding mechanism towards unambiguous labels decisions.

Subsequently, an overview regarding the organization of this work is given:

In *Chapter 2*, the necessary mathematical background for this work is presented. The basic notation used throughout this thesis is laid out in Section 2.1. The reader is assumed to be familiar with the basic definitions and facts from differential geometry and convex analysis presented in the corresponding appendices A and B. Section 2.2 introduces the necessary fundamental concepts and results from information geometry needed to define and investigate the dynamical formulation of the image labeling problem on the assignment manifold in Section 2.3.

In *Chapter 3*, the process of inferring label assignments through the Riemannian gradient descent flow and the corresponding numerical integration with the geometric Euler method are considered. For this, Section 3.1 defines the log-barrier method on the assignment manifold and Section 3.2 introduces special affine coordinates as well as the

Lojasiewicz inequality for analytic functions. After these mathematical preparations, the established convergence theory of gradient flows for analytic functions in Euclidean space is transferred to Riemannian gradient flows on the assignment manifold in Section 3.3. Section 3.4 deals with the corresponding theory for the numerical integration through the geometric Euler method.

Chapter 4 is concerned with the variational formulation of the assignment flow. In Section 4.1, it is shown that even though the assignment flow itself is not a Riemannian gradient flow, it can alternatively be parameterized by its dominant component, called *S-flow*, which in turn admits the characterization as a Riemannian gradient flow. Subsequently, the corresponding potential is investigated and basic properties are evaluated with two academical examples. A continuous-domain variational formulation is studied in Section 4.2. After establishing well-posedness of the associated optimization problem and deriving a numerical algorithm for solving it, the close relation of this approach to the assignment flow is illustrated by an experiment. In the end, a PDE characterization of solutions is obtained by a ‘formal’ derivation.

Finally, in *Chapter 5*, an alternative approach for optimizing discrete functions related to discrete graphical models is presented. For this, a relaxed variational model on the assignment manifold is derived in Section 5.2 using entropy regularized local Wasserstein distances. This derivation is based on the smoothed local polytope relaxation, which will be introduced in Section 5.1. Following the corresponding Riemannian gradient flow of the variational model results in an alternative inference process for discrete graphical models using parallel ‘Wasserstein messages’ along edges. In contrast to established methods, the local marginalization constraints are always satisfied and a smooth rounding mechanism towards integral assignments is incorporated in the inference process. Basic properties of this approach are evaluated with academical experiments in Section 5.3, including a comparison with two established methods in the field.

A summary of this thesis together with a short list of further research directions is presented in *Chapter 6*.

Chapter 2

Preliminaries

In this chapter, the central mathematical objects of this thesis are defined, the so called *assignment manifold*, encoding fully probabilistic label assignments, together with the *assignment flow*, inferring label configurations on the assignment manifold. Before this is done, the fundamental concepts from information geometry are introduced, necessary to define and investigate the dynamical formulation of the image labeling problem on the assignment manifold. The reader is assumed to be familiar with the basic definitions and results from differential geometry and convex analysis as presented in Appendix A and B.

2.1. Basic Notation

In the following, an overview of the notation for standard mathematical objects used throughout this work is given. For the notation regarding differential geometry and convex analysis, the reader is referred to the corresponding appendices A and B. Unless otherwise stated, the Einstein summation convention is used (see appendix A).

For $n \in \mathbb{N} = \{1, 2, \dots\}$, the first n natural numbers are denoted by

$$[n] := \{1, 2, \dots, n-1, n\}$$

and the n -dimensional vector containing only ones by $\mathbb{1}_n := (1, 1, \dots, 1) \in \mathbb{R}^n$. The standard basis of \mathbb{R}^n is given by $\mathcal{B}_n := \{e_1, \dots, e_n\} \subset \mathbb{R}^n$.

For two indices $i, j \in \mathbb{N}$, the Kronecker delta is denoted by δ_{ij} and takes the values $\delta_{ij} = 1$ if $i = j$ and $\delta_{ij} = 0$ else. The indicator function of a set $S \subset X$ is defined as

$$\chi_S: X \rightarrow \{0, 1\}, \quad x \mapsto \chi_S(x) = \begin{cases} 1 & , \text{ for } x \in S \\ 0 & , \text{ for } x \notin S. \end{cases} \quad (2.1)$$

For a differentiable function $f: U \rightarrow \mathbb{R}$, with $U \subset \mathbb{R}^n$ open, the ordinary gradient is denoted by¹ ∂f and the Hessian by $\text{Hess } f$. The dependence of a linear map $F: V \rightarrow W$ between two vector spaces V and W on the argument x is denoted by $F[x]$, for example $F[A] = B^\top A^\top + AB$ for matrices $A \in \mathbb{R}^{m \times n}$ and $B \in \mathbb{R}^{n \times d}$. If the action of F on x is explicitly given by matrix multiplication, then also Fx is used. The kernel (nullspace)

¹As subdifferentials of a function will not occur in this thesis, there is no danger of confusion.

and image (range) of a linear mapping F is denoted by $\ker(F)$ and $\text{Im}(F)$. If $U \subset V$ is a linear subspace of a Euclidean vector space $(V, \langle \cdot, \cdot \rangle)$, then the orthogonal projection onto U is denoted by $P_U: V \rightarrow U$ and the orthogonal complement of U in V by U^\perp .

Due to the Einstein summation convention, basis vectors will always have lower and vector coordinates always upper indices, e.g. if $x \in \mathbb{R}^n$, then $x = x^i e_i$. Unless otherwise stated, a matrix $A \in \mathbb{R}^{m \times n}$ will be identified with an element of the product space

$$\mathbb{R}^{m \times n} \cong (\mathbb{R}^n)^m = \prod_{i \in [m]} \mathbb{R}^n,$$

that is, the i -th component of $A = (A_i)_{i \in [m]}$ is given by the i -th row vector of A , again denoted by $A_i \in \mathbb{R}^n$. Expressing this row vector A_i in coordinates gives $A_i = A_i^j e_j$. Thus, an element of a matrix $A \in \mathbb{R}^{m \times n}$ will be indexed by A_i^j , where $i \in [m]$ is the row index and $j \in [n]$ the column index. The j -th column vector of A is therefore denoted by A^j .

The standard inner product of two vectors $x, y \in \mathbb{R}^n$ is denoted by $\langle x, y \rangle$ and the induced Euclidean norm by $\|\cdot\|$, other norms will always be indicated by a corresponding subscript. If $M \subset \mathbb{R}^n$ is a submanifold, then the canonical Riemannian metric given by the induced Euclidean metric is sometimes denoted by $E = \langle \cdot, \cdot \rangle$ to simplify notation, especially in the context of Riemannian gradients. Furthermore, the Frobenius inner product of two matrices $A, B \in \mathbb{R}^{m \times n}$ is given by

$$\langle A, B \rangle := \text{tr}(A^\top B) = \sum_{i \in [m], j \in [n]} A_i^j B_i^j = \sum_{i \in [m]} \langle A_i, B_i \rangle = \sum_{j \in [n]} \langle A^j, B^j \rangle,$$

and induces the Frobenius matrix norm, again denoted by $\|\cdot\|$. The closure of a set M in \mathbb{R}^n or $\mathbb{R}^{m \times n}$ with respect to $\|\cdot\|$ is indicated by \overline{M} and the interior by $\text{int}(M) := \overline{M} \setminus M$. Furthermore, open Euclidean balls with radius $r > 0$ around a point $x \in \mathbb{R}^n$ are always denoted by $B_r(x)$ and similarly for balls around $X \in \mathbb{R}^{m \times n}$.

Inequalities between two vectors or matrices are meant componentwise, i.e. if $x = x^i e_i$ and $y = y^i e_i$ are vectors in \mathbb{R}^n , then $x > y$ means $x^i > y^i$ for all $i \in [n]$. The Hadamard product, i.e. componentwise multiplication of matrices $A, B \in \mathbb{R}^{m \times n}$, is denoted by $A \bullet B$ and componentwise division for $B > 0$ by $\frac{A}{B}$ or A/B respectively. Define $A^{\bullet 0}$ to be the identity matrix and inductively $A^{\bullet k} := A \bullet A^{\bullet(k-1)}$ for $k \in \mathbb{N}$. For two vectors $x, y \in \mathbb{R}^n$, the Hadamard product is simply denoted by $xy := x \bullet y$, since there is no confusion with matrix multiplication. Also, for $x, y, z \in \mathbb{R}^n$ and $A, B, C \in \mathbb{R}^{m \times n}$ the relations

$$xy = \text{Diag}(x)y, \quad \langle xy, z \rangle = \langle x, yz \rangle \quad \text{and} \quad \langle A \bullet B, C \rangle = \langle A, B \bullet C \rangle$$

hold. The componentwise application of a given scalar function $f: \mathbb{R} \rightarrow \mathbb{R}$ to a vector $x = x^i e_i \in \mathbb{R}^n$ is defined by $f(x) := f(x^i) e_i$, e.g. $e^x = (e^{x^1}, \dots, e^{x^n}) \in \mathbb{R}^n$. Similarly, $f(X)$ denotes the componentwise application of f to a matrix $X \in \mathbb{R}^{m \times n}$.

2.2. Information Geometry

The notion of a dually flat manifold originates in the field of information geometry, where families of probability distributions, such as exponential families, are treated as manifolds. There, the investigation of intrinsic geometric properties of these statistical manifolds naturally leads to the concept of dually flat structures, which provides a rich mathematical framework with applications in statistical inference, information theory, machine learning and many more, see [AN07], [Ama16], [AJVLS17] and references therein. These basic information geometric concepts will be a powerful tool for defining and investigating the dynamical formulation of image labeling on the assignment manifold throughout this work.

In the following, the general concept of a dually flat manifold together with some of the fundamental properties are introduced, based on the aforementioned references. Then, the natural dually flat structure for the space of discrete probability distributions with full support, used to encode label decisions in the subsequent sections, is considered.

2.2.1. Dually Flat Manifolds

Let (S, g) be a Riemannian manifold. Two affine connections ∇ and ∇^* on S are *dual*, if for all vector fields $X, Y, Z \in \mathfrak{X}(S)$

$$Zg(X, Y) = g(\nabla_Z X, Y) + g(X, \nabla_Z^* Y) \quad (2.2)$$

holds. The triple (g, ∇, ∇^*) is called a *dualistic structure* on S . The manifold S together with the choice of a dualistic structure is a *dualistic manifold*, denoted by (S, g, ∇, ∇^*) .

For a given connection ∇ there exists a unique dual connection ∇^* , implying the equality $(\nabla^*)^* = \nabla$. Uniqueness also results in self-duality $(\nabla^g)^* = \nabla^g$ for the Levi-Civita connection ∇^g associated to the Riemannian metric g .

A *statistical manifold* is a dualistic manifold (S, g, ∇, ∇^*) with ∇ and ∇^* torsion free. Since ∇ and ∇^* are dual connections, $\nabla' := \frac{1}{2}(\nabla + \nabla^*)$ is a metric connection on (S, g) . Because ∇ and ∇^* are additionally torsion free, so is ∇' and as a consequence, equals the Levi-Civita connection $\nabla^g = \nabla'$. Furthermore, the dual connections ∇ and ∇^* of the statistical manifold S can be encoded by a symmetric 3-tensor as follows.

Theorem 2.2.1. *For every statistical manifold (S, g, ∇, ∇^*) there is an associated symmetric 3-tensor via the construction*

$$\mathcal{T}(X, Y, Z) := g(\nabla_X^* Y - \nabla_X Y, Z) \quad \text{for } X, Y, Z \in \mathfrak{X}(S)$$

Conversely, any symmetric 3-tensor on a Riemannian manifold (S, g) results in a statistical manifold (S, g, ∇, ∇^) , where ∇ is defined by the equation*

$$g(\nabla_X Y, Z) = g(\nabla_X^g Y, Z) - \frac{1}{2}\mathcal{T}(X, Y, Z) \quad \text{for all } X, Y, Z \in \mathfrak{X}(S)$$

and ∇^ is uniquely determined by ∇ through the duality condition (2.2).*

Proof. See [AJVLS17, Thm. 4.1] and [AJVLS17, Thm. 4.2]. \square

A dualistic manifold (S, g, ∇, ∇^*) is called *dually flat manifold* if both dual connections ∇ and ∇^* are flat. Since flat connections are also torsion free, a dually flat manifold is always also a statistical manifold.

The next result shows that any dually flat structure is locally induced by dually convex functions defined on dual affine coordinates.

Theorem 2.2.2. *Let (S, g, ∇, ∇^*) be a dually flat manifold. For any ∇ -affine coordinate system θ on $U \subset S$, there exists a dual coordinate system η on U which is ∇^* -affine. Also, there are smooth convex functions $\psi(\theta)$ and $\varphi(\eta)$ (convex with respect to the coordinates) related by a Legendre transformation*

$$\varphi(\eta) = \max_{\theta} \{ \langle \theta, \eta \rangle - \psi(\theta) \} = \psi^*(\eta),$$

inducing the dual affine coordinates

$$\eta = \partial\psi(\theta) \quad \text{and} \quad \theta = \partial\varphi(\eta) \quad \text{with} \quad \psi(\theta) + \varphi(\eta) - \langle \theta, \eta \rangle = 0, \quad (2.3)$$

as well as the Riemannian structure

$$g_{ij} = g \left(\frac{\partial}{\partial\theta^i}, \frac{\partial}{\partial\theta^j} \right) = \frac{\partial^2}{\partial\theta^i \partial\theta^j} \psi \quad \text{and} \quad g_{ij}^* = g \left(\frac{\partial}{\partial\eta^i}, \frac{\partial}{\partial\eta^j} \right) = \frac{\partial^2}{\partial\eta^i \partial\eta^j} \varphi \quad (2.4)$$

with $g^{ij} = g_{ij}^*$. Furthermore, the components \mathcal{F}_{ijk} of the symmetric 3-tensor \mathcal{F} from Theorem 2.2.1, encoding the dual torsion free connections ∇ and ∇^* , are given by

$$\mathcal{F}_{ijk} = \frac{\partial^3}{\partial\theta^i \partial\theta^j \partial\theta^k} \psi, \quad (2.5)$$

showing that ψ completely induces the dually flat structure.

Proof. For a proof see [AJVLS17, Thm. 4.4] as well as [AN07, Thm. 3.6]. \square

Following the construction of [AN07, Sec. 3.4], there is a uniquely determined local divergence for every dually flat manifold (S, g, ∇, ∇^*) , called the *canonical local divergence*. Let θ and η be dual ∇ - and ∇^* -affine coordinate systems on an open set $U \subset S$ together with their respective convex potentials $\psi(\theta)$ and $\varphi(\eta)$. For $p, q \in U$, the canonical divergence associated with ψ is defined by

$$\begin{aligned} D_{\psi}(p||q) &:= \psi(\theta(p)) + \varphi(\eta(q)) - \langle \theta(p), \eta(q) \rangle \\ &\stackrel{(2.3)}{=} \psi(\theta(p)) - \psi(\theta(q)) - \langle \partial\psi(\theta(q)), \theta(p) - \theta(q) \rangle = D_{\psi}(\theta(p), \theta(q)), \end{aligned} \quad (2.6)$$

which is nothing else than the Bregman divergence (B.7). Dually, there is the corresponding canonical divergence associated with φ by exchanging the role of ψ and η , resulting in

$$D_{\varphi}(p||q) = \varphi(\eta(p)) + \psi(\theta(q)) - \langle \eta(p), \theta(q) \rangle = D_{\varphi}(\eta(p), \eta(q)). \quad (2.7)$$

Comparing (2.6) and (2.7) shows that the two divergences are given by the same expressions and only differ by swapping the arguments. This motivates to define the *dual canonical divergence* as

$$D_\psi^*(p\|q) := D_\varphi(p\|q) = D_\psi(q\|p).$$

Furthermore, they also induce the Riemannian metric by

$$\frac{\partial^2}{\partial\theta^i\partial\theta^j}D_\psi(p\|q) = g_{ij} \quad \text{as well as} \quad \frac{\partial^2}{\partial\eta^i\partial\eta^j}D_\psi(p\|q) = g^{ij}$$

and it can be shown that $D_\psi(p\|q)$ is invariant under affine coordinate transformations. Thus, (2.6) and its dual are indeed uniquely determined by the dually flat structure.

2.2.2. Discrete Probability Distributions with Full Support

Probability distributions on a discrete set \mathcal{X} with a finite number of elements $|\mathcal{X}| = n$ are identified as points on the *probability simplex*

$$\Delta := \{p \in \mathbb{R}^n \mid \langle \mathbb{1}_n, p \rangle = 1 \text{ and } p \geq 0\} = \text{conv}(\mathcal{B}_n). \quad (2.8)$$

Hence, the set of discrete probability distributions on \mathcal{X} with full support is represented by the manifold

$$\mathcal{S} := \{p \in \Delta \mid p > 0\} = \text{rint}(\Delta), \quad (2.9)$$

with constant tangent space

$$T_p\mathcal{S} = \{v \in \mathbb{R}^n \mid \langle \mathbb{1}_n, v \rangle = 0\} =: T_{\mathcal{S}} \quad \forall p \in \mathcal{S} \quad (2.10)$$

and trivial tangent bundle $T\mathcal{S} = \mathcal{S} \times T_{\mathcal{S}}$. In the following, the natural dually flat structure of \mathcal{S} is introduced, based on [Ama16] and [AJVLS17].

The manifold \mathcal{S} can be viewed as an exponential family (see [Ama16, Sec. 2.2.2]) by defining the natural parameters $\theta = \theta(p) \in \mathbb{R}^{n-1}$ of a point $p = p^i e_i \in \mathcal{S}$ as

$$\theta^i = \log \frac{p^i}{p^n} \quad \text{for } i \in [n-1], \quad (2.11)$$

with the associated convex cumulant generating function

$$\psi(\theta) = \log (1 + \langle \mathbb{1}_{n-1}, e^\theta \rangle) = -\log p^n. \quad (2.12)$$

The resulting dual coordinates $\eta = \eta(p) \in \mathbb{R}^{n-1}$ are

$$\eta^i = p^i \quad \text{for } i \in [n-1] \quad (2.13)$$

with the *negative entropy* as corresponding dual convex function

$$\varphi(\eta) = \langle \eta, \log \eta \rangle + (1 - \langle \mathbb{1}_{n-1}, \eta \rangle) \log (1 - \langle \mathbb{1}_{n-1}, \eta \rangle) = \langle p, \log p \rangle =: -H(p). \quad (2.14)$$

Therefore, the natural dually flat structure of \mathcal{S} is induced by the strictly convex negative entropy $-H(p)$. The resulting Riemannian metric

$$g_p: T_{\mathcal{S}} \times T_{\mathcal{S}} \rightarrow \mathbb{R}, \quad (u, v) \mapsto g_p(u, v) = \left\langle u, \text{Diag} \left(\frac{1}{p} \right) v \right\rangle, \quad \forall p \in \mathcal{S}, \quad (2.15)$$

is called *Fisher-Rao (information) metric* and plays an important role for estimation theory in statistics and related fields, see [AN07], [AJVLS17] and references therein. The related dual connections, induced by (2.5) through Theorem 2.2.1, are denoted by $\nabla^{(e)}$ and $\nabla^{(m)} = (\nabla^{(e)})^*$ and called e - and m -connection respectively. With this $(\mathcal{S}, g, \nabla^{(e)}, \nabla^{(m)})$ is a dually flat manifold and the above introduced dual coordinates θ in (2.11) and η in (2.13) are dual e - and m -affine global coordinates of \mathcal{S} . The corresponding maximal m - and e -geodesics at $p \in \mathcal{S}$ in the direction $v \in T_{\mathcal{S}}$ are given by (see [AJVLS17, Prop. 2.5])

$$\gamma_v^{(m)}: (t^-, t^+) \rightarrow \mathcal{S}, \quad t \mapsto p + tv \quad (2.16a)$$

$$\gamma_v^{(e)}: \mathbb{R} \rightarrow \mathcal{S}, \quad t \mapsto \frac{pe^{\frac{t}{p}}}{\langle p, e^{\frac{t}{p}} \rangle}, \quad (2.16b)$$

where $(t^-, t^+) \subset \mathbb{R}$ is the maximal interval for $\gamma_v^{(m)}$ with $t^- < 0 < t^+$. Therefore, the resulting exponential maps are

$$\text{Exp}^{(m)}: \mathcal{E}^{(m)} \rightarrow \mathcal{S}, \quad (p, v) \mapsto \text{Exp}_p^{(m)}(v) = p + v \quad (2.17a)$$

$$\text{Exp}^{(e)}: \mathcal{S} \times T_{\mathcal{S}} \rightarrow \mathcal{S}, \quad (p, v) \mapsto \text{Exp}_p^{(e)}(v) = \frac{pe^{\frac{v}{p}}}{\langle p, e^{\frac{v}{p}} \rangle}, \quad (2.17b)$$

with $\mathcal{E}^{(m)} = \{(p, v) \mid p + v \in \mathcal{S}\} \subset T\mathcal{S} = \mathcal{S} \times T_{\mathcal{S}}$. Furthermore, the canonical divergences associated with ψ and φ from (2.6) and (2.7) in this setting are given by the KL divergence from (B.12) and its dual (see [AJVLS17, Eq. (4.78)]),

$$D_{\psi}(p||q) = \text{KL}^*(p, q) = \text{KL}(q, p), \quad D_{\varphi}(p||q) = D_{\psi}^*(p||q) = \text{KL}(p, q)$$

Remark 2.2.1. The exponential maps $\text{Exp}^{(m)}$ and $\text{Exp}^{(e)}$ corresponding to $\nabla^{(m)}$ and $\nabla^{(e)}$ are *not* the exponential map Exp^g with respect to the Levi-Civita connection ∇^g induced by the Riemannian metric on \mathcal{S} . Consequently, the affine geodesics (2.16) are *not* length-minimizing with respect to the Riemannian structure g . But locally, they provide a close approximation [ÅPSS17, Prop. 3] and are more convenient for numerical computations.

There is an alternative characterization of the Fisher-Rao metric on \mathcal{S} . For this, consider the part of the sphere with radius two, denoted by $2\mathbb{S}^n$, in the positive orthant of \mathbb{R}^n , i.e.

$$2\mathbb{S}_{>0}^n := 2\mathbb{S}^n \cap \mathbb{R}_{>0}^n = \{x \in \mathbb{R}^n \mid \|x\|^2 = 2, x > 0\}.$$

2.3. Image Labeling by Geometric Assignment

This manifold is identified with \mathcal{S} via the following diffeomorphism, called *sphere map*,

$$\xi: \mathcal{S} \rightarrow 2\mathbb{S}_{>0}^n, \quad p \mapsto \xi(p) := 2\sqrt{p}.$$

The submanifold $2\mathbb{S}_{>0}^n \subset \mathbb{R}^n$ has a canonical Riemannian metric given by the induced Euclidean metric $E = \langle \cdot, \cdot \rangle$ on \mathbb{R}^n .

Proposition 2.2.3. [*AJVLS17, Prop. 2.1*]. *The sphere map ξ is an isometry between the Riemannian manifolds (\mathcal{S}, g) and $(2\mathbb{S}_{>0}^n, E)$, i.e. the Fisher-Rao metric is the pullback of the standard Euclidean metric under ξ ,*

$$g_p(u, v) = \langle d\xi(p)[u], d\xi(p)[v] \rangle = \left\langle \frac{u}{\sqrt{p}}, \frac{v}{\sqrt{p}} \right\rangle,$$

for all $p \in \mathcal{S}$ and $u, v \in T_{\mathcal{S}}$.

As a consequence of this relation between \mathcal{S} and $2\mathbb{S}_{>0}^n$, there is an explicit expression for the Riemannian distance d_g on \mathcal{S} , given by

$$d_g(p, q) = d_{\mathbb{S}^n}(\sqrt{p}, \sqrt{q}) = 2 \arccos(\langle \sqrt{p}, \sqrt{q} \rangle), \quad (2.18)$$

as well as an explicit expression for the geodesics on (\mathcal{S}, g) , see [*ÅPSS17, Proposition 2*] for details. Because all geodesics of the sphere $2\mathbb{S}^n$ eventually leave the positive orthant in finite time, the Riemannian manifolds $(2\mathbb{S}_{>0}^n, E)$ and (\mathcal{S}, g) are *not complete*.

2.3. Image Labeling by Geometric Assignment

In this section, the dynamical formulation of image labeling on the assignment manifold together with the required definitions and geometric concepts from [*ÅPSS17*] and [*Sch20*] are introduced. Even so, the main area of application in this thesis will be in the context of image labeling, the smooth geometric assignment approach is developed in full generality, i.e. for any given data with values in an abstract metric space defined on an arbitrary graph. Thus, the framework is also applicable to manifold valued images, spatio-temporal data in $\mathbb{R} \times \mathbb{R}^d$, graphs representing a discretized submanifold in \mathbb{R}^d and many more.

First, the labeling problem on a graph with respect to some given data and a predefined set of labels is formalized. Next, the assignment manifold, encoding the label decisions on the graph, is introduced together with the induced dually flat structure and the resulting Riemannian gradient, as well as the replicator operator and the lifting map. These concepts are then combined to define the assignment flow, a spatially coupled dynamical system on the assignment manifold for inferring label assignments. Finally, geometric Runge-Kutta methods for numerically integrating the assignment flow on the assignment manifold are briefly discussed.

2.3.1. The Labeling Problem on Graphs

Let $\mathcal{G} = (\mathcal{V}, \mathcal{E})$ be an undirected graph with $m := |\mathcal{V}|$ vertices. Throughout this text, the identification $\mathcal{V} = [m]$, resulting from any numbering of the vertices, will be used for convenience. Suppose some data

$$f: \mathcal{V} \rightarrow \mathcal{F}, \quad i \mapsto f(i) =: f_i \in \mathcal{F} \quad (2.19)$$

defined on \mathcal{G} with *feature* values f_i in a metric space $(\mathcal{F}, d_{\mathcal{F}})$, called *feature space*, together with *prototypical features* or *labels*

$$\mathcal{X} = \{\ell_1, \dots, \ell_n\} \subset \mathcal{F} \quad (2.20)$$

is given, with $|\mathcal{X}| = n$. Each label ℓ_j represents a class j of features. The *labeling task* or *labeling problem* corresponds to finding a *task specific label assignment* $\mathcal{V} \rightarrow \mathcal{X}$, assigning a class label to each node, depending on the given data f in a local spatial context encoded by the graph structure. Since the number of vertices m is finite, label assignments can equivalently be viewed as elements of \mathcal{X}^m .

The spatial relation between the data points f_i , represented by the adjacency relation of the graph, induces neighborhoods

$$\mathcal{N}_i = \{k \in \mathcal{V} \mid ik \in \mathcal{E}\}, \quad \forall i \in \mathcal{V}, \quad (2.21)$$

where ik is shorthand for the undirected edge $\{i, k\} \in \mathcal{E}$. Unless otherwise stated,

$$i \in \mathcal{N}_i \quad \forall i \in \mathcal{V} \quad (2.22)$$

is always assumed. As a consequence of the graph being undirected, the neighborhoods satisfy the relations

$$k \in \mathcal{N}_i \Leftrightarrow i \in \mathcal{N}_k, \quad \forall i, k \in \mathcal{V}, \quad (2.23)$$

meaning that feature f_k is spatially related to feature f_i if and only if f_i is related to f_k . For various calculations, it will be convenient to use the indicator function of the neighborhoods \mathcal{N}_i from (2.1), for $i \in \mathcal{V}$, which take the form

$$\chi_{\mathcal{N}_i}: \mathcal{V} \rightarrow \{0, 1\}, \quad j \mapsto \chi_{\mathcal{N}_i}(j) = \begin{cases} 1 & , \text{ for } j \in \mathcal{N}_i \\ 0 & , \text{ else.} \end{cases} \quad (2.24)$$

As a result of the symmetry relation of the neighborhood structure in (2.23), the equality

$$\chi_{\mathcal{N}_i}(j) = \chi_{\mathcal{N}_j}(i) \quad \forall i, j \in \mathcal{V} \quad (2.25)$$

follows. Furthermore, weights $\omega_{ik} \in \mathbb{R}$ for all $k \in \mathcal{N}_i$ may be associated to every neighborhood \mathcal{N}_i from 2.21, fulfilling

$$\omega_{ik} > 0 \quad \text{and} \quad \sum_{k \in \mathcal{N}_i} \omega_{ik} = 1 \quad \forall i \in \mathcal{V}. \quad (2.26)$$

2.3. Image Labeling by Geometric Assignment

These weights quantify the influence of feature f_j on f_i in the spatial neighborhood $j \in \mathcal{N}_i$ and are used to parametrize the regularization property of the assignment flow below.

The graph \mathcal{G} may result from discretizing the image domain $\Omega \subset \mathbb{R}^2$ of a given (gray-value) image $\Omega \rightarrow \mathbb{R}$. In this case, each node indexes a position $x_i \in \Omega$ and neighboring nodes $k \in \mathcal{N}_i$ represent spatial locations x_k with small distance $\|x_i - x_k\|$ to x_i . The features f_i are then called *image features* and are extracted from the raw image at pixel i in a preprocessing step. The resulting labeling task is referred to as *image labeling*.

In this setting, a standard graph for representing rectangular digital images is the image *grid graph* $\mathcal{G}_g = (\mathcal{V}_g, \mathcal{E}_g)$ from low-level image processing. The vertex set is given by $\mathcal{V}_g = [n_x] \times [n_y] \subset \mathbb{Z} \times \mathbb{Z}$, representing the $n_x \times n_y$ pixel grid of the image, $n_x, n_y \in \mathbb{N}$. For a given radius $r \in \mathbb{N}$, the neighborhood \mathcal{N}_i at vertex $i \in \mathcal{V}_g$ is chosen to be the $\|\cdot\|_{\max}$ ball in \mathcal{V}_g centered at i , i.e.

$$\mathcal{N}_i = \{j \in \mathcal{V}_g \mid \|i - j\|_{\max} \leq r\}.$$

These neighborhoods are also called ‘ $N \times N$ neighborhoods’, because for a vertex in the interior of the pixel grid, \mathcal{N}_i is given by the $N \times N$ pixel patch centered at i , where $N = 2r + 1$. This neighborhood structure uniquely determines the edge set \mathcal{E}_g of the grid graph \mathcal{G}_g .

2.3.2. Assignment Manifold

Every label $\ell_j \in \mathcal{X}$ can be encoded as the vertex e_j of the probability simplex Δ from (2.8), with e_j being the j -th standard basis vector of \mathbb{R}^n . This results in the identification

$$\mathcal{X} \subset \Delta.$$

It is therefore natural to allow fully probabilistic label assignments on the manifold \mathcal{S} of discrete probability distributions with full support from (2.9). Points $p \in \mathcal{S}$ sufficiently close to e_j are interpreted as unique label assignments $\ell_j \in \mathcal{X}$.

In the same way as global discrete label assignments $\mathcal{V} \rightarrow \mathcal{X}$ are encoded as points in the product space \mathcal{X}^m , also global probabilistic label assignment $\mathcal{V} \rightarrow \mathcal{S}$ may be represented on the product space of probability distributions with full support.

Definition 2.3.1 (Assignment Manifold). The set of global probabilistic label assignments is called *assignment manifold* and defined by the product space

$$\mathcal{W} := \prod_{i \in \mathcal{V}} \mathcal{S}. \quad (2.27)$$

Remark 2.3.1. In the following, points on the assignment manifold will always be denoted by upper-case letters.

The fact that the tangent space $T_{\mathcal{S}}$ of \mathcal{S} is constant together with the identification (A.4) for the tangent space of the product manifold \mathcal{W} , implies that the assignment manifold also has a constant *tangent space*

$$T_P\mathcal{W} = \prod_{i \in \mathcal{V}} T_{P_i}\mathcal{S} = \prod_{i \in \mathcal{V}} T_{\mathcal{S}} =: \mathcal{T}_{\mathcal{W}}, \quad \forall P = (P_i)_{i \in \mathcal{V}} \in \mathcal{W},$$

and therefore a trivial tangent bundle $T\mathcal{W} = \mathcal{W} \times \mathcal{T}_{\mathcal{W}}$.

Since a point $p \in \mathcal{S} \subset \mathbb{R}^n$ has coordinates $p = p^j e_j$ in the standard basis e_j of \mathbb{R}^n , the i -th component of a point $P = (P_i)_{i \in \mathcal{V}} \in \mathcal{W}$ has coordinates $P_i = P_i^j e_j$. As a consequence, \mathcal{W} is identified with the following embedding into $\mathbb{R}^{m \times n}$

$$\mathcal{W} = \{W \in \mathbb{R}^{m \times n} \mid W\mathbf{1}_n = \mathbf{1}_m \text{ and } W_i^j > 0 \text{ for all } i \in [m], j \in [n]\}. \quad (2.28)$$

Thus, points $W \in \mathcal{W}$ are row-stochastic ($m \times n$) matrices, where the i -th row vector, denoted by $W_i = W_i^j e_j \in \mathcal{S}$, represents the label assignments for node $i \in \mathcal{V}$. Due to this embedding of \mathcal{W} , the tangent space $\mathcal{T}_{\mathcal{W}}$ can be identified with

$$\mathcal{T}_{\mathcal{W}} = \{V \in \mathbb{R}^{m \times n} \mid V\mathbf{1}_n = 0\}.$$

Therefore, every row vector $V_i = V_i^j e_j$ of a tangent vector $V \in \mathcal{T}_{\mathcal{W}}$ is contained in $T_{\mathcal{S}}$, for every $i \in \mathcal{V}$.

As a consequence of the natural dually flat structure of \mathcal{S} , induced by the negative entropy (see Section 2.2.2), this probabilistic encoding of label assignments allows for a geometric model of the labeling task within the rich framework of information geometry. In the following, the product dually flat structure of \mathcal{W} is investigated and subsequently the replicator operator as well as the lifting map are introduced together with their basic properties.

Dually Flat Structure of the Assignment Manifold

The dually flat structure of the factors \mathcal{S} naturally carries over to the product space \mathcal{W} in the following way.

Let $P \in \mathcal{W}$. For the i -th factor \mathcal{S} of \mathcal{W} , $i \in \mathcal{V}$, denote the e -affine coordinates (2.11) by $\theta_i = \theta_i(P_i) \in \mathbb{R}^{n-1}$ and the dual m -affine coordinates (2.13) by $\eta_i = \eta_i(P_i) \in \mathbb{R}^{n-1}$ as well as the corresponding convex function (2.12) by $\psi_i(\theta_i)$ and dual convex function (2.14) by $\varphi_i(\eta_i)$. Furthermore, define the global product coordinates of \mathcal{W} by

$$\theta := (\theta_i)_{i \in \mathcal{V}} \quad \text{and} \quad \eta := (\eta_i)_{i \in \mathcal{V}} \quad (2.29)$$

together with the associated convex functions

$$\psi(\theta) := \sum_{i \in \mathcal{V}} \psi_i(\theta_i) \quad \text{and} \quad \varphi(\eta) := \sum_{i \in \mathcal{V}} \varphi_i(\eta_i).$$

Since ψ factorizes, the conjugate function of ψ is given by

$$\psi^*(\eta) = \max_{\theta = (\theta_i)} \left\{ \sum_{i \in \mathcal{V}} (\langle \theta_i, \eta_i \rangle - \psi_i(\theta_i)) \right\} = \sum_{i \in \mathcal{V}} \max_{\theta_i} \{ \langle \theta_i, \eta_i \rangle - \psi_i(\theta_i) \} = \varphi(\eta),$$

2.3. Image Labeling by Geometric Assignment

showing that θ and η are global dual e - and m -affine coordinates of \mathcal{W} , induced by the negative *global entropy*, or again simply called *entropy*, on \mathcal{W} defined by

$$H_{\mathcal{W}}(P) := \sum_{i \in \mathcal{V}} H(P_i) \stackrel{(2.29)}{=} - \sum_{i \in \mathcal{V}} \varphi_i(\eta_i) = -\varphi(\eta), \quad \forall P \in \mathcal{W}. \quad (2.30)$$

By Theorem 2.2.2, ψ induces a Riemannian metric with coordinates

$$g_{P(\theta)} \left(\frac{\partial}{\partial \theta_k^i}, \frac{\partial}{\partial \theta_l^j} \right) = \frac{\partial^2}{\partial \theta_k^i \partial \theta_l^j} \psi(\theta) = \delta_{kl} \frac{\partial^2}{\partial \theta_k^i \partial \theta_k^j} \psi_k(\theta_k) = \delta_{kl} g_{P_k(\theta_k)} \left(\frac{\partial}{\partial \theta_k^i}, \frac{\partial}{\partial \theta_k^j} \right)$$

at $P \in \mathcal{W}$, where δ_{kl} is the Kronecker delta. For $V, U \in \mathcal{T}_{\mathcal{W}}$, these coordinates of the Riemannian metric result in

$$g_P(V, U) = V_k^i U_l^j g_P \left(\frac{\partial}{\partial \theta_k^i}, \frac{\partial}{\partial \theta_l^j} \right) = V_k^i U_k^j g_{P_k} \left(\frac{\partial}{\partial \theta_k^i}, \frac{\partial}{\partial \theta_k^j} \right) = \sum_{k \in \mathcal{V}} g_{P_k}(V_k, U_k).$$

Therefore, the Riemannian metric of the dually flat structure $(\mathcal{W}, g, \nabla^{(e)}, \nabla^{(m)})$, induced by the negative global entropy $H_{\mathcal{W}}$ from (2.30), is given by the Riemannian product metric, again called Fisher-Rao metric and denoted by g . Again due to the special factorization of ψ and φ , the canonical divergence between $P, Q \in \mathcal{W}$ is the *global KL divergence*, or again simply called *KL divergence*, given by

$$D_{\varphi}(P||Q) = \sum_{i \in \mathcal{V}} D_{\varphi_i}(P_i||Q_i) = \sum_{i \in \mathcal{V}} \text{KL}(P_i, Q_i) = \left\langle P, \log \left(\frac{P}{Q} \right) \right\rangle =: \text{KL}(P, Q). \quad (2.31)$$

Replicator Operator, Riemannian Gradient and Lifting Map

To simplify notation and streamline calculations in the following, it will be advantageous to introduce the *replicator operator* and the *lifting map* from [Sch20] together with their basic properties and relations.

For every $p \in \mathcal{S}$, the *replicator operator* is the linear map $R_p: \mathbb{R}^n \rightarrow T_{\mathcal{S}}$, defined by

$$R_p := \text{Diag}(p) - pp^{\top} \in \mathbb{R}^{n \times n}, \quad (2.32)$$

and the *lifting map* by

$$\exp_p: \mathbb{R}^n \rightarrow \mathcal{S}, \quad x \mapsto \exp_p(x) := \frac{pe^x}{\langle p, e^x \rangle}. \quad (2.33)$$

Furthermore, the *barycenter*, given by the uniform distribution, is denoted by

$$\mathbb{1}_{\mathcal{S}} := \frac{1}{n} \mathbb{1}_n \in \mathcal{S} \quad (2.34)$$

and the orthogonal projection $P_{T_S} : \mathbb{R}^n \rightarrow T_S$ with respect to the standard inner product on \mathbb{R}^n is given by the matrix

$$P_{T_S} := I_n - \mathbb{1}_S \mathbb{1}_n^\top \in \mathbb{R}^{n \times n}. \quad (2.35)$$

The next two lemmas collect some basic properties for the replicator operator and the lifting map frequently used in the subsequent chapters.

Lemma 2.3.1. *The symmetric matrix $R_p \in \mathbb{R}^{n \times n}$ satisfies the following properties:*

- (1) $R_p P_{T_S} = R_p = P_{T_S} R_p$ for all $p \in \mathcal{S}$ and $\ker(R_p) = \mathbb{R}\mathbb{1}$.
- (2) Restricting the linear map R_p to T_S results in a linear isomorphism $R_p : T_S \rightarrow T_S$ for every $p \in \mathcal{S}$ with inverse

$$(R_p|_{T_S})^{-1} = P_{T_S} \text{Diag} \left(\frac{1}{p} \right) : T_S \rightarrow T_S, \quad v \mapsto P_{T_S} \frac{v}{p}. \quad (2.36)$$

- (3) The replicator operator R_p and the variance of a vector $x \in \mathbb{R}^n$ with respect to the probability distribution $p \in \mathcal{S}$ are connected by the identity

$$\langle x, R_p x \rangle = \text{Var}_p(x) \geq 0. \quad (2.37)$$

Thus, R_p is a positive semi-definite symmetric matrix and has real eigenvalues in the interval $0 \leq \lambda_1 \leq \dots \leq \lambda_n \leq \frac{1}{2}$. The restricted map $R_p|_{T_S}$ is a symmetric positive definite endomorphism on T_S .

Remark 2.3.2. Strictly speaking, the restriction of R_p to T_S and its inverse should always be denoted by $R_p|_{T_S}$ and $(R_p|_{T_S})^{-1}$. However, to simplify notation only R_p and R_p^{-1} are used in the following. This will not be a source of confusion, because solving an equation $R_p x = y \in T_S$ for $x \in \mathbb{R}^n$ only introduced an additional projection P_{T_S} due to property (1), i.e.

$$y = R_p x = R_p P_{T_S} x \quad \Leftrightarrow \quad R_p^{-1} y = P_{T_S} x.$$

Proof. To (1): Let $p \in \mathcal{S}$ be arbitrary and take any $x \in \mathbb{R}^n$. Then

$$\langle R_p x, \mathbb{1}_n \rangle = \langle p x, \mathbb{1}_n \rangle - \langle x, p \rangle \langle p, \mathbb{1}_n \rangle = \langle x, p \rangle - \langle x, p \rangle = 0,$$

showing that $R_p x \in T_S$ and therefore also $P_{T_S} R_p = R_p$. Since P_{T_S} and R_p are symmetric,

$$R_p P_{T_S} = (P_{T_S} R_p)^\top = R_p^\top = R_p.$$

Let $p \in \mathcal{S}$ and $x \in \mathbb{R}^n$. Because $p > 0$, it follows

$$x \in \ker(R_p) \quad \Leftrightarrow \quad 0 = R_p x = p(x - \langle x, p \rangle \mathbb{1}_n) \quad \Leftrightarrow \quad x \in \mathbb{R}\mathbb{1}_n.$$

To (2): Since $\mathbb{R}\mathbb{1}_n = \ker(R_p)$ is the orthogonal complement of T_S , the decomposition $\mathbb{R}^n = \mathbb{R}\mathbb{1}_n \oplus T_S$ follows and therefore also $\ker(R_p|_{T_S}) = 0$. As a consequence, the

2.3. Image Labeling by Geometric Assignment

endomorphism $R_p|_{T_S}$ is an isomorphism. To verify that the inverse is given by (2.36), take an arbitrary $v \in T_S$. Keeping $\langle v, \mathbb{1}_n \rangle = 0$ in mind,

$$R_p P_{T_S} \text{Diag} \left(\frac{1}{p} \right) v = R_p \frac{v}{p} = v - \langle v, \mathbb{1}_n \rangle p = v.$$

To (3): Let $x = x^i e_i \in \mathbb{R}^n$ and $p = p^i e_i \in \mathcal{S}$. It follows

$$\langle x, R_p x \rangle = \langle x, p x \rangle - \langle x, p \rangle^2 = \sum_{i \in [n]} (x^i - \langle x, p \rangle)^2 p^i = \text{Var}_p(x) \geq 0,$$

proving (2.37) and that R_p is indeed positive semi-definite. Because of $\mathbb{R}^n = \mathbb{R}\mathbb{1}_n \oplus T_S$, any $x \in T_S$ implies $x \notin \mathbb{R}\mathbb{1}_n$. Therefore, the above equation also yields $\langle x, R_p|_{T_S} x \rangle = \text{Var}_p(x) > 0$ for all $0 \neq x \in T_S$, showing that $R_p|_{T_S}: T \rightarrow T$ is positive-definite.

Since R_p is symmetric, all eigenvalues λ_i are real. For $p = p^i e_i \in \mathcal{S}$, the i -th absolute row sum of R_p is given by

$$\sum_{j \in [n]} |(R_p)_{ij}| = p^i(1 - p^i) + p^i \sum_{i \neq j \in [n]} p^j = 2p^i(1 - p^i) = 2^{-1} - 2(p^i - 2^{-1})^2,$$

resulting in $\|R_p\|_\infty = \max_{i \in [n]} \sum_{j \in [n]} |(R_p)_{ij}| \leq \frac{1}{2}$. Thus, if λ is an eigenvalue with corresponding eigenvector $x_\lambda \neq 0$, then the estimate

$$|\lambda| \|x_\lambda\|_\infty = \|\lambda x_\lambda\|_\infty = \|R_p x_\lambda\|_\infty \leq \|R_p\|_\infty \|x_\lambda\|_\infty \leq \frac{1}{2} \|x_\lambda\|_\infty$$

holds. Because R_p is positive semi-definite, all eigenvalues fulfill $0 \leq \lambda \leq \frac{1}{2}$. \square

Lemma 2.3.2. *The following properties hold for the lifting map (2.33):*

(1) *The lifting map implicitly projects onto T_S , i.e.*

$$\exp_p(P_{T_S} x) = \exp_p(x), \quad \forall x \in \mathbb{R}^n. \quad (2.38)$$

(2) *The restriction $\exp_p: T_S \rightarrow \mathcal{S}$ is a diffeomorphism for every $p \in \mathcal{S}$ with inverse*

$$\exp_p^{-1}: \mathcal{S} \rightarrow T_S, \quad q \mapsto \exp_p^{-1}(q) := P_{T_S} \log \frac{q}{p}. \quad (2.39)$$

The differentials of \exp_p and \exp_p^{-1} at $v \in T_S$ and $q \in \mathcal{S}$, respectively, are given by

$$d\exp_p(v)[u] = R_{\exp_p(v)} u \quad \text{and} \quad d\exp_p^{-1}(q)[u] = R_q^{-1} u \quad \forall u \in T_S. \quad (2.40)$$

(3) *For every $p \in \mathcal{S}$, the maps \exp_p and $\text{Exp}_p^{(e)}$ are related by $\text{Exp}_p^{(e)} \circ R_p = \exp_p$. As a consequence, the inverse of the e -exponential map at $p \in \mathcal{S}$ is globally defined and given by*

$$(\text{Exp}_p^{(e)})^{-1} = R_p \circ \exp_p^{-1}: \mathcal{S} \rightarrow T_S. \quad (2.41)$$

- (4) If \mathbb{R}^n is viewed as an abelian group, then $\exp: \mathbb{R}^n \times \mathcal{S} \rightarrow \mathcal{S}$ given by $(v, p) \mapsto \exp_p(v)$ defines a Lie-group action, i.e.

$$\exp_p(v + u) = \exp_{\exp_p(u)}(v) \quad \text{and} \quad \exp_p(0) = p \quad \forall v, u \in T_{\mathcal{S}} \quad \text{and} \quad \forall p \in \mathcal{S}. \quad (2.42)$$

Furthermore, the following identities hold for all $p, q, a \in \mathcal{S}$ and $v \in \mathbb{R}^n$

$$\exp_p(v) = \exp_q(v + \exp_q^{-1}(p)) \quad (2.43a)$$

$$\exp_q^{-1}(p) = -\exp_p^{-1}(q) \quad (2.43b)$$

$$\exp_q^{-1}(a) = \exp_p^{-1}(a) - \exp_p^{-1}(q). \quad (2.43c)$$

- (5) For $x \in \mathbb{R}^n$ and $p \in \mathcal{S}$, the lifting map is characterized by

$$\exp_p(-x) = \operatorname{argmin}_{q \in \Delta} \{ \langle q, x \rangle + \operatorname{KL}(q, p) \}. \quad (2.44)$$

Remark 2.3.3.

- (1) Similar to Remark 2.3.2, the restriction of \exp_p to $T_{\mathcal{S}}$ and its inverse should always be denoted by $\exp_p|_{T_{\mathcal{S}}}$ and $(\exp_p|_{T_{\mathcal{S}}})^{-1}$. However, as a consequence of property (1)

$$q = \exp_p(x) = \exp_p|_{T_{\mathcal{S}}}(P_{T_{\mathcal{S}}}x) \quad \Leftrightarrow \quad (\exp_p|_{T_{\mathcal{S}}})^{-1}(q) = P_{T_{\mathcal{S}}}x$$

for all $x \in \mathbb{R}^n$ and $p, q \in \mathcal{S}$. Hence, in order to simplify notation \exp_p and \exp_p^{-1} will be used in the following, by keeping in mind that an additional projection enters the equation if \exp_p^{-1} is applied.

- (2) The characterization of \exp_p in (2.44) was already derived in [BT03] as a special case for solving convex optimization problems $\min_{x \in C} f(x)$. There it is shown that the mirror descent method [NY83] can be viewed as a nonlinear projected subgradient method using Bregman divergences, i.e.

$$x^{k+1} = \partial\varphi^*(\partial\varphi(x^k) - h_k \partial f(x^k)) = \operatorname{argmin}_{x \in \Delta} \{ h_k \langle x, \partial f(x^k) \rangle + D_{\varphi}(x, x^k) \}$$

where $h_k > 0$ is the step size and φ a smooth strictly convex function fulfilling some additional technical assumptions. If the convex function is defined on the probability simplex $f: \Delta \rightarrow \mathbb{R}$ and φ is chosen as the negative entropy, then $D_{\varphi} = \operatorname{KL}$ and the characterization (2.44) follows in the form

$$x^{k+1} = \exp_{x^k}(-t_k \partial f(x^k)).$$

Proof. To (1): Take $x \in \mathbb{R}^n$ and $\alpha \in \mathbb{R}$. Then $e^{x+\alpha \mathbf{1}_n} = e^x e^{\alpha}$ and therefore also $\exp_p(x + \alpha \mathbf{1}_n) = \exp_p(x)$. Due to $P_{T_{\mathcal{S}}}x = x - \langle x, \mathbf{1}_n \rangle \mathbf{1}_{\mathcal{S}}$ by (2.35), the previous identity directly implies the statement.

Statement (2) is shown by a direct computation. Fix $p \in \mathcal{S}$ and let q be any point in \mathcal{S} . Then by property (1),

$$\exp_p\left(P_{T_{\mathcal{S}}}\log\frac{q}{p}\right) = \exp_p\left(\log\frac{q}{p}\right) = \frac{p^{\frac{q}{p}}}{\langle p, \frac{q}{p} \rangle} = \frac{q}{\langle \mathbf{1}_n, q \rangle} = q.$$

2.3. Image Labeling by Geometric Assignment

For an arbitrary $v \in T_S$, it follows from $\ker(P_{T_S}) = \mathbb{R}\mathbf{1}$ that

$$P_{T_S} \log \left(\frac{\exp_p(v)}{p} \right) = P_{T_S} \log \left(\frac{e^v}{\langle p, e^v \rangle} \right) = P_{T_S} (v - (\log \langle p, e^v \rangle) \mathbf{1}_n) = P_{T_S} v = v.$$

The differentials are calculated using (A.3). For this, let $u \in T_S$ and define $\gamma(t) := v + tu$ as well as $\beta(t) := q + tu$ for sufficiently small $t \in \mathbb{R}$. Using (2.32) and (2.36), leads to

$$\begin{aligned} \left. \frac{d}{dt} \frac{pe^{\gamma(t)}}{\langle p, e^{\gamma(t)} \rangle} \right|_{t=0} &= \frac{pe^v}{\langle p, e^v \rangle} u - \frac{pe^v}{\langle p, e^v \rangle^2} \langle pe^v, u \rangle = R_{\exp_p(v)} u, \\ \left. \frac{d}{dt} P_{T_S} \log \frac{\beta(t)}{p} \right|_{t=0} &= P_{T_S} \frac{p u}{q p} = P_{T_S} \frac{u}{q} = R_q^{-1} u. \end{aligned}$$

Regarding (3), the definitions for $\text{Exp}_p^{(e)}$ in (2.17b) and \exp_p in (2.33) together with property (1) directly imply

$$\text{Exp}_p^{(e)}(v) = \exp_p \left(\frac{v}{p} \right) = \exp_p \left(P_{T_S} \frac{v}{p} \right) = \exp_p(R_p^{-1}v) \quad \forall v \in T_S,$$

which is equivalent to $\text{Exp}_p^{(e)} R_p = \exp_p$. Since R_p and \exp_p restricted to T_S are invertible, so is $\text{Exp}_p^{(e)}$ with inverse given by (2.41).

To (4): Properties (2.42) defining the group action are directly verified

$$\exp_{\exp_p(u)}(v) = \frac{\frac{pe^u}{\langle p, e^u \rangle} e^v}{\langle \frac{pe^u}{\langle p, e^u \rangle}, e^v \rangle} = \frac{pe^{u+v}}{\langle p, e^{u+v} \rangle} = \exp_p(u+v).$$

Now, suppose $p, q, a \in \mathcal{S}$ and $v \in \mathbb{R}^n$ are arbitrary. The group action property together with $p = \exp_q(\exp_q^{-1}(p))$ yield

$$\exp_p(v) = \exp_{\exp_q(\exp_q^{-1}(p))}(v) = \exp_q(v + \exp_q^{-1}(p)),$$

which proves (2.43a). To show (2.43b), set $v_a := \exp_p^{-1}(a)$ and substitute this vector into (2.43a). Applying \exp_q^{-1} to both sides then gives

$$\exp_q^{-1}(a) = \exp_q^{-1}(\exp_p(v_a)) = v_a + \exp_q^{-1}(p) = \exp_p^{-1}(a) + \exp_q^{-1}(p). \quad (2.45)$$

Setting $a = q$ in this equation, (2.43b) is obtained from

$$0 = \exp_q^{-1}(q) = \exp_p^{-1}(q) + \exp_q^{-1}(p).$$

Using $\exp_q^{-1}(p) = -\exp_p^{-1}(q)$ in (2.45) results in (2.43c).

To (5): The constraints of the optimization problem in (2.44) are $\langle q, \mathbf{1}_n \rangle - 1 = 0$ and $q \geq 0$. Therefore, the overall optimization problem is convex (B.19) and the KKT optimality conditions (B.18) are sufficient. Because the objective $\langle q, x - \log p \rangle + \langle p, \log p \rangle$ is

strictly convex, the minimizer q^* is unique. In order to determine this unique minimizer, consider the Lagrangian (B.15) of the form

$$L(q, \lambda, \nu) = \langle x, q \rangle + \text{KL}(q, p) + \lambda(\langle q, \mathbb{1}_n \rangle - 1) - \langle \nu, q \rangle,$$

with Lagrange multipliers $\lambda \in \mathbb{R}$ and $\nu \in \mathbb{R}^n$, $\nu \geq 0$. The KKT-conditions (B.18) for the minimizer q^* and corresponding multipliers λ^* , ν^* are given by

$$0 = \partial_q L(q^*, \lambda^*, \nu^*) = x + \log q^* - \log p + (1 + \lambda^*)\mathbb{1}_n - \nu^* = 0 \quad (2.46a)$$

$$1 = \langle q^*, \mathbb{1}_n \rangle, \quad q^* \geq 0, \quad \nu^* \geq 0, \quad \langle \nu^*, q^* \rangle = 0. \quad (2.46b)$$

Rearranging (2.46a) yields

$$\log q^* = \nu^* - x + \log p - (1 + \lambda^*)\mathbb{1}_n \quad \Leftrightarrow \quad q^* = e^{\nu^* - x} p e^{-(1 + \lambda^*)}.$$

Therefore, $q^* > 0$ and (2.46b) implies $\nu^* = 0$. Furthermore,

$$1 = \langle \mathbb{1}_n, q^* \rangle = \langle e^{-x}, p \rangle e^{-(1 + \lambda^*)}.$$

As a consequence, the minimizer q^* has the form

$$q^* = e^{-x} p e^{-(1 + \lambda^*)} = \frac{p e^{-x}}{\langle p, e^{-x} \rangle} = \exp_p(-x). \quad \square$$

As shown in [AJVLS17, Prop. 2.2] and [PSS17, Prop. 1], the Riemannian gradient and the Euclidean gradient of a function are related by the replicator operator. This relation can easily be derived by using the above properties of the replicator operator.

Lemma 2.3.3. *Suppose $J: \mathcal{S} \rightarrow \mathbb{R}$ is C^1 . Additionally to the Fisher-Rao metric g , let $E = \langle \cdot, \cdot \rangle$ be the standard Euclidean metric on $\mathcal{S} \subset \mathbb{R}^n$. Then the Riemannian gradient $\text{grad}_g J(p)$ of (\mathcal{S}, g) and the Riemannian gradient $\text{grad}_E J(p)$ of (\mathcal{S}, E) are related by*

$$\text{grad}_g J(p) = R_p \text{grad}_E J(p). \quad (2.47)$$

If J is defined on an open subset $U \subset \mathbb{R}^n$ containing \mathcal{S} , then $\text{grad}_E J(p) = P_{T_S} \partial J(p)$ and the relation takes the form

$$\text{grad}_g J(p) = R_p \partial J(p). \quad (2.48)$$

Remark 2.3.4. As a consequence of this relation, the Riemannian gradient of J represents a replicator equation with fitness function ∂J or $\text{grad}_e J$ respectively, selecting the assignment with the highest fitness, a fact well known in evolutionary game dynamics [HS03].

Proof. Let $p \in \mathcal{S}$ and $v \in T_S$. By the definition of the Riemannian gradient,

$$\langle \text{grad}_E J(p), v \rangle = dJ(p)[v] = g_p(\text{grad}_g J(p), v) = \langle P_{T_S} \text{Diag} \left(\frac{1}{p} \right) \text{grad}_g J(p), v \rangle.$$

2.3. Image Labeling by Geometric Assignment

Since v was arbitrary, the equality

$$\text{grad}_E J(p) = P_{T_S} \text{Diag} \left(\frac{1}{p} \right) \text{grad}_g J(p)$$

follows. Multiplying the above equation by R_p and keeping in mind that $P_{T_S} \text{Diag}(p^{-1})$ is the inverse of R_p on T_S by Lemma 2.3.1 (2), the relation (2.47) is established. If J is defined on the set U containing \mathcal{S} , then $dJ(p)[v] = \langle \partial J(p), v \rangle = \langle P_{T_S} \partial J(p), v \rangle$ for all $v \in T_S$, proving $\text{grad}_E J(p) = P_{T_S} \partial J(p)$. Due to $R_p P_{T_S} = R_p$ by Lemma 2.3.1 (1), also (2.48) follows. \square

All the introduced concepts on \mathcal{S} naturally extend to the product manifold \mathcal{W} . The global uniform distribution, given by the uniform distribution in every row and again called *barycenter*, is denoted by

$$\mathbb{1}_{\mathcal{W}} := (\mathbb{1}_{\mathcal{S}}, \dots, \mathbb{1}_{\mathcal{S}}) = \mathbb{1}_m \mathbb{1}_{\mathcal{S}}^{\top} \in \mathcal{W},$$

where the second equality is due to the embedding (2.28). All the mappings P_{T_S} , R , exp and $\text{Exp}^{(e)}$ as well as their inverses also carry over to the assignment manifold as product maps (see (A.5)) and are again denoted by the same symbols, e.g. for $X \in \mathbb{R}^{m \times n}$, $V \in \mathcal{T}_{\mathcal{W}}$ and $W \in \mathcal{W}$, given by

$$\begin{aligned} P_{\mathcal{T}_{\mathcal{W}}}[X] &= (P_{T_S} X_i)_{i \in [m]} \in \mathcal{T}_{\mathcal{W}}, \\ R_W[X] &= (R_{W_i} X_i)_{i \in [m]} \in \mathcal{T}_{\mathcal{W}}, \\ \text{Exp}_W^{(e)}(V) &= (\text{Exp}_{W_i}^{(e)}(V_i))_{i \in \mathcal{V}} \in \mathcal{W} \end{aligned}$$

and so on. Also most of the properties from Lemma 2.3.2 and Lemma 2.3.2 are still valid. As a result of the factorization

$$\min_{P \in \Delta^m} \{ \langle P, X \rangle + \text{KL}(P, W) \} = \sum_{i \in \mathcal{V}} \min_{P_i \in \Delta} \{ \langle P_i, X_i \rangle + \text{KL}(P_i, W_i) \} \quad (2.49)$$

for $W \in \mathcal{W}$ and $X \in \mathbb{R}^{m \times n}$, also the characterization (2.44) and the corresponding interpretation of the lifting map in Remark 2.3.3 (2) are valid on \mathcal{W}

$$\text{exp}_W(-X) = \text{argmin}_{P \in \Delta^m} \{ \langle P, X \rangle + \text{KL}(P, W) \}. \quad (2.50)$$

As a direct consequence of the Fisher-Rao metric on \mathcal{W} being a product metric, the same relation between the Riemannian and Euclidean gradient as in Lemma 2.3.3 holds.

Corollary 2.3.4. *Let $J: \mathcal{W} \rightarrow \mathbb{R}$ be C^1 and consider the Fisher-Rao metric g as well as the standard Euclidean metric $E = \langle \cdot, \cdot \rangle$ on \mathcal{W} . Then the Riemannian gradients $\text{grad}_g J(W)$ of (\mathcal{W}, g) and $\text{grad}_E J(W)$ of (\mathcal{W}, E) are related by*

$$\text{grad}_g J(W) = R_W[\text{grad}_E J(W)], \quad \forall W \in \mathcal{W}. \quad (2.51)$$

If J is defined on an open set $U \subset \mathbb{R}^{m \times n}$ containing \mathcal{W} , then $\text{grad}_E J(W) = P_{\mathcal{T}_{\mathcal{W}}}[\partial J(W)]$ and the relation takes the form

$$\text{grad}_g J(W) = R_W[\partial J(W)], \quad \forall W \in \mathcal{W}. \quad (2.52)$$

Remark 2.3.5. As a result of the identification in (2.3.2), the gradients $\text{grad}_g J(W)$, $\text{grad}_E J(W)$ and $\partial J(W)$ are real $m \times n$ matrices. For $i \in \mathcal{V}$, the i -th row of these matrices is denoted by $\text{grad}_{g,i} J(W)$, $\text{grad}_{E,i} J(W)$ and $\partial_i J(W)$ respectively, representing the change of J with respect to the i -th row W_i of W . Locally at a vertex $i \in \mathcal{V}$, (2.52) takes the form

$$\text{grad}_{g,i} J(W) = R_{W_i} \partial_i J(W), \quad \forall W \in \mathcal{W}. \quad (2.53)$$

Since $\partial_i J(W)$ generally not only depends on W_i but also on assignments W_j at other locations $j \in \mathcal{V}$, the Riemannian gradient $\text{grad}_g J(W)$ represents a spatially coupled replicator equation with fitness $\text{grad}_E J$ or ∂J respectively.

2.3.3. Assignment Flow

Motivated by the relation (2.52) between the Riemannian and the Euclidean gradient, the dynamical selection process of the assignment flow is modeled as a spatially coupled replicator equation, combining three distinct objectives: (I) selecting the *best label fit* at every location $i \in \mathcal{V}$ while (II) minimizing the deviation to neighboring assignments in a small neighborhood around i for *spatial regularization* and (III) gradually *enforcing* unambiguous labels decisions. In the following, the construction of the assignment flow is explained in more detail.

Based on the given data (2.19) and labels (2.20) with values in the feature (metric) space $(\mathcal{F}, d_{\mathcal{F}})$, the label fit is measured by the *distance matrix* $D_{\mathcal{F}} \in \mathbb{R}^{m \times n}$ with i -th row defined by

$$D_{\mathcal{F}i} := (d_{\mathcal{F}}(f_i, \ell_1), \dots, d_{\mathcal{F}}(f_i, \ell_n)) \in \mathbb{R}^n, \quad \text{for all } i \in \mathcal{V}. \quad (2.54)$$

This distance information is *lifted* onto the assignment manifold by the following *likelihood matrix*

$$L(W) := \exp_W(-D_{\mathcal{F}}/\rho) \in \mathcal{W}, \quad (2.55a)$$

$$L_i(W) = L_i(W_i) = \frac{W_i e^{-\frac{1}{\rho} D_{\mathcal{F}i}}}{\langle W_i, e^{-\frac{1}{\rho} D_{\mathcal{F}i}} \rangle}, \quad \rho > 0, \quad i \in \mathcal{V}, \quad (2.55b)$$

where $\rho > 0$ is a scaling parameter to normalize the a-priori unknown scale of the distances induced by the features f_i depending on the application at hand. As a result of (2.49) and (2.50), the likelihood vector L_i is characterized by

$$L_i(W_i) = \operatorname{argmin}_{p \in \Delta} \{ \rho \langle W_i, D_{\mathcal{F}i} \rangle + \text{KL}(p, W_i) \}.$$

and can be interpreted as selecting the best label assignment at every $i \in \mathcal{V}$ while taking the current assignment state $W_i \in \mathcal{S}$ into account through the KL divergence, with the tradeoff controlled by ρ .

This representation of the data on the assignment manifold \mathcal{W} is regularized in the local neighborhoods (2.21) using the associated weights (2.26) to obtain the *similarity matrix* $S(W) \in \mathcal{W}$, with i -th row $S_i(W)$ defined through the condition

$$0 = \sum_{k \in \mathcal{N}_i} \omega_{ik} (\text{Exp}_{S_i(W)}^{(e)})^{-1}(L_k(W_k)) \quad \forall i \in \mathcal{V}. \quad (2.56)$$

2.3. Image Labeling by Geometric Assignment

If the e -exponential map $\text{Exp}^{(e)}$ is replaced by the exponential map Exp^g with respect to the Riemannian structure (Levi-Civita connection), then the above condition would be the optimality condition (A.16) used to determine the Riemannian center of mass. In view of Remark 2.2.1, this interpretation of the similarity matrix is only approximately true mathematically. However, as the next proposition shows, it is still correct conceptually: $S_i(W)$ moves W_i towards the normalized geometric mean of the likelihood vectors L_k for $k \in \mathcal{N}_i$.

Proposition 2.3.5. *For every $i \in \mathcal{V}$ and $W \in \mathcal{W}$, the i -th row $S_i(W)$ of the similarity matrix $S(W) \in \mathcal{W}$ is uniquely determined through condition (2.56) and can be explicitly expressed as*

$$S_i(W) = \exp_{\mathbb{1}_S} \left(\sum_{k \in \mathcal{N}_i} \omega_{ik} \left(\exp_{\mathbb{1}_S}^{-1}(W_k) - \frac{1}{\rho} D_{\mathcal{F}k} \right) \right). \quad (2.57)$$

Denoting the weighted geometric mean of the likelihood vectors in the neighborhood \mathcal{N}_i around $i \in \mathcal{V}$ with weights $\omega_i = (\omega_{ik})_{k \in \mathcal{N}_i}$ by

$$\text{gm}^{\omega_i} \{L_k(W_k)\}_{k \in \mathcal{N}_i} := \prod_{k \in \mathcal{N}_i} (L_k(W_k))^{\omega_{ik}},$$

the similarity matrix is equivalently characterized as the normalized geometric mean, which is the weighted center of mass with respect to the canonical KL divergence on \mathcal{S}

$$S_i(W) = \frac{\text{gm}^{\omega_i} \{L_k(W_k)\}_{k \in \mathcal{N}_i}}{\langle \mathbb{1}_n, \text{gm}^{\omega_i} \{L_k(W_k)\}_{k \in \mathcal{N}_i} \rangle} = \underset{p \in \Delta}{\text{argmin}} \left\{ \sum_{k \in \mathcal{N}_i} \omega_{ik} \text{KL}(p, L_k(W_k)) \right\}. \quad (2.58)$$

Remark 2.3.6. In a similar way, the normalized geometric mean was already derived in [ÅPSS17, Lem. 5] as a reasonable approximation of the underlying Riemannian mean with respect to the Fisher-Rao metric.

Proof. To simplify notation in this proof, the explicit dependency of the similarity and likelihood vectors on W is dropped and they are simply denoted by S_i and L_k . Next, note that by (2.43a), the likelihood vector at $k \in \mathcal{V}$ can be expressed as

$$L_k = \exp_{W_k}(-D_{\mathcal{F}k}/\rho) = \exp_{\mathbb{1}_S}(\exp_{\mathbb{1}_S}^{-1}(W_k) - D_{\mathcal{F}k}/\rho) \quad (2.59)$$

and by (2.43c), the following identity holds

$$\exp_{S_i}^{-1}(L_k) = \exp_{\mathbb{1}_S}^{-1}(L_k) - \exp_{\mathbb{1}_S}^{-1}(S_k). \quad (2.60)$$

Applying the inverse of $R_{S_i(W)}$ to (2.56) (the inverse of $\text{Exp}_{S_i}^{(e)}$ only takes values in T_S) and using the explicit expression for $(\text{Exp}_{S_i}^{(e)})^{-1}$ from (2.41) yields,

$$\begin{aligned} 0 &= R_{S_i(W)}^{-1} \sum_{k \in \mathcal{N}_i} \omega_{ik} (\text{Exp}_{S_i(W)}^{(e)})^{-1}(L_k(W_k)) = \sum_{k \in \mathcal{N}_i} \omega_{ik} \exp_{S_i(W)}^{-1}(L_k) \\ &\stackrel{(2.60)}{=} \sum_{k \in \mathcal{N}_i} \omega_{ik} \exp_{\mathbb{1}_S}^{-1}(L_k) - \exp_{\mathbb{1}_S}^{-1}(S_k). \end{aligned}$$

Bringing $\exp_{\mathbb{1}_S}^{-1}(S_k)$ to the other side and applying $\exp_{\mathbb{1}_S}$ finally results in

$$S_k = \exp_{\mathbb{1}_S} \left(\sum_{k \in \mathcal{N}_i} \omega_{ik} \exp_{\mathbb{1}_S}^{-1}(L_k) \right) \stackrel{(2.59)}{=} \exp_{\mathbb{1}_S} \left(\sum_{k \in \mathcal{N}_i} \omega_{ik} (\exp_{\mathbb{1}_S}^{-1}(W_k) - D_{\mathcal{F}_k}/\rho) \right),$$

showing uniqueness and existence for every $W \in \mathcal{W}$. The connection to the normalized geometric mean is established by continuing the first equality of the above equation

$$\begin{aligned} S_k &= \exp_{\mathbb{1}_S} \left(\sum_{k \in \mathcal{N}_i} \omega_{ik} \exp_{\mathbb{1}_S}^{-1}(L_k) \right) \stackrel{(2.39)}{=} \exp_{\mathbb{1}_S} \left(P_{T_S} \sum_{k \in \mathcal{N}_i} \omega_{ik} \log(L_k) \right) \\ &\stackrel{(2.38)}{=} \exp_{\mathbb{1}_S} \left(\log \left(\prod_{k \in \mathcal{N}_i} L_k^{\omega_{ik}} \right) \right) = \frac{\text{gm}^{\omega_i} \{L_k(W_k)\}_{k \in \mathcal{N}_i}}{\langle \mathbb{1}_n, \text{gm}^{\omega_i} \{L_k(W_k)\}_{k \in \mathcal{N}_i} \rangle}. \end{aligned}$$

Let $a \in \mathbb{R}_{>0}^n$ and consider the problem of minimizing the generalized KL divergence $\text{KL}(q, a)$ (B.13) with respect to $q \in \Delta$ for fixed a . Because the argmin does not depend on constant terms,

$$\begin{aligned} \text{argmin}_{q \in \Delta} \{ \text{KL}(q, a) \} &= \text{argmin}_{q \in \Delta} \{ \langle q, -\log a \rangle + \text{KL}(q, \mathbb{1}_S) \} \\ &\stackrel{(2.44)}{=} \exp_{\mathbb{1}_S}(\log a) = \frac{a}{\langle \mathbb{1}_n, a \rangle}. \end{aligned}$$

With this, the second equality in (2.58) directly follows from the observation

$$\sum_{k \in \mathcal{N}_i} \omega_{ik} \text{KL}(q, L_k) = \text{KL} \left(q, \prod_{k \in \mathcal{N}_i} L_k^{\omega_{ik}} \right). \quad \square$$

The inference of label assignments is defined as a dynamical system evolving on the statistical manifold \mathcal{W} steered by the similarity matrix, which quantifies label decisions in a spatial context.

Definition 2.3.2 (Assignment Flow). The *assignment flow* on \mathcal{W} is the dynamical system

$$\dot{W}(t) = R_{W(t)}[S(W(t))], \quad W(0) = \mathbb{1}_{\mathcal{W}}. \quad (2.62)$$

Because every $S_i(W)$, $i \in \mathcal{V}$ depends on the assignments W_k in a neighborhood $k \in \mathcal{N}_i$ (see Proposition 2.3.5), the assignment flow is a system of spatially coupled replicator equations. Integrating this flow yields smooth curves $W_i(t) \in \mathcal{S}$ for every pixel $i \in \mathcal{V}$ emanating from $W_i(0) = \mathbb{1}_S$, which approach a label state $W_i(t)$ for sufficiently large $t > 0$ and hence a unique label assignment after trivial rounding.

2.3.4. Geometric Numerical Integration of the Assignment Flow

If a given ODE on a manifold can be represented by a Lie group action, then geometric Runge-Kutta methods on the manifold can be used for integration, see [MK99] and references therein. In the following, the application of this approach in [ZSPS20] to the assignment flow is summarized.

Due to Lemma 2.3.2(4), setting $\Lambda(V, W) := \exp_W(V)$ defines a Lie group action on the assignment manifold $\Lambda: \mathcal{T}_\mathcal{W} \times \mathcal{W} \rightarrow \mathcal{W}$. Since the Lie group in the present case is given by the flat abelian vector space $\mathcal{T}_\mathcal{W}$, the geometric Runge-Kutta method on the assignment manifold is considerably simplified. Overall, the resulting approach for integrating an arbitrary vector field $F: \mathcal{W} \rightarrow \mathcal{T}_\mathcal{W}$ is as follows. Suppose, the ODE

$$\dot{W}(t) = R_{W(t)}[F(W(t))], \quad W(0) = \mathbb{1}_\mathcal{W} \quad (2.63)$$

on the assignment manifold is given. Then the parametrization $W(t) = \exp_{\mathbb{1}_\mathcal{W}}(V(t))$ yields an equivalent reparametrized ODE

$$\dot{V}(t) = F(W(t)) = F(\exp_{\mathbb{1}_\mathcal{W}}(V(t))), \quad V(0) = 0 \quad (2.64)$$

purely evolving on the vector space $\mathcal{T}_\mathcal{W}$. There, standard Runge-Kutta methods (see e.g. [HPW93]) can now be used for numerical integration. Translating these update schemes back onto \mathcal{W} , yields geometric Runge-Kutta methods on \mathcal{W} induced by the Lie-group action $\Lambda = \exp$.

Remark 2.3.7. Notice, that the assumption $F(W) \in \mathcal{T}_\mathcal{W}$ is crucial, because the transformation of the ODE (2.63) onto $\mathcal{T}_\mathcal{W}$ in (2.64) uses the inverse of R_W , which only exists for elements from $\mathcal{T}_\mathcal{W}$ but not for those from $\mathbb{R}^{m \times n}$. However, as already mentioned in Remark 2.3.2 this is no limitation. Suppose any vector field $G: \mathcal{W} \rightarrow \mathbb{R}^{m \times n}$ is given. Then the relation $R_W = R_W P_{\mathcal{T}_\mathcal{W}}$ from Lemma 2.3.1(1) allows to consider instead the vector field

$$F(W) := P_{\mathcal{T}_\mathcal{W}}[G(W)] \in \mathcal{T}_\mathcal{W},$$

without changing the underlying ODE (2.63) for $W(t)$.

An important special case for numerically integrating the assignment flow (2.64), sufficient for most applications (see the discussion in [ZSPS20]), is the explicit Euler method on the vector space $\mathcal{T}_\mathcal{W}$, i.e.

$$V^{(k+1)} = V^{(k)} + h_k F(W^{(k)}), \quad W^{(k)} = \exp_{\mathbb{1}_\mathcal{W}}(V^{(k)}), \quad V^{(0)} = 0 \quad (2.65)$$

with step-size $h_k > 0$. Due to the Lie-group action, this update scheme translates to the geometric Euler integration on \mathcal{W} , given by

$$W^{(k+1)} = \exp_{W^{(k)}}(h_k F(W^{(k)})), \quad W^{(0)} = \mathbb{1}_\mathcal{W}, \quad (2.66)$$

with step-size $h_k > 0$.

Chapter 3

General Variational Models on the Assignment Manifold

In the assignment flow framework from Section 2.3, the inference of assignment configurations is done by following a certain dynamical system, a spatially coupled replicator equation, of the general form

$$\dot{W}(t) = R_{W(t)}[F(W(t))] \quad (3.1)$$

with a vector field $F: \mathcal{W} \rightarrow \mathcal{T}_{\mathcal{W}}$ acting as fitness function. During inference, a label assignment with locally highest fitness is selected. In case of the assignment flow (2.62), the fitness is given by the similarity matrix, consisting of weighted geometric means of likelihood vectors in spatial neighborhoods, according to Proposition 2.3.5.

The more classical strategy for image labeling would be a variational approach (see e.g. [LS11], [KAH⁺15] and references therein), i.e. finding an optimal labeling with respect to an *objective function*, measuring the quality of label assignments depending on the domain of application. In the present case of fully probabilistic assignments on \mathcal{W} , this would mean to devise a function $J: \mathcal{W} \rightarrow \mathbb{R}$ in such a way that minimizers correspond to desired assignment configurations. In this approach, inference of assignments is done by finding global minimizers of the optimization problem

$$\inf_{W \in \mathcal{W}} \{J(W)\}.$$

Since there is a difference between methods for integrating a flow and optimizing a function, the two mentioned approaches follow different philosophies. In the first case, the focus of numerical algorithms is on closely following the dynamics of the system with minimal deviation over a certain period of time, [HPW93]. In the second case, the aim is on finding a global minimizer of J , irrespective of whether the chosen method follows any specific dynamics or which minimizer is found, [NW06].

Motivated by [ÅPSS17], the approach of variational models for image labeling on \mathcal{W} in this thesis is to combine both viewpoints: minimize the objective function J through the dynamics of the Riemannian gradient descent flow with respect to the Fisher-Rao metric. Due to the relation between the Fisher-Rao and Euclidean gradient from Corollary 2.3.4, the resulting dynamical system has the form

$$\dot{W}(t) = -\text{grad}_g J(W(t)) = R_{W(t)}[-\text{grad}_E J(W(t))], \quad W(0) = W_0 \in \mathcal{W} \quad (3.2)$$

and fits into the general formulation (3.1) of the assignment flow for inferring label assignments through spatially coupled replicator equations with fitness $F = -\text{grad}_E J$. As a consequence of

$$\frac{d}{dt}J(W(t)) = g_{W(t)}(\text{grad}_g J(W(t)), \dot{W}(t)) = -\|\text{grad}_g J(W(t))\|_{g,W(t)}^2 \leq 0, \quad (3.3)$$

the function values of J are minimized along solutions $W(t)$ of (3.2).

In order to avoid issues arising from the fact that (\mathcal{W}, g) is not a complete Riemannian manifold and minimizers of J may lie on the boundary of \mathcal{W} , a slightly perturbed version J_ε of the original variational model with preferable convergence properties is introduced in the next Section 3.1. This is done by prohibiting arbitrary certain label decisions using the log-barrier method, a standard interior point approach in optimization, see e.g. [NN87, Ter96]. For all practical purposes, this perturbed version is a sufficiently close approximation to the original function J and only has minimizers that stay a small fixed distance away from the boundary, ensuring the numerical integration of the Riemannian gradient flow (3.2) stays on \mathcal{W} . The main class of variational models in this work are analytic functions on \mathcal{W} . Therefore, after some preparations in Section 3.2, it will be shown in the subsequent Sections 3.3 and 3.4 that the perturbed model J_ε allows to transfer the convergence and stability results for the gradient flow and numerical integration of analytic functions on \mathbb{R}^n from [AMA05] and [AK06] to the assignment manifold. Furthermore, convergence rates for the Riemannian gradient flow and the geometric Euler discretization are derived using the approach of [BDL07] and [AB09]. For this thesis to be as self-contained as possible, the results and involved concepts are fully developed and proven in detail.

3.1. Log-Barrier Perturbation of the Variational Model

Throughout this chapter, $J: \mathcal{W} \rightarrow \mathbb{R}$ is always assumed to be at least C^2 and lower bounded, i.e.

$$\inf_{W \in \mathcal{W}} \{J(W)\} > -\infty.$$

Since (\mathcal{W}, g) is not a complete Riemannian manifold (see Section 2.2.2), curves can leave \mathcal{W} in finite time. Also, minimizers of J may lie on the boundary of $\overline{\mathcal{W}} = \Delta^m$ outside of \mathcal{W} , representing arbitrary certain label decisions. In this case, solutions of the Riemannian gradient flow might converge to a boundary point, leading to asymptotic singular behavior. Optimization approaches in this scenario often assume J to be defined on an open set containing $\overline{\mathcal{W}} = \Delta^m$ and additionally to be convex, for proving convergence results for the integral curves, see e.g. [ABB04] and references therein. In the following, neither of these assumptions will be made.

As already mentioned in [ÅPSS17], there is an additional practical issue using numerical integration methods on the assignment manifold in applications. Numerically, only finite precision is available to represent real numbers on a computer, resulting in a difference between mathematical and numerical positivity. Therefore, if the integral

3.1. Log-Barrier Perturbation of the Variational Model

curve of the Riemannian gradient flow is to close to the boundary of \mathcal{W} , the numerical integration method might leave the manifold.

In order to avoid these issues, the log-barrier approach of interior point methods for optimization problems is applied, see e.g. [NN87, Ter96]. For this, consider the following optimization problem on a convex domain given by equality and inequality constraints of the form

$$\min_{x \in \mathbb{R}^d} \{\Phi(x)\} \quad \text{subject to} \quad Ax = b, \Psi_i(x) \geq 0, \forall i \in [K]$$

where $A \in \mathbb{R}^{c \times d}$, $b \in \mathbb{R}^c$ and $\Phi, \Psi_i: \mathbb{R}^d \rightarrow \mathbb{R}$, with Ψ_i convex for all $i \in [K]$. In the present case of the assignment manifold, the relevant inequality constraints are $W > 0$ for $W \in \mathbb{R}^{m \times n}$. The log-barrier method consists of penalizing the inequality constraints by $-\log(\Psi_i(x))$ for $i \in [K]$ and adding them all to the objective Φ with a sufficiently small factor $0 < \varepsilon$, resulting in the approximate optimization problem

$$\min_{x \in \mathbb{R}^d} \left\{ \Phi(x) - \varepsilon \sum_{i \in [K]} \log(\Psi_i(x)) \right\} \quad \text{subject to} \quad Ax = b.$$

Since this is a minimization problem and $-\log(\Psi_i(x)) \rightarrow \infty$ for $\Psi_i(x) \rightarrow 0$, all points $x \in \mathbb{R}^d$ with $\Psi_i(x) = 0$ for any $i \in [K]$ are avoided.

Motivated by this approach, the log-barrier function for the constraints $W > 0$ of the assignment manifold is defined as follows.

Definition 3.1.1. The *log-barrier function* $\xi: \mathcal{W} \rightarrow \mathbb{R}$ for $W \in \mathcal{W}$ is given by

$$\xi(W) := -\frac{1}{n} \sum_{i \in [m]} \sum_{j \in [n]} \log(W_i^j) = -\langle \log(W), \mathbb{1}_{\mathcal{W}} \rangle = -\sum_{i \in \mathcal{V}} \langle \log(W_i), \mathbb{1}_{\mathcal{S}} \rangle \quad (3.4)$$

Due to $0 < W_i^j < 1$, this function is non-negative on \mathcal{W} . It also has the property that if $(W^{(k)})_{k \in \mathbb{N}}$ is a sequence in \mathcal{W} converging to a boundary point, then the corresponding log-barrier values diverge towards infinity, $\lim_{k \rightarrow \infty} \xi(W^{(k)}) = \infty$. With this, the perturbed variational model can be defined next.

Definition 3.1.2. The *perturbed variational model* $J_\varepsilon: \mathcal{W} \rightarrow \mathbb{R}$ is defined by

$$J_\varepsilon(W) := J(W) - \varepsilon \xi(W) = J(W) - \varepsilon \langle \log(W), \mathbb{1}_{\mathcal{W}} \rangle, \quad W \in \mathcal{W}, \quad (3.5)$$

for a sufficiently small $0 < \varepsilon \ll 1$.

The interpretation of J_ε from the image labeling point of view is as follows: besides measuring the *quality* of a probabilistic assignment with J , also an additional "price" for more *certain label decisions* is included in the model.

All local minimizers of J_ε less or equal a certainty value stay a small fixed distance away from the boundary. This can be seen by noticing that all level sets of J_ε are compact in $\mathbb{R}^{m \times n}$, as shown next. Since function values along integral curves $W(t)$ of the Riemannian gradient descent flow are decreasing by (3.3), a minimum amount of uncertainty is introduced in the model J_ε , preventing $W(t)$ to reach the boundary.

Definition 3.1.3. The level set of a function $\Phi: \mathcal{W} \rightarrow \mathbb{R}$ for $\alpha \in \mathbb{R}$ is given by

$$\text{lev}_\alpha(\Phi) := \Phi^{-1}((-\infty, \alpha]) = \{W \in \mathcal{W}: \Phi(W) \leq \alpha\}.$$

Lemma 3.1.1. The level sets $\text{lev}_\alpha(J_\varepsilon) \subset \mathcal{W}$ are compact.

Proof. Because $\mathcal{W} \subset \mathbb{R}^{m \times n}$ is bounded with respect to the Euclidean norm $\|\cdot\|$, so is $\text{lev}_\alpha(J_\varepsilon)$. To show the level set is compact, it remains to show $\text{lev}_\alpha(J_\varepsilon)$ is closed as a subset of $\mathbb{R}^{m \times n}$. For this, let $(W^{(k)})_{k \in \mathbb{N}} \subset \text{lev}_\alpha(J_\varepsilon) \subset \mathcal{W}$ be a sequence converging to some $W^* \in \overline{\text{lev}_\alpha(J_\varepsilon)} \subset \overline{\mathcal{W}} = \Delta^m$. As a result of $\inf_{W \in \mathcal{W}} J(W) =: J^* > -\infty$, the estimate

$$\alpha \geq J_\varepsilon(W^{(k)}) \geq J^* - \frac{\varepsilon}{n} \langle \log(W^{(k)}), \mathbb{1}_m \mathbb{1}_n^\top \rangle$$

shows that the log-barrier is bounded on the whole sequence, implying $W^* \in \mathcal{W}$. Since J_ε is continuous on \mathcal{W} , the estimate $\alpha \geq J_\varepsilon(W^*)$ follows, proving $\text{lev}_\alpha(J_\varepsilon)$ is closed and therefore also compact. \square

The perturbed variational model J_ε also results in a perturbed dynamical system for image labeling through the Riemannian gradient of J_ε .

Lemma 3.1.2. For $W \in \mathcal{W}$, the Euclidean and Fisher-Rao gradients of J_ε are

$$\begin{aligned} \text{grad}_E J_\varepsilon(W) &= \text{grad}_E J(W) - \varepsilon P_{\mathcal{T}_W} [\mathbb{1}_\mathcal{W}/W] \\ \text{grad}_g J_\varepsilon(W) &= \text{grad}_g J(W) + \varepsilon(W - \mathbb{1}_\mathcal{W}) \end{aligned}$$

Proof. The log-barrier function is well defined on $\mathbb{R}_{>0}^{m \times n}$ with gradient $\partial \xi(W) = -\mathbb{1}_\mathcal{W}/W$ for $W \in \mathcal{W}$. Since $\mathcal{W} \subset \mathbb{R}_{>0}^{m \times n}$, Corollary 2.3.4 gives

$$\text{grad}_E \xi(W) = -P_{\mathcal{T}_W} [\mathbb{1}_\mathcal{W}/W] \quad \text{and} \quad \text{grad}_g \xi(W) = -R_W [\mathbb{1}_\mathcal{W}/W]$$

The i -th row of $\text{grad}_g \xi(W)$ reads

$$-R_{W_i} \left[\frac{\mathbb{1}_\mathcal{S}}{W_i} \right] = - \left(W_i \frac{\mathbb{1}_\mathcal{S}}{W_i} - \left\langle W_i, \frac{\mathbb{1}_\mathcal{S}}{W_i} \right\rangle W_i \right) = (W_i - \mathbb{1}_\mathcal{S}),$$

where the last equality follows from $\langle \mathbb{1}_\mathcal{S}, \mathbb{1}_n \rangle = 1$ by the definition of the barycenter $\mathbb{1}_\mathcal{S}$ from (2.34). \square

In this chapter, the convergence properties for the *perturbed Riemannian gradient descent flow*, induced by the perturbed variational model J_ε , of the form

$$\dot{W}(t) = -\text{grad}_g J_\varepsilon(W(t)) = -\text{grad}_g J(W) + \varepsilon(\mathbb{1}_\mathcal{W} - W), \quad W(0) = W^0 \in \mathcal{W}, \quad (3.6)$$

is investigated. Compared to the unperturbed version (3.2), any integral curve $W(t)$ of this flow is now additionally slightly pushed away from the boundary and towards the barycenter $\mathbb{1}_\mathcal{W}$ of \mathcal{W} through the perturbation term. Therefore, adding the log-barrier can be interpreted as adding a "force field", preventing $W(t)$ from getting arbitrarily

close to the boundary.

Next, the behavior of critical points of J_ε for small perturbation parameter ε converging towards zero is considered. It will be shown that if a sequence of parameters ε_k decreases towards zero and the corresponding sequence of interior critical points $W^{(k)}$ of J_{ε_k} converges to an interior point $W^* \in \mathcal{W}$, then W^* is a critical point of the original objective function J . Thus, for most practical applications in image labeling, the perturbed model J_ε will be a good approximation to the original function J for sufficiently small $\varepsilon > 0$.

Proposition 3.1.3. *Let $(\varepsilon_k)_{k \in \mathbb{N}} \subset \mathbb{R}_{>0}$ be such that $\lim_{k \rightarrow \infty} \varepsilon_k = 0$. If $(W^{(k)})_{k \in \mathbb{N}} \subset \mathcal{W}$ is a sequence of critical points of J_{ε_k} , i.e. $\text{grad}_E J_{\varepsilon_k}(W^{(k)}) = 0$, converging to some interior point $W^* \in \mathcal{W}$, then W^* is a critical point of J , i.e. $\text{grad}_E J(W^*) = 0$.*

Proof. The gradient $\text{grad}_E J_\varepsilon$ evaluated at $W^{(k)}$ gives

$$0 = \text{grad}_E J_\varepsilon(W^{(k)}) = \text{grad}_E J(W^{(k)}) - \varepsilon_k \text{grad}_E \xi(W^{(k)}) \quad \forall k \in \mathbb{N}.$$

Since $W^* \in \mathcal{W}$, the expression $\text{grad}_E \xi(W^*)$ is well defined and $\|\text{grad}_E \xi(W^{(k)})\|$ is a bounded sequence converging towards $\|\text{grad}_E \xi(W^*)\|$. As a consequence of the continuity of $\text{grad}_E J$ on \mathcal{W} , it therefore follows

$$\|\text{grad}_E J(W^*)\| = \lim_{k \rightarrow \infty} \|\text{grad}_E J(W^{(k)})\| = \lim_{k \rightarrow \infty} \varepsilon_k \|\text{grad}_E \xi(W^{(k)})\| = 0. \quad \square$$

This statement also holds in the case where J is defined on an open set $U \subset \mathbb{R}^{m \times n}$ containing $\overline{W} = \Delta^m$ and local minimizers of $J: \Delta^m \rightarrow \mathbb{R}$ possibly lie on the boundary. According to [RW09, Thm. 6.12], a necessary first-order condition for a point W^* in the convex set Δ^m to be locally optimal is given by the variational inequality

$$\langle \partial J(W^*), P - W^* \rangle \geq 0 \quad \forall P \in \Delta^m. \quad (3.7)$$

Proposition 3.1.4. *Assume J is defined on some open set $U \subset \mathbb{R}^{m \times n}$ containing the closure $\overline{W} = \Delta^m$ and let $(\varepsilon_k)_{k \in \mathbb{N}} \subset \mathbb{R}_{>0}$ be a sequence with $\lim_{k \rightarrow \infty} \varepsilon_k = 0$. If $(W^{(k)})_{k \in \mathbb{N}} \subset \mathcal{W}$ is a sequence of critical points of J_{ε_k} , i.e. $\text{grad}_E J_{\varepsilon_k}(W^{(k)}) = 0$, converging to some $W^* \in \Delta^m$, then W^* is a critical point of J , i.e. the variational inequality (3.7) for W^* is fulfilled.*

Proof. Due to the fact that the log-barrier is well-defined on $\mathbb{R}_{>0}^{m \times n}$, the perturbed function $J_\varepsilon = J + \varepsilon \xi$ is defined on $U \cap \mathbb{R}_{>0}^{m \times n}$ with ordinary gradient $\partial J_\varepsilon = \partial J + \varepsilon \partial \xi$. By Corollary 2.3.4, the Euclidean Riemannian gradient of J_ε is given by $\text{grad}_E J_\varepsilon(W) = P_{\mathcal{T}_W}[\partial J_\varepsilon(W)]$. Therefore, the relation

$$0 = \text{grad}_E J_{\varepsilon_k}(W^{(k)}) = P_{\mathcal{T}_W}[\partial J(W^{(k)})] + \varepsilon_k P_{\mathcal{T}_W}[\partial \xi(W^{(k)})] \quad (3.8)$$

holds for all $k \in \mathbb{N}$. Since ξ is convex on $\mathbb{R}_{>0}^{m \times n}$, the first-order convexity condition (B.4) for an arbitrary $P \in \mathcal{W}$ gives

$$\begin{aligned} \xi(P) &\geq \xi(W^{(k)}) + \langle \partial \xi(W^{(k)}), P - W^{(k)} \rangle \\ &= \xi(W^{(k)}) + \langle P_{\mathcal{T}_W}[\partial \xi(W^{(k)})], P - W^{(k)} \rangle, \end{aligned} \quad (3.9)$$

where the last equality follows from the fact that $P - W^{(k)} \in \mathcal{T}_{\mathcal{W}}$ for all $k \in \mathbb{N}$. Combining this inequality with the above relation results in

$$\begin{aligned} \langle \partial J(W^{(k)}), P - W^{(k)} \rangle &= \langle P_{\mathcal{T}_{\mathcal{W}}}[\partial J(W^{(k)})], P - W^{(k)} \rangle \\ &\stackrel{(3.8)}{=} -\varepsilon_k \langle P_{\mathcal{T}_{\mathcal{W}}}[\partial \xi(W^{(k)})], P - W^{(k)} \rangle \\ &\stackrel{(3.9)}{\geq} \varepsilon_k \xi(W^{(k)}) - \varepsilon_k \xi(P) \geq -\varepsilon_k \xi(P) \end{aligned}$$

for $P \in \mathcal{W}$ and all $k \in \mathbb{N}$, where the last inequality holds due to $\xi(W) \geq 0$ for all W . As a consequence, taking the limit $k \rightarrow \infty$ on both sides gives

$$\langle \partial J(W^*), P - W^* \rangle \geq 0, \quad \forall P \in \mathcal{W}.$$

Because the function $P \mapsto \langle \partial J(W^*), P - W^* \rangle$ is continuous on $\mathbb{R}^{m \times n}$, the variational inequality is fulfilled on all of Δ^m . \square

A critical but non-optimal point. In the remaining part of this section, a function $J: \mathcal{W} \rightarrow \mathbb{R}$ is constructed such that the points $W^{(k)} \in \mathcal{W}$ are local minimizers of J_{ε_k} but the limit point W^* is only a critical point of J and not a local minimizer. Thus, in this sense the previous two statements are the best one can hope for the log-barrier method on the assignment manifold.

Before the example can be constructed, consider the Hessian $\text{Hess}_E \Phi$ of a C^2 function $\Phi: \mathcal{W} \rightarrow \mathbb{R}$ from (A.17), with respect to the induced Euclidean metric $E = \langle \cdot, \cdot \rangle$ on \mathcal{W} . Since (\mathcal{W}, E) is a flat, parallel transport is the identity. Since the covariant derivative of a vector field $Y: \mathcal{W} \rightarrow \mathcal{T}_{\mathcal{W}}$ can be recovered through parallel transport by (A.8), the following expression holds for every $V \in \mathcal{T}_{\mathcal{W}} = T_W \mathcal{W}$

$$\nabla_V Y(W) = \lim_{t \rightarrow 0} \frac{1}{t} (Y(W + tV) - Y(W)) = \frac{d}{dt} Y(W + tV)|_{t=0} = dY(W)[V]. \quad (3.10)$$

Therefore, the Hessian of Φ evaluated at $W \in \mathcal{W}$ in direction $V \in \mathcal{T}_{\mathcal{W}}$ is given by

$$\text{Hess}_E \Phi(W)[V] = \nabla_V^E \text{grad}_E \Phi(W) = d \text{grad}_E \Phi(W)[V]. \quad (3.11)$$

Let $\eta: \mathcal{W} \rightarrow U_{\mathcal{W}}$ be the isometric chart from Corollary 3.2.3. Since the coordinates of $\text{grad}_E \Phi(W)$ in this chart are $\partial \hat{\Phi}(\eta)$, the coordinates of $\text{Hess}_E \Phi(W)$ are given by $\text{Hess} \hat{\Phi}(\eta)$. Thus, if $\text{grad}_E \Phi(W) = 0$ and $\text{Hess}_E \Phi(W)$ is positive definite, then W is a strict local minimum of Φ .

Next, determine the unique minimizer of the log barrier ξ on \mathcal{W} . Since ξ is strictly convex on $\mathbb{R}_{>0}^{m \times n}$, so is ξ on \mathcal{W} and thus the minimizer is unique if it exists. As a consequence of Corollary 2.3.4, the gradient of ξ is given by

$$\text{grad}_E \xi(W) = P_{\mathcal{T}_{\mathcal{W}}}[\partial \xi(W)] = -P_{\mathcal{T}_{\mathcal{W}}}\left[\frac{\mathbb{1}_{\mathcal{W}}}{W}\right]$$

and therefore, according to (3.11), the Hessian has the form

$$\text{Hess}_E \xi(W)[V] = \frac{d}{dt} P_{\mathcal{T}_{\mathcal{W}}}[\partial \xi(W + tV)]|_{t=0} = P_{\mathcal{T}_{\mathcal{W}}}[\text{Hess} \xi(W)[V]] = P_{\mathcal{T}_{\mathcal{W}}}\left[\frac{V}{W \bullet 2}\right],$$

3.1. Log-Barrier Perturbation of the Variational Model

for $V \in \mathcal{T}_{\mathcal{W}}$. Note, that for all $W \in \mathcal{W}$ and $0 \neq V \in \mathcal{T}_{\mathcal{W}}$

$$\left\langle V, \text{Hess}_E \xi(W)[V] \right\rangle = \left\langle V, \frac{V}{W \bullet 2} \right\rangle = \sum_{i \in [m]} \sum_{j \in [n]} \left(\frac{V_i^j}{W_i^j} \right)^2 > 0. \quad (3.12)$$

Since $\text{grad}_E \xi(\mathbb{1}_{\mathcal{W}}) = -P_{\mathcal{T}_{\mathcal{W}}}[\mathbb{1}_m \mathbb{1}_n^\top] = 0$, it follows that $\mathbb{1}_{\mathcal{W}}$ is a local minimizer and thus the unique global minimizer of ξ on \mathcal{W} .

After these preparations, define the function

$$J(W) := \sum_{i \in m} \sum_{j \in n} (W_i^j - \frac{1}{n})^3 = \langle (W - \mathbb{1}_{\mathcal{W}}) \bullet 3, \mathbb{1}_m \mathbb{1}_n \rangle.$$

The gradient and Hessian of J at $W \in \mathcal{W}$ are given by

$$\text{grad}_E J(W) = 3P_{\mathcal{T}_{\mathcal{W}}}[(W - \mathbb{1}_{\mathcal{W}}) \bullet 2] \quad \text{Hess}_E J(W)[V] = 6(W - \mathbb{1}_{\mathcal{W}}) \bullet V$$

for all $V \in \mathcal{T}_{\mathcal{W}}$. Evaluating these expressions at $\mathbb{1}_{\mathcal{W}}$ gives $\text{grad}_E J(\mathbb{1}_{\mathcal{W}}) = 0$ and $\text{Hess}_E J(\mathbb{1}_{\mathcal{W}}) = 0$. As a consequence of this, it follows for the perturbed model J_ε

$$\begin{aligned} \text{grad}_E J_\varepsilon(\mathbb{1}_{\mathcal{W}}) &= \text{grad}_E J(\mathbb{1}_{\mathcal{W}}) + \varepsilon \text{grad}_E \xi(\mathbb{1}_{\mathcal{W}}) = 0 \\ \text{Hess}_E J_\varepsilon(\mathbb{1}_{\mathcal{W}}) &= \text{Hess}_E J(\mathbb{1}_{\mathcal{W}}) + \varepsilon \text{Hess}_E \xi(\mathbb{1}_{\mathcal{W}}) = \varepsilon \text{Hess}_E \xi(\mathbb{1}_{\mathcal{W}}). \end{aligned}$$

Since $\text{Hess}_E \xi(\mathbb{1}_{\mathcal{W}})$ is positive definite, the point $J_\varepsilon(\mathbb{1}_{\mathcal{W}})$ is a strict local minimum. However, $\mathbb{1}_{\mathcal{W}}$ is not a minimizer of J , as shown next. For this, let $r > 0$ and assume $n = |\mathcal{X}| \geq 3$ labels are given. Define

$$W_{\pm r} := \mathbb{1}_{\mathcal{W}} \pm r \mathbb{1}_m \left(e_1^\top - \frac{1}{n-1} \sum_{j=2}^n e_j^\top \right). \quad (3.13)$$

Because of $W_{\pm r} \mathbb{1}_m = \mathbb{1}_n$ and $W_{\pm r} > 0$ for $r > 0$ sufficiently small, $W_{\pm r} \in \mathcal{W}$ follows. To determine the function values of J at $W_{\pm r}$, note that $(\mathbb{1}_m e_j^\top) \bullet (\mathbb{1}_m e_i^\top) = \delta_{ij} \mathbb{1}_m e_j$ holds, where δ_{ij} is the Kronecker delta. With this,

$$\begin{aligned} J(W_{\pm r}) &= \pm r^3 \left\langle \left(\mathbb{1}_m e_1^\top - \frac{1}{n-1} \sum_{j=2}^n \mathbb{1}_m e_j^\top \right) \bullet 3, \mathbb{1}_m \mathbb{1}_n^\top \right\rangle \\ &= \pm r^3 \left\langle \mathbb{1}_m e_1^\top - \frac{1}{(n-1)^3} \sum_{j=2}^n \mathbb{1}_m e_j^\top, \mathbb{1}_m \mathbb{1}_n^\top \right\rangle = \pm r^3 m \left(1 - \frac{1}{(n-1)^2} \right). \end{aligned}$$

Since $r^3 m \left(1 - \frac{1}{(n-1)^2} \right) > 0$ and $J(\mathbb{1}_{\mathcal{W}}) = 0$, the function value of $W_{\pm r}$ are

$$J(W_{+r}) > 0 = J(\mathbb{1}_{\mathcal{W}}) > J(W_{-r}) \quad (3.14)$$

for every sufficiently small $r > 0$, showing that $J(\mathbb{1}_{\mathcal{W}})$ is not a local minimum. Thus, if $\varepsilon_k > 0$ is any sequence with $\lim_{k \rightarrow \infty} \varepsilon_k = 0$, then $W^{(k)} := \mathbb{1}_{\mathcal{W}}$ is a local minimizer of J_{ε_k} for all $k \in \mathbb{N}$, but $\lim_{k \rightarrow \infty} W^{(k)} = \mathbb{1}_{\mathcal{W}}$ is not a local minimizer of J .

Even so the presented example shows that critical limit points are not guaranteed to be optimal, this will rarely happen in practice, as the parameters of objective functions usually contain random measurement errors in reality and therefore prevent such ‘pathological’ cases.

3.2. Mathematical Preparations

3.2.1. Euclidean Isometric m -Affine Coordinates

Subsequently, an alternative pair of m - and e -affine coordinates is introduced, such that the m -affine coordinates are an Euclidean isometry between $\mathcal{S} \subset \mathbb{R}^n$ and an open set $U \subset \mathbb{R}^{n-1}$ equipped with their corresponding induced Euclidean metric. This m -affine chart naturally extends to the product manifold \mathcal{W} and provides a convenient way of proving some of the results in this and subsequent chapters. These coordinates are then also used to characterize convex functions on the assignment manifold \mathcal{W} independent of any specific m -affine coordinate chart.

Construction of the m - and e -Affine Coordinates

For the construction of the Euclidean isometric m -affine coordinates, consider the linear map $G: \mathbb{R}^n \rightarrow \mathbb{R}$ defined by $G(x) := \langle \mathbf{1}_n, x \rangle$. It follows from linear algebra that the set

$$A := G^{-1}(1) = \{x \in \mathbb{R}^n \mid \langle x, \mathbf{1}_n \rangle = 1\}$$

is an affine subspace of \mathbb{R}^n . Due to the definition of \mathcal{S} in (2.9) and the structure of the resulting tangent space $T_{\mathcal{S}}$ in (2.10), the identities $\mathcal{S} = A \cap \mathbb{R}_{\geq 0}^n$ and $\ker(G) = T_{\mathcal{S}}$ follow. Also note that the orthogonal projection $P_{T_{\mathcal{S}}} = I_n - \mathbf{1}_{\mathcal{S}}\mathbf{1}_n^{\top}$ from (2.35) has kernel $\ker(P_{T_{\mathcal{S}}}) = \mathbb{R}\mathbf{1}_n$, where $\mathbf{1}_{\mathcal{S}}$ is the barycenter of \mathcal{S} from (2.34). Thus, the affine space A can be represented by

$$A = \ker(G) + \mathbf{1}_{\mathcal{S}} = T_{\mathcal{S}} + \mathbf{1}_{\mathcal{S}},$$

Choose an orthonormal basis of $T_{\mathcal{S}}$

$$\mathcal{B}_{T_{\mathcal{S}}} = \{b_1, \dots, b_{n-1}\} \subset T_{\mathcal{S}} \subset \mathbb{R}^n \quad (3.15)$$

and define the matrix with i -th column given by the basis vector b_i as

$$B := (b_1 \mid \dots \mid b_{n-1}) \in \mathbb{R}^{n \times (n-1)}. \quad (3.16)$$

Since $\mathcal{B}_{T_{\mathcal{S}}}$ is an orthonormal basis, the relations

$$B^{\top}B = I_{n-1} \quad \text{and} \quad BB^{\top} = P_{T_{\mathcal{S}}} \quad (3.17)$$

follow, where I_{n-1} denotes the identity matrix. Therefore, a global affine chart of the affine manifold $A = T_{\mathcal{S}} + \mathbf{1}_{\mathcal{S}}$ together with its inverse is given by

$$F: A \mapsto \mathbb{R}^{n-1}, \quad x \mapsto B^{\top}(x - \mathbf{1}_{\mathcal{S}}) \quad \text{and} \quad F^{-1}: \mathbb{R}^{n-1} \rightarrow A, \quad y \mapsto By + \mathbf{1}_{\mathcal{S}}. \quad (3.18)$$

Lemma 3.2.1. *The chart $F: A \rightarrow \mathbb{R}^{n-1}$ from (3.18) is an isometry, where $A \subset \mathbb{R}^n$ and \mathbb{R}^{n-1} are viewed as Riemannian manifolds with the standard inner product $\langle \cdot, \cdot \rangle$.*

Proof. The tangent space of A is constant and given by $T_x A = T_{\mathcal{S}}$ for every $x \in A$. The differential of F at $x \in A$ has the form

$$dF(x): T_{\mathcal{S}} \rightarrow \mathbb{R}^{n-1}, \quad u \mapsto dF(x)[u] = B^{\top} u. \quad (3.19)$$

Now, let $u \in T_{\mathcal{S}}$. With respect to $\mathcal{B}_{T_{\mathcal{S}}}$, u has the coordinates $u = \hat{u}^i b_i = B\hat{u}$ with $B^{\top} u = \hat{u}$. For $x \in A$ and $u, v \in T_{\mathcal{S}}$, it therefore follows

$$\langle u, v \rangle = \langle B\hat{u}, B\hat{v} \rangle \stackrel{(3.17)}{=} \langle \hat{u}, \hat{v} \rangle = \langle B^{\top} u, B^{\top} v \rangle \stackrel{(3.19)}{=} \langle dF(x)[u], dF(x)[v] \rangle. \quad \square$$

Since $\mathcal{S} = A \cap \mathbb{R}_{>0}^n$, the chart F from (3.18) also defines a chart for \mathcal{S} into the open set $U := F(\mathcal{S}) \subset \mathbb{R}^{n-1}$, by

$$\eta := F|_{\mathcal{S}}: \mathcal{S} \rightarrow U, \quad p \mapsto B^{\top}(p - \mathbb{1}_{\mathcal{S}}) \quad (3.20a)$$

$$\eta^{-1} := (F^{-1}|_U): U \rightarrow \mathcal{S}, \quad \eta \mapsto B\eta + \mathbb{1}_{\mathcal{S}}. \quad (3.20b)$$

Proposition 3.2.2. *If $\mathcal{S} \subset \mathbb{R}^n$ is viewed as a Riemannian submanifold with the induced Euclidean metric $E = \langle \cdot, \cdot \rangle$, then the chart $\eta: \mathcal{S} \rightarrow U$ from (3.20) is an isometry between (\mathcal{S}, E) and $(U, \langle \cdot, \cdot \rangle)$. Furthermore, η is an m -affine coordinate system for $(\mathcal{S}, g, \nabla^{(e)}, \nabla^{(m)})$, with the negative entropy as associated convex function*

$$\varphi(\eta) = \langle B\eta + \mathbb{1}_{\mathcal{S}}, \log(B\eta + \mathbb{1}_{\mathcal{S}}) \rangle = -H(p), \quad (3.21)$$

for $\eta = \eta(p)$, $p \in \mathcal{S}$. The corresponding dual e -affine coordinates are given by

$$\theta: \mathcal{S} \rightarrow \mathbb{R}^{n-1}, \quad p \mapsto B^{\top} \log(p) \quad \text{and} \quad \theta^{-1}: \mathbb{R}^{n-1} \rightarrow T_{\mathcal{S}}, \quad \theta \mapsto p(\theta) = \frac{e^{B\theta}}{\langle \mathbb{1}_n, e^{B\theta} \rangle} \quad (3.22)$$

with corresponding conjugate convex function

$$\psi(\theta) = \log(\langle \mathbb{1}_{n-1}, e^{B\theta} \rangle), \quad (3.23)$$

where B is the matrix from (3.16).

Remark 3.2.1. The formulas in (3.22) and (3.23) suggest to think of $T_{\mathcal{S}}$ as an abstract basis independent e -affine coordinate system with coordinate chart

$$\begin{aligned} \mathcal{S} \ni p &\mapsto v(p) = P_{T_{\mathcal{S}}} \log(p) = \exp_{\mathbb{1}_{\mathcal{S}}}^{-1}(p) \in T_{\mathcal{S}} \\ T_{\mathcal{S}} \ni v &\mapsto p(v) = \frac{e^v}{\langle \mathbb{1}_n, e^v \rangle} = \exp_{\mathbb{1}_{\mathcal{S}}}(v) \in \mathcal{S}, \end{aligned}$$

as well as convex function $\psi: T_{\mathcal{S}} \rightarrow \mathbb{R}$ and conjugate convex function $\varphi: \mathcal{S} \rightarrow \mathbb{R}$ given by

$$\psi(v) = \log(\langle \mathbb{1}_n, e^v \rangle) = \text{logexp}(v) \quad \text{and} \quad \psi^*(p) = \varphi(p) = -H(p),$$

where the function logexp above is the well-known *log-exponential function* (see e.g. [RW09]). Thus, (\mathcal{S}, E) as a flat Riemannian submanifold of the affine space A , may be viewed as an abstract basis independent m -affine coordinate system.

Proof. Due to $\eta = F|_{\mathcal{S}}$, the isometry property directly follows from Lemma 3.2.1. To show that η is m -affine, consider the m -affine coordinate system $\bar{\eta}$ from (2.13) and the coordinate change $\alpha := \bar{\eta}\eta^{-1}: \mathbb{R}^{n-1} \rightarrow \mathbb{R}^{n-1}$. The chart $\bar{\eta}$ can be expressed by the linear map

$$\bar{\eta}(p) = Mp, \quad \text{with the matrix } M := (I_{n-1}, 0_{n-1}) \in \mathbb{R}^{(n-1) \times n},$$

where I_{n-1} denotes the identity matrix and $0_{n-1} \in \mathbb{R}^{n-1}$ the zero vector. Since the inverse of η is given as an affine map $p(\eta) = B\eta + \mathbb{1}_{\mathcal{S}}$ by (3.18), the coordinate change α is again an affine map

$$\alpha(\eta) = \bar{\eta}(p(\eta)) = C\eta + c, \quad \text{with } C := MB \quad \text{and} \quad c := M\mathbb{1}_{\mathcal{S}}.$$

Because α is a diffeomorphism, the differential $d\alpha(\eta) = C$ is invertible, i.e. $C \in \text{GL}_n(\mathbb{R})$. As a result of the characterization (A.11) in the Appendix A.3.3, η is also an m -affine coordinate chart. The formula in (3.21) for the corresponding convex function is just the coordinate expression $\varphi(\eta) = -\hat{H}(\eta) = -H(p(\eta))$ of the negative entropy on \mathcal{S} in η coordinates.

To obtain the conjugate convex function and e -coordinates, consider the optimization problem $\psi(\theta) = \max_{\eta} \{\langle \theta, \eta \rangle - \varphi(\eta)\}$ with optimality condition

$$\theta = \partial\varphi(\eta) = B^{\top} \log(B\eta + \mathbb{1}_{\mathcal{S}}), \quad (3.24)$$

where the formula for the gradient follows from the fact that $B^{\top}\mathbb{1}_{\mathcal{S}} = 0$ as a result of $\mathbb{1}_{\mathcal{S}}$ being orthogonal to all basis vectors b_1, \dots, b_{n-1} from (3.15). With $p = p(\eta) = B\eta + \mathbb{1}_{\mathcal{S}}$, the desired expression $\theta(p) = B^{\top} \log(p)$ in (3.22) directly follows. Multiplying (3.24) by B yields

$$B\theta = BB^{\top} \log(p) \stackrel{(3.17)}{=} P_{T_{\mathcal{S}}} \log(p) \stackrel{(2.35)}{=} \log(p) - \frac{\langle \log(p), \mathbb{1}_n \rangle}{n} \mathbb{1}_n.$$

Because $e^{\beta\mathbb{1}_n} = e^{\beta}\mathbb{1}_n$, for every $\beta \in \mathbb{R}$, setting $\beta := -\langle \log(p), \mathbb{1}_n \rangle \frac{1}{n} \in \mathbb{R}$ gives

$$e^{B\theta} = e^{\log(p) + \beta\mathbb{1}_n} = pe^{\beta}.$$

As a consequence of $e^{\beta} \in \mathbb{R}$ together with the constraint $1 = \langle \mathbb{1}_n, p \rangle$, the identity $e^{\beta} = \langle \mathbb{1}_n, e^{B\theta} \rangle$ follows, resulting in the expression $p(\theta)$ for the inverse θ^{-1} on the right-hand side of (3.22).

For proving (3.23), let $\theta \in \mathbb{R}^{n-1}$. Taking the logarithm of the expression for $p(\theta)$ on the right-hand side of (3.22) yields

$$\log(p(\theta)) = B\theta - (\log \langle \mathbb{1}_n, e^{B\theta} \rangle) \mathbb{1}_n. \quad (3.25)$$

The η coordinates of $p(\theta)$ are $\eta(\theta) = B^{\top}(p(\theta) - \mathbb{1}_{\mathcal{S}}) = B^{\top}p(\theta)$, where the last equality again follows from $B^{\top}\mathbb{1}_{\mathcal{S}} = 0$. Since

$$\langle \theta, \eta(\theta) \rangle = \langle \theta, B^{\top}p(\theta) \rangle = \langle B\theta, p(\theta) \rangle \stackrel{(3.25)}{=} -H(p(\theta)) + \log \langle \mathbb{1}_n, e^{B\theta} \rangle, \quad (3.26)$$

the conjugate convex function $\psi(\theta) = \varphi^*(\theta)$ is given by

$$\psi(\theta) = \langle \theta, \eta(\theta) \rangle - \varphi(\eta(\theta)) \stackrel{(3.21)}{=} \langle \theta, \eta(\theta) \rangle + H(p(\theta)) \stackrel{(3.26)}{=} \log \langle \mathbb{1}_n, e^{B\theta} \rangle. \quad \square$$

As a direct consequence of the product structure of \mathcal{W} and Proposition 3.2.2, also the corresponding product m -coordinate chart $\eta: \mathcal{W} \rightarrow U_{\mathcal{W}} := \prod_{i \in [m]} U \subset \mathbb{R}^{m \times (n-1)}$ from (2.29) is an isometry with respect to the standard Euclidean inner product.

Corollary 3.2.3. *If $\mathcal{W} \subset \mathbb{R}^{m \times n}$ is viewed as Riemannian submanifold with the induced Euclidean metric $E = \langle \cdot, \cdot \rangle$, then the m -affine chart $\eta: \mathcal{W} \rightarrow U_{\mathcal{W}}$ from (2.29) is an isometry between (\mathcal{W}, E) and $(U_{\mathcal{W}}, \langle \cdot, \cdot \rangle)$.*

Characterization of Convexity on the Assignment Manifold

The characterization of convexity and strong convexity through Bregman divergences in Section B.3 is only valid for functions defined on a convex set with nonempty interior. However, the convex set $\mathcal{W} \subset \mathbb{R}^{m \times n}$ has no nonempty interior and therefore, the above mentioned criterion via Bregman divergences only holds in an m -affine chart. In the following, a coordinate independent way for characterizing convex and strongly convex functions on \mathcal{W} is given. For this, let E be the induced Euclidean metric of $\mathcal{W} \subset \mathbb{R}^{m \times n}$ and suppose $\Phi: \mathcal{W} \rightarrow \mathbb{R}$ is a C^1 function. Define $D_{\Phi}: \mathcal{W} \times \mathcal{W} \rightarrow \mathbb{R}$ by

$$D_{\Phi}(P, W) := \Phi(P) - \Phi(W) - \langle \text{grad}_E \Phi(W), P - W \rangle, \quad \forall P, W \in \mathcal{W}. \quad (3.27)$$

This function is linear in Φ , i.e. if $\alpha, \beta \in \mathbb{R}$ and $\Psi, \Phi \in C^1(\mathcal{W})$, then

$$D_{\alpha\Phi + \beta\Psi} = \alpha D_{\Phi} + \beta D_{\Psi}.$$

As the next Lemma shows, using this coordinate independent Bregman divergence on \mathcal{W} , convexity and strong convexity can be characterized in the same way as in Section B.3.

Lemma 3.2.4. *Let $\eta: \mathcal{W} \rightarrow U_{\mathcal{W}}$ be the isometric chart from Corollary 3.2.3 with respect to the Euclidean metric E on \mathcal{W} . If a subset $K \subset \mathcal{W}$ is convex, then also $\hat{K} := \eta(K)$ is convex and a function $\Phi: K \rightarrow \mathbb{R}$ is convex if and only if the coordinate function $\hat{\Phi}: \hat{K} \rightarrow \mathbb{R}$ is convex. If $\Phi: K \rightarrow \mathbb{R}$ is additionally C^1 , then*

$$D_{\Phi}(P, W) = D_{\hat{\Phi}}(\eta(P), \eta(W)) \quad (3.28)$$

for all $P, W \in K$ and the following characterizations hold:

$$\Phi \text{ is convex on } K \Leftrightarrow \forall P, W \in K, \quad D_{\Phi}(P, W) \geq 0 \quad (3.29)$$

$$\Phi \text{ is } \sigma\text{-strongly convex on } K \Leftrightarrow \forall P, W \in K, \quad D_{\Phi}(P, W) \geq \frac{\sigma}{2} \|P - W\|^2. \quad (3.30)$$

Proof. It is first shown that for all $r \in [0, 1]$ and $P, W \in \mathcal{W}$ the equality

$$\eta(rP + (1-r)W) = r\eta(P) + (1-r)\eta(W) \quad (3.31)$$

holds. Since η is a product chart $\eta = (\eta_i)_{i \in \mathcal{V}}$ by (2.29), it suffices to show (3.31) for each component $\eta_i: \mathcal{S} \rightarrow U$ from (3.20), with $i \in \mathcal{V}$. Let $P_i, W_i \in \mathcal{S}$ and $r \in [0, 1]$. Due to $\eta_i(p) = B^{\top}(p - \mathbb{1}_{\mathcal{S}})$ for $p \in \mathcal{S}$, it immediately follows

$$\eta_i(rP_i + (1-r)W_i) = rB^{\top}(P_i - \mathbb{1}_{\mathcal{S}}) + (1-r)B^{\top}(W_i - \mathbb{1}_{\mathcal{S}}) = r\eta_i(P_i) + (1-r)\eta_i(W_i),$$

establishing (3.31) on \mathcal{W} . Due to η being a bijection, equality (3.31) directly implies that convexity of $K \subset \mathcal{W}$ is equivalent to the convexity of $\hat{K} \subset U_{\mathcal{W}}$ and that $\Phi: K \rightarrow \mathbb{R}$ is convex if and only if $\hat{\Phi}: \hat{K} \rightarrow \mathbb{R}$ is convex.

Next, the equality (3.28) is proven. For this, suppose Φ is C^1 . In the following, the notation $\text{grad}_{E,i} \Phi(W)$ and $\partial_i \hat{\Phi}(\eta)$ from Remark 2.3.5 is used to denote the i -th row of the gradients, representing the change with respect to W_i and η_i respectively. Because $\eta: (\mathcal{W}, E) \rightarrow (U_{\mathcal{W}}, \langle \cdot, \cdot \rangle)$ is an isometry, Lemma A.4.1 gives

$$\partial \hat{\Phi}(W) = d\eta(W)[\text{grad}_E \Phi(W)].$$

As a result of the expression $\eta_i(p) = B^\top(p - \mathbb{1}_{\mathcal{S}})$ for $p \in \mathcal{S}$ on each component $i \in \mathcal{V}$ by (3.20), the i -th row of the gradients are related by

$$\partial_i \hat{\Phi}(\eta(W)) = d\eta_i(W)[\text{grad}_{E,i} \Phi(W)] = B^\top \text{grad}_{E,i} \Phi(W). \quad (3.32)$$

Define $\eta_P := \eta(P)$ and $\eta_W := \eta(W)$ as well as $\eta_{P_i} := \eta_i(P_i)$ and $\eta_{W_i} := \eta_i(W_i)$ for the components, with $i \in \mathcal{V}$. According to (3.20), the inverse of $\eta_i(P_i)$ has the form $P_i(\eta_i) = B\eta_i + \mathbb{1}_{\mathcal{S}}$, implying

$$P_i - W_i = B(\eta_{P_i} - \eta_{W_i}). \quad (3.33)$$

Combining these equations shows the following relation for all components $i \in \mathcal{V}$

$$\langle \text{grad}_{E,i} \Phi(W), P_i - W_i \rangle \stackrel{(3.33)}{=} \langle B^\top \text{grad}_{E,i} \Phi(W), \eta_{P_i} - \eta_{W_i} \rangle \stackrel{(3.32)}{=} \langle \partial_i \hat{\Phi}(\eta_W), \eta_{P_i} - \eta_{W_i} \rangle,$$

resulting in the desired equality

$$\begin{aligned} D_\Phi(P, W) &= \Phi(P) - \Phi(W) - \langle \text{grad}_E \Phi(W), P - W \rangle \\ &= \hat{\Phi}(\eta_P) - \hat{\Phi}(\eta_W) - \langle \partial \hat{\Phi}(\eta_W), \eta_P - \eta_W \rangle = D_{\hat{\Phi}}(\eta_P, \eta_W). \end{aligned}$$

To show (3.29), assume Φ is convex on K . By the first part, this is true if and only if $\hat{\Phi}$ is convex on \hat{K} , which in turn is equivalent to $D_\Phi(P, W) = D_{\hat{\Phi}}(\eta_P, \eta_W) \geq 0$ for all $P, W \in K$ by (B.9).

For proving (3.30), suppose Φ is σ -strongly convex. Since η is a Euclidean isometry, it follows $\|P - W\| = \|\eta_P - \eta_W\|$ and therefore by definition, Φ is σ -strongly convex if and only if $\hat{\Phi}$ is σ -strongly convex, which in turn is equivalent to

$$D_\Phi(P, W) = D_{\hat{\Phi}}(\eta_P, \eta_W) \geq \frac{\sigma}{2} \|\eta_P - \eta_W\| = \frac{\sigma}{2} \|P - W\|^2, \quad (3.34)$$

by (B.10). □

Lemma 3.2.5. *The negative global entropy $-H_{\mathcal{W}}$ from (2.30) is n^{-1} -strongly convex.*

Proof. Due to Proposition B.2.1, the negative entropy $-H$ is 1-strongly convex on $\mathcal{S} = \text{rint}(\Delta)$ with respect to $\|\cdot\|_1$ and therefore

$$D_{-H}(p, q) = \text{KL}(p, q) \geq \frac{1}{2} \|p - q\|_1^2 \quad \forall p, q \in \mathcal{S} \quad (3.35)$$

by (B.10). As a consequence of the norm estimate $\|x\|_1^2 \geq n^{-1}\|x\|^2$ for $x \in \mathbb{R}^n$ together with the identity $\text{KL}(P, W) = D_{-H_{\mathcal{W}}}(P, W)$ and the corresponding factorization from (2.31), it follows

$$D_{-H_{\mathcal{W}}}(P, W) \stackrel{(2.31)}{=} \sum_{i \in \mathcal{V}} \text{KL}(P_i, W_i) \stackrel{(3.35)}{\geq} \frac{1}{2} \sum_{i \in \mathcal{V}} \|P_i - W_i\|_1^2 \geq \frac{n^{-1}}{2} \|P - W\|^2$$

for all $P, W \in \mathcal{W}$. As a result of Lemma 3.2.4, the negative entropy $-H_{\mathcal{W}}$ is indeed n^{-1} -strongly convex on \mathcal{W} . \square

3.2.2. Analytic Functions and the Łojasiewicz Inequality

Recall (e.g. from [KP02]) that a *real analytic manifold* M is a smooth manifold whose coordinate transitions are real analytic. A function $\Phi: M \rightarrow \mathbb{R}$ on an analytic manifold M is *real analytic* if for each coordinate chart φ on M , the coordinate representation $\hat{\Phi} = \Phi \circ \varphi^{-1}$ is real analytic. Therefore, viewing \mathcal{W} as an affine manifold by the m -affine charts, it is also a real analytic manifold and a smooth function $\Phi: \mathcal{W} \rightarrow \mathbb{R}$ is analytic if and only if it is analytic in any m -affine chart.

The fundamental property for proving convergence of analytic gradient flows in \mathbb{R}^n is the Łojasiewicz inequality.

Lemma 3.2.6. [*Łojasiewicz inequality*] *Let $U \subset \mathbb{R}^d$ be an open set, $\phi: U \rightarrow \mathbb{R}$ a real analytic function and $z \in U$. Then there exist a neighborhood $U_L \subset U$ of z and constants $c > 0$, $\mu \in [0, 1)$ such that*

$$\|\nabla\phi(x)\| \geq c|\phi(x) - \phi(z)|^\mu \quad \text{for all } x \in U_L, \quad (3.36)$$

where the convention $0^0 = 0$ is adopted in the case $\mu = 0$. The exponent μ is also called the *Łojasiewicz exponent*.

Proof. See [IL65] or [BM88]. \square

There are generalizations of the Łojasiewicz inequality to analytic Riemannian manifolds [Lag07] as well as to the large class of subanalytic functions [BDL07], used to prove convergence for subgradient differential inclusions. For ease of exposition, the Łojasiewicz inequality is directly shown to hold on \mathcal{W} via the above introduced m -affine isometric coordinates.

Corollary 3.2.7. [*Łojasiewicz inequality on \mathcal{W}*] *Let $\Phi: \mathcal{W} \rightarrow \mathbb{R}$ be analytic and $Z \in \mathcal{W}$. Let $E = \langle \cdot, \cdot \rangle$ be the induced Euclidean metric on $\mathcal{W} \subset \mathbb{R}^{m \times n}$. Then there exists a neighborhood $U_L \subset \mathcal{W}$ of Z and constants $C > 0$, $\mu \in [0, 1)$ such that*

$$\|\text{grad}_E \Phi(W)\| \geq C|\Phi(W) - \Phi(Z)|^\mu \quad \text{for all } W \in U_L, \quad (3.37)$$

with the convention $0^0 = 0$ in the case $\mu = 0$.

Proof. Let $\eta: \mathcal{W} \rightarrow U_{\mathcal{W}}$ be the m -affine isometric chart from Corollary 3.2.3, where $\mathcal{W} \subset \mathbb{R}^{m \times n}$ is equipped with metric E . By assumption, $\hat{\Phi} = \Phi \circ \eta^{-1}: U_{\mathcal{W}} \rightarrow \mathbb{R}$ is analytic. Define $\eta_Z := \eta(Z) \in U_{\mathcal{W}}$. By Lemma 3.2.6, there exists a neighborhood $\bar{U}_L \subset U_{\mathcal{W}}$ of η_Z , on which the Lojasiewicz inequality (3.36) holds with exponent $\mu \in [0, 1)$ and constant $C > 0$. Set $U_L := \eta^{-1}(\bar{U}_L)$. Since $\|\partial \hat{\Phi}(\eta(W))\| = \|\text{grad}_E \Phi(W)\|$, as a consequence of Lemma A.4.1 and the fact that η is an isometry, the inequality

$$C|\Phi(W) - \Phi(Z)|^\mu = C|\hat{\Phi}(\eta(W)) - \hat{\Phi}(\eta_Z)|^\mu \leq \|\partial \hat{\Phi}(\eta(W))\| = \|\text{grad}_E \Phi(W)\|$$

holds for all $W \in U_L$, proving the statement. \square

3.3. Perturbed Riemannian Gradient Descent Flows for Optimization

In the following, convergence properties of the perturbed Riemannian gradient flow (3.6) are investigated. After proving some basic relations between $\|\cdot\|$ and $\|\cdot\|_g$ in Section 3.3.1, general properties of the Riemannian gradient descent flow for J_ε are shown in Section 3.3.2. As the counterexamples from [PDM12] and [AMA05] in the Euclidean case demonstrate, integral curves of gradient flows do not necessarily converge to a single point. However, for gradient flows of analytic functions in \mathbb{R}^d , it can be shown that bounded integral curves indeed converge [AMA05]. Even stability results [AK06] and convergence rates are available [BDL07] in this case. Proving the corresponding statements on the assignment manifold will be done in Section 3.3.3.

3.3.1. Basic Estimates

In order to proof the convergence results in the remaining part of this section, some basic relations between $\|\cdot\|$ and $\|\cdot\|_g$ are needed. Establishing these relations will be done in the following. First, the situation on one factor \mathcal{S} of \mathcal{W} is considered.

Lemma 3.3.1. *For all $p \in \mathcal{S}$ and $u, v \in T_{\mathcal{S}}$, the identity*

$$g_p(v, R_p u) = \langle v, u \rangle \tag{3.38}$$

and the inequality

$$\|R_p u\| \leq \|R_p u\|_{g,p} \leq \|u\| \tag{3.39}$$

hold. Furthermore, for every compact subset $K \subset \mathcal{S}$, there exist constants $C_K, C'_K > 0$ such that

$$C_K \|u\| \leq \|R_p u\|_{g,p} \leq C'_K \|R_p u\| \quad \forall p \in K \text{ and } \forall u \in T_{\mathcal{S}}. \tag{3.40}$$

Proof. The identity in (3.38) is a consequence of

$$g_p(v, R_p u) \stackrel{(2.15)}{=} \left\langle v, \text{Diag} \left(\frac{1}{p} \right) R_p u \right\rangle = \left\langle v, P_{T_{\mathcal{S}}} \text{Diag} \left(\frac{1}{p} \right) R_p u \right\rangle \stackrel{(2.36)}{=} \langle v, u \rangle.$$

3.3. Perturbed Riemannian Gradient Descent Flows for Optimization

The inequality on the right-hand side of (3.39) follows from

$$\|R_p u\|_{g,p}^2 \stackrel{(3.38)}{=} \langle u, R_p u \rangle \leq \|u\|^2,$$

where the last estimate results from all eigenvalues of R_p being upper bounded by $1/2$ according to Lemma 2.3.1 (3). Define $R_p u =: v_p = v_p^i e_i$. Since the components of $p = p^i e_i \in \mathcal{S}$ are contained in the interval $0 < p^i < 1$, the inequality on the left-hand side of (3.39) is a result of

$$\|v_p\|_{g,p}^2 \stackrel{(2.15)}{=} (v_p^i)^2 \frac{1}{p^i} \geq \|v_p\|^2.$$

To show (3.40), let $K \subset \mathcal{S}$ be compact. The minimal eigenvalue $\lambda_{\min}(R_p|_{T_{\mathcal{S}}})$ of $R_p|_{T_{\mathcal{S}}}$ continuously depends on $p \in \mathcal{S}$ and is positive by Lemma 2.3.1 (3). Thus, a minimal positive eigenvalue $C_k^2 := \min_{p \in K} \{\lambda_{\min}(R_p|_{T_{\mathcal{S}}})\} > 0$ exists on K , implying

$$\|R_p\|_{g,u}^2 \stackrel{(3.38)}{=} \langle u, R_p u \rangle \geq \lambda_{\min}(R_p|_{T_{\mathcal{S}}}) \|u\|^2 \geq C_k^2 \|u\|^2,$$

for all $u \in T_{\mathcal{S}}$ and $p \in K$. Similarly, the function $\alpha(p) := \max_{i \in [n]} \{(p^i)^{-1}\}$ continuously depends on $p = p^i e_i \in \mathcal{S}$ and obtains a maximal value $(C'_K)^2 := \max_{p \in K} \{\alpha(p)\} > 0$ on the compact set K . As a consequence, using $R_p u = v_p = v_p^i e_i$ from above yields

$$\|v_p\|_{g,p}^2 \stackrel{(2.15)}{=} (v_p^i)^2 \frac{1}{p^i} \leq \alpha(p) \|v_p\|^2 \leq (C'_K)^2 \|v_p\|^2$$

for all $u \in T_{\mathcal{S}}$ and $p \in K$. □

Because the Fisher-Rao metric g on \mathcal{W} is a product metric, the equality (3.38) and inequality (3.39) directly carry over to \mathcal{W} , i.e. if $W \in \mathcal{W}$ and $U, V \in \mathcal{T}_{\mathcal{W}}$, then

$$g_W(V, R_W[U]) = \langle V, U \rangle, \tag{3.41}$$

$$\|R_W[U]\| \leq \|R_W[U]\|_{g,W} \leq \|U\| \tag{3.42}$$

hold. For transferring the third inequality (3.40) to \mathcal{W} , suppose $K \subset \mathcal{W}$ is a compact subset. Since the canonical projection onto the i -th factor $\pi_i: \mathcal{W} \rightarrow \mathcal{S}$, defined by $\pi_i(W) = W_i$, is continuous, also $K_i := \pi_i(K) \subset \mathcal{S}$ is compact. Let $C_{K_i}, C'_{K_i} > 0$ be the constants fulfilling (3.40) on $K_i \subset \mathcal{S}$ on the i -th factor of \mathcal{W} . Then, the constants $C_K := \min_{i \in \mathcal{V}} \{C_{K_i}\} > 0$ and $C'_K := \max_{i \in \mathcal{V}} \{C'_{K_i}\} > 0$ satisfy the inequality

$$C_k \|U\| \leq \|R_W[U]\|_{g,W} \leq C'_K \|R_W[U]\| \quad \forall W \in K \text{ and } \forall U \in \mathcal{T}_{\mathcal{W}}. \tag{3.43}$$

As a direct consequence of the relation between the Riemannian gradient and Euclidean gradient through the replicator operator in Corollary 2.3.4, the above inequalities on \mathcal{W} yield the following statement.

Corollary 3.3.2. *Let $J: \mathcal{W} \rightarrow \mathbb{R}$ be C^1 . Then, for all $W \in \mathcal{W}$, the Riemannian gradient $\text{grad}_g J(W)$ of the Fisher-Rao metric g and the Riemannian gradient $\text{grad}_E J(W)$ of the Euclidean metric $E = \langle \cdot, \cdot \rangle$ on \mathcal{W} fulfill*

$$g_W(V, \text{grad}_g J(W)) = \langle V, \text{grad}_E J(W) \rangle = \langle V, \partial J(W) \rangle, \quad (3.44)$$

where the last equality holds if J is defined on an open set $U \subset \mathbb{R}^{m \times n}$ containing \mathcal{W} , and the inequality

$$\|\text{grad}_g J(W)\| \leq \|\text{grad}_g J(W)\|_{g,W} \leq \|\text{grad}_E J(W)\| \quad (3.45)$$

is satisfied. Furthermore, for any compact set $K \subset \mathcal{W}$, there are constants $C_K, C'_K > 0$ such that

$$C_K \|\text{grad}_E J(W)\| \leq \|\text{grad}_g J(W)\|_{g,W} \leq C'_K \|\text{grad}_g J(W)\| \quad \forall W \in K. \quad (3.46)$$

3.3.2. General Properties of Perturbed Riemannian Gradient Flows

Following the Riemannian gradient flow for minimizing J_ε on the assignment manifold is related to general optimization approaches on Riemannian manifolds, see [ABB04] and references therein. In [ABB04] the optimization framework is developed for Riemannian metrics induced by Legendre functions on convex subsets of \mathbb{R}^d . However, most approaches rely on the objective function also to be defined outside the manifold, so as to be well behaved on the boundary. In contrast, in the present setting J is only assumed to be defined on \mathcal{W} and lower bounded.

First, it is shown that integral curves of the perturbed Riemannian gradient flow (3.6) are well defined in the sense that they exist for all future time.

Proposition 3.3.3. *For every initial condition $W(0) \in \mathcal{W}$, there exists a unique solution $W(t)$ of the perturbed Riemannian gradient descent flow (3.6) for all $t \geq 0$. The function values $J_\varepsilon(W(t))$ are monotonically decreasing and converge towards*

$$\lim_{t \rightarrow +\infty} J_\varepsilon(W(t)) = \inf_{t \geq 0} \{J_\varepsilon(W(t))\} > -\infty. \quad (3.47)$$

For $\alpha \in \mathbb{R}$, the compact level sets $\text{lev}_\alpha(J_\varepsilon)$ are positively invariant, i.e. $W(0) \in \text{lev}_\alpha(J_\varepsilon)$ implies $W(t) \in \text{lev}_\alpha(J_\varepsilon)$ for all $t \geq 0$.

Proof. Let $\alpha \in \mathbb{R}$ and assume $W(0) \in \text{lev}_\alpha(J_\varepsilon)$. By the fundamental theorem on flows A.2.1, there exists a unique maximal solution $W: I \rightarrow \mathcal{W}$ of (3.6), where $I \subset \mathbb{R}$ is an open interval containing 0. Define $T_M := \sup I \in (0, +\infty]$. Because of (3.3), the value $J_\varepsilon(W(t))$ is monotonically decreasing in t , implying $\alpha \geq J_\varepsilon(W(0)) \geq J_\varepsilon(W(t))$ and therefore $W(t) \in \text{lev}_\alpha(J_\varepsilon)$ for all $t \in [0, T_M)$. Due to the compactness of $\text{lev}_\alpha(J_\varepsilon)$ by Lemma 3.1.1, the Escape Lemma A.2.2 implies that $T_M = +\infty$, showing that $\text{lev}_\alpha(J_\varepsilon)$ is positively invariant. The convergence of the function values $J_\varepsilon(W(t))$ to the infimum in (3.47) also follows from the monotonicity (3.3) by a standard argument. Since every point $W(0) \in \mathcal{W}$ is always contained in the level set $\text{lev}_{\alpha_0}(J_\varepsilon)$ with $\alpha_0 := J_\varepsilon(W(0))$, the statement for an arbitrary point on \mathcal{W} follows. \square

3.3. Perturbed Riemannian Gradient Descent Flows for Optimization

As one would expected, the Riemannian gradient of J_ε converges towards zero for $t \rightarrow \infty$. The proof follows the one in [Jos17, Lemma 8.4.4], however, with different assumptions. The argument makes use of Barbalat's lemma, stated next.

Lemma 3.3.4 (Barbalat's lemma). *Suppose $\varphi: [0, \infty) \rightarrow [0, \infty)$ is uniformly continuous, i.e. for every $\varepsilon > 0$ there exists a $\delta > 0$ such that $|t_1 - t_2| < \delta$ for $t_1, t_2 \in [0, \infty)$ implies $|\varphi(t_1) - \varphi(t_2)| < \varepsilon$. If $\int_0^\infty \varphi(t) dt < \infty$, then $\lim_{t \rightarrow \infty} \varphi(t) = 0$.*

Proof. See e.g. [Kha02] □

Remark 3.3.1. If $\varphi: [0, \infty) \rightarrow [0, \infty)$ is Lipschitz, i.e. there exists an $L > 0$ such that

$$|\varphi(t_1) - \varphi(t_2)| \leq L|t_1 - t_2| \quad \text{for all } t_1, t_2 \in [0, \infty), \quad (3.48)$$

then φ is also uniformly continuous, by choosing $\delta := \frac{\varepsilon}{L} > 0$ for any given $\varepsilon > 0$.

Proposition 3.3.5. *If $W(t) \in \mathcal{W}$ is an integral curve of the perturbed Riemannian gradient descent flow (3.6) then $\lim_{t \rightarrow \infty} \text{grad}_g J_\varepsilon(W(t)) = 0$.*

Proof. By Proposition 3.3.3, the solution $W(t) \in \mathcal{W}$ of (3.6) exists for all $t \geq 0$, is contained in the compact set $K := \text{lev}_{\alpha_0}(J_\varepsilon)$, with $\alpha_0 := J_\varepsilon(W(0))$, and the function values $J_\varepsilon(W(t))$ converge monotonically decreasing to $\lim_{t \rightarrow \infty} J_\varepsilon(W(t)) =: J_\varepsilon^* > -\infty$. As a result of

$$J_\varepsilon(W(t_1)) - J_\varepsilon(W(t_2)) = - \int_{t_1}^{t_2} \frac{d}{dt} J_\varepsilon(W(t)) dt \stackrel{(3.3)}{=} \int_{t_1}^{t_2} \|\text{grad}_g J_\varepsilon(W(t))\|_{g, W(t)}^2 dt$$

and Corollary 3.3.2, the overall estimate

$$\infty > J_\varepsilon(W(0)) - J_\varepsilon^* = \int_0^\infty \|\text{grad}_g J_\varepsilon(W(t))\|_{g, W(t)}^2 dt \stackrel{(3.45)}{\geq} \int_0^\infty \|\text{grad}_g J_\varepsilon(W(t))\|^2 dt$$

follows. Define $0 \leq \|\text{grad}_g J_\varepsilon(W(t))\|^2 =: \varphi(t)$. It is shown that φ is Lipschitz continuous on $[0, \infty)$ by proving $\dot{\varphi}(t)$ is bounded on $[0, \infty)$. For this, represent φ as the composition $\varphi(t) = g(W(t))$ with $g: \mathcal{W} \rightarrow \mathbb{R}$ defined by $g(W) := \|\text{grad}_g J_\varepsilon(W)\|^2$. Because J is C^2 , the function g is C^1 . Equipping \mathcal{W} with the standard Euclidean metric $E = \langle \cdot, \cdot \rangle$ yields the continuous gradient $\text{grad}_E g: \mathcal{W} \rightarrow \mathcal{T}_\mathcal{W}$. Since K is compact, there exists a constant $L > 0$ simultaneously bounding g and $\|\text{grad}_E g\|^2$ on K . As a result of $W(t) \in K$ for all $t \geq 0$ the estimate

$$|\dot{\varphi}(t)| = |\langle \text{grad}_E g(W(t)), \dot{W}(t) \rangle| \leq \|\text{grad}_E g(W(t))\| \|\text{grad}_g J_\varepsilon(W(t))\| \leq L^2$$

follows, showing that φ is indeed Lipschitz continuous on $[0, \infty)$. Lemma 3.3.4 together with Remark 3.3.1 then implies $\lim_{t \rightarrow \infty} \|\text{grad}_g J_\varepsilon(W(t))\|^2 = 0$. □

3.3.3. Convergence Analysis for Analytic Variational Models

As already mentioned above, integral curve of gradient fields do not necessarily converge to a single point. Thus, in order to prove any convergence results, additional assumptions on the function J_ε have to be made. E.g. in [ABB04], a convexity assumption results in a convergent statement for the corresponding integral curves [ABB04, Thm. 4.7] as well as in convergence rates [ABB04, Prop. 4.4]. Since J is not assumed to be convex, the focus will be on analytic variational models for the remaining part of this section. For this class of functions, the Łojasiewicz inequality results in convergence statements for integral curves of the corresponding gradient flow, as first shown by Łojasiewicz in [Loj82]. See [AMA05] for a review of the chase in \mathbb{R}^d , [Lag07] for the general case of analytic Riemannian manifolds and [BDL07] for a generalization to subgradient differential inclusions for subanalytic functions.

In the following, convergence for analytic J_ε on the assignment manifold will be shown based on the case for analytic function in \mathbb{R}^d from [AMA05]. This way, the parallels between the present continuous-time case and the geometric Euler discretization discussed in the next Section 3.4 will become most apparent. Subsequently, the stability results from [AK06] are shown to also hold on the assignment manifold and finally, also convergence rates are proven based on [BDL07].

The key argument, underlying the following proofs is the fact that the Łojasiewicz inequality can be used to find an estimate of the arc length for integral curves in various situations. The corresponding statement in Lemma 3.3.7 below is a general formulation, extracted from the proofs in [AK06] and [AMA05].

Lemma 3.3.6. *Let $\alpha \in \mathbb{R}$. Then, there exists a constant $C > 0$ such that for any initial condition $W(0) \in \text{lev}_\alpha(J_\varepsilon)$, the flow $W(t)$ from (3.6) fulfills*

$$\frac{d}{dt} J_\varepsilon(W(t)) \leq -C \|\text{grad}_E J_\varepsilon(W(t))\| \|\dot{W}(t)\| \quad \text{for all } t \geq 0.$$

Furthermore, $\frac{d}{dt} J_\varepsilon(W(t_0)) = 0$ for some $t_0 \geq 0$ then $\dot{W}(t) = 0$ for all $t \geq t_0$.

Remark 3.3.2. The presentation in [AMA05] follows the generalization of gradient flows from [Lag02]. The first condition is called *angle condition* and the second one *weak decrease condition*. To prove convergence, a flow only has to fulfill these two conditions.

Proof. If $\frac{d}{dt} J_\varepsilon(W(t_0)) = 0$ for some t_0 , then $\text{grad}_g J_\varepsilon(W(t_0)) = 0$ as a consequence of

$$\frac{d}{dt} J_\varepsilon(W(t)) = - \|\text{grad}_g J_\varepsilon(W(t))\|_{g,W(t)}^2. \quad (3.49)$$

Since integral curves are unique by Theorem A.2.1, the solution is given by the constant curve $W(t) = W(t_0)$ for all $t \geq t_0$ and therefore $\frac{d}{dt} W(t) = 0$ follows. To prove the first statement, note that due to Proposition 3.3.3, the flow $W(t) \in \mathcal{W}$ with initial condition $W(0) \in \text{lev}_\alpha(J_\varepsilon) =: K_\alpha$ is contained in the compact set K_α for all $t \geq 0$. By Corollary 3.3.2, there exists a constant $C > 0$ such that

$$\begin{aligned} & \|\text{grad}_g J_\varepsilon(W(t))\|_{g,W(t)} \geq C \|\text{grad}_E J_\varepsilon(W(t))\| \\ \text{and} \quad & \|\text{grad}_g J_\varepsilon(W(t))\|_{g,W(t)} \geq \|\text{grad}_g J_\varepsilon(W(t))\| = \|\dot{W}(t)\| \end{aligned}$$

3.3. Perturbed Riemannian Gradient Descent Flows for Optimization

for all $t \geq 0$. Combining these inequalities with (3.49), results in the first statement. \square

Lemma 3.3.7. *Let $J_\varepsilon: \mathcal{W} \rightarrow \mathbb{R}$ be analytic, $Z \in \mathcal{W}$ and $\alpha \in \mathbb{R}$. Suppose $U_L \subset \mathcal{W}$ is a neighborhood of $Z \in \mathcal{W}$ on which the Łojasiewicz gradient inequality with exponent $\mu \in [0, 1)$ is satisfied. Then there exists a constant $C > 0$ with the following property. For any solution $W(t)$ of the Riemannian gradient flow (3.6) with $W(0) \in \text{lev}_\alpha(J_\varepsilon)$, if $J_\varepsilon(W(t)) \geq J_\varepsilon(Z)$ and $W(t) \in U_L$ is satisfied for $t \in [t_1, t_2]$, then the arc length of $W(t)$ on $[t_1, t_2]$ with respect to the Euclidean metric $\|\cdot\|$ is bounded by*

$$\int_{t_1}^{t_2} \|\dot{W}(t)\| dt \leq C (J_\varepsilon(W(t_1)) - J_\varepsilon(Z))^{1-\mu}. \quad (3.50)$$

Proof. To simplify notation, define $\Phi(t) := J_\varepsilon(W(t)) - J_\varepsilon(Z)$. By Lemma 3.3.6 there exists a $C' > 0$ such that any solution $W(t)$ of (3.6) with $W(0) \in \text{lev}_\alpha(J_\varepsilon)$ satisfies $\frac{d}{dt} J_\varepsilon(W(t)) \leq -C' \|\nabla J_\varepsilon(W(t))\| \|\dot{W}(t)\|$ for all $t \geq 0$. Let $C'' > 0$ and $\mu \in [0, 1)$ be the constants of the Łojasiewicz inequality on U_L and define

$$C := ((1 - \mu)C'C'')^{-1} > 0.$$

If $W(t)$ is a solution of the Riemannian gradient descent flow with $W(0) \in \text{lev}_\alpha(J_\varepsilon)$ satisfying $W(t) \in U_L$ on $[t_1, t_2]$, then

$$\frac{d}{dt} \Phi(t) \leq -C' \|\nabla J_\varepsilon(W(t))\| \|\dot{W}(t)\| \leq -C'C'' |\Phi(t)|^\mu \|\dot{W}(t)\| \quad \forall t \in [t_1, t_2]. \quad (3.51)$$

The remaining proof is divided into two cases.

First assume $\Phi(t) > 0$ on $[t_1, t_2]$. It follows by the definition of C that

$$\frac{d}{dt} (\Phi(t))^{1-\mu} = (1 - \mu) \frac{1}{(\Phi(t))^\mu} \frac{d}{dt} \Phi(t) \leq -\frac{1}{C} \|\dot{W}(t)\| \stackrel{(3.51)}{\leq} 0 \quad \forall t \in [t_1, t_2].$$

As a consequence of this and $\mu < 1$, the arc length is upper bounded by

$$\begin{aligned} \int_{t_1}^{t_2} \|\dot{W}(t)\| dt &\leq -C \int_{t_1}^{t_2} \frac{d}{dt} (\Phi(t))^{1-\mu} dt \\ &= C \left[(\Phi(t_1))^{1-\mu} - (\Phi(t_2))^{1-\mu} \right] \leq C (\Phi(t_1))^{1-\mu} \end{aligned}$$

where the last inequality holds due to $(\Phi(t_2))^{1-\mu} \geq 0$.

Now, suppose $\Phi(t) > 0$ on $[t_1, t_2]$ is not true. Since $\Phi(t) \geq 0$ on $[t_1, t_2]$ by assumption, the existence of

$$T := \inf \{t \in [t_1, t_2] \mid \Phi(t) = 0\} < t_2$$

is implied. The condition $\Phi(T) = 0$ translates to $J_\varepsilon(W(T)) = J_\varepsilon(Z)$. As a result of the monotonicity of $J_\varepsilon(W(t))$ from Proposition 3.3.3, the equality $J_\varepsilon(W(t)) = J_\varepsilon(Z)$ for $t \in [T, t_2]$ follows. Therefore $\frac{d}{dt} J_\varepsilon(W(t)) = 0$ on $[T, t_2]$, implying

$$\dot{W}(t) = 0 \quad \forall t \geq T \quad (3.52)$$

by Lemma 3.3.6. Due to the $\Phi(t) > 0$ for all $t \in [t_1, T)$, by the choice of T , the above estimate from the first case can be applied on $[t_1, T)$ resulting in

$$\int_{t_1}^{t_2} \|\dot{W}(t)\| dt \stackrel{(3.52)}{=} \int_{t_1}^T \|\dot{W}(t)\| dt \leq C(\Phi(t_1))^{1-\mu}. \quad \square$$

After these preparations, it is now possible to prove the convergence of integral curves for analytic J_ε on the assignment manifold.

Theorem 3.3.8. *Assume $J_\varepsilon: \mathcal{W} \rightarrow \mathbb{R}$ is analytic and let $W(t) \in \mathcal{W}$ be the solution of the perturbed gradient descent flow (3.6) with $W(0) \in \text{lev}_\alpha(J_\varepsilon)$. Then there exists a critical point $W^* \in \text{lev}_\alpha(J_\varepsilon) \subset \mathcal{W}$ of J_ε , i.e. $\text{grad}_g J_\varepsilon(W^*) = 0$, such that $\lim_{t \rightarrow \infty} W(t) = W^*$.*

Proof. The adapted proof of [AMA05, Thm. 2.2] on \mathcal{W} is given, using Lemma 3.3.7 for estimating the arc length of $W(t)$. By Proposition 3.3.3, the flow $W(t)$ is contained in the compact set $\text{lev}_\alpha(J_\varepsilon) =: K_\alpha$. Thus, $W(t)$ has an accumulation point W^* in K_α , i.e. there is a sequence $0 < t_1 < t_2 < \dots$ with $\lim_{k \rightarrow \infty} t_k = \infty$ such that $\lim_{k \rightarrow \infty} W(t_k) = W^*$. Because $J_\varepsilon(W(t))$ is monotonically decreasing in t , the continuity of J_ε implies

$$J_\varepsilon(W^*) = \lim_{k \rightarrow \infty} J_\varepsilon(W(t_k)) = \lim_{t \rightarrow \infty} J_\varepsilon(W(t)). \quad (3.53)$$

Similarly, the continuity of $\text{grad}_g J_\varepsilon: \mathcal{W} \rightarrow \mathcal{T}_\mathcal{W}$ and Proposition 3.3.5 give

$$\text{grad}_g J_\varepsilon(W^*) = \lim_{k \rightarrow \infty} \text{grad}_g J_\varepsilon(W(t_k)) = \lim_{t \rightarrow \infty} \text{grad}_g J_\varepsilon(W(t)) = 0,$$

showing W^* is indeed a critical point of J_ε .

As a consequence of J_ε being analytic on \mathcal{W} , Corollary 3.2.7 yields the exists of a neighborhood $U_L \subset \mathcal{W}$ of W^* on which the Łojasiewicz inequality holds with exponent $\mu \in [0, 1)$. In the following, it will be shown by contradiction that for arbitrarily small $r > 0$, with $\overline{B}_r(W^*) \subset U_L$, the curve $W(t)$ eventually enters $B_r(W^*)$ and never leaves. Since r is arbitrarily small, it then follows that $W(t)$ converges to W^* .

Assume an arbitrary $r > 0$ with $\overline{B}_r(W^*) \subset U_L$ is given. Let $C > 0$ be the constant from Lemma 3.3.7 corresponding to the choice $Z = W^*$. The fact that W^* is an accumulation point of the curve $W(t)$ together with (3.53) implies the existence of a time $t_1 \geq 0$ such that

$$\|W(t_1) - W^*\| < \frac{r}{4} \quad \text{and} \quad C|J_\varepsilon(W(t_1)) - J_\varepsilon(W^*)|^{1-\mu} < \frac{r}{4}. \quad (3.54)$$

Now, suppose $W(t)$ would leave $B_r(W^*)$ on $[t_1, \infty)$, i.e.

$$t_2 := \inf \{t > t_1 \mid \|W(t) - W^*\| = r\} > t_1$$

exists. The fact that $W(t) \in \overline{B}_r(W^*) \subset U_L$ on $[t_1, t_2]$ by the choice of t_2 together with $J_\varepsilon(W(t)) \geq J_\varepsilon(W^*)$ due to the monotonicity of $J_\varepsilon(W(t))$ shows that the assumptions of Lemma 3.3.7 with constant C are fulfilled on $[t_1, t_2]$. The resulting estimate of the arc length by (3.50) gives

$$\|W(t_2) - W(t_1)\| \leq \int_{t_1}^{t_2} \|\dot{W}(t)\| dt \leq C(J_\varepsilon(W(t_1)) - J_\varepsilon(W^*))^{1-\mu} \stackrel{(3.54)}{<} \frac{r}{4}.$$

3.3. Perturbed Riemannian Gradient Descent Flows for Optimization

It then follows $\|W(t_2) - W^*\| \leq \|W(t_2) - W(t_1)\| + \|W(t_1) - W^*\| < \frac{r}{4} + \frac{r}{4} = \frac{r}{2}$, contradicting the choice of t_2 . Thus $W(t)$ has to be contained in $B_r(W^*)$ for all $t \geq t_1$, proving the statement. \square

Stability of the Riemannian Gradient Flow for J_ε

Even if the objective function is C^∞ , local minima are not necessarily stable equilibria of the corresponding gradient flow, as the counterexample from [AK06, Prop. 2] in the Euclidean case shows. There are also C^∞ functions with stable equilibria which are not local minima. However, in [AK06] it is shown that for analytic functions on \mathbb{R}^d , local minima are in one to one correspondence with stable equilibria of the gradient flow. The same holds for strict local minima and asymptotically stable equilibria.

In the following, this is also proven for the Riemannian gradient descent flow of J_ε on the assignment manifold, where stability will be understood with respect to the $\|\cdot\|$ norm on $\mathbb{R}^{m \times n}$.

Definition 3.3.1 (Stability). Let $F: \mathcal{W} \rightarrow \mathcal{T}_{\mathcal{W}}$ be a vector field on \mathcal{W} . Consider the dynamical system $\dot{W}(t) = F(W(t))$ and suppose $\bar{W} \in \mathcal{W}$ is an equilibrium point, i.e. $F(\bar{W}) = 0$ holds.

- (1) \bar{W} is *(Lyapunov) stable*, if for every $r > 0$ there is a $\delta = \delta(r) > 0$ such that if $\|W(0) - \bar{W}\| < \delta$, then $\|W(t) - \bar{W}\| < r$ for all $t \geq 0$.
- (2) \bar{W} is *asymptotically stable*, if it is stable and a constant $\delta > 0$ can be chosen such that if $\|W(0) - \bar{W}\| < \delta$ then $\lim_{t \rightarrow \infty} W(t) = \bar{W}$.

The stability results on the assignment manifold \mathcal{W} are directly shown using the Łojasiewicz inequality on \mathcal{W} from Corollary 3.2.7.

Theorem 3.3.9. *Let $J_\varepsilon: \mathcal{W} \rightarrow \mathbb{R}$ be analytic. Then $Z \in \mathcal{W}$ is a local minimum of J_ε if and only if Z is a stable equilibrium of the Riemannian gradient descent flow (3.6).*

Proof. The first direction is an adapted version from the proof of [AK06, Thm. 3] and is similar to the argument in Theorem 3.3.8. For this, assume Z is a local minimum of J_ε . Due to the local minimality, there exists a neighborhood $U_m \subset \mathcal{W}$ of Z such that $J_\varepsilon(Q) \geq J_\varepsilon(Z)$ for all $Q \in U_m$ and $\text{grad}_g J_\varepsilon(Z) = 0$, showing that Z is an equilibrium of the Riemannian gradient flow (3.6). Since J_ε is analytic, there is a neighborhood $U_L \subset \mathcal{W}$ of Z from Corollary 3.2.7 on which the Łojasiewicz inequality is fulfilled with exponent $\mu \in [0, 1)$. Assume an arbitrary $r > 0$ with $\bar{B}_r(Z) \subset U_m \cap U_L$ is given. Choose α sufficiently large such that also $\bar{B}_r(Z) \subset \text{lev}_\alpha(J_\varepsilon)$ holds and let $C > 0$ be the constant from Lemma 3.3.7 corresponding to the choices of α and Z . Then, by the continuity of J_ε , there is a $0 < \delta < \frac{r}{4}$ such that

$$C|J_\varepsilon(X) - J_\varepsilon(Z)|^{1-\mu} < \frac{r}{4} \quad \forall X \in B_\delta(Z). \quad (3.55)$$

Now, suppose an arbitrary $W(0) \in B_\delta(Z)$ is chosen. It is shown by contradiction that $W(t) \in B_r(Z)$ holds for all $t \geq 0$. Assume $W(t)$ leaves $B_r(Z)$ at some point, i.e.

$$T := \inf \{t \geq 0 \mid \|W(t) - Z\| = r\}$$

exists. Then $W(t) \in \overline{B}_r(Z) \subset U_L \cap U_m$ for all $t \in [0, T]$ by the choice of T , resulting in $J_\varepsilon(W(t)) \geq J_\varepsilon(Z)$ on $[0, T]$. Since α was chosen such that $\overline{B}_r(Z) \subset \text{lev}_\alpha(J_\varepsilon)$, the starting point $W(0)$ is contained in $\text{lev}_\alpha(J_\varepsilon)$. Overall, the assumptions of Lemma 3.3.7 with constant C from above are satisfied, resulting in the arc length estimate

$$\|W(T) - W(0)\| \leq \int_0^T \|\dot{W}(t)\| dt \leq C |J_\varepsilon(W(0)) - J_\varepsilon(Z)|^{1-\mu} \stackrel{(3.55)}{<} \frac{r}{4}. \quad (3.56)$$

It then follows $\|W(T) - Z\| \leq \|W(T) - W(0)\| + \|W(0) - Z\| < \frac{r}{4} + \delta < \frac{r}{2}$, contradicting the choice of T . Thus $W(t) \in B_r(Z)$ for all $t \geq 0$ must be true, showing that the local minimum Z is indeed a stable equilibrium.

As for the other direction, suppose Z is a stable equilibrium. Since J_ε is analytic, Corollary 3.2.7 gives a neighborhood $U_L \subset \mathcal{W}$ of Z on which the Łojasiewicz inequality (3.44) with constants $C > 0$ and $\mu \in [0, 1)$ is fulfilled. Choose any $r > 0$ with $\overline{B}_r(Z) \subset U_L$. Because Z is stable, there is a $\delta = \delta(r) > 0$ such that $W(t) \in B_r(Z)$ for all $t \geq 0$ if $W(0) \in B_\delta(Z)$. To show Z is a local minimum, let $X \in B_\delta(Z)$ be arbitrary. According to Theorem 3.3.8 the trajectory $W(t)$ with initial condition $W(0) := X$ converges towards a point $W^* \in \mathcal{W}$, the values $J_\varepsilon(W(t))$ are monotonically decreasing and the gradient vanishes

$$0 = \text{grad}_g J_\varepsilon(W^*) = R_{W^*} [\text{grad}_E J_\varepsilon(W^*)].$$

Due to the invertibility of R_{W^*} by Lemma 2.3.1, also $\text{grad}_E J_\varepsilon(W^*) = 0$ follows. Since $W(t)$ is contained in $B_r(Z)$ for all $t \geq 0$, the limit point W^* lies in the closure $\overline{B}_r(Z)$. Because r was chosen to guarantee $\overline{B}_r(Z) \subset U_L$, the Łojasiewicz inequality

$$C |J_\varepsilon(W^*) - J_\varepsilon(Z)|^\mu \leq \|\text{grad}_E J_\varepsilon(W^*)\| = 0,$$

resulting in $J_\varepsilon(W^*) = J_\varepsilon(Z)$. As a result of the monotonicity of $J_\varepsilon(W(t))$,

$$J_\varepsilon(X) = J_\varepsilon(W(0)) \geq J_\varepsilon(W(t)) \geq J_\varepsilon(W^*) = J_\varepsilon(Z)$$

follows. Since $X \in B_\delta(Z)$ was arbitrary, the equilibrium Z is a local minimum of J_ε . \square

Theorem 3.3.10. *Let $J_\varepsilon: \mathcal{W} \rightarrow \mathbb{R}$ be analytic. Then $Z \in \mathcal{W}$ is a strict local minimum of J_ε if and only if Z is an asymptotically stable equilibrium of the Riemannian gradient descent flow (3.6).*

Proof. Suppose $Z \in \mathcal{W}$ is a strict local minimum, i.e. there is a neighborhood $U_m \subset \mathcal{W}$ of Z such that $J_\varepsilon(X) > J_\varepsilon(Z)$ for all $X \in U_m$ with $X \neq Z$. By Corollary 3.2.7, there exists a neighborhood $U_L \subset \mathcal{W}$ of Z on which the Łojasiewicz inequality with exponent $\mu \in [0, 1)$ and constant $C > 0$ is fulfilled. Choose $r > 0$ sufficiently small such that $\overline{B}_r(Z) \subset U_m \cap U_L$. Since strict local optima are also local optima, it follows from Theorem 3.3.9 that Z is a stable equilibrium of the flow, thus there is a $\delta > 0$ such that if $W(0) \in B_\delta(Z)$ then $W(t) \in B_r(Z) \subset U_m$ for all $t \geq 0$. For any such $W(0) \in B_\delta(Z)$, Theorem 3.3.8 shows the convergence of $W(t) \in B_r(Z)$ towards a critical point $W^* \in \overline{B}_r(Z) \subset U_L$, i.e. $\text{grad}_g J_\varepsilon(W^*) = 0$. Due to the invertibility of R_{W^*} by

3.3. Perturbed Riemannian Gradient Descent Flows for Optimization

Lemma 2.3.1 and $\text{grad}_g J_\varepsilon(W^*) = R_{W^*}[\text{grad}_E J_\varepsilon(W^*)]$, also $\text{grad}_E J_\varepsilon(W^*) = 0$. The Lojasiewicz inequality then implies

$$C|J_\varepsilon(W^*) - J_\varepsilon(Z)|^\mu \leq \|\text{grad}_E J_\varepsilon(W^*)\| = 0, \quad (3.57)$$

showing that $J_\varepsilon(W^*) = J_\varepsilon(Z)$. Because W^* is an element of U_m and Z is a strict minimum, the equality $J_\varepsilon(W^*) = J_\varepsilon(Z)$ implies $Z = W^* = \lim_{t \rightarrow \infty} W(t)$. This proves the asymptotic stability of Z .

Conversely, suppose, Z is an asymptotically stable equilibrium, i.e. Z is stable and there is a $\delta > 0$ such that $\lim_{t \rightarrow \infty} W(t) = Z$ for all $W(0) \in B_\delta(Z)$. Since Z is stable, Theorem 3.3.9 shows that Z is a local minimum on some neighborhood U_m . By choosing a sufficiently small $\delta > 0$, Z is a local minimum on $B_\delta(Z) \subset U_m$. It remains to show Z is also strict on $B_\delta(Z)$. For this, suppose $J_\varepsilon(Z) = J_\varepsilon(X)$ holds for some $X \in B_\delta(Z)$. As a consequence of Z being asymptotically stable, the flow $W(t)$ with initial condition $W(0) = X$ converges towards Z . According to Proposition 3.3.3 the corresponding function values $J_\varepsilon(W(t))$ are monotonically decreasing, resulting in the inequality

$$J_\varepsilon(Z) = J_\varepsilon(X) = J_\varepsilon(W(0)) \geq J_\varepsilon(W(t)) \geq \lim_{t \rightarrow \infty} J_\varepsilon(W(t)) = J_\varepsilon(Z).$$

This shows $J_\varepsilon(W(t)) = J_\varepsilon(Z)$ is constant for all $t \geq 0$ and $\frac{d}{dt} J_\varepsilon(W(t)) = 0$ follows. Lemma 3.3.6 then implies $\dot{W}(t) = 0$ for all $t \geq 0$, proving that $W(t)$ is constant and hence $X = W(0) = \lim_{t \rightarrow \infty} W(t) = Z$ holds. This establishes the strict minimality of Z on $B_\delta(Z)$. \square

Convergence Rates of the Riemannian Gradient Flow for J_ε

The derivation of convergence rates for bounded solutions of subgradient differential inclusions from [BDL07] can be adapted to obtain convergence rates for the perturbed Riemannian gradient descent flow (3.6). The argument relies on comparing solutions of differential equations on \mathbb{R} .

Lemma 3.3.11 (Comparison Lemma). *Consider the scalar differential equation*

$$\dot{y}(t) = f(t, y(t)), \quad y(t_0) = y_0 \quad (3.58)$$

where $f(t, y)$ is continuous in t and locally Lipschitz in y , for all $t \geq 0$ and all $y \in I \subset \mathbb{R}$. Let $[t_0, T)$ be a maximal interval of existence of the solution $y(t)$ (T could be infinite) and suppose $y(t) \in I$ for all $t \in [t_0, T)$. Let $\sigma(t)$ be a continuous function satisfying the differential inequality

$$\dot{\sigma}(t) \leq f(t, \sigma(t)), \quad \sigma(t_0) \leq y_0, \quad (3.59)$$

with $\sigma(t) \in I$ for all $t \in [t_0, T)$. Then $\sigma(t) \leq y(t)$ for all $t \in [t_0, T)$.

Proof. See e.g. [Kha02] \square

Theorem 3.3.12. *Let $J_\varepsilon: \mathcal{W} \rightarrow \mathbb{R}$ be analytic and suppose $W(t) \in \mathcal{W}$ is a solution of the perturbed gradient descent flow (3.6) converging towards $W^* \in \mathcal{W}$. Let U_L be a neighborhood of W^* on which the Lojasiewicz inequality is fulfilled with exponent $\mu \in [0, 1)$. Then the following estimates hold for $t \rightarrow \infty$*

(1) *If $\mu \in [0, \frac{1}{2})$, then $W(t)$ converges to W^* in finite time.*

(2) *If $\mu = \frac{1}{2}$, then there exist $\beta, C > 0$ such that*

$$\|W(t) - W^*\| \leq Ce^{-\beta t}. \quad (3.60)$$

(3) *If $\mu \in (\frac{1}{2}, 1)$, then there exist $\beta, C > 0$ such that*

$$\|W(t) - W^*\| \leq C(t + \beta)^{-\frac{1-\mu}{2\mu-1}}. \quad (3.61)$$

Proof. The proof follows the one for the convergence rates in [BDL07], with some necessary modifications. Since $W(t)$ converges to W^* , there is a $T > 0$ such that $W(t) \in U_L$ for all $t \geq T$. Because $J_\varepsilon(W(t))$ is monotonically decreasing by Proposition 3.3.3, also $J_\varepsilon(W(t)) \geq J_\varepsilon(W^*)$ for all $t \geq T$ is fulfilled. Therefore, all the assumptions for Lemma 3.3.7 are satisfied and there exists a $C' > 0$ such that

$$\sigma(t) := \int_t^\infty \|\dot{W}(t)\| dt \leq C'(J_\varepsilon(W(t)) - J_\varepsilon(Z))^{1-\mu} < \infty \quad \text{for all } t \geq T. \quad (3.62)$$

The following two properties

$$\|W(t) - W^*\| \leq \sigma(t) \quad \text{and} \quad \dot{\sigma}(t) = -\|\dot{W}(t)\| \quad (3.63)$$

show that $\sigma(t)$ is non-negative and monotonically decreasing. Below, the convergence rates are proven using the above comparison lemma together with a differential inequality of $\sigma(t)$, which is derived now. For this, suppose $\mu \in (0, 1)$. Then (3.62) and the Lojasiewicz inequality (3.2.7) on U_L with constant $\bar{C} > 0$ imply

$$\sigma(t) \leq C'(J_\varepsilon(W(t)) - J_\varepsilon(Z))^{1-\mu} \leq \bar{C} \|\text{grad}_E J_\varepsilon(W(t))\|^{\frac{1-\mu}{\mu}}. \quad (3.64)$$

Since $\text{lev}_{\alpha_0}(J_\varepsilon) =: K_{\alpha_0}$ with $\alpha_0 := J_\varepsilon(W(0))$ is positively invariant and compact by Proposition 3.3.3, it follows $W(t) \in K_{\alpha_0}$ for all $t \geq 0$. According to (3.46) of Corollary 3.3.2, there is a constant $C_{\alpha_0} > 0$ such that

$$C_{\alpha_0} \|\text{grad}_E J_\varepsilon(W(t))\| \leq \|\text{grad}_g J_\varepsilon(W(t))\| \quad \text{for all } t \geq 0. \quad (3.65)$$

With this and $\bar{C}' := \bar{C}C_{\alpha_0}^{-\frac{1-\mu}{\mu}} > 0$, the estimation of $\sigma(t)$ in (3.64) can be continued as

$$\begin{aligned} \sigma(t) &\leq \bar{C}' \|\text{grad}_E J_\varepsilon(W(t))\|^{\frac{1-\mu}{\mu}} \leq \bar{C}' \|\text{grad}_g J_\varepsilon(W(t))\|^{\frac{1-\mu}{\mu}} \\ &= \bar{C}' \|\dot{W}(t)\|^{\frac{1-\mu}{\mu}} \stackrel{(3.63)}{=} \bar{C}' (-\dot{\sigma}(t))^{\frac{1-\mu}{\mu}}. \end{aligned}$$

3.3. Perturbed Riemannian Gradient Descent Flows for Optimization

Rearranging this inequality and setting $\nu := \frac{\mu}{1-\mu}$ as well as $L := (\overline{C}')^{-\nu} > 0$, results in

$$\dot{\sigma}(t) \leq -L(\sigma(t))^\nu.$$

The smooth function $\mathbb{R}_{>0} \rightarrow \mathbb{R}_{>0}$, given by $y \mapsto L(y)^\nu$, is locally Lipschitz and the comparison lemma can be applied in the following arguments to obtain convergence rates. For this, consider the autonomous ODE

$$\dot{y}(t) = -L(y(t))^\nu \quad \text{with} \quad y(0) := \sigma(0) \geq 0 \quad (3.66)$$

and assume a solution on $[0, \tau)$ exists. Then

$$\|W(t) - W^*\| \stackrel{(3.63)}{\leq} \sigma(t) \leq y(t) \quad (3.67)$$

for all $t \in [0, \tau)$, according to the comparison lemma 3.3.11.

In the following, $W(0) \neq W^*$ is always assumed, resulting in $\sigma(0) > 0$. In order to prove the convergence rates, it remains to find solutions of $y(t)$ with initial condition $y(0) = \sigma(0) > 0$ depending on the value of $\mu \in (0, 1)$.

To (1): If $\mu = 0$, then $|J_\varepsilon(W(t)) - J_\varepsilon(W^*)|^\mu = 1$ for $J_\varepsilon(W(t)) \neq J_\varepsilon(W^*)$ and $0^0 = 0$ otherwise, according to the adopted convention. Proposition 3.3.5 and the Łojasiewicz inequality with constant \overline{C} then give

$$\overline{C}|J_\varepsilon(W(t)) - J_\varepsilon(W^*)|^\mu \leq \|\text{grad}_E J_\varepsilon(W(t))\| \rightarrow 0 \quad \text{for } t \rightarrow \infty. \quad (3.68)$$

Hence, there is a T_0 with $J_\varepsilon(W(t)) = J_\varepsilon(W^*)$ for all $t \geq T_0$, resulting in $\frac{d}{dt} J_\varepsilon(W(t)) = 0$ for $t \geq T_0$. Lemma 3.3.6 then implies $\dot{W}(t) = 0$ for $t \geq T_0$, showing that $W(t)$ is constant from T_0 onward. Since $W(t)$ converges towards W^* , the equality $W(t) = W^*$ for $t \geq T_0$ follows, proving convergence in finite time.

Now suppose $\mu \in (0, \frac{1}{2})$. Then, $\nu = \frac{\mu}{1-\mu} \in (0, 1)$ and by separation of variables, the solution

$$y(t) = (\sigma(0)^{1-\nu} - (1-\nu)Lt)^{\frac{1}{1-\nu}} \quad \text{for } 0 \leq t \leq \frac{\sigma(0)^{1-\nu}}{(1-\nu)L} =: \tau \quad (3.69)$$

for the ODE (3.66) is found. For $t = \tau$, the value $y(\tau) = 0$ together with (3.67) implies $W(\tau) = W^*$, showing that $W(t)$ converges in finite time.

To (2): If $\mu = \frac{1}{2}$, then $\nu = \frac{\mu}{1-\mu} = 1$ and the ODE (3.66) takes the form $\dot{y} = -Ly$. Thus, the solution of the initial value problem is given by $y(t) = \sigma(0)e^{-Lt}$ for all $t \geq 0$. Due to (3.67), setting $C := \sigma(0) > 0$ and $\beta := L > 0$ results in the desired estimate.

To (3): If $\mu \in (\frac{1}{2}, 1)$, then $\nu = \frac{\mu}{1-\mu} > 1$ and thus $\nu - 1 > 0$. By separation of variables, the solution

$$y(t) = ((\nu - 1)Lt + \sigma(0)^{-(\nu-1)})^{-\frac{1}{\nu-1}} = C(t + \beta)^{-\frac{1}{\nu-1}} \quad \text{for all } t \geq 0 \quad (3.70)$$

for the ODE (3.66) is found, with $C := ((\nu - 1)L)^{-\frac{1}{\nu-1}} > 0$ and $\beta := \frac{\sigma(0)^{-(\nu-1)}}{(\nu-1)L} > 0$. Because of $\frac{1}{\nu-1} = \frac{1-\mu}{2\mu-1}$, the desired estimate for $\|W(t) - W^*\|$ follows from (3.67). \square

3.4. Numerical Integration of the Perturbed Riemannian Gradient Descent Flow

Recall the geometric integration framework from Section 2.3.4 for numerically integrating flows of the form $\dot{W}(t) = R_{W(t)}[F(W(t))]$ with an arbitrary vector field $F: \mathcal{W} \rightarrow \mathcal{T}_{\mathcal{W}}$. Due to the relation between the Fisher-Rao and the Euclidean gradient in Corollary 2.3.4, the Riemannian gradient descent flow (3.6) fits into this integration scheme with the vector field $F(W) = -\text{grad}_E J_\varepsilon(W)$.

In general, there is a difference between numerically integrating a vector field and numerically optimizing a function. In the first case, it is important to develop methods to accurately follow the dynamics given by the vector field, see e.g. [HPW93]. In the second case, the focus is on minimization and methods trying to find descent directions by preferably using second-order information, without the need to track any specific integral curve, see e.g. [NW06]. The explicit Euler method is the simplest approach that can be viewed as both, a method for numerically integrating the flow and for optimizing J_ε . Therefore, in the following, convergence will only be investigated for the geometric Euler integration (2.66) on \mathcal{W} .

As it turns out, most of the results in the continuous-time setting from the previous Section 3.3 carry over to the corresponding statements for the geometric Euler in the discrete-time case. In Section 3.4.1 the geometric Euler is revisited and connections to existing numerical optimization techniques in the literature are pointed out. Section 3.4.2 introduces the concept of L -smooth adaptability from [BSTV18], a weaker form of the Lipschitz condition for determining step-sizes. Subsequently, this concept is used in Section 3.4.3 to inspect general properties of the geometric Euler with Armijo step-size selection. Similar to the continuous-time setting, convergence and stability results for iterative optimization schemes are known for analytic functions on \mathbb{R}^d [AMA05] as well as convergence rates [AB09]. In Section 3.4.4, these results are shown to also hold for analytic J_ε on the assignment manifold.

3.4.1. Geometric Euler Integration

The explicit geometric Euler integration (2.66), for integrating the Riemannian gradient descent flow (3.6) takes the form

$$W^{(k+1)} = \exp_{W^{(k)}}\left(-h_k \text{grad}_E J_\varepsilon(W^{(k)})\right), \quad W^{(0)} \in \mathcal{W}, \quad (3.71)$$

with step-size $h_k > 0$. Using the characterization of \exp_W in (2.50) and keeping in mind that the argmin does not depend on constant terms, results in the expression

$$W^{(k+1)} = \operatorname{argmin}_{W \in \Delta^m} \left\{ h_k \langle \text{grad}_E J_\varepsilon(W^{(k)}), W - W^{(k)} \rangle + \text{KL}(W, W^{(k)}) \right\}. \quad (3.72)$$

As already mentioned in Remark 2.3.3 (2), this clearly demonstrates the connection between geometric Euler integration of the Riemannian gradient descent flow and the Bregman projected (sub)gradient methods in optimization, as e.g. in [BT03]. In [RM15],

it was proven that this relation holds in general between natural gradient descent updates, originally proposed in [Ama98], and mirror descent updates with respect to the convex function inducing the dually flat structure on the manifold.

The geometric Euler (3.71) is also related to line-search methods on manifolds as in [AMS08], based on the concept of retractions. A retraction for a general manifold M is a smooth mapping $\mathcal{R}: TM \rightarrow M$ such that for every $x \in M$, $\mathcal{R}_x: T_x M \rightarrow M$ fulfills $\mathcal{R}_x(0) = x$ and $d\mathcal{R}_x(0)[v] = v$ for every $v \in T_x M$. The line-search method on M for minimizing a given function $\Phi: M \rightarrow \mathbb{R}$ is based on the update $x_{k+1} = \mathcal{R}_{x_k}(h_k \zeta_k)$, where $\zeta_k \in T_{x_k} M$ and $h_k > 0$ are a suitable chosen search direction for minimizing Φ and a positive step-size. Consider the exponential map $\text{Exp}^{(e)}: TW = \mathcal{W} \times \mathcal{T}_{\mathcal{W}} \rightarrow \mathcal{W}$ corresponding to the e -connection. Since $\text{Exp}^{(e)}$ is an exponential map, it obviously fulfills all the requirements to be a retraction on \mathcal{W} . Thus $\mathcal{R} = \text{Exp}^{(e)}$ can be chosen. Keeping in mind the relations $\text{Exp}_W^{(e)} \circ R_W = \exp_W$ for all $W \in \mathcal{W}$ from Lemma 2.3.2 (3) and $\text{grad}_g J_\varepsilon(W) = R_W[\text{grad}_E J_\varepsilon(W)]$ from Corollary 2.3.4, results in

$$\begin{aligned} W^{(k+1)} &= \mathcal{R}_{W^{(k)}}(-h_k \text{grad}_g J_\varepsilon(W^{(k)})) = \text{Exp}_{W^{(k)}}^{(e)}(R_{W^{(k)}}[-h_k \text{grad}_E J_\varepsilon(W^{(k)})]) \\ &= \exp_{W^{(k)}}(-h \text{grad}_E J_\varepsilon(W^{(k)})). \end{aligned}$$

Therefore, the geometric Euler update can also be interpreted as a line-search method on \mathcal{W} in the setting of [AMS08], with the choice $\text{Exp}^{(e)}$ as retraction.

To simplify notation for the subsequent analysis of the geometric Euler scheme (3.71), the following map is defined.

Definition 3.4.1. Define the *geometric Euler map* $\text{GE}: \mathbb{R} \times \mathcal{W} \rightarrow \mathcal{W}$ by

$$(h, W) \mapsto \text{GE}_h(W) := \exp_W(-h \text{grad}_E J_\varepsilon(W)). \quad (3.73)$$

A *geometric Euler (GE) sequence* is a sequence of the form

$$W^{(k+1)} = \text{GE}_{h_k}(W^{(k)}), \quad W^{(0)} \in \mathcal{W} \quad (3.74)$$

with step-sizes $h_k > 0$ for all $k \in \mathbb{N}$.

The next lemma collects some important basic properties of the geometric Euler map, relevant for the convergence analysis below.

Lemma 3.4.1. *Let $h > 0$. Then $\text{grad}_E J_\varepsilon(W) = 0$ if and only if $W = \text{GE}_h(W)$. Additionally, the inequality*

$$h \langle \text{grad}_E J_\varepsilon(W), \text{GE}_h(W) - W \rangle + \text{KL}(\text{GE}_h(W), W) \leq 0 \quad (3.75)$$

holds for all $h > 0$ and $W \in \mathcal{W}$

Proof. Let $\text{grad}_E J_\varepsilon(W) = 0$. Because \exp_W is a Lie group action by Lemma 2.3.2, it directly follows $\text{GE}_h(W) = \exp_W(0) = W$. If $W = \text{GE}_h(W) = \exp_W(-h \text{grad}_E J_\varepsilon(W))$, then it again follows from Lemma 2.3.2 that

$$0 = \exp_W^{-1}(W) = \exp^{-1}(\text{GE}_h(W)) = -h \text{grad}_E J_\varepsilon(W).$$

Since $h > 0$, $\text{grad}_E J_\varepsilon(W) = 0$ follows. To prove inequality (3.75), define

$$F_{h,W}(P) := h \langle \text{grad}_E J_\varepsilon(W), P - W \rangle + \text{KL}(P, W) \quad \forall P \in \mathcal{W}.$$

With this, the characterization of the geometric Euler step in (3.72) is expressed as $\text{GE}_h(W) = \exp_W(-h \text{grad}_E J_\varepsilon(W)) = \text{argmin}_{P \in \Delta^m} \{F_{h,W}(P)\}$, implying the inequality

$$F_{h,W}(\text{GE}_h(W)) = \min_{P \in \Delta^m} \{F_{h,W}(P)\} \leq F_{h,W}(W) = 0. \quad \square$$

3.4.2. L -smooth Adaptability

In order to establish convergence results, it is usually assumed (e.g. [BT03]) that J_ε is convex and globally Lipschitz continuous. Since neither of these assumptions are given in the present case, the concept of L -smooth adaptability, introduced in [BSTV18], is used in a slightly modified version. This concept can be viewed as a generalized Lipschitz condition and is applied to derive the sufficient decrease property of the geometric Euler update for a suitable choice of step-sizes, depending on the constant L .

Definition 3.4.2 (L -smooth adaptable (L -smad) [BSTV18]). Let $\Phi, \Psi: \mathcal{W} \rightarrow \mathbb{R}$ be two C^1 functions and additionally assume Ψ is convex. Then, the pair (Φ, Ψ) is called L -smooth adaptable (L -smad) on a convex subset $K \subset \mathcal{W}$, if there exists a constant $L > 0$ such that $L\Psi - \Phi$ is convex on K .

For proving convergence results, an alternative characterization of the L -smad condition as in [BSTV18, Lemma 2.1] is more convenient. This characterization is also valid on the assignment manifold, as shown next.

Corollary 3.4.2. Let $\Phi, \Psi: \mathcal{W} \rightarrow \mathbb{R}$ be C^1 and suppose Ψ is convex. Then (Φ, Ψ) is L -smad on a convex subset $K \subset \mathcal{W}$ if and only if

$$\Phi(P) - \Phi(W) - \langle \text{grad}_E \Phi(W), P - W \rangle \leq LD_\Psi(P, W) \quad \forall P, W \in K.$$

Proof. Due to Lemma 3.2.4, $L\Psi - \Phi$ is convex on K if and only if

$$0 \leq D_{L\Psi - \Phi}(P, W) = LD_\Psi(P, W) - D_\Phi(P, W) \quad \forall P, W \in K.$$

Bringing $D_\Phi(P, W)$ to the left-hand side together with the definition of D_Φ from (3.28), shows the equivalent characterization. \square

The next proposition gives a sufficient condition on Φ and Ψ such that (Φ, Ψ) is L -smad on compact convex subsets of \mathcal{W} . As a consequence of this, it will be shown that $(J_\varepsilon, -H_{\mathcal{W}})$ is always L -smad on compact convex subsets of the assignment manifold, where $H_{\mathcal{W}}$ is the global entropy from (2.30).

Proposition 3.4.3. Let $\Phi, \Psi: \mathcal{W} \rightarrow \mathbb{R}$ be C^2 and assume Ψ is σ -strongly convex with respect to a norm $\|\cdot\|_p$ on $\mathbb{R}^{m \times n}$. Then, for any compact convex subset $K \subset \mathcal{W}$ there exists a constant $L > 0$, such that (Φ, Ψ) is L -smad on K .

Proof. Let $\eta: \mathcal{W} \rightarrow U_{\mathcal{W}}$ be the isometric chart from Corollary 3.2.3. If $K \subset \mathcal{W}$ is compact convex, then so is $\hat{K} := \eta(K) \subset U_{\mathcal{W}}$, according to Lemma 3.2.4. Define the C^2 function $\alpha_L := L\Psi - \Phi$, with constant $L > 0$ and consider the coordinate expressions $\hat{\alpha}_L$, $\hat{\Psi}$ and $\hat{\Phi}$. Since any two norms on $\mathbb{R}^{m \times n}$ are equivalent, there exists a constant $\nu > 0$ with $\|X\|_p \geq \nu\|X\|$ for all $X \in \mathbb{R}^{m \times n}$. Thus, the fact that Ψ is σ -strongly convex with respect to $\|\cdot\|_p$ and (B.10) gives

$$D_{\hat{\Psi}}(P, W) \geq \frac{\sigma}{2}\|P - W\|_p^2 \geq \frac{\nu\sigma}{2}\|P - W\|^2 \quad \forall P, W \in \hat{K},$$

showing that $\hat{\Psi}$ is $\bar{\sigma} := \nu\sigma$ -strongly convex on \hat{K} (i.e. with respect to $\|\cdot\|$). Due to the characterization (B.6),

$$\langle X, \text{Hess } \hat{\Psi}(\eta)[X] \rangle \geq \bar{\sigma}\|X\|^2 \quad \forall \eta \in U_{\mathcal{W}} \text{ and } \forall X \in \mathbb{R}^{m \times n} \quad (3.76)$$

follows. Denote the maximal eigenvalue of $\text{Hess } \hat{\Phi}(\eta)$ by $\lambda_{\max}^{\hat{\Phi}}(\eta)$. As a consequence of \hat{K} being compact and $\lambda_{\max}^{\hat{\Phi}}(\eta)$ continuously depending on η , the maximum eigenvalue $M_K := \max_{\eta \in \hat{K}} \lambda_{\max}^{\hat{\Phi}}(\eta)$ exists and results in

$$\langle X, \text{Hess } \hat{\Phi}(\eta)[X] \rangle \leq \lambda_{\max}^{\hat{\Phi}}(\eta)\|X\|^2 \leq M_K\|X\|^2 \quad \forall \eta \in U_{\mathcal{W}} \text{ and } \forall X \in \mathbb{R}^{m \times n}. \quad (3.77)$$

Combining the estimates (3.76) and (3.77) finally gives

$$\langle X, \text{Hess } \hat{\alpha}_L(\eta)[X] \rangle \geq (L\bar{\sigma} - M_K)\|X\|^2 \quad (3.78)$$

for all $\eta \in U_{\mathcal{W}}$ and $X \in \mathbb{R}^{m \times n}$. Hence, $L\bar{\sigma} - M_K > 0$ can be achieved by choosing a sufficiently large value for the constant L . This results in $\text{Hess } \hat{\alpha}_L(\eta)$ being positive definite for all $\eta \in \hat{K}$, implying the convexity of $\hat{\alpha}_L$ on \hat{K} . Then, also $\alpha_L = L\Psi - \Phi$ is convex on K , according to Lemma 3.2.4 and proves that (Φ, Ψ) is L -smad on K . \square

Corollary 3.4.4. *For every compact convex subset $K \subset \mathcal{W}$, there exists an $L > 0$ such that $(J_\varepsilon, -H_{\mathcal{W}})$ is L -smad on K .*

Proof. Since $-H_{\mathcal{W}}$ is n^{-1} -strongly convex on \mathcal{W} and $-H_{\mathcal{W}}$ as well as J_ε are C^2 , the statement directly follows from Proposition 3.4.3. \square

Similar to [BSTV18, Lemma 4.1] the L -smad property of $(J_\varepsilon, -H_{\mathcal{W}})$ on compact convex subsets guarantees a sufficient decrease of the objective function values for the geometric Euler updates (3.71).

Lemma 3.4.5 (sufficient decrease). *Let $\alpha \in \mathbb{R}$. Then there is a constant $L > 0$ such that for any parameter $\tau \in [0, 1)$ and step-size $h \in (0, L^{-1}(1 - \tau)]$, the inequality*

$$J_\varepsilon(\text{GE}_h(W)) \leq J_\varepsilon(W) + \tau \langle \text{grad}_E J_\varepsilon(W), \text{GE}_h(W) - W \rangle \leq J_\varepsilon(W) \quad (3.79)$$

holds for all $W \in \text{lev}_\alpha(J_\varepsilon)$, where GE is the geometric Euler map from (3.73).

Proof. By Lemma B.1.1, $K_\alpha := \text{conv}(\text{lev}_\alpha(J_\varepsilon))$ is a compact convex subset of \mathcal{W} . Choose an arbitrarily large $R > 0$. Since the geometric Euler map $\text{GE}: \mathbb{R} \times \mathcal{W} \rightarrow \mathcal{W}$ from (3.73) is continuous, so is $J_\varepsilon \circ \text{GE}: \mathbb{R} \times \mathcal{W} \rightarrow \mathbb{R}$ and obtains a maximum on the compact set $[0, R] \times K_\alpha$, denoted by

$$\bar{\alpha} := \max_{(h,W) \in [0,R] \times K_\alpha} \{J_\varepsilon(\text{GE}_h(W))\} \geq \alpha. \quad (3.80)$$

Define $K_{\bar{\alpha}} := \text{conv}(\text{lev}_{\bar{\alpha}} J_\varepsilon)$. Again by Lemma B.1.1, also $K_{\bar{\alpha}}$ is a compact convex subset of \mathcal{W} and as a consequence of Corollary 3.4.4, there exists a constant $L_{\bar{\alpha}} > 0$ such that $(J_\varepsilon, -H_{\mathcal{W}})$ is $L_{\bar{\alpha}}$ -smad on $K_{\bar{\alpha}}$. Define the desired constant L as

$$L := \max\{L_{\bar{\alpha}}, R^{-1}\} > 0.$$

Notice that $(J_\varepsilon, -H_{\mathcal{W}})$ is also L -smad on $K_{\bar{\alpha}}$, because of $L \geq L_{\bar{\alpha}}$. Since $\alpha \leq \bar{\alpha}$, the inclusion $\text{lev}_\alpha(J_\varepsilon) \subset \text{lev}_{\bar{\alpha}}(J_\varepsilon)$ and thus also $K_\alpha \subset K_{\bar{\alpha}}$ hold.

Now, let $\tau \in [0, 1)$ and $h \in (0, L^{-1}(1 - \tau)]$. Due to the definition of $L > 0$, the inequalities

$$h \leq R \quad \text{and} \quad L < h^{-1}(1 - \tau) \quad (3.81)$$

follow. Suppose an arbitrary $W \in \text{lev}_\alpha(J_\varepsilon)$ is given. Then, (h, W) is contained in $[0, R] \times K_\alpha$ and implies $\text{GE}_h(W) \in K_{\bar{\alpha}}$, as a result of (3.80). Tanks to the equivalent characterization of the L -smad property in Corollary 3.4.2 and the fact that $W, \text{GE}_h(W) \in K_{\bar{\alpha}}$, the inequality

$$J_\varepsilon(\text{GE}_h(W)) - J_\varepsilon(W) - \langle \text{grad}_E J_\varepsilon(W), \text{GE}_h(W) - W \rangle \leq L \text{KL}(\text{GE}_h(W), W) \quad (3.82)$$

holds. Furthermore, the choice of h and Lemma 3.4.1 give

$$L \text{KL}(\text{GE}_h(W), W) \stackrel{(3.81)}{\leq} h^{-1}(1 - \tau) \text{KL}(\text{GE}_h(W), W) \quad (3.83a)$$

$$\stackrel{(3.75)}{\leq} -(1 - \tau) \langle \text{grad}_E J_\varepsilon(W), \text{GE}_h(W) - W \rangle. \quad (3.83b)$$

Overall, the established inequalities lead to

$$\begin{aligned} J_\varepsilon(\text{GE}_h(W)) - J_\varepsilon(W) &\stackrel{(3.82)}{\leq} \langle \text{grad}_E J_\varepsilon(W), \text{GE}_h(W) - W \rangle + L \text{KL}(\text{GE}_h(W), W) \\ &\stackrel{(3.83)}{\leq} \tau \langle \text{grad}_E J_\varepsilon(W), \text{GE}_h(W) - W \rangle, \end{aligned}$$

proving the inequality on the left-hand side of (3.79). The one on the right-hand side follows from $\langle \text{grad}_E J_\varepsilon(W), \text{GE}_h(W) - W \rangle \leq -h^{-1} \text{KL}(\text{GE}_h(W), W) \leq 0$, due to Lemma 3.4.1. \square

3.4.3. Geometric Euler with Armijo Step-Size

The sufficient decrease result in Lemma 3.4.5 shows that a constant $L > 0$ exists such that if the constant step-size $h \in (0, L^{-1}(1 - \tau))$, with $\tau \in (0, 1)$, is chosen in the geometric

Euler update (3.71), then for every $W^{(0)} \in \text{lev}_\alpha(J_\varepsilon)$ the function values $J_\varepsilon(W^{(k)})$ are decreasing. However, in order to choose a constant step-size this way, one has to know or estimate the constant L . This might be infeasible in practice. An alternative approach for obtaining step-sizes which decrease the function value $J_\varepsilon(W^{(k)})$ without knowing L is given by Armijo step-size selection via line-search. This is a well-known technique for step-size selection in optimization problems on real vector spaces [NW06] as well as for optimization on manifolds [AMS08].

In the following, Armijo step-size selection for the geometric Euler on \mathcal{W} is introduced and basic convergence properties are proven.

Definition 3.4.3 (Armijo step-size). Suppose a *descent parameter* $\tau \in (0, 1)$, a *diminishing factor* $s \in (0, 1)$ and a *maximal step-size* $h_{\max} > 0$ is given. Define the function

$$\beta: \mathbb{N} \rightarrow \mathbb{R}, \quad j \mapsto \beta(j) := s^j h_{\max} > 0. \quad (3.84)$$

For $W \in \mathcal{W}$, let $j_{\min}(W) \in \mathbb{N}$ be the smallest integer such that the *Armijo condition*

$$J_\varepsilon(\text{GE}_{\beta(j)}(W)) \leq J_\varepsilon(W) + \tau \langle \text{grad}_E J_\varepsilon(W), \text{GE}_{\beta(j)}(W) - W \rangle \quad \text{for } j \in \mathbb{N} \quad (3.85)$$

is fulfilled, where GE is the geometric Euler map (3.73). The *Armijo step-size* for $W \in \mathcal{W}$ is defined by

$$h_{\tau, s, h_{\max}}(W) := \beta(j_{\min}) = \tau^{j_{\min}} h_{\max} > 0. \quad (3.86)$$

Remark 3.4.1. As a consequence of

$$g_W(\text{grad}_g J_\varepsilon(W), \text{GE}_h(W) - W) = \langle \text{grad}_E J_\varepsilon(W), \text{GE}_h(W) - W \rangle,$$

resulting from $\text{GE}_h(W) - W \in \mathcal{T}_W$ together with (3.44), the Armijo condition (3.85) is exactly the same as the one on manifolds in [AMS08]. However, in what follows the presented version will be more convenient for proving the convergence results and additionally highlights the connection to other optimization techniques in the literature, such as [BSTV18].

Choosing the Armijo step-size for the geometric Euler sequence (3.74) avoids to determine L from Lemma 3.4.5 and potentially allows for a larger step-size locally, while still ensuring the sufficient decrease of the generated sequence. Algorithmically, the Armijo step-size is calculated by successively computing the sequence

$$\beta(0), \beta(1), \beta(2), \dots$$

until the Armijo condition (3.85) is satisfied. The next lemma shows that this procedure always terminates.

Lemma 3.4.6 (Armijo line-search terminates). *Suppose $\tau, s \in (0, 1)$ and $h_{\max} > 0$ are given. Then for every $\alpha \in \mathbb{R}$ there exists a minimal step-size $0 < h_{\min} \leq h_{\max}$ such that the Armijo step-size (3.86) is a well-defined function*

$$h_{\tau, s, h_{\max}}: \text{lev}_\alpha(J_\varepsilon) \rightarrow [h_{\min}, h_{\max}], \quad (3.87)$$

taking only finitely many values, i.e. $|h_{\tau, s, h_{\max}}(\text{lev}_\alpha(J_\varepsilon))| < \infty$.

Proof. Again by Lemma B.1.1 and the compactness of $\text{lev}_\alpha(J_\varepsilon)$, the set $\text{conv}(\text{lev}_\alpha)$ is compact convex. Due to the sufficient decrease property in Lemma 3.4.5, there exists a constant L , such that

$$J_\varepsilon(\text{GE}_h(W)) - J_\varepsilon(W) \leq \tau \langle \text{grad}_E J_\varepsilon(W), \text{GE}_h(W) - W \rangle \quad (3.88)$$

for all $W \in \text{lev}_\alpha(J_\varepsilon)$ and $h \in (0, L^{-1}(1 - \tau)]$. As a result of $s \in (0, 1)$, the function $\beta: \mathbb{N} \rightarrow \mathbb{R}$ from (3.84) is strictly monotonically decreasing and $\lim_{j \rightarrow \infty} \beta(j) = 0$. Thus, there exists the minimal integer $l_{\min} \geq 0$ (not to be confused with the minimal integer in Definition 3.4.3) such that

$$h_{\min} := \beta(l_{\min}) \leq L^{-1}(1 - \tau).$$

Because of $h_{\min} \in (0, L^{-1}(1 - \tau)]$, the sufficient decrease condition (3.88) is fulfilled and therefore also the Armijo condition (3.85). As a consequence of this, the smallest integer $j_{\min}(W)$ satisfying the Armijo condition is upper bounded by l_{\min} and has to be one of the finitely many candidates $0 \leq 1 \leq \dots \leq l_{\min}$. Therefore, the Armijo line-search sequence $\beta(0), \beta(1), \dots$ terminates and $h_{\tau, s, h_{\max}}(W)$ is well-defined for every $W \in \text{lev}_\alpha(J_\varepsilon)$, taking only one of the finitely many possible values

$$h_{\max} = \beta(0) \geq \beta(1) \geq \dots \geq \beta(l_{\min}) = h_{\min} \quad \square$$

In the remaining part of this section, it will be shown that geometric Euler sequences with Armijo step-size inherit the corresponding convergence properties from their continuous counterpart in Section 3.3. For this, it will be convenient to introduce the following notation.

Definition 3.4.4 (geometric Euler sequence with Armijo step-size (GEA)). Let the parameters $\tau, s \in (0, 1)$ and $h_{\max} > 0$ be given. The *geometric Euler map with Armijo step-size* $\text{GE}^A: \mathcal{W} \rightarrow \mathcal{W}$ is defined as

$$W \mapsto \text{GE}^A(W) := \text{GE}_{h(W)}(W)$$

where GE is the geometric Euler map from (3.73) and $h(W) = h_{\tau, s, h_{\max}}(W)$ the Armijo step-size (3.86). The discrete-time dynamical system

$$W^{(k+1)} = \text{GE}^A(W^{(k)}), \quad W^{(0)} \in \mathcal{W} \quad (3.89)$$

is called *geometric Euler sequence with Armijo step-size (GEA)* and the step-size in iteration $k \in \mathbb{N}$ is denoted by $h_k := h(W^{(k)}) > 0$.

In order to study the convergence behavior of GEA-sequences, some basic estimates involving the map GE^A are needed. These are given in the next preparatory lemma.

Lemma 3.4.7. *Let $\alpha \in \mathbb{R}$ and suppose the parameters $\tau, s \in (0, 1)$ as well as $h_{\max} > 0$ are given for the geometric Euler with Armijo step-size. Then,*

$$J_\varepsilon(\text{GE}^A(W)) \leq J_\varepsilon(W), \quad \forall W \in \text{lev}_\alpha(J_\varepsilon) \quad (3.90)$$

and there are constants $C_1, C_2 > 0$ as well as $\bar{C}_1, \bar{C}_2 > 0$ such that

$$C_1 \|\text{GE}^A(W) - W\| \leq \|\text{grad}_E J_\varepsilon(W)\| \leq C_2 \|\text{GE}^A(W) - W\|, \quad (3.91)$$

$$\bar{C}_1 \|\text{GE}^A(W) - W\|^2 \leq J_\varepsilon(W) - J_\varepsilon(\text{GE}^A(W)) \leq \bar{C}_2 \|\text{GE}^A(W) - W\| \quad (3.92)$$

hold for all $W \in \text{lev}_\alpha(J_\varepsilon)$.

Remark 3.4.2. Suppose $(W^{(k)})$ is a GEA-sequence with starting point $W^{(0)} \in \mathcal{W}$ and parameters $\tau, s \in (0, 1)$, $h_{\max} > 0$. Then the inequalities (3.91) and (3.92) say that any of the quantities $\|\text{grad}_E J_\varepsilon(W^{(k)})\|$, $\|W^{(k)} - W^{(k-1)}\|$ or $J_\varepsilon(W^{(k-1)}) - J_\varepsilon(W^{(k)})$ can be used as a criterion for terminating the sequence.

Also, notice that the inequality on the left-hand side of (3.92) really involves the squared Euclidean distance.

Proof. The well-known fact that continuously differentiable maps are Lipschitz continuous on compact convex sets is frequently used in the following. For this, note that the set $K_\alpha := \text{conv}(\text{lev}_\alpha(J_\varepsilon))$ is compact convex by Lemma B.1.1. For simplicity, denote the Armijo step-size (3.86) by $h_W := h_{\tau, s, h_{\max}}(W)$.

First, (3.90) is proven. As a result of Lemma 3.4.6, there is a minimal step-size such that $0 < h_{\min} \leq h_W \leq h_{\max}$ for all $W \in \text{lev}_\alpha(J_\varepsilon)$. Since $h(W)$ fulfills the Armijo condition (3.85), Lemma 3.4.1 gives

$$J_\varepsilon(W) - J_\varepsilon(\text{GE}^A(W)) \geq -\tau \langle \text{grad}_E J_\varepsilon(W), \text{GE}^A(W) - W \rangle \quad (3.93a)$$

$$\geq \frac{\tau}{h_W} \text{KL}(\text{GE}^A(W), W) \geq 0, \quad (3.93b)$$

implying the inequality $J_\varepsilon(\text{GE}^A(W)) \leq J_\varepsilon(W)$ for all $W \in \text{lev}_\alpha(J_\varepsilon)$. It also follows that $J_\varepsilon(\text{GE}^A(W)) \leq J_\varepsilon(W) \leq \alpha$ and thus $\text{GE}^A(W) \in \text{lev}_\alpha(J_\varepsilon)$ for all $W \in \text{lev}_\alpha(J_\varepsilon)$.

Next, the inequality (3.91) is shown. For this, note that $\exp_{\mathbb{1}_{\mathcal{W}}}: \mathcal{T}_{\mathcal{W}} \rightarrow \mathcal{W}$ and $\exp_{\mathbb{1}_{\mathcal{W}}}^{-1}: \mathcal{W} \rightarrow \mathcal{T}_{\mathcal{W}}$ from Section 2.3 are continuously differential. Since K_α is compact convex, $\exp_{\mathbb{1}_{\mathcal{W}}}^{-1}$ is Lipschitz continuous with some constant $L_2 > 0$. Inequality (3.90) for the function values shows $\text{GE}^A(W) \in K_\alpha$ for all $W \in \text{lev}_\alpha(J_\varepsilon)$, resulting in

$$\|\exp_{\mathbb{1}_{\mathcal{W}}}^{-1}(\text{GE}^A(W)) - \exp_{\mathbb{1}_{\mathcal{W}}}^{-1}(W)\| \leq L_2 \|\text{GE}^A(W) - W\|. \quad (3.94)$$

By continuity of $\exp_{\mathbb{1}_{\mathcal{W}}}^{-1}$, the set $\exp_{\mathbb{1}_{\mathcal{W}}}^{-1}(K_\alpha)$ is compact and $\text{conv}(\exp_{\mathbb{1}_{\mathcal{W}}}^{-1}(K_\alpha)) =: M_\alpha$ compact convex, due to Lemma B.1.1. Hence, $\exp_{\mathbb{1}_{\mathcal{W}}}$ is Lipschitz continuous on M_α with some constant $L_1 > 0$. Set $V := \exp_{\mathbb{1}_{\mathcal{W}}}^{-1}(W)$ as well as $U := \exp_{\mathbb{1}_{\mathcal{W}}}^{-1}(\text{GE}^A(W))$. The fact that $U, V \in M_\alpha$ for $W \in \text{lev}_\alpha(J_\varepsilon)$ then implies

$$\|\text{GE}^A(W) - W\| = \|\exp_{\mathbb{1}_{\mathcal{W}}}(U) - \exp(V)\| \leq L_1 \|U - V\|. \quad (3.95)$$

As a result of Lemma 2.3.2 together with the definition of $\text{GE}^A(W)$, the identity

$$-h_W \text{grad}_E J_\varepsilon(W) = \exp_W^{-1}(\text{GE}^A(W)) \stackrel{(2.43c)}{=} \exp_{\mathbb{1}_{\mathcal{W}}}^{-1}(\text{GE}^A(W)) - \exp_{\mathbb{1}_{\mathcal{W}}}^{-1}(W) \quad (3.96)$$

follows. Thus, combining (3.96) with (3.94) and (3.95), keeping $h_{\min} \leq h_W \leq h_{\max}$ in mind and setting $C_1 := (h_{\max} L_1)^{-1} > 0$ as well as $C_2 := h_{\min}^{-1} L_2 > 0$, finally proves the inequality (3.91).

At last, (3.92) is shown. Due to $-H_{\mathcal{W}}$ being n^{-1} -strongly convex by Lemma 3.2.5,

$$\text{KL}(\text{GE}^A(W), W) \geq \frac{n^{-1}}{2} \|\text{GE}^A(W) - W\|^2$$

holds all $W \in \text{lev}_\alpha(J_\varepsilon)$. Combining this with (3.93) and defining $\bar{C}_1 := \tau(2h_{\max}n)^{-1} > 0$ results in the first inequality of (3.92). Because K_α is compact convex, J_ε is Lipschitz continuous with some constant $\bar{C}_2 > 0$ and the second inequality of (3.92) follows from the fact that $J_\varepsilon(W) - J_\varepsilon(\text{GE}^A(W)) \geq 0$. \square

With the estimates from the previous lemma, the discrete analog of Proposition 3.3.3 and 3.3.5 regarding the Riemannian gradient flow can now be shown for GEA-sequences.

Proposition 3.4.8. *Suppose the parameters $\tau, s \in (0, 1)$ and $h_{\max} > 0$ are given. If $(W^{(k)})_{k \in \mathbb{N}}$ is a GEA-sequence with $W^{(0)} \in \mathcal{W}$, then the function values $J_\varepsilon(W^{(k)})$ are monotonically decreasing with limit value*

$$\lim_{k \rightarrow +\infty} J_\varepsilon(W^{(k)}) = \inf_{k \in \mathbb{N}} \{J_\varepsilon(W^{(k)})\} > -\infty. \quad (3.97)$$

Furthermore, $\lim_{k \rightarrow \infty} \text{grad}_E J_\varepsilon(W^{(k)}) = 0$ as well as $\lim_{k \rightarrow \infty} \text{grad}_g J_\varepsilon(W^{(k)}) = 0$ and

$$\lim_{k \rightarrow \infty} \|W^{(k+1)} - W^{(k)}\| = 0.$$

For $\alpha \in \mathbb{R}$, the compact level sets $\text{lev}_\alpha(J_\varepsilon)$ are positively invariant, i.e. $W^{(0)} \in \text{lev}_\alpha(J_\varepsilon)$ implies $W^{(k)} \in \text{lev}_\alpha(J_\varepsilon)$ for all $k \in \mathbb{N}$.

Proof. Let $\alpha \in \mathbb{R}$ and assume $W^{(0)} \in \text{lev}_\alpha(J_\varepsilon)$. According to (3.90) from Lemma 3.4.7, the sequence of function values $J_\varepsilon(W^{(k)})$ is monotonically decreasing and therefore fulfills $J_\varepsilon(W^{(k)}) \leq J_\varepsilon(W^{(0)}) \leq \alpha$ for all $k \in \mathbb{N}$, showing the positive invariance of $\text{lev}_\alpha(J_\varepsilon)$. Due to the monotonicity of the function values, the convergence in (3.97) to the limit value $J_\varepsilon^* := \inf_{k \in \mathbb{N}} \{J_\varepsilon(W^{(k)})\}$ follows.

As a consequence of Lemma 3.4.7 and the fact that $\text{lev}_\alpha(J_\varepsilon)$ is positively invariant, there exist constants $C, C' > 0$ such that

$$C \|\text{grad}_E J_\varepsilon(W^{(k)})\|^2 \stackrel{(3.91)}{\leq} C' \|W^{(k+1)} - W^{(k)}\|^2 \stackrel{(3.92)}{\leq} J_\varepsilon(W^{(k)}) - J_\varepsilon(W^{(k+1)})$$

is fulfilled for all $k \in \mathbb{N}$, resulting in

$$\begin{aligned} C \lim_{k \rightarrow \infty} \|\text{grad}_E J_\varepsilon(W^{(k)})\|^2 &\leq C' \lim_{k \rightarrow \infty} \|W^{(k+1)} - W^{(k)}\|^2 \\ &\leq \lim_{k \rightarrow \infty} \left(J_\varepsilon(W^{(k)}) - J_\varepsilon(W^{(k+1)}) \right) = J_\varepsilon^* - J_\varepsilon^* = 0. \end{aligned}$$

Because of $\|\text{grad}_g J_\varepsilon(W)\| \leq \|\text{grad}_E J_\varepsilon(W)\|$ by Corollary 3.3.2, also $\text{grad}_g J_\varepsilon(W^{(k)})$ converges to zero.

Since any starting point $W^{(0)} \in \mathcal{W}$ is always contained in the level set $\text{lev}_{\alpha_0}(J_\varepsilon)$ with $\alpha_0 := J_\varepsilon(W^{(0)})$, the statements also hold for an arbitrary $W^{(0)} \in \mathcal{W}$. \square

Remark 3.4.3. All that was needed in the preceding proof are the inequality on the right-hand side of (3.91) and the one on the left-hand side of (3.92). In the more general setting of non-convex composite functions in [BSTV18], sequences fulfilling an analogue of these two inequalities plus an additional continuity assumption for the objective function are called *gradient-like descent sequences*. These properties are all that is needed to prove the corresponding results in a more abstract setting, cf. [BSTV18, Prop. 4.1].

3.4.4. Convergence Analysis for Analytic Variational Models

Similar to the continuous-time case, the iterates of numerical methods for minimizing a C^∞ function do not necessarily converge to a single point, see the counterexample from [AMA05] in \mathbb{R}^d . Therefore, some additional assumptions on J_ε are again needed to ensure convergence of the iterates. Once more, the focus will be on analytic variational models in the remaining part of this section. Also in this case, the Lojasiewicz inequality can be used to obtain convergence and stability results of the corresponding discrete-time dynamical system, as proven in [AMA05] for analytic functions on \mathbb{R}^d . In [AB09], even convergence rates are derived. In the following, these results are proven for GEA-sequences on \mathcal{W} under the assumption of J_ε being analytic.

As in the analysis for continuous-time setting in Section 3.3.3, the key argument for proving the results is the fact that the Lojasiewicz inequality can be used to estimate the sum of the length of line segments between iterates, the discrete analogue of the arc length. The corresponding discrete-time version of Lemma 3.3.7 will be proven below.

Corollary 3.4.9. *Let $\alpha \in \mathbb{R}$ and suppose the parameters $\tau, s \in (0, 1)$ and $h_{\max} > 0$ are given. Then, there exists a constant $C > 0$ such that any GEA-sequence $(W^{(k)})_{k \in \mathbb{N}}$ with $W^{(0)} \in \text{lev}_\alpha(J_\varepsilon)$ satisfies*

$$J_\varepsilon(W^{(k)}) - J_\varepsilon(W^{(k+1)}) \geq C \|\text{grad}_E J_\varepsilon(W^{(k)})\| \|W^{(k+1)} - W^{(k)}\| \quad (3.98)$$

for all integers $k \geq 0$. Furthermore, $J_\varepsilon(W^{(k_0+1)}) = J_\varepsilon(W^{(k_0)})$ for some $k_0 \in \mathbb{N}$ implies $W^{(k_0)} = W^{(k)}$ for all $k \geq k_0$.

Remark 3.4.4. These two conditions together are called *strong descent conditions* and are all that is assumed in [AMA05, Thm. 3.2] to prove convergence for analytic functions. This assumption is sufficiently general to cover the analysis of trust-region methods in [AMA05, Sec. 4.2].

Proof. First note that the set $\text{lev}_\alpha(J_\varepsilon)$ is positive invariant by Proposition 3.4.8 and therefore contains $W^{(k)}$ for all $k \in \mathbb{N}$. As a consequence of Lemma 3.4.7, there are constants $\overline{C}_1 > 0$ and $C_2 > 0$ such that

$$\begin{aligned} J_\varepsilon(W^{(k)}) - J_\varepsilon(W^{(k+1)}) &\geq \overline{C}_1 \|W^{(k+1)} - W^{(k)}\|^2 \\ C_2 \|W^{(k+1)} - W^{(k)}\| &\geq \|\text{grad}_E J_\varepsilon(W^{(k)})\| \end{aligned}$$

holds for all $k \in \mathbb{N}$. Combining these inequalities and setting $C := \overline{C}_1 C_2^{-1} > 0$ proves the first statement. For the second statement, assume $J_\varepsilon(W^{(k_0+1)}) = J_\varepsilon(W^{(k_0)})$ for some

$k_0 \in \mathbb{N}$. Then the above inequality gives

$$0 = J_\varepsilon(W^{(k_0)}) - J_\varepsilon(W^{(k_0+1)}) \geq \bar{C}_1 \|W^{(k_0+1)} - W^{(k_0)}\|^2,$$

implying $W^{(k_0+1)} = W^{(k_0)}$. By induction, it follows

$$W^{(k+1)} = \text{GE}^A(W^{(k)}) = \text{GE}^A(W^{(k_0)}) = W^{(k_0+1)} = W^{(k_0)}$$

for $k \geq k_0$. □

Lemma 3.4.10. *Let $J_\varepsilon: \mathcal{W} \rightarrow \mathbb{R}$ be analytic, $Z \in \mathcal{W}$ and $\alpha \in \mathbb{R}$. Suppose the parameter $\tau, s \in (0, 1)$ as well as $h_{\max} > 0$ are given and $U_L \subset \mathcal{W}$ is a neighborhood of Z on which the Łojasiewicz inequality with exponent $\mu \in [0, 1)$ holds. Then there exists a constant $C > 0$ with the following property. For any GEA-sequence $(W^{(k)})_{n \in \mathbb{N}}$ with $W^{(0)} \in \text{lev}_\alpha(J_\varepsilon)$, if there are $k_0 < k_1$ such that $J_\varepsilon(W^{(k)}) \geq J_\varepsilon(Z)$ and $W^{(k)} \in U_L$ for $k_0 \leq k \leq k_1$, then the sum of the length of line segments of $W^{(k)}$, for $k_0 \leq k \leq k_1$, with respect to the Euclidean metric $\|\cdot\|$ is bounded by*

$$\sum_{k=k_0}^{k_1-1} \|W^{(k+1)} - W^{(k)}\| \leq C \left(J_\varepsilon(W^{(k_0)}) - J_\varepsilon(Z) \right)^{1-\mu}. \quad (3.99)$$

Proof. To simplify notation during the proof, define $\Phi(W) := J_\varepsilon(W) - J_\varepsilon(Z)$. Due to Corollary 3.4.9 there exists a constant $C' > 0$ such that for any GEA-sequence with $W^{(0)} \in \text{lev}_\alpha(J_\varepsilon)$ the inequality (3.98) is satisfied for all $k \in \mathbb{N}$. Let $C'' > 0$ and $\mu \in [0, 1)$ be the constants of the Łojasiewicz inequality on U_L from Corollary 3.2.7 and define

$$C := ((1 - \mu)C'C'')^{-1} > 0.$$

If $(W^{(k)})_{k \in \mathbb{N}}$ is a GEA-sequence with $W^{(0)} \in \text{lev}_\alpha(J_\varepsilon)$ and $W^{(k)} \in U_L$ for $k_0 \leq k \leq k_1$, then combining (3.98) and the Łojasiewicz inequality gives

$$\begin{aligned} \Phi(W^{(k)}) - \Phi(W^{(k+1)}) &\geq C' \|\text{grad}_E \Phi(W^{(k)})\| \|W^{(k+1)} - W^{(k)}\| \\ &\geq C' C'' |\Phi(W^{(k)})|^\mu \|W^{(k+1)} - W^{(k)}\| \end{aligned}$$

for $k_0 \leq k \leq k_1$. The remaining proof is divided into two cases.

First assume $\Phi(W^{(k)}) > 0$ for $k_0 \leq k < k_1$. Then the above inequality together with the definition of C results in

$$\|W^{(k+1)} - W^{(k)}\| \leq (1 - \mu)C \frac{\Phi(W^{(k)}) - \Phi(W^{(k+1)})}{(\Phi(W^{(k)}))^\mu} \quad \text{for } k_0 \leq k < k_1. \quad (3.100)$$

Because of $\mu \geq 0$, choosing $\zeta \in \mathbb{R}$ in the interval $0 \leq \Phi(W^{(k+1)}) \leq \zeta \leq \Phi(W^{(k)})$ gives $(\Phi(W^{(k)}))^{-\mu} \leq \zeta^{-\mu}$. As a consequence of this and the fact that $\mu < 1$, the inequality

$$\begin{aligned} \frac{\Phi(W^{(k)}) - \Phi(W^{(k+1)})}{(\Phi(W^{(k)}))^\mu} &= \int_{\Phi(W^{(k+1)})}^{\Phi(W^{(k)})} \frac{1}{(\Phi(W^{(k)}))^\mu} d\zeta \leq \int_{\Phi(W^{(k+1)})}^{\Phi(W^{(k)})} \frac{1}{\zeta^\mu} d\zeta \\ &= (1 - \mu)^{-1} \left((\Phi(W^{(k)}))^{1-\mu} - (\Phi(W^{(k+1)}))^{1-\mu} \right) \end{aligned}$$

holds for $k_0 \leq k < k_1$. Combining this with (3.100) results in the overall estimate for the sum of line segments

$$\begin{aligned} \sum_{k=k_0}^{k_1-1} \|W^{(k+1)} - W^{(k)}\| &\leq C \sum_{k=k_0}^{k_1-1} \left((\Phi(W^{(k)}))^{1-\mu} - (\Phi(W^{(k+1)}))^{1-\mu} \right) \\ &= C \left((\Phi(W^{(k_0)}))^{1-\mu} - (\Phi(W^{(k_1)}))^{1-\mu} \right) \leq C (\Phi(W^{(k_0)}))^{1-\mu}, \end{aligned}$$

where the last inequality is a consequence of $(\Phi(W^{(k_1)}))^{1-\mu} \geq 0$.

Now suppose $\Phi(W^{(k)}) > 0$ for $k_0 \leq k < k_1$ is not true. Since $\Phi(W^{(k)}) \geq 0$ for $k_0 \leq k \leq k_1$ by assumption, the existence of

$$K := \min \{ l \in \mathbb{N} \mid k_0 \leq l < k_1 \text{ and } \Phi(W^{(l)}) = 0 \} < k_1$$

follows. Since the condition $\Phi(W^{(l)}) = 0$ is equivalent to $J_\varepsilon(W^{(l)}) = J_\varepsilon(Z)$, the monotonicity of the function values $J_\varepsilon(W^{(k)})$ from Proposition 3.4.8 results in the equality $J_\varepsilon(W^{(k)}) = J_\varepsilon(Z)$ for $K \leq k \leq k_1$. As a consequence of $K < k_1$, this equality holds at least for K and $K+1$, i.e. $J_\varepsilon(W^{(K)}) = J_\varepsilon(Z) = J_\varepsilon(W^{(K+1)})$. Thus, Corollary 3.4.9 implies

$$W^{(k)} = W^{(K)} \quad \forall k \geq K. \quad (3.101)$$

Due to $\Phi(W^{(k)}) > 0$ for $k_0 \leq k < K$ by the choice of K , the estimate from the first case can be applied for the length of line segments on $k_0 \leq k \leq K$ resulting in

$$\sum_{k=k_0}^{k_1-1} \|W^{(k+1)} - W^{(k)}\| \stackrel{(3.101)}{=} \sum_{k=k_0}^{K-1} \|W^{(k+1)} - W^{(k)}\| \leq C (\Phi(W^{(k_0)}))^{1-\mu}. \quad \square$$

Applying this estimate for the sum of the length of line segments, convergence for GEA-sequences of analytic J_ε can now be proven.

Theorem 3.4.11. *Let $J_\varepsilon: \mathcal{W} \rightarrow \mathbb{R}$ be analytic and assume $(W^{(k)})_{k \in \mathbb{N}}$ is a GEA-sequence with $W^{(0)} \in \text{lev}_\alpha(J_\varepsilon)$ and parameters $\tau, s \in (0, 1)$ as well as $h_{\max} > 0$. Then there exists a critical point $W^* \in \text{lev}_\alpha(J_\varepsilon)$ of J_ε , i.e. $\text{grad}_g J_\varepsilon(W^*) = 0$, such that $\lim_{k \rightarrow \infty} W^{(k)} = W^*$.*

Proof. For completeness, the adapted proof of [AMA05, Thm. 3.2] on \mathcal{W} is given, using Lemma 3.4.10 for estimating the sum of line segments. Due to Proposition 3.4.8, the sequence is contained in the compact set $\text{lev}_\alpha(J_\varepsilon) =: K_\alpha$ and therefore has an accumulation point $W^* \in K_\alpha$, i.e. there is a subsequence $k_1 < k_2 < \dots$ with $\lim_{j \rightarrow \infty} W^{(k_j)} = W^*$. As a consequence of the continuity of J_ε , it follows

$$J_\varepsilon(W^*) = \lim_{j \rightarrow \infty} J_\varepsilon(W^{(k_j)}) = \lim_{k \rightarrow \infty} J_\varepsilon(W^{(k)}). \quad (3.102)$$

Similarly, the continuity of $\text{grad}_g J_\varepsilon: \mathcal{W} \rightarrow \mathcal{T}_\mathcal{W}$ and Proposition 3.4.8 imply

$$\text{grad}_g J_\varepsilon(W^*) = \lim_{j \rightarrow \infty} \text{grad}_g J_\varepsilon(W^{(k_j)}) = \lim_{k \rightarrow \infty} \text{grad}_g J_\varepsilon(W^{(k)}) = 0,$$

showing that W^* is a critical point of J_ε .

As a consequence of J_ε being analytic on \mathcal{W} , Corollary 3.2.7 yields the exists of a neighborhood $U_L \subset \mathcal{W}$ of W^* on which the Lojasiewicz inequality holds with exponent $\mu \in [0, 1)$. In the following, it will be shown by contradiction that for arbitrarily small $r > 0$, with $\overline{B}_r(W^*) \subset U_L$, the iterates $W^{(k)}$ eventually enter $B_r(W^*)$ and never leave. Since r is arbitrarily small, it then follows that $W^{(k)}$ converges to W^* .

Assume an arbitrary $r > 0$ with $\overline{B}_r(W^*) \subset U_L$ is given. Let $C > 0$ be the constant from Lemma 3.4.10 corresponding to the choice $Z = W^*$. As a consequence of $\lim_{k \rightarrow \infty} \|W^{(k+1)} - W^{(k)}\| = 0$ from Proposition 3.4.8 together with (3.102) and the fact that $W^* = \lim_{j \rightarrow \infty} W^{(k_j)}$, there exists an index $k_0 \in \mathbb{N}$ such that

$$\|W^{(k+1)} - W^{(k)}\| < \frac{r}{6} \quad \forall k \geq k_0 \quad (3.103a)$$

$$\|W^{(k_0)} - W^*\| < \frac{r}{6} \quad (3.103b)$$

$$C(J_\varepsilon(W^{(k_0)}) - J_\varepsilon(W^*))^{1-\mu} < \frac{r}{6} \quad (3.103c)$$

holds simultaneously. Now suppose $W^{(k)}$ would leave $B_r(W^*)$ for some $k \geq k_0$, i.e.

$$K := \min \{k > k_0 \mid \|W^{(k)} - W^*\| \geq r\} > k_0$$

exists. The inequalities (3.103a) and (3.103b) result in

$$\|W^{(k_0+1)} - W^*\| \leq \|W^{(k_0+1)} - W^{(k_0)}\| + \|W^{(k_0)} - W^*\| \leq \frac{r}{6} + \frac{r}{6} < r, \quad (3.104)$$

from which $W^{(k_0+1)} \in B_r(W^*)$ and therefore $k_0 < K - 1$ follows. The fact that $W^{(k)}$ is contained in $\overline{B}_r(W^*)$ for $k_0 \leq k \leq K - 1$ by the choice of K together with $J_\varepsilon(W^{(k)}) \geq J_\varepsilon(W^*)$ due to the monotonicity of $J_\varepsilon(W^{(k)})$ shows that the assumptions of Lemma 3.4.10 with constant C for $k_0 \leq k \leq K - 1$ are fulfilled. The resulting upper bound for the sum of line segments then gives

$$\|W^{(K-1)} - W^{(k_0)}\| \leq \sum_{k=k_0}^{K-2} \|W^{(k+1)} - W^{(k)}\| \leq C(J_\varepsilon(W^{(k_0)}) - J_\varepsilon(W^*))^{1-\mu} \stackrel{(3.103c)}{<} \frac{r}{6}.$$

Combining all these estimates yields

$$\|W^{(K)} - W^*\| \leq \|W^{(K)} - W^{(K-1)}\| + \|W^{(K-1)} - W^{(k_0)}\| + \|W^{(k_0)} - W^*\| < \frac{r}{2},$$

contradicting the choice of K . Therefore, $W^{(k)}$ has to be contained in $B_r(W^*)$ for all $k \geq k_0$, proving the statement. \square

Stability of GEA-Sequences

The stability analysis for Riemannian gradient descent flows of analytic J_ε carries over to GEA-sequences, viewed as a discrete-time dynamical system induced by the map GE^A . Again, stability with respect to the Euclidean norm on $\mathbb{R}^{m \times n}$ is considered.

Definition 3.4.5. Let $F: \mathcal{W} \rightarrow \mathcal{W}$ be a continuous map. Consider the discrete-time dynamical system $W^{(k+1)} = F(W^{(k)})$ on \mathcal{W} and suppose $\overline{W} \in \mathcal{W}$ is a fixed point, i.e. $\overline{W} = F(\overline{W})$.

- (1) \overline{W} is (Lyapunov) stable, if for every $r > 0$ there is a $\delta = \delta(r) > 0$ such that if $\|W^{(0)} - \overline{W}\| < \delta$, then $\|W^{(k)} - \overline{W}\| < r$ for all integers $k \geq 0$.
- (2) \overline{W} is asymptotically stable, if it is stable and a constant δ can be chosen such that if $\|W^{(0)} - \overline{W}\| < \delta$ then $\lim_{k \rightarrow \infty} W^{(k)} = \overline{W}$.

In [AMA05, Prop. 3.3], stability of local minima is shown for discrete dynamical systems on \mathbb{R}^d fulfilling the strong descent conditions from Corollary 3.4.9 together with an additional termination criterion. A similar result is also presented in [AMS08] for sequences generated by retractions on a manifold. Subsequently, analogue stability statements as for the continuous-time case are directly proven for GEA-sequences on the assignment manifold.

Theorem 3.4.12. Let $J_\varepsilon: \mathcal{W} \rightarrow \mathbb{R}$ be analytic and suppose the parameters $\tau, r \in (0, 1)$ as well as $h_{\max} > 0$ are given. Then $Z \in \mathcal{W}$ is a local minimum of J_ε if and only if Z is a GEA stable fixed point.

Proof. The first direction is an adapted version from the proof of [AMA05, Prop. 3.3] and is similar to the argument in Theorem 3.4.11. For this, assume Z is a local minimum of J_ε . Then, there exists a neighborhood $U_m \subset \mathcal{W}$ of Z such that $J_\varepsilon(P) \geq J_\varepsilon(Z)$ for all $P \in U_m$ and $\text{grad}_E J_\varepsilon(Z) = 0$. According to Lemma 3.4.1, $Z = \text{GE}^A(Z)$ follows, showing that Z is a GEA fixed point. Due to J_ε being analytic, there is also a neighborhood $U_L \subset \mathcal{W}$ of Z by Corollary 3.2.7 on which the Łojasiewicz inequality is fulfilled with exponent $\mu \in [0, 1)$. Assume an arbitrary $r > 0$ with $\overline{B}_r(Z) \subset U_m \cap U_L$ is given and choose α sufficiently large such that $\overline{B}_r(Z) \subset \text{lev}_\alpha(J_\varepsilon)$ holds. Let $C > 0$ be the constant from Lemma 3.4.10 corresponding to the choices for α and Z . By Lemma 3.4.7, there exists a constant $C' > 0$ with

$$\|\text{GE}^A(W) - W\| \leq C' \|\text{grad}_E J_\varepsilon(W)\| \quad \forall W \in \text{lev}_\alpha(J_\varepsilon).$$

As a consequence of the continuity of J_ε and $\text{grad}_E J_\varepsilon$, there exists a $0 < \delta < \frac{r}{6}$ such that simultaneously

$$\|\text{GE}^A(P) - P\| < \frac{r}{6} \quad \text{and} \quad C(J_\varepsilon(P) - J_\varepsilon(Z))^{1-\mu} < \frac{r}{6} \quad (3.105)$$

for all $P \in B_\delta(Z)$ holds. Now suppose an arbitrary $W^{(0)} \in B_\delta(Z)$ is chosen. It is shown by contradiction that the whole GEA-sequence $W^{(k)}$ lies in $B_r(Z)$. Assume $W^{(k)}$ leaves $B_r(Z)$ for some integer $k > 0$, i.e.

$$K := \inf \{k > 0 \mid \|W^{(k)} - Z\| \geq r\} > 0$$

exists. Due to (3.105), $\|W^{(1)} - W^{(0)}\| < r$ follows, which in turn implies $0 < K - 1$. The fact that $W^{(k)}$ is contained in $B_r(Z) \subset U_L \cap U_m$ for $0 \leq k \leq K - 1$ by the choice

of K , results in $J_\varepsilon(W^{(k)}) \geq J_\varepsilon(Z)$ for $0 \leq k \leq K-1$. Since α was chosen such that $\overline{B}_r(Z) \subset \text{lev}_\alpha(J_\varepsilon)$, the starting point $W^{(0)}$ also lies in $\text{lev}_\alpha(J_\varepsilon)$. Overall, the assumptions of Lemma 3.4.10 with constant C are satisfied, resulting in the estimate

$$\|W^{(K-1)} - W^{(0)}\| \leq \sum_{k=0}^{K-2} \|W^{(k+1)} - W^{(k)}\| \leq C(J_\varepsilon(P) - J_\varepsilon(Z))^{1-\mu} \stackrel{(3.105)}{<} \frac{r}{6}.$$

Combining all the estimates yields

$$\|W^{(K)} - W^{(0)}\| \leq \|W^{(K)} - W^{(K-1)}\| + \|W^{(K-1)} - W^{(0)}\| + \|W^{(0)} - Z\| < \frac{r}{2},$$

contradicting the choice of K . Thus $W^{(k)} \in B_r(Z)$ for all integers $k \geq 0$ has to be true, proving that Z is a stable fixed point.

For the other direction, suppose Z is a stable fixed point. Because J_ε is analytic, there is a neighborhood $U_L \subset \mathcal{W}$ of Z by Corollary 3.2.7 on which the Łojasiewicz inequality with constant $C > 0$ and exponent $\mu \in [0, 1)$ is fulfilled. Choose any $r > 0$ with $\overline{B}_r(Z) \subset U_L$. Since Z is stable, there is a $\delta = \delta(r) > 0$ such that if $W^{(0)} \in B_\delta(Z)$ then $W^{(k)} \in B_r(Z)$ for all $k \geq 0$. To show Z is a local minimum, let $P \in B_\delta(Z)$ be arbitrary. By Theorem 3.4.11, the GEA-sequence $W^{(k)}$ with $W^{(0)} := P$ converges towards a critical point $W^* \in \mathcal{W}$, the function values $J_\varepsilon(W^{(k)})$ are monotonically decreasing and the gradient at W^* vanishes. Due to

$$0 = \text{grad}_g J_\varepsilon(W^*) = R_{W^*} [\text{grad}_E J_\varepsilon(W^*)]$$

and the invertibility of R_{W^*} by Lemma 2.3.1, also $\text{grad}_E J_\varepsilon(W^*) = 0$ follows. As $W^{(k)}$ is contained in $\overline{B}_r(Z)$ for all $k \geq 0$, so is the limit point W^* . As a result of $\overline{B}_r(Z) \subset U_L$, the Łojasiewicz inequality

$$C \|J_\varepsilon(W^*) - J_\varepsilon(Z)\|^\mu \leq \|\text{grad}_E J_\varepsilon(W^*)\| = 0$$

shows $J_\varepsilon(W^*) = J_\varepsilon(Z)$. As a consequence of the monotonicity of $J_\varepsilon(W^{(k)})$,

$$J_\varepsilon(P) = J_\varepsilon(W^{(0)}) \geq J_\varepsilon(W^{(k)}) \geq J_\varepsilon(W^*) = J_\varepsilon(Z)$$

follows. Since $P \in B_\delta(Z)$ was arbitrary, the fixed point Z is a local minimum of J_ε . \square

Theorem 3.4.13. *Let $J_\varepsilon: \mathcal{W} \rightarrow \mathbb{R}$ be analytic and suppose $\tau, r \in (0, 1)$ as well as $h_{\max} > 0$ are given. Then Z is a strict local minimum of J_ε if and only if Z is a GEA asymptotically stable fixed point.*

Proof. Assume Z is a strict local minima of J_ε . Then, $\text{grad}_E J_\varepsilon(Z) = 0$ and there exists a neighborhood $U_m \subset \mathcal{W}$ of Z such that $J_\varepsilon(P) > J_\varepsilon(Z)$ for all $P \in U_m$ with $P \neq Z$. By Corollary 3.2.7, there is a neighborhood U_L of Z on which the Łojasiewicz inequality is valid with constants $C > 0$ and $\mu \in [0, 1)$. Fix a radius $r > 0$ such that $\overline{B}_r(Z) \subset U_m \cap U_L$. According to the previous Theorem 3.4.12, local minima are stable fixed points. Thus there is a $\delta > 0$ such that $W^{(0)} \in B_\delta(Z)$ implies $W^{(k)} \in B_r(Z)$ for all integers $k \geq 0$.

Due to Theorem 3.4.11, the GEA-sequence converges to a fixed point $W^* \in \overline{B}_r(Z) \subset U_L$ with $\text{grad}_E J_\varepsilon(W^*) = 0$. Therefore, the Łojasiewicz inequality on U_L gives

$$C|J_\varepsilon(W^*) - J_\varepsilon(Z)|^\mu \leq \|\text{grad}_E J_\varepsilon(W^*)\| = 0,$$

implying $J_\varepsilon(W^*) = J_\varepsilon(Z)$. Since Z is a strict minimum on U_m and $W^* \in \overline{B}_r(Z) \subset U_m$ by the choice of $r > 0$, equality of the function values results in $Z = W^* = \lim_{k \rightarrow \infty} W^{(k)}$. Thus, the asymptotic stability of Z is established.

Now suppose Z is an asymptotically stable fixed point, i.e. Z is stable and there is a $\delta > 0$ such that $W^{(0)} \in B_\delta(Z)$ implies $\lim_{k \rightarrow \infty} W^{(k)} = Z$. Due to the stability of Z , the previous Theorem 3.4.12 shows the local minimality of Z . By choosing a sufficiently small $\delta > 0$, Z can be assumed to be a minimum on $B_\delta(Z)$. It remains to show Z is also strict on $B_\delta(Z)$. For this, suppose $J_\varepsilon(Z) = J_\varepsilon(P)$ for some $P \in B_\delta(Z)$. As a consequence of Z being asymptotically stable, the iterates $W^{(k)}$ with starting point $W^{(0)} = P$ converge towards Z . By Proposition 3.4.8 the function values $J_\varepsilon(W^{(k)})$ are monotonically decreasing, resulting in the inequality

$$J_\varepsilon(Z) = J_\varepsilon(P) = J_\varepsilon(W^{(k)}) \geq J_\varepsilon(W^{(0)}) \geq \lim_{k \rightarrow \infty} J_\varepsilon(W^{(k)}) = J_\varepsilon(Z).$$

Therefore, $J_\varepsilon(W^{(k)}) = J_\varepsilon(Z)$ is constant for all $k \in \mathbb{N}$. Corollary 3.4.9 then implies that the whole sequence $W^{(k)}$ is constant, resulting in $P = W^{(0)} = \lim_{k \rightarrow \infty} W^{(k)} = Z$. Hence, Z must be a strict minimum on $B_\delta(Z)$. \square

Convergence Rates of GEA-Sequences

In the following, the convergence rates for bounded Bregman proximal gradient sequences from [BSTV18] are proven for GEA-sequences, based on the original proof in [AB09].

Theorem 3.4.14. *Let J_ε be analytic and suppose the parameters $\tau, r \in (0, 1)$ as well as $h_{\max} > 0$ are given. Assume $(W^{(k)})_{k \in \mathbb{N}}$ is a GEA-sequence converging to $W^* \in \mathcal{W}$ and let U_L be a neighborhood of W^* on which the Łojasiewicz inequality is fulfilled with exponent $\mu \in [0, 1)$. Then the following estimates hold for $k \rightarrow \infty$*

(1) *If $\mu = 0$, then $W^{(k)}$ converges in a finite number of steps.*

(2) *If $\mu \in (0, \frac{1}{2}]$, then exist constants $C > 0$ and $\zeta \in (0, 1)$ such that*

$$\|W^{(k)} - W^*\| \leq C\zeta^k.$$

(3) *If $\mu \in (\frac{1}{2}, 1)$, then there exists a $C > 0$ such that*

$$\|W^{(k)} - W^*\| \leq Ck^{-\frac{1-\mu}{2\mu-1}}.$$

Proof. The proof is an adapted version of the one in [AB09] with some necessary modifications. Because $W^{(k)}$ converges to W^* , there exists a $K > 0$ such that $W^{(k)} \in U_L$ for

all $k \geq K$. Also, $J_\varepsilon(W^{(k)}) \geq \lim_{k \rightarrow \infty} J_\varepsilon(W^{(k)}) = J_\varepsilon(W^*)$ by Proposition 3.4.8. Therefore, with the choices $Z = W^*$ and $\alpha = J_\varepsilon(W^{(0)})$, all assumptions of Lemma 3.4.10 are fulfilled and there exists a $C' > 0$ with

$$\sigma_k := \sum_{l=k}^{\infty} \|W^{(l+1)} - W^{(l)}\| \leq C' |J_\varepsilon(W^{(k)}) - J_\varepsilon(W^*)|^{1-\mu} < \infty, \quad \text{for all } k \geq K. \quad (3.106)$$

By definition of σ_k and the triangle inequality,

$$\sigma_k \geq \|W^{(k)} - W^*\| \quad \text{and} \quad \sigma_k - \sigma_{k+1} = \|W^{(k+1)} - W^{(k)}\| \quad \text{for all } k \in \mathbb{N}. \quad (3.107)$$

This equation shows that σ_k is non-negative and monotonically decreasing in k . Thus,

$$\exists k_0 \geq K: \sigma_{k_0} = 0 \quad \Rightarrow \quad \forall k \geq k_0: 0 = \sigma_k \geq \|W^{(k)} - W^*\|. \quad (3.108)$$

In this case, $W^{(k)} = W^*$ is constant for all $k \geq k_0$ and hence, the sequence converges to W^* in a finite number of steps.

To (1): If $\mu = 0$, then $|J_\varepsilon(W^{(k)}) - J_\varepsilon(W^*)|^\mu = 1$ for $J_\varepsilon(W^{(k)}) \neq J_\varepsilon(W^*)$ and $0^0 = 0$ otherwise, according to the adopted convention. Because $W^{(k)} \in U_L$ for $k \geq K$ and $\lim_{k \rightarrow \infty} \text{grad}_E J_\varepsilon(W^{(k)}) = 0$ by Proposition 3.4.8, the Łojasiewicz inequality implies

$$C |J_\varepsilon(W^{(k)}) - J_\varepsilon(W^*)|^\mu \leq \|\text{grad}_E J_\varepsilon(W^{(k)})\| \rightarrow 0 \quad \text{for } k \rightarrow \infty.$$

Hence, there exists a $k_0 \geq K$ with $J_\varepsilon(W^{(k)}) = J_\varepsilon(W^*)$ being constant for all $k \geq k_0$. Then, the estimate (3.106) implies $\sigma_{k_0} = 0$ and as a consequence of (3.108) the sequence $W^{(k)}$ converges to W^* in finitely many steps.

According to Lemma 3.4.7, there exists a constant $C_2 > 0$ with

$$\|\text{grad}_E J_\varepsilon(W^{(k)})\| \leq C_2 \|W^{(k+1)} - W^{(k)}\| \quad \forall k \in \mathbb{N}.$$

Therefore, (3.106) together with the Łojasiewicz inequality on U_L and the above estimate for $\|\text{grad}_E J_\varepsilon(W^{(k)})\|$ imply

$$\begin{aligned} \sigma_k &\leq C' |J_\varepsilon(W^{(k)}) - J_\varepsilon(W^*)|^{1-\mu} \leq C'' \|\text{grad}_E J_\varepsilon(W^{(k)})\|^{\frac{1-\mu}{\mu}} \\ &\leq \tilde{C} \|W^{(k+1)} - W^{(k)}\|^{\frac{1-\mu}{\mu}} = \tilde{C} (\sigma_k - \sigma_{k+1})^{\frac{1-\mu}{\mu}} \end{aligned} \quad (3.109)$$

for $k \geq K$, with suitable choices for $C'', \tilde{C} > 0$.

To (2): If $\mu \in (0, \frac{1}{2}]$, then $1 \leq \frac{1-\mu}{\mu}$. Because $\lim_{k \rightarrow \infty} \|W^{(k+1)} - W^{(k)}\| = 0$ by Proposition 3.4.8, the above chosen constant K can be assumed to be sufficiently large, such that additionally to $W^{(k)} \in U_L$ also $\sigma_k - \sigma_{k+1} = \|W^{(k+1)} - W^{(k)}\| < 1$ for $k \geq K$ holds. In this situation, (3.109) gives

$$\sigma_{k+1} \leq \sigma_k \leq \tilde{C} (\sigma_k - \sigma_{k+1})^{\frac{1-\mu}{\mu}} \leq \tilde{C} (\sigma_k - \sigma_{k+1}) \quad \text{for } k \geq K,$$

where the first inequality follows from the monotonicity of σ_k . Rearranging yields

$$\sigma_{k+1} \leq \frac{\tilde{C}}{1 + \tilde{C}} \sigma_k \quad \text{for } k \geq K.$$

Define $\zeta := \frac{\tilde{C}}{1+\tilde{C}} \in (0, 1)$. Then, it follows from induction that

$$\sigma_k \leq \zeta^{k-K} \sigma_K = C \zeta^k \quad \text{for } k \geq K,$$

with $C := \zeta^{-K} \sigma_K > 0$.

To (3): Since $\mu \in (\frac{1}{2}, 1)$, the variable $\rho := \frac{\mu}{1-\mu}$ is contained in $\rho \in (1, \infty)$. First, suppose $\sigma_{k_0} = 0$ for some $k_0 \geq K$. Then (3.108) again implies $W^{(k)} = W^*$ for all $k \geq k_0$, showing that $W^{(k)}$ converges in finitely many steps and the estimate for the rate of convergence trivially holds. Thus, in the following $\sigma_k > 0$ for $k \geq K$ is assumed. If $t > 0$ is chosen in the interval $0 < \sigma_{k+1} \leq t \leq \sigma_k$, then $\sigma_k^{-\rho} \leq t^{-\rho}$. Define the constant $\tilde{C}' := \tilde{C}^\rho (\rho - 1)^{-1} > 0$. With this, (3.109) can equivalently be rewritten as

$$\begin{aligned} 1 &\leq \tilde{C}^\rho (\sigma_k - \sigma_{k+1}) \sigma_k^{-\rho} = \tilde{C}^\rho \int_{\sigma_{k+1}}^{\sigma_k} \sigma_k^{-\rho} dt \leq \tilde{C}^\rho \int_{\sigma_{k+1}}^{\sigma_k} t^{-\rho} dt \\ &= \frac{\tilde{C}^\rho}{1-\rho} (\sigma_k^{1-\rho} - \sigma_{k+1}^{1-\rho}) = \tilde{C}' (\sigma_{k+1}^{1-\rho} - \sigma_k^{1-\rho}), \end{aligned}$$

for $k \geq K$. By telescopic canceling and $\sigma_K^{1-\rho} > 0$,

$$k - K = \sum_{l=K}^{k-1} 1 \leq \tilde{C}' \sum_{l=K}^{k-1} (\sigma_{l+1}^{1-\rho} - \sigma_l^{1-\rho}) = \tilde{C}' (\sigma_k^{1-\rho} - \sigma_K^{1-\rho}) \leq \tilde{C}' \sigma_k^{1-\rho} \quad \text{for } k \geq K.$$

Therefore, if $k \geq 2K$, then

$$2^{-1}k \leq k - K \leq \tilde{C}' \sigma_k^{1-\rho}. \quad (3.110)$$

Due to the definition of ρ , the expression $0 > 1 - \rho = (1 - 2\mu)(1 - \mu)^{-1}$ follows. Hence, rearranging the above inequality and keeping $1 - \rho < 0$ in mind, yields

$$\|W^{(k)} - W^*\| \stackrel{(3.107)}{\leq} \sigma_k \stackrel{(3.110)}{\leq} (\tilde{C}' 2)^{-\frac{1}{1-\rho}} k^{\frac{1}{1-\rho}} = C k^{-\frac{1-\mu}{2\mu-1}} \quad \text{for } k \geq 2K,$$

with $C := (\tilde{C}' 2)^{-\frac{1}{1-\rho}} > 0$, establishing the desired asymptotic estimate. \square

Chapter 4

Variational Formulation of the Assignment Flow

Comparing the Riemannian gradient descent flow induced by a C^1 function $J: \mathcal{W} \rightarrow \mathbb{R}$

$$\dot{W} = -\text{grad}_g J(W) = -R_W[\text{grad}_E J(W)]$$

with the specific form of the assignment flow

$$\dot{W} = R_W[S(W)],$$

raises the following natural question: Does there exist a potential J such that the assignment flow is a Riemannian gradient descent flow with respect to J , i.e. does the equality $R_W S(W) = -\text{grad}_g J(W)$ hold?

This question will be answered in the beginning of Section 4.1, by proving that no such potential exists (Section 4.1.1). Subsequently, a novel parameterization of the assignment flow is derived by separating a dominant component of the flow, called *S-flow*, that completely determines the remaining component and hence essentially characterizes the assignment flow (Section 4.1.2). As it turns out, the *S-flow* *does* correspond to a non-convex potential, under an additional symmetry assumption with respect to the weights (2.26) that parameterize the similarity matrix (2.57). This potential can be decomposed into two components which clearly identify the two main interacting processes of the assignment flow: regularization and gradually enforcing integral assignments.

Based on this result, a corresponding *continuous-domain variational* formulation is considered in Section 4.2. Well-posedness of the resulting optimization problem is proven (Section 4.2.2), which is not immediate due to nonconvexity, and an algorithm that computes a locally optimal assignment is proposed (Section 4.2.4). A numerical example demonstrates that the PDE-based approach reproduces results obtained with the above discrete-domain variational formulation of the *S-flow*. Finally, a PDE that characterizes global minimizers of the nonconvex objective function is derived under an unrealistic regularity assumption, providing yet another interpretation of the assignment flow.

This chapter is based on a preliminary version of the presented results currently submitted for publication and is available as preprint [SS19b].

4.1. Discrete-Domain Variational Model

In the following, the question from the introduction of this chapter will be negatively answered in Section 4.1.1, by showing that for all practical purposes a potential for the assignment flow does not exist. However, in Section 4.1.2, the assignment flow is decoupled into two separate flows, where one flow, called *S-flow*, steers the other and in this sense dominates the assignment flow. Under the additional assumption that the weights ω_{ij} of the similarity map $S(W)$ in (2.57) are symmetric, it is shown that the dominating *S-flow* is indeed a Riemannian gradient flow induced by a nonconvex potential. This result is the basis for the continuous-domain formulation of the assignment flow studied in Sections 4.2 below. Finally, some basic properties of this potential flow are evaluated by investigating two academical image labeling problems.

4.1.1. Nonexistence of a Potential

In Theorem 4.1.2 below, it is shown that under some mild assumptions on the distance matrix $D_{\mathcal{F}}$ (2.54), which are always fulfilled in practice, no potential J exists that induces the assignment flow (2.62). In order to prove this result, explicit expressions for the differential $dS(W)$ of the similarity map (2.56) and its transpose $dS(W)^\top$ with respect to the standard Euclidean structure on $\mathbb{R}^{m \times n}$ are derived next.

Lemma 4.1.1. *The i -th row of the differential $dS(W)$ is given by*

$$dS_i(W)[X] = \sum_{j \in \mathcal{N}_i} \omega_{ij} R_{S_i(W)} \frac{X_j}{W_j} \quad \text{for all } X \in \mathcal{T}_{\mathcal{W}} \text{ and } i \in \mathcal{V}.$$

Furthermore, the i -th row of the adjoint differential $dS(W)^\top: \mathcal{T}_{\mathcal{W}} \rightarrow \mathcal{T}_{\mathcal{W}}$ with respect to the standard Euclidean inner product on $\mathcal{T}_{\mathcal{W}} \subset \mathbb{R}^{m \times n}$ is given by

$$dS_i(W)^\top[X] = \sum_{j \in \mathcal{N}_i} \omega_{ji} P_{T_S} \frac{R_{S_j(W)} X_j}{W_i} \quad \text{for every } X \in \mathcal{T}_{\mathcal{W}} \text{ and } i \in \mathcal{V}.$$

Proof. Define the map $F_i: \mathcal{W} \rightarrow \mathbb{R}^n$ by $F_i(W) := \sum_{j \in \mathcal{N}_i} \omega_{ij} (\exp_{\mathbb{1}_S}^{-1}(W_j) - \frac{1}{\rho} D_{\mathcal{F}_j})$ for all $W \in \mathcal{W}$. Let $\gamma: (-\varepsilon, \varepsilon) \rightarrow \mathcal{W}$ be a smooth curve, with $\varepsilon > 0$, $\gamma(0) = W$ and $\dot{\gamma}(0) = X$. It then follows for the differential of F_i

$$dF_i(W)[X] = \frac{d}{dt} F_i(\gamma(t)) \Big|_{t=0} = \sum_{j \in \mathcal{N}_i} \omega_{ij} \frac{d}{dt} \exp_{\mathbb{1}_S}^{-1}(\gamma_j(t)) \Big|_{t=0} \stackrel{(2.40)}{=} \sum_{j \in \mathcal{N}_i} \omega_{ij} P_{T_S} \frac{X_j}{W_j}.$$

As a consequence of the explicit expression $S_i(W) = \exp_{\mathbb{1}_S}(F_i(W))$ for the i -th row of the similarity map from Proposition 2.3.5, the differential of S_i is given by

$$\begin{aligned} dS_i(W)[X] &= d \exp_{\mathbb{1}_S}(F_i(W)) [dF_i(W)[X]] \stackrel{(2.40)}{=} R_{\exp_{\mathbb{1}_S}(F_i(W))} dF_i(W)[X] \\ &= R_{S_i(W)} \sum_{j \in \mathcal{N}_i} \omega_{ij} P_{T_S} \frac{X_j}{W_j} = \sum_{j \in \mathcal{N}_i} \omega_{ij} R_{S_i(W)} \frac{X_j}{W_j}, \end{aligned}$$

where $R_{S_i(W)}P_{T_S} = R_{S_i(W)}$ from Lemma 2.3.1 was used to obtain the last equation.

Now let $W \in \mathcal{W}$ as well as $X, Y \in \mathcal{T}_W$ be arbitrary. The symmetry of the matrix $R_{S_i(W)} \in \mathbb{R}^{n \times n}$ and the indicator function of the neighborhoods $\chi_{\mathcal{N}_i}$ (2.24) together with their corresponding symmetry relation (2.25) result in

$$\begin{aligned}
 \langle dS(W)[X], Y \rangle &= \sum_{i \in \mathcal{V}} \langle dS_i(W)[X], Y_i \rangle = \sum_{i \in \mathcal{V}} \sum_{j \in \mathcal{N}_i} \omega_{ij} \left\langle R_{S_i(W)} \frac{X_j}{W_j}, Y_i \right\rangle \\
 &= \sum_{i \in \mathcal{V}} \sum_{j \in \mathcal{V}} \chi_{\mathcal{N}_i}(j) \omega_{ij} \left\langle \frac{X_j}{W_j}, R_{S_i(W)} Y_i \right\rangle = \sum_{i \in \mathcal{V}} \sum_{j \in \mathcal{V}} \chi_{\mathcal{N}_j}(i) \omega_{ij} \left\langle X_j, \frac{R_{S_i(W)} Y_i}{W_j} \right\rangle \quad (4.1) \\
 &= \sum_{j \in \mathcal{V}} \sum_{i \in \mathcal{N}_j} \omega_{ij} \left\langle X_j, P_{T_S} \frac{R_{S_i(W)} Y_i}{W_j} \right\rangle = \sum_{j \in \mathcal{V}} \left\langle X_j, \sum_{i \in \mathcal{N}_j} \omega_{ij} P_{T_S} \frac{R_{S_i(W)} Y_i}{W_j} \right\rangle.
 \end{aligned}$$

On the other hand,

$$\langle dS(W)[X], Y \rangle = \langle X, dS(W)^\top[Y] \rangle = \sum_{j \in \mathcal{V}} \left\langle X_j, dS_j(W)^\top[Y] \right\rangle. \quad (4.2)$$

Because (4.1) and (4.2) hold for all $X, Y \in \mathcal{T}_W$, the formula for $dS_i(W)^\top[X]$ is proven. \square

In order to prove the following nonexistence result, it will be assumed that for at least on node i the corresponding row in the distance matrix $D_{\mathcal{F}_i}$ is not constant, i.e. there is at least one preferred label choice based on the distance information. Since in reality any measured data contains errors, this assumption will always be fulfilled in practice.

Theorem 4.1.2. *Suppose $|\mathcal{X}| = n \geq 3$ and there exists a node $i \in \mathcal{V}$ such that the distance vector $D_{\mathcal{F}_i} \in \mathbb{R}^n$ is not constant, i.e. $D_{\mathcal{F}_i} \notin \mathbb{R}\mathbf{1}_n$. Then no potential function $J: \mathcal{W} \rightarrow \mathbb{R}$ exists satisfying $R_W[S(W)] = -\text{grad}_g J(W)$, i.e. the assignment flow (2.62) is not a Riemannian gradient descent flow.*

Proof. According to Lemma 2.3.1, $R_W[S(W)] = R_W[P_{\mathcal{T}_W}[S(W)]]$ and $R_W: \mathcal{T}_W \rightarrow \mathcal{T}_W$ is invertible. Therefore, the question of the existence of a potential $J: \mathcal{W} \rightarrow \mathbb{R}$ for the assignment flow (2.62) can be transferred to the Euclidean setting by applying $(R_W|_{\mathcal{T}_W})^{-1}$ to both sides of the equation $R_W[S(W)] = -\text{grad}_g J(W) = R_W[-\text{grad}_E J(W)]$, resulting in

$$P_{\mathcal{T}_W}[S(W)] = -\text{grad}_E J(W) \in \mathcal{T}_W.$$

Consider the Riemannian Hessian $\text{Hess}_E J$ from (A.17). In this Euclidean setting,

$$-\text{Hess}_E J(W) \stackrel{(3.11)}{=} -d\text{grad}_E J(W) = d(P_{\mathcal{T}_W} \circ S)(W) = P_{\mathcal{T}_W} dS(W) = dS(W),$$

where the last two equations follows due to $P_{\mathcal{T}_W}$ being linear and $dS(W): \mathcal{T}_W \rightarrow \mathcal{T}_W$. Since the Riemannian Hessian is symmetric by (A.18), it follows that if a potential J

exists, then $\text{Hess}_E J(W)$ and therefore also $dS(W)$ must be symmetric with respect to the Euclidean inner product for every $W \in \mathcal{W}$.

Hence, in order to prove that a potential cannot exist, it is shown that $dS(W)$ is not symmetric at every point $W \in \mathcal{W}$. To this end, a point $W \in \mathcal{W}$ and tangent vector $X \in \mathcal{T}_W$ with $dS(W)[X] - dS(W)^\top[X] \neq 0$ are constructed. It suffices to show

$$dS_j(W)[X] - dS_j(W)^\top[X] \neq 0 \quad \text{for some row index } j \in \mathcal{V}. \quad (4.3)$$

To simplify notation, the j -th row of the distance matrix $D_{\mathcal{F}j}$ is denoted by D_j in the remainder of the proof. Due to the hypothesis,

$$D_i = D_{\mathcal{F}i} \neq \mathbb{R}\mathbf{1}_n. \quad (4.4)$$

Let $k, l \in [n]$ be label indices such that

$$D_i^k = \min_{s \in [n]} D_i^s \quad \text{and} \quad D_i^l = \max_{s \in [n]} D_i^s.$$

Relation (4.4) implies $D_i^k < D_i^l$, resulting in

$$e^{-\frac{1}{\rho}D_i^k} > e^{-\frac{1}{\rho}D_i^l}. \quad (4.5)$$

Using the standard basis \mathcal{B}_n of \mathbb{R}^n , define

$$u := e_k - e_l \in T_{\mathcal{S}}, \quad e_k, e_l \in \mathcal{B}_n. \quad (4.6)$$

Since $n \geq 3$, there is also a point

$$p \in \mathcal{S} \quad \text{with} \quad p \neq \mathbf{1}_{\mathcal{S}} \quad \text{and} \quad p_k = p_l, \quad (4.7)$$

e.g. by choosing $0 < \alpha < \frac{1}{n}$ and setting $p_k = p_l = \alpha$ and $p_r = (n-2)^{-1}(1-2\alpha)$ for all indices $r \notin \{k, l\}$.

With these choices, define the point $W \in \mathcal{W}$, by setting

$$W_j := \exp_p\left(\frac{1}{\rho}D_j\right) \quad \text{for all } j \in \mathcal{V}.$$

According to (2.43a), the j -th row of W can be expressed as $W_j = \exp_{\mathbf{1}_{\mathcal{S}}}(v + \frac{1}{\rho}D_j)$, with $v := \exp_{\mathbf{1}_{\mathcal{S}}}^{-1}(p)$. The expression for the r -th row of the similarity matrix from Proposition 2.3.5 then implies

$$\begin{aligned} S_r(W) &= \exp_{\mathbf{1}_{\mathcal{S}}}\left(\sum_{j \in \mathcal{N}(r)} \omega_{rj} \left(\exp_{\mathbf{1}_{\mathcal{S}}}^{-1}(W_j) - \frac{1}{\rho}D_j\right)\right) \\ &= \exp_{\mathbf{1}_{\mathcal{S}}}\left(\sum_{j \in \mathcal{N}(r)} \omega_{rj} v\right) = \exp_{\mathbf{1}_{\mathcal{S}}}(v) = p, \end{aligned} \quad (4.8)$$

for all $r \in \mathcal{V}$. Now, define the tangent vector $X \in \mathcal{T}_{\mathcal{W}}$ by

$$X_k = \begin{cases} u \in T_{\mathcal{S}}, & \text{if } k = i \\ 0, & \text{if } k \neq i. \end{cases}$$

Using the expressions for $dS_i(W)$ and $dS_i(W)^\top$ from Lemma 4.1.1, one obtains

$$\begin{aligned} dS_i(W)[X] - dS_i(W)^\top[X] &= \omega_{ii} R_{S_i(W)} \frac{X_i}{W_i} - \omega_{ii} P_{\mathcal{T}_{\mathcal{W}}} \frac{R_{S_i(W)} X_i}{W_i} \\ &\stackrel{(4.8)}{=} \omega_{ii} R_p \frac{u}{\exp_p(\frac{1}{\rho} D_i)} - \omega_{ii} P_{\mathcal{T}_{\mathcal{W}}} \frac{R_p u}{\exp_p(\frac{1}{\rho} D_i)} \\ &\stackrel{(2.33)}{=} \omega_{ii} \langle p, e^{\frac{1}{\rho} D_i} \rangle \left(R_p \frac{ue^{-\frac{1}{\rho} D_i}}{p} - P_{\mathcal{T}_{\mathcal{W}}} \left(\frac{e^{-\frac{1}{\rho} D_i}}{p} R_p u \right) \right). \end{aligned} \quad (4.9)$$

Since $\omega_{ii} \langle p, e^{\frac{1}{\rho} D_i} \rangle > 0$, only the expression inside the brackets has to be checked. As for the first term, using the definition of R_p (2.32), one obtains

$$R_p \frac{ue^{-\frac{1}{\rho} D_i}}{p} = ue^{-\frac{1}{\rho} D_i} - \langle u, e^{-\frac{1}{\rho} D_i} \rangle p.$$

Setting $a := (\langle e^{-\frac{1}{\rho} D_i}, \mathbb{1}_{\mathcal{S}} \rangle \mathbb{1}_n - e^{-\frac{1}{\rho} D_i})$, it follow for the second term

$$P_{\mathcal{T}_{\mathcal{W}}} \left(\frac{e^{-\frac{1}{\rho} D_i}}{p} R_p u \right) = P_{\mathcal{T}_{\mathcal{W}}} \left(e^{-\frac{1}{\rho} D_i} u - \langle u, p \rangle e^{-\frac{1}{\rho} D_i} \right) = e^{-\frac{1}{\rho} D_i} u - \langle u, e^{-\frac{1}{\rho} D_i} \rangle \mathbb{1}_{\mathcal{S}} + \langle u, p \rangle a.$$

Thus, the term inside the brackets in (4.9) reads

$$\begin{aligned} R_p \frac{ue^{-\frac{1}{\rho} D_i}}{p} - P_{\mathcal{T}_{\mathcal{W}}} \left(\frac{e^{-\frac{1}{\rho} D_i}}{p} R_p u \right) &= -\langle u, e^{-\frac{1}{\rho} D_i} \rangle p + \langle u, e^{-\frac{1}{\rho} D_i} \rangle \mathbb{1}_{\mathcal{S}} - \langle u, p \rangle a \\ &= \langle u, e^{-\frac{1}{\rho} D_i} \rangle (\mathbb{1}_{\mathcal{S}} - p) - \langle u, p \rangle a. \end{aligned}$$

The choices of u and p in (4.6) and (4.7) imply

$$\langle u, e^{-\frac{1}{\rho} D_i} \rangle = e^{-\frac{1}{\rho} D_i^k} - e^{-\frac{1}{\rho} D_i^l} \stackrel{(4.5)}{>} 0 \quad \text{and} \quad \langle u, p \rangle = p_k - p_l = 0$$

such that

$$\langle u, e^{-\frac{1}{\rho} D_i} \rangle (\mathbb{1}_{\mathcal{S}} - p) - \langle u, p \rangle a = (e^{-\frac{1}{\rho} D_i^k} - e^{-\frac{1}{\rho} D_i^l}) (\mathbb{1}_{\mathcal{S}} - p) \neq 0.$$

can be concluded. This proves (4.3) and consequently the theorem. \square

4.1.2. S-Parameterization and Variational Model

Even though Theorem 4.1.2 says that no potential exists for the assignment flow in general, in this section a "hidden" potential flow is revealed under an additional symmetry assumption on the weights ω_{ij} from (2.26). To this end, the assignment flow is decoupled into two components, where one component depends on the second one. The dominating second one, therefore, provides a new parameterization of the assignment flow. Assuming symmetry of the averaging weights, i.e. $\omega_{ij} = \omega_{ji}$, the dominating flow becomes a Riemannian gradient descent flow. The corresponding potential defined on a continuous domain will be studied in the subsequent Section 4.2.

For notational efficiency, all weights (2.26) are collected into the *averaging matrix*

$$\Omega^\omega \in \mathbb{R}^{m \times m} \text{ with } (\Omega^\omega)_i^j := \chi_{\mathcal{N}_i}(j)\omega_{ij} = \begin{cases} \omega_{ij} & \text{if } j \in \mathcal{N}_i, \\ 0 & \text{else} \end{cases}, \quad \text{for } i, j \in \mathcal{V}, \quad (4.10)$$

where $\chi_{\mathcal{N}_i}(j)$ is the indicator function of the neighborhoods (2.24). Due to the properties of the weights,

$$\Omega^\omega \mathbf{1}_m = \mathbf{1}_m \quad (4.11)$$

holds and the symmetry of the averaging matrix Ω^ω is equivalent to the symmetry $\omega_{ij} = \omega_{ji}$ of the weights.

For an arbitrary matrix $M \in \mathbb{R}^{m \times n}$, the average of its row vectors using the weights indexed by the neighborhood \mathcal{N}_i is given by the corresponding row vectors of the matrix $\Omega^\omega M$, i.e.

$$\sum_{k \in \mathcal{N}_i} \omega_{ik} M_k = (\Omega^\omega M)_i, \quad \forall i \in \mathcal{V}. \quad (4.12)$$

Next, a new representation of the assignment flow is introduced based the averaging matrix.

Proposition 4.1.3. *The assignment flow (2.62) is equivalent to the system*

$$\dot{W} = R_W[\bar{S}] \quad \text{with } W(0) = \mathbf{1}_W \quad (4.13a)$$

$$\dot{\bar{S}} = R_{\bar{S}}[\Omega^\omega \bar{S}] \quad \text{with } \bar{S}(0) = S(\mathbf{1}_W). \quad (4.13b)$$

Remark 4.1.1. Observe that the flow $W(t)$ is completely determined by $\bar{S}(t)$. In the following, the dominating part (4.13b) is referred to as the *S-flow*. In order to stress the underlying connection to the assignment flow and to simplify notation, the *S-flow* \bar{S} is again denoted by S .

Proof. Let $W(t)$ be a solution of the assignment flow, i.e. $\dot{W}_i = R_{W_i} S_i(W)$ for all $i \in \mathcal{V}$. Set $\bar{S}(t) := S(W(t))$. Then (4.13a) is immediate from the assumption on W . Using the expression for $dS_i(W)$ from Lemma 4.1.1 gives

$$\dot{\bar{S}}_i = \frac{d}{dt} S(W)_i = dS_i(W)[\dot{W}] = \sum_{j \in \mathcal{N}_i} \omega_{ij} R_{S_i(W)} \frac{\dot{W}_j}{W_j}. \quad (4.14)$$

Since W solves the assignment flow and $\ker(R_{S_i(W)}) = \mathbb{R}\mathbf{1}_n$ by Lemma 2.3.1, it follows from the explicit expression (2.32) of $R_{S_i(W)}$ that

$$\begin{aligned} R_{S_i(W)} \frac{\dot{W}_j}{W_j} &= R_{S_i(W)} \frac{R_{W_j} S_j(W)}{W_j} = R_{S_i(W)} \left(S_j(W) - \langle W_j, S_j(W) \rangle \mathbf{1}_n \right) \\ &= R_{S_i(W)} S_j(W). \end{aligned}$$

Substitution of this identity into (4.14) and keeping $S_i(W) = \bar{S}_i$ in mind, results in

$$\dot{\bar{S}}_i = \sum_{j \in \mathcal{N}_i} \omega_{ij} R_{S_i(W)} S_j(W) = R_{\bar{S}_i} \sum_{j \in \mathcal{N}_i} \omega_{ij} \bar{S}_j \stackrel{(4.12)}{=} R_{\bar{S}_i} (\Omega^\omega \bar{S})_i \quad \text{for all } i \in \mathcal{V}.$$

Collecting these vectors as row vectors of the matrix $\dot{\bar{S}}$ gives (4.13b). \square

Next, it will be shown that the S -flow, which essentially determines the assignment flow (Remark 4.1.1), becomes a Riemannian descent flow under the additional assumption that the averaging matrix (4.10) is symmetric.

Proposition 4.1.4. *Suppose the weights defining the similarity matrix in (2.56) are symmetric, i.e. $(\Omega^\omega)^\top = \Omega^\omega$. Then the S -flow (4.13b) is a Riemannian gradient decent flow $\dot{S} = -\text{grad}_g J(S)$, induced by the potential*

$$J(S) := -\frac{1}{2} \langle S, \Omega^\omega S \rangle, \quad S \in \mathcal{W}. \quad (4.15)$$

Proof. Since J is defined on all of $\mathbb{R}^{m \times n}$ and Ω^ω is symmetric, the ordinary gradient is given by $\partial J(S) = -\Omega^\omega S$. Due to Corollary 2.3.4, the Riemannian gradient is expressed as $\text{grad}_g J(S) = R_S[\partial J(S)] = -R_S[\Omega^\omega S]$. \square

It is interesting to note that the decoupling of the assignment flow in the continuous-time case has an analogue in the discrete-time setting. Due to Proposition 4.1.4, this discretization of the S -flow (4.17b) is nothing else than the corresponding geometric Euler discretization of the Riemannian gradient descent flow with respect to the objective function J .

Proposition 4.1.5. *The geometric Euler integration (2.66) of the assignment flow (2.62) with step-sizes $h_k > 0$, given by*

$$W^{(k+1)} = \exp_{W^{(k)}}(h_k S(W^{(k)})) \quad (4.16)$$

is equivalent to the geometric Euler integration of the decoupled system (4.13), given by

$$W^{(k)} = \exp_{W^{(k)}}(h_k \bar{S}^{(k)}) \quad \text{with } W^{(0)} = \mathbf{1}_W \quad (4.17a)$$

$$\bar{S}^{(k)} = \exp_{\bar{S}^{(k)}}(h_k \Omega^\omega \bar{S}^{(k)}) \quad \text{with } \bar{S}^{(0)} = S(\mathbf{1}_W). \quad (4.17b)$$

Proof. Assume $W^{(k)}$ is the discrete-time solution of the assignment flow given by (4.16) and define $\bar{S}^{(k)} := S(W^{(k)})$ for all $k \in \mathbb{N}$. Then (4.17a) is a direct consequence of the assumption on $W^{(k)}$. Using (2.43a), $W_i^{(k+1)}$ can be rewritten as

$$W_i^{(k+1)} = \exp_{W_i^{(k)}}(h_k \bar{S}_i^{(k)}) = \exp_{\mathbb{1}_S}(\exp_{\mathbb{1}_S}^{-1}(W^{(k)}) + h_k \bar{S}_i^{(k)}) \quad (4.18)$$

for every $i \in \mathcal{V}$. As a result of the explicit expression (2.57) for $\bar{S}_i^{(k)} = S_i(W^{(k)})$ from Proposition 2.3.5, it follows

$$\begin{aligned} \exp_{\mathbb{1}_S}^{-1}(\bar{S}_i^{(k+1)}) &\stackrel{(2.57)}{=} \sum_{j \in \mathcal{N}_i} \omega_{ij} \left(\exp_{\mathbb{1}_S}^{-1}(W_j^{(k+1)}) - \frac{1}{\rho} D_{\mathcal{F}j} \right) \\ &\stackrel{(4.18)}{=} \sum_{j \in \mathcal{N}_i} \omega_{ij} \left(\exp_{\mathbb{1}_S}^{-1}(W_j^{(k)}) - \frac{1}{\rho} D_{\mathcal{F}j} \right) + h_k \sum_{j \in \mathcal{N}_i} \omega_{ij} \bar{S}_j^{(k)} \\ &\stackrel{(2.57)}{=} \exp_{\mathbb{1}_S}^{-1}(\bar{S}_i^{(k)}) + h_k \left(\Omega^\omega \bar{S}^{(k)} \right)_i, \end{aligned}$$

where the last equality also used the relation (4.12) for the last term. Applying $\exp_{\mathbb{1}_S}$ to both sides and again using (2.43a) gives

$$\bar{S}_i^{(k+1)} = \exp_{\mathbb{1}_S} \left(\exp_{\mathbb{1}_S}^{-1}(\bar{S}_i^{(k)}) + h_k \left(\Omega^\omega \bar{S}^{(k)} \right)_i \right) = \exp_{\bar{S}_i^{(k)}} \left(h_k \left(\Omega^\omega \bar{S}^{(k)} \right)_i \right) \quad \text{for all } i \in \mathcal{V}.$$

Collecting these vectors as row vectors of the matrix $\dot{\bar{S}}$ results in (4.17b). \square

In the following, an alternative expression for the objective function J is derived. For this, consider the matrix

$$L_{\mathcal{G}} = I_m - \Omega^\omega \in \mathbb{R}^{m \times m}, \quad (4.19)$$

where I_m denotes the identity matrix. Since $I_m = \text{Diag}(\Omega^\omega \mathbb{1}_m)$ by (4.11) is the degree matrix of the symmetric averaging matrix Ω^ω , $L_{\mathcal{G}}$ can be regarded as Laplacian (matrix) of the underlying undirected weighted graph $\mathcal{G} = (\mathcal{V}, \mathcal{E})$ ¹. For the analysis of the S -flow it will be convenient to rewrite the potential (4.15) accordingly.

Proposition 4.1.6. *Under the assumption of Proposition 4.1.4, the potential (4.15) can be written in the form*

$$J(S) = \frac{1}{2} \langle S, L_{\mathcal{G}} S \rangle - \frac{1}{2} \|S\|^2 = \frac{1}{4} \sum_{i \in \mathcal{V}} \sum_{j \in \mathcal{N}_i} \omega_{ij} \|S_i - S_j\|^2 - \frac{1}{2} \|S\|^2. \quad (4.20)$$

The matrix $L_{\mathcal{G}}$ is symmetric, positive semidefinite and $L_{\mathcal{G}} \mathbb{1}_n = 0$.

¹For undirected graphs, the graph Laplacian is commonly defined by the weighted *adjacency* matrices with diagonal entries 0, whereas $\Omega_{ii}^\omega = \omega_{ii} > 0$. The diagonal entries do not affect the quadratic form (4.20), however.

Proof. From the expression of the Laplacian (4.19) and the potential (4.15),

$$J(S) = -\frac{1}{2}(\langle S, (\Omega^\omega - I_m)S \rangle + \langle S, S \rangle) = \frac{1}{2}(\langle S, L_G S \rangle - \|S\|^2)$$

directly follows. Thus, the focus will be on the double sum of (4.20).

First, note that $\|S_j - S_i\|^2 = \langle S_j, S_j - S_i \rangle + \langle S_i, S_i - S_j \rangle$. As a consequence of the symmetry relation $\chi_{\mathcal{N}_i}(j) = \chi_{\mathcal{N}_j}(i)$ for the indicator functions of the neighborhoods (2.24) as well as the symmetry assumption on the weights $\omega_{ij} = \omega_{ji}$, the identity

$$\begin{aligned} \sum_{i \in \mathcal{V}} \sum_{j \in \mathcal{N}_i} \omega_{ij} \langle S_j, S_j - S_i \rangle &= \sum_{i, j \in \mathcal{V}} \chi_{\mathcal{N}_i}(j) \omega_{ij} \langle S_j, S_j - S_i \rangle = \sum_{i, j \in \mathcal{V}} \chi_{\mathcal{N}_j}(i) \omega_{ji} \langle S_j, S_j - S_i \rangle \\ &= \sum_{j \in \mathcal{V}} \sum_{i \in \mathcal{N}_j} \omega_{ji} \langle S_j, S_j - S_i \rangle = \sum_{i \in \mathcal{V}} \sum_{j \in \mathcal{N}_i} \omega_{ij} \langle S_i, S_i - S_j \rangle \end{aligned} \quad (4.21)$$

follows, where the last equality results from renaming the indices i and j . Thus, using the properties of the weights (2.26),

$$\begin{aligned} \sum_{i \in \mathcal{V}} \sum_{j \in \mathcal{N}_i} \omega_{ij} \|S_i - S_j\|^2 &= \sum_{i \in \mathcal{V}} \sum_{j \in \mathcal{N}_i} \omega_{ij} \langle S_j, S_j - S_i \rangle + \sum_{i \in \mathcal{V}} \sum_{j \in \mathcal{N}_i} \omega_{ij} \langle S_i, S_i - S_j \rangle \\ &\stackrel{(4.21)}{=} 2 \sum_{i \in \mathcal{V}} \sum_{j \in \mathcal{N}_i} \omega_{ij} \langle S_i, S_i - S_j \rangle = 2 \sum_{i \in \mathcal{V}} \left\langle S_i, S_i - \sum_{j \in \mathcal{N}_i} \omega_{ij} S_j \right\rangle \\ &= 2 \sum_{i \in \mathcal{V}} \langle S_i, (L_G S)_i \rangle = 2 \langle S, L_G S \rangle. \end{aligned}$$

The properties of L_G follow from the symmetry of Ω^ω , nonnegativity of the quadratic form in the above equation and definition (4.19). \square

The expression in (4.20) allows to clearly identify the two competing ‘forces’ governing the S -flow, and due to the decomposition (4.13) also the assignment flow: *regularization* through the convex term

$$J_{\text{reg}}(S) := \frac{1}{2} \langle S, L_G S \rangle = \frac{1}{4} \sum_{i \in \mathcal{V}} \sum_{j \in \mathcal{N}_i} \omega_{ij} \|S_i - S_j\|^2, \quad S \in \mathcal{W}, \quad (4.22)$$

favoring constant assignments and *integrality enforcing* through the concave part

$$J_{\text{int}}(S) := -\frac{1}{2} \|S\|^2, \quad S \in \mathcal{W}. \quad (4.23)$$

Lemma 4.1.7. *For all $p \in \Delta$ the inequality $\|p\| \leq 1$ holds and $\|p\| = 1$ if and only if p is a standard basis vectors of \mathbb{R}^n , i.e. $p \in \mathcal{B}_n$.*

Proof. The first inequality and the ‘if’ statement are obvious. As for the ‘only if’, suppose $p = p^i e_i \notin \mathcal{B}_n$, i.e. $p^i < 1$ for all $i \in [n]$. Then $(p^i)^2 < p^i$ and $\|p\|^2 < \|p\|_1 = 1$. \square

As a consequence of this property, the integrality term J_{int} attains its minimum

$$\min_{S \in \mathcal{W}} \{J_{\text{int}}(S)\} = -\frac{1}{2}m \quad (4.24)$$

only at the vertices of the simplex, representing integral (unique) label decisions. Therefore, in contrast to classical methods, where a post-processing step is needed to achieve integrality, the dynamics of the S -flow (and therefore also the assignment flow) has a built in state depending mechanism to continuously enforce integrality.

Introducing an additional parameter $\alpha > 0$ in the model enables to trade off the influence of integrality enforcing against regularization

$$J_\alpha(S) := J_{\text{reg}} + \alpha J_{\text{int}} = \frac{1}{2} \langle S, L_{\mathcal{G}} S \rangle - \alpha \frac{1}{2} \|S\|^2, \quad S \in \mathcal{W}. \quad (4.25)$$

Since J_α is a continuous function on the compact set $\overline{\mathcal{W}} = \Delta^m$, the existence of minimizers on Δ^m is ensured. For α tending towards 0, the integrality enforcing term J_{int} vanishes in the limit and the model reduces to a convex function $J_\alpha = J_{\text{reg}}$ with global minimizers given by constant assignments. For very large α , the dynamics is dominated by the integrality term J_{int} and the influence of regularization through J_{reg} is greatly diminished.

Since the function J_α is defined on all of $\mathbb{R}^{m \times n}$, the ordinary gradient is given by

$$\partial J_\alpha(S) = (L_{\mathcal{G}} - \alpha I_m) S \stackrel{(4.19)}{=} ((1 - \alpha)I_m - \Omega^\omega) S, \quad \forall S \in \mathcal{W},$$

where I_m denotes the $m \times m$ identity matrix. The resulting Riemannian gradient descent flow on the assignment manifold \mathcal{W} has the form

$$\dot{S} = -\text{grad}_g J_\alpha(S) = R_S[(\alpha I_m - L_{\mathcal{G}})S], \quad S(0) = S(\mathbb{1}_{\mathcal{W}}) \in \mathcal{W}.$$

4.1.3. Experiments

In the following, two academical examples are presented to illustrate and assess basic properties of the S -flow under the symmetry assumption $(\Omega^\omega)^\top = \Omega^\omega$ of the weights. For this, the framework of log-barrier perturbed objective functions from Chapter 3 is applied and GEA-sequences from Section 3.4.3 are used for numerical integration of the resulting perturbed Riemannian gradient flow. Both examples are represented on the grid graph from Section 2.3.1.

Perturbed model and flow. The perturbed variational model is given by

$$J_{\alpha;\varepsilon}(S) := (J_\alpha)_\varepsilon(S) = J_\alpha(S) - \varepsilon \langle \log(S), \mathbb{1}_{\mathcal{W}} \rangle, \quad S \in \mathcal{W}, \quad (4.26)$$

with $0 < \varepsilon \ll 1$. By Lemma 3.1.2, the Euclidean gradient has the form

$$\text{grad}_E J_{\alpha;\varepsilon}(S) = P_{\mathcal{T}_{\mathcal{W}}}[(L_{\mathcal{G}} - \alpha I_m)S - \varepsilon \mathbb{1}_{\mathcal{W}}/S], \quad S \in \mathcal{W}, \quad (4.27)$$

resulting in the perturbed Riemannian gradient flow

$$\dot{S} = R_S[(\alpha I_m - L_G)S] + \varepsilon(\mathbb{1}_{\mathcal{W}} - S), \quad S(0) = S(\mathbb{1}_{\mathcal{W}}) \in \mathcal{W}. \quad (4.28)$$

Due to $J_{\alpha;\varepsilon}: \mathcal{W} \rightarrow \mathbb{R}$ being analytic, the convergence and stability results from Section 3.3.3 apply.

Numerical integration. For parameters $\tau, s \in (0, 1)$ and $h_{\max} > 0$, the general update scheme of a GEA-sequence (3.89) is of the form

$$S^{(k+1)} = \text{GE}^A(S^{(k)}) = \exp_{S^{(k)}}\left(-h_k \text{grad}_E J_{\alpha;\varepsilon}(S^{(k)})\right), \quad S^{(0)} = S(\mathbb{1}_{\mathcal{W}}) \in \mathcal{W}, \quad (4.29)$$

where the step-size $h_k = h(S^{(k)}) > 0$ is the Armijo step-size (3.86) depending on the choices for the descent parameter τ , the diminishing factor s and the maximal step-size h_{\max} . Replacing the Euclidean gradient by the explicit expression in (4.27) and using the fact that the liftmap implicitly projects onto $\mathcal{T}_{\mathcal{W}}$ according to (2.38), the update scheme reads

$$S^{(k+1)} = \exp_{S^{(k)}}\left(h_k\left((\alpha I_m - L_G)S^{(k)} + \varepsilon\mathbb{1}_{\mathcal{W}}/S^{(k)}\right)\right), \quad S^{(0)} = S(\mathbb{1}_{\mathcal{W}}).$$

As a consequence of $J_{\alpha;\varepsilon}: \mathcal{W} \rightarrow \mathbb{R}$ being analytic, the convergence and stability results from Section 3.4 are valid.

Termination criterion. In both experiments, the *normalized relative change* of $J_{\alpha;\varepsilon}$

$$\text{nrc}J_{\alpha;\varepsilon}(S^{(k)}) := \frac{J_{\alpha;\varepsilon}(S^{(k)}) - J_{\alpha;\varepsilon}(S^{(k+1)})}{h_k |J_{\alpha;\varepsilon}(S^{(k)})|} \geq 0 \quad (4.30)$$

is used as convergence criterion. Using the properties of the liftmap from Lemma 2.3.2, it can be shown that for $h_k \rightarrow 0$, the nrc of $J_{\alpha;\varepsilon}$ approaches

$$-\frac{\frac{d}{dh_k} J_{\alpha;\varepsilon}(S^{(k)})|_{h_k=0}}{|J_{\alpha;\varepsilon}(S^{(k)})|} = \frac{\|\text{grad}_g J_{\alpha;\varepsilon}(S^{(k)})\|_{g,S^{(k)}}^2}{|J_{\alpha;\varepsilon}(S^{(k)})|} \geq 0 \quad (4.31)$$

and is therefore an approximation of the relative continuous-time change (3.3) for the underlying Riemannian gradient flow.

Symmetric uniform weights. Consider a general grid graph $\mathcal{G}_g = (\mathcal{V}_g, \mathcal{E}_g)$. For a vertex $i \in \mathcal{V}_g$ in the interior of the grid with an associated $N \times N$ neighborhood \mathcal{N}_i , uniform weights $\omega_{ij} = \frac{1}{|\mathcal{N}_i|} = \frac{1}{N^2}$ for all $j \in \mathcal{N}_i$ are chosen. Since $|\mathcal{N}_i| < N^2$ for vertices $i \in \mathcal{V}$ close to the boundary of the grid, symmetry of the weights can only be ensured if $\omega_{ij} = \frac{1}{N^2}$ for $i \neq j \in \mathcal{N}_i$ and the remaining mass is concentrated at the center weight ω_{ii} . Overall, the *symmetric uniform weights*, used in the following examples, are defined as

$$\omega_{ij} := \begin{cases} \frac{1}{N^2} & , \text{ for } i \neq j \\ \frac{1}{N^2}(1 + N^2 - |\mathcal{N}_i|) & , \text{ for } i = j. \end{cases} \quad (4.32)$$

Unbiased Geometric Regularization

The image labeling experiment from [ÅPSS17, Fig. 6] is used to evaluate the influence of ρ and the neighborhood size $|\mathcal{N}_i| = N \times N$ on the performance of geometric regularization of the S -flow in an unbiased way. The spatial structure of the data is given by a grid graph \mathcal{G}_g with $\mathcal{V} = [256] \times [256]$ pixels (see Section 2.3.1). In order for the distance matrix not to be biased towards any specific label, every pixel can take one of 31 possible discrete values with uniform distance between the values. This is modeled on the set of standard basis vectors in \mathbb{R}^{31} as metric space and labels space

$$\mathcal{F} = \mathcal{B}_{31} = \{e_1, \dots, e_{31}\} = \mathcal{X}$$

with distance measure $d_{\mathcal{F}}(f, f') := \|f - f'\|_1$. Thus, for any given input data $f: \mathcal{V}_g \rightarrow \mathcal{F}$, the entries of the distance matrix are given by

$$D_{\mathcal{F}_i}^j = \|e_i - e_j\|_1 = \begin{cases} 2 & , \text{ for } i \neq j \\ 0 & , \text{ else} \end{cases}$$

and are therefore unbiased towards any label. The underlying ground truth pattern together with a noisy version used as input for the model $J_{\alpha;\varepsilon}$ (4.26) is depicted on the left in Figure 4.1, where the 31 elements of $\mathcal{F} = \mathcal{X}$ are encoded by 31 different colors for visualization purposes. Symmetric uniform weights (4.32) are used for regularization together with the integrality enforcing parameter $\alpha = 1$ and perturbation parameter $\varepsilon = 10^{-10}$. For the GEA update scheme (4.29), the chosen parameters are $\tau = 0.01$, $s = 0.5$ and $h_{\max} = 0.5$. The iteration is terminated if the nrc of $J_{\alpha;\varepsilon}$ (4.30) drops below the threshold of 10^{-6} . In all experiments, the step-size of the last iterate was maximal, i.e. $h_k = 0.5$, meaning the function value in the last iteration changed less than $5 \cdot 10^{-7}$ percent.

The 3 by 3 image array on the right-hand side of Figure 4.1 shows the influence of different choices for $\rho \in \{0.01, 0.1, 1.0\}$ and $N \in \{3, 5, 11\}$ on the regularization properties of the model $J_{\alpha;\varepsilon}$. The color values of each image represent the expected label value $\mathbb{E}_{S_i}[\mathcal{X}] = \sum_{j \in [31]} S_i^j \ell_j$ for every pixel i , given the assignments S after termination of the sequence. Increasing the neighborhood size results in more regularized assignments but also in an increasing loss of pattern structure by favoring rounded edges. The effect of ρ appears to depend on the given neighborhood size N . For a small size of $N = 3$, larger ρ values produce less noisy assignments, while for a larger size of $N = 11$, an increase of ρ leads to an additional loss in spatial structure, as can be seen in the last row for the bottom right structure of the images. In the case of $N = 5$, the effect of ρ in the parameter range $(0.01, 1.0)$ seem negligible.

In Figure 4.2, the effect of different neighborhood sizes N and parameters ρ on nrc $J_{\alpha;\varepsilon}$ as well as the average values of J_{int} and J_{reg} can be seen. The *left column* of Figure 4.2 corresponds to the choices of $N \in \{3, 5, 11\}$ for fixed $\rho = 1.0$. In this case, the values of $\frac{1}{m} J_{\text{int}}$ (top left) rapidly decrease within the first 300 iterations, slightly delayed for increased neighborhood sizes N . Since $\frac{1}{m} J_{\text{int}}$ has the minimal value of $-\frac{1}{2}$ by (4.24), corresponding to integral assignments, this plot shows that unique label decisions are

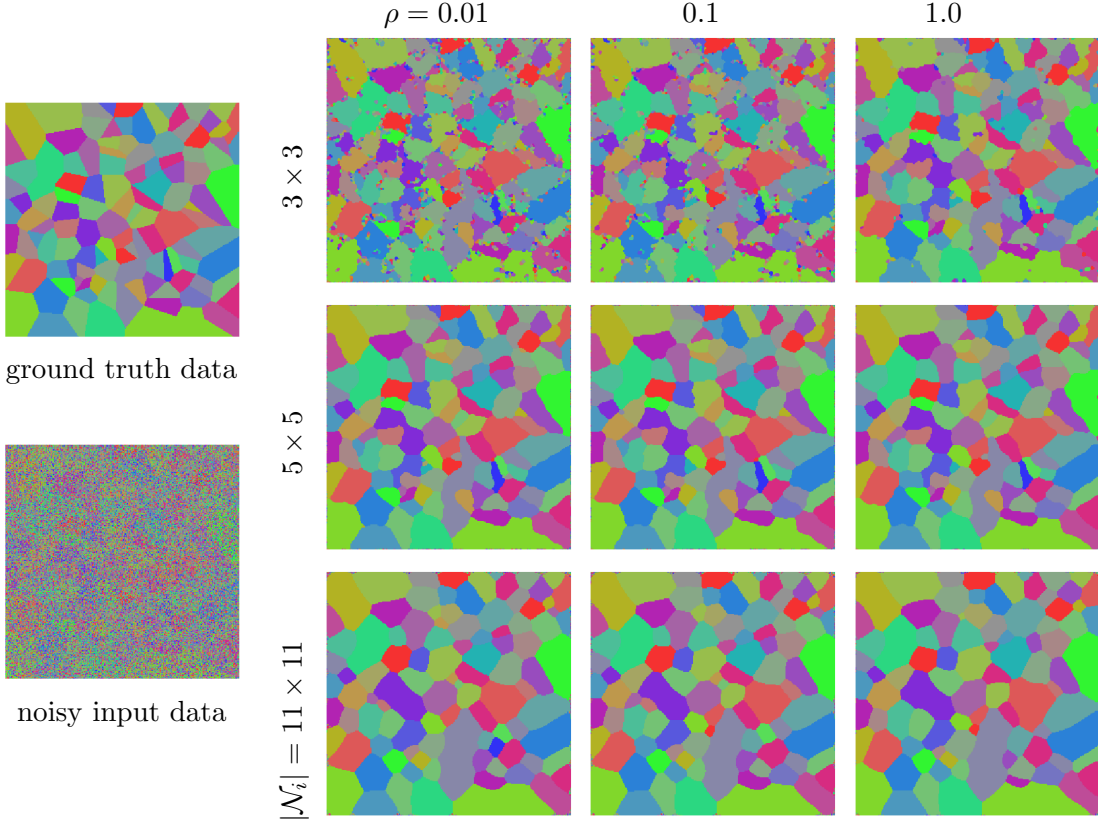


Figure 4.1.: Influence of the parameter ρ and neighborhood size N on the regularization of the S -flow model $J_{\alpha;\varepsilon}$ (4.26) with $\alpha = 1$ and $\varepsilon = 10^{-10}$. **Left:** The underlying ground truth pattern together with the noisy version used as input of the model. The data is given on a 256×256 pixel grid, where each pixel can take one of 31 possible discrete values, encoded by 31 different color values for visualization purposes. **Right:** The results for varying $\rho \in \{0.01, 0.1, 1\}$ and $N \in \{3, 5, 11\}$ after reaching the termination criterion with a threshold of 10^{-6} . The images depict the expected label value $\mathbb{E}_{S_i}[\mathcal{X}] = \sum_{j \in [31]} S_i^j \ell_j$ given the assignment S_i for every pixel i .

enforced in the early phase of the minimization process, while the remaining time is mostly spend for regularization. Since the Euclidean distance $\|S_i - S_j\|^2$ between two assignment vectors is maximal if S_i and S_j are two distinct integral assignments, i.e. if S_i and S_j are distinct vertices of the simplex Δ , the early integrality enforcement amplifies the Euclidean distance between different assignments and therefore leads to an increase of $\frac{1}{m} J_{\text{reg}}$ (middle left). Larger neighborhood sizes N result in higher values for $\frac{1}{m} J_{\text{reg}}$ and longer runtime until the convergence criterion is fulfilled (bottom left), as more spatial information is incorporated in the regularization measure. The (log-scale) plot on the bottom left depicts the corresponding nrc $J_{\alpha;\varepsilon}$ curves.

For the *right column* of Figure 4.2, corresponding to the choices $\rho \in \{0.01, 0.1, 1\}$ for

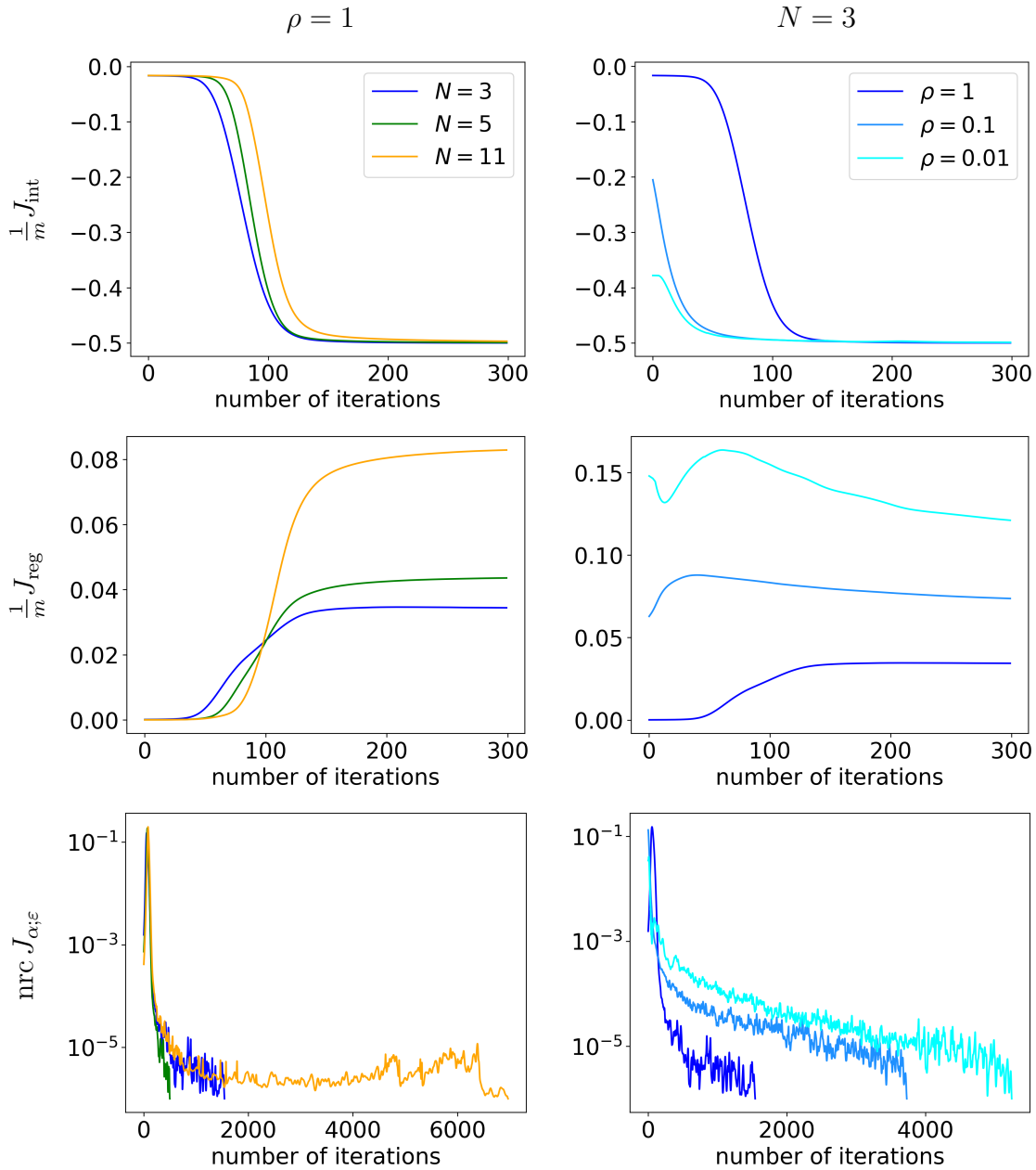


Figure 4.2.: Influence of varying neighborhood sizes N (left column with fixed $\rho = 1$) and parameter values ρ (right column with fixed $N = 3$) on the average values of the integrality enforcing and regularization terms J_{int} (4.23) (top row) and J_{reg} (4.22) (middle row) in the first 300 iterations as well as the normalized relative change $\text{nrc } J_{\alpha;\varepsilon}$ (4.30) (bottom row) for all iterations.

fixed neighborhood size $N = 3$, consider the initial condition $S(\mathbb{1}_{\mathcal{W}})$ of the S -flow. Due to Proposition 2.3.5

$$S_i(\mathbb{1}_{\mathcal{W}}) = \exp_{\mathbb{1}_S} \left(-\frac{1}{\rho} a_i \right), \quad \forall i \in \mathcal{V}_g,$$

with the average vectors $a_i := \sum_{j \in \mathcal{N}_i} \omega_{ij} D_{\mathcal{F}j} \in \mathbb{R}^n$. From this expression, it can be seen that the influence of the averaged data a_i is diminished for large values of ρ . In the limit $\lim_{\rho \rightarrow \infty} S_i(\mathbb{1}_{\mathcal{W}}) = \mathbb{1}_S$, in which case any information is lost. On the other hand, for ρ tending towards 0, it can be shown (see Lemma 5.2.15 below) that if a_i has a unique minimal entry (always fulfilled in practice due to random noise in the data), say $a_i^{j_0}$, then $\lim_{\rho \rightarrow 0} S_i(\mathbb{1}_{\mathcal{W}}) = e_{j_0}$, i.e. $S_i(\mathbb{1}_{\mathcal{W}})$ converges to the vertex e_{j_0} of Δ representing the label $\ell_{j_0} \in \mathcal{X}$.

As a consequence of this, $\frac{1}{m} J_{\text{int}}$ starts at lower values (top right) for smaller ρ , because the starting point $S(\mathbb{1}_{\mathcal{W}})$ gets closer to an integral assignment. As in the case for varying N , the value of $\frac{1}{m} J_{\text{int}}$ decreases in the first 300 iterations and thereby enforces integrality, more rapidly for smaller values of ρ , while the remaining time is mostly spend for regularization. Similarly, $\frac{1}{m} J_{\text{reg}}$ starts at lower values (middle right) for larger ρ , as the starting point $S(\mathbb{1}_{\mathcal{W}})$ is getting closer to the barycenter and thereby diminishes the Euclidean distance between different assignments. As before, the integrality enforcement in the first phase leads to an increase in $\frac{1}{m} J_{\text{reg}}$. The log-scale plots of $\text{nrc} J_{\alpha;\varepsilon}$ (bottom right) confirms, that for larger values of ρ less time is spend for regularization, leading to faster convergence.

Influence of the Integrality Enforcing Term

In this experiment, the effect of the integrality parameter α on the model $J_{\alpha;\varepsilon}$ (4.26) is investigated. The grid graph \mathcal{G}_g (see Section 2.3.1) with $\mathcal{V}_g = [100] \times [100]$ and neighborhood size $N = 3$ represents the spatial structure of the 100×100 noisy RGB-image $f: \mathcal{V}_g \rightarrow [0, 1]^3$, depicted in Figure 4.3, used as input. The distance measure of the RGB feature space $\mathcal{F} := [0, 1]^3$ is given by $d_{\mathcal{F}}(f, f') = \|f - f'\|_1/3$ and 8 prototypical colors (Figure 4.3 top right) are chosen as labels \mathcal{X} . Again, symmetric uniform weights (4.32) are used for regularization together with $\rho = 0.1$ and perturbation parameter $\varepsilon = 10^{-10}$. For the GEA update scheme (4.29), the values $\tau = 0.01$, $s = 0.5$ and $h_{\text{max}} = 0.5$ are chosen and the iteration is terminated if the nrc of $J_{\alpha;\varepsilon}$ (4.30) drops below the threshold of 10^{-6} or the maximum number of 25000 iterations is reached.

The middle and bottom row of Figure 4.3 show the influence for the parameter choices $\alpha \in \{0, 0.1, 0.5, 0.7, 1, 2\}$ on the model $J_{\alpha;\varepsilon}$. Again, the color values of each image represent the expected label value $\mathbb{E}_{S_i}[\mathcal{X}] = \sum_{j \in [31]} S_i^j \ell_j$ for every pixel i , given the assignments S after termination of the sequence. For $\alpha = 0$, the model reduces to the convex function $J_{0;\varepsilon} = J_{\text{reg}}$ (4.22), with the set of minimizers given by uniform assignment. The sequence converges to such an optimal point in the interior of the assignment manifold, resulting in a uniform brownish expected value. The choice $\alpha = 0.1$ is sufficient to push the sequence towards an integral assignment, however, the influence of the integrality enforcing term compared to the regularizer is too weak to preserve any

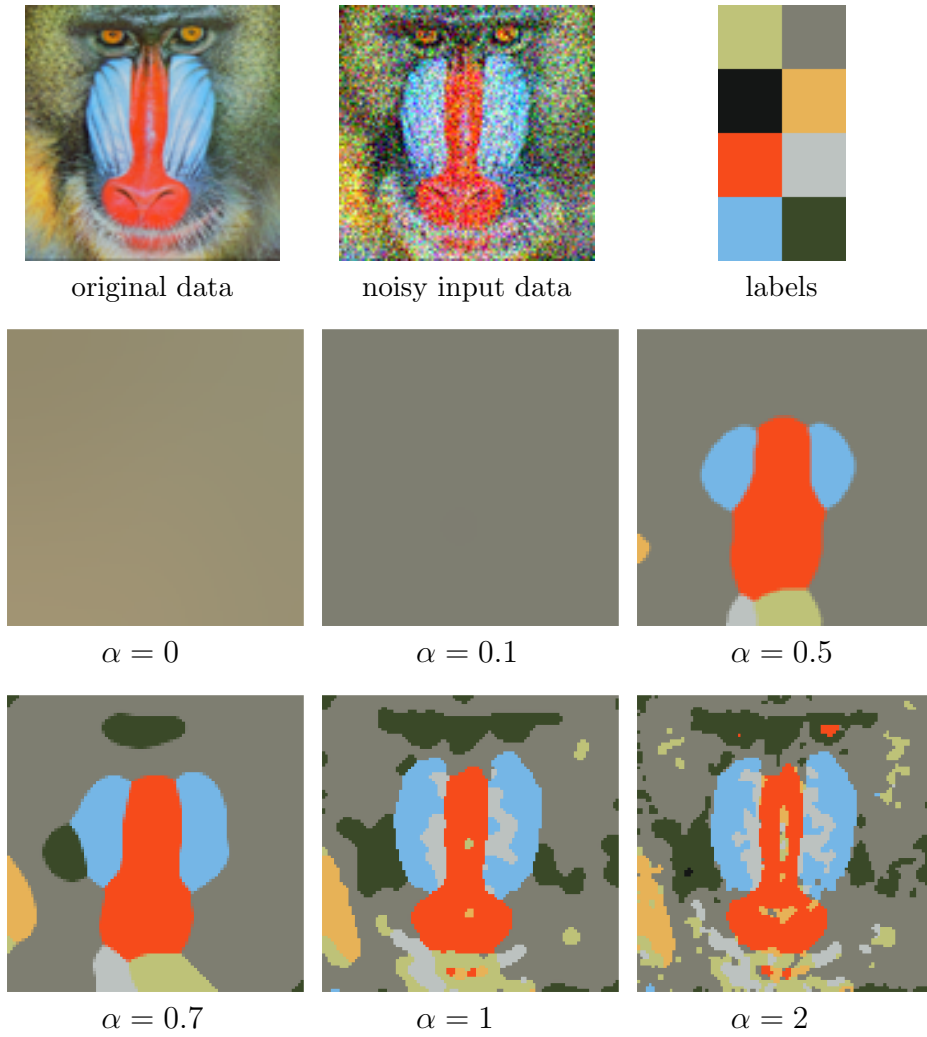


Figure 4.3.: Effect of the integrality parameter α on the S -flow model $J_{\alpha;\varepsilon}$ (4.26) with the choices $\varepsilon = 10^{-10}$, $\rho = 0.1$ and neighborhood size $N = 3$. **Top row:** The underlying 100×100 pixel RGB-image together with the noisy input version of the model and 8 prototypical colors used as labels. **Middle and bottom row:** Results for varying values of α after reaching the termination criterion with a threshold of 10^{-6} . The images again show the expected color label $\mathbb{E}_{S_i}[\mathcal{X}] = \sum_{j \in [8]} S_i^j \ell_j$ given the assignment S_i at every pixel i .

image structure and therefore results in a uniform integral assignment. For larger values $\alpha \geq 0.5$, an increasing amount of the image structure is preserved.

Figure 4.4 shows the influence of the parameter values $\alpha \in \{0, 0.1, 0.5, 0.7, 1, 2\}$ on $\frac{1}{m} J_{\text{int}}$ (4.23), $\frac{1}{m} J_{\text{reg}}$ (4.22) and $\text{nrc} J_{\alpha;\varepsilon}$ (4.30) in the first 500 iterations, as well as the effect on $\text{nrc} J_{\alpha;\varepsilon}$ up to the maximum number of 25000 iterations. For $\alpha = 0$, the maximum number of iteration was reached, while in all other cases the nrc of $J_{\alpha;\varepsilon}$

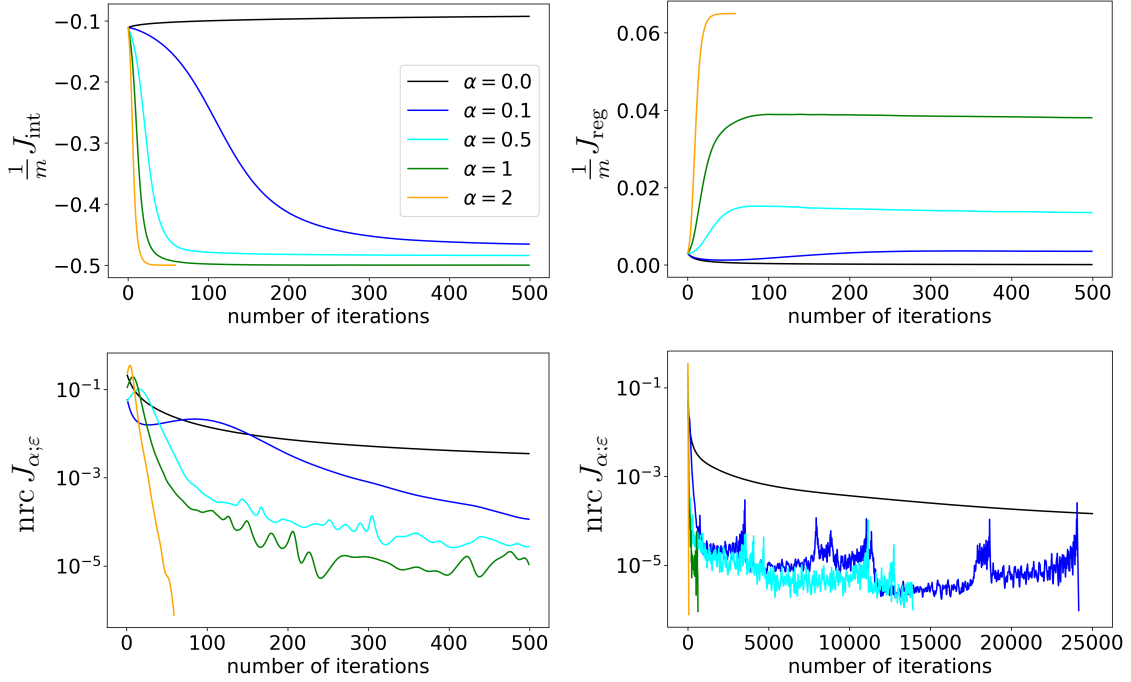


Figure 4.4.: Influence of the integrality parameter α on the average integrality values $\frac{1}{m} J_{\text{int}}$ (4.23) (top left), regularization values $\frac{1}{m} J_{\text{reg}}$ (4.22) (top right) and nrc of $J_{\alpha;\epsilon}$ (4.30) (bottom left) for the first 500 iterations. Additionally, the nrc of $J_{\alpha;\epsilon}$ up to the maximum number of 25000 iterations is shown (bottom right).

dropped below 10^{-6} (bottom right) first. Larger values of α cause more emphasis on the minimization of J_{int} (top left), leading to a faster decay in the value and therefore also a faster convergence towards integral assignments (bottom row). For smaller values of α , the influence of J_{int} is diminished and more time is spend on minimizing J_{reg} , resulting in smaller values for J_{reg} (top right) and therefore more regularized assignments.

4.2. Continuous-Domain Variational Model

In this section, a continuous-domain variational formulation of the potential from Proposition 4.1.6 is studied. The following considerations are confined to the case of uniform weights (2.26) and neighborhoods (2.21) that only contain the nearest neighbors of each vertex i , such that L_G becomes the discretized ordinary Laplacian. As a result, the minimization of the following functional with $\alpha \geq 0$ is consider

$$J_\alpha : H^1(\mathcal{M}; \mathbb{R}^n) \rightarrow \mathbb{R}, \quad S \mapsto J_\alpha(S) := \int_{\mathcal{M}} \|DS(x)\|^2 - \alpha \|S(x)\|^2 dx. \quad (4.33)$$

Throughout this section, $\mathcal{M} \subset \mathbb{R}^2$ is a simply-connected bounded open subset in the Euclidean plane. Parameter α controls the interaction between regularization and en-

forcing integrality when the function values of S are restricted to the probability simplex $S(x) \in \mathcal{S}$ for all $x \in \mathcal{M}$.

In the following, well-posedness for vanishing (Section 4.2.2) and Dirichlet boundary conditions (Section 4.2.3), respectively, are proven and the set of minimizers in the former case is explicitly specified. The gradient descent flow corresponding to the latter case, initialized by means of given data and with parameter value $\alpha = 1$, may be seen as a continuous-domain extension of the assignment flow, that is parameterized according to (4.1.3) and operates at the smallest spatial scale in terms of the size $|\mathcal{N}_i|$ of uniform neighborhoods (2.21) (in the discrete formulation (2.62): nearest neighbor averaging). This is illustrated by a numerical example (Section 4.2.4), based on discretizing (4.33) and applying an algorithm that mimics the S -flow and converges to a local minimum of the non-convex functional (4.33), by solving a sequence of convex programs.

It is pointed out that \mathcal{M} could be turned into a Riemannian manifold using a metric that reflects images features (edges etc.), as was proposed with the Laplace-Beltrami framework for image denoising [KMS00]. In this work the focus is on the essential point, however, that distinguishes image *denoising* from image *labeling*, i.e. the interaction of the two terms in (4.33) which essentially is a consequence of the information geometry of the assignment manifold \mathcal{W} from Section 2.3.2.

4.2.1. Background on Functional Analysis

Subsequently, a few basic facts and definitions regarding Sobolev spaces are listed from [Zie89, ABM14] and the corresponding notation is fixed. In the following, $\Omega \subset \mathbb{R}^d$ denotes an open bounded domain.

The inner product and the norm of functions $f, g \in L^2(\Omega)$ is denoted by

$$(f, g)_\Omega = \int_\Omega fg dx, \quad \|f\|_\Omega = (f, f)_\Omega^{1/2}.$$

Functions f_1 and f_2 are equivalent and identified whenever they merely differ pointwise on a Lebesgue-negligible set of measure zero. f_1 and f_2 then are said to be equal a.e. (almost everywhere). $H^1(\Omega) = W^{1,2}(\Omega)$ denotes the Sobolev space of functions f with square-integrable weak derivatives $D^\alpha f$ up to order one. $H^1(\Omega)$ is a Hilbert space with inner product and norm denoted by

$$(f, g)_{1;\Omega} = \sum_{|\alpha| \leq 1} (D^\alpha f, D^\alpha g)_\Omega, \quad \|f\|_{1;\Omega} = \left(\sum_{|\alpha| \leq 1} \|D^\alpha f\|_\Omega^2 \right)^{1/2}. \quad (4.34)$$

Lemma 4.2.1 ([Zie89, Cor. 2.1.9]). *If Ω is connected, $u \in H^1(\Omega)$ and $Du = 0$ a.e. on Ω , then u is equivalent to a constant function on Ω .*

The closure in $H^1(\Omega)$ of the set of test functions $C_c^\infty(\Omega)$ that are compactly supported on Ω , is the Sobolev space

$$H_0^1(\Omega) = \overline{C_c^\infty(\Omega)} \subset H^1(\Omega).$$

It contains all functions in $H^1(\Omega)$ whose boundary values on $\partial\Omega$ (in the sense of traces) vanish. The space $H^1(\Omega; \mathbb{R}^d)$, with $2 \leq d \in \mathbb{N}$ contains vector-valued functions f whose component functions f_i , $i \in [d]$ are in $H^1(\Omega)$. For notational efficiency, the norm of $f \in H^1(\Omega; \mathbb{R}^d)$ is again denoted by

$$\|f\|_{1;\Omega} = \left(\sum_{i \in [d]} \|f_i\|_{1;\Omega}^2 \right)^{1/2},$$

as in the scalar case (4.34). It will be clear from the context if f is scalar- or vector-valued.

The compactness theorem of Rellich-Kondrakov [ABM14, Thm. 5.3.3] says that the canonical embedding

$$H_0^1(\Omega) \hookrightarrow L^2(\Omega)$$

is compact, i.e. every bounded subset in $H_0^1(\Omega)$ is relatively compact in $L^2(\Omega)$. This extends to the vector-valued case

$$H_0^1(\Omega; \mathbb{R}^d) \hookrightarrow L^2(\Omega; \mathbb{R}^d) \quad (4.35)$$

since $H_0^1(\Omega; \mathbb{R}^d)$ is isomorphic to $H_0^1(\Omega) \times \cdots \times H_0^1(\Omega)$ and likewise for $L^2(\Omega; \mathbb{R}^d)$. The dual space of $H_0^1(\Omega)$ is commonly denoted by $H^{-1}(\Omega) = (H_0^1(\Omega))'$. Accordingly, this is extended to the vector valued case $H^{-1}(\Omega; \mathbb{R}^d) = (H_0^1(\Omega; \mathbb{R}^d))'$.

Strong and weak convergence of a sequence (f_k) is written as $f_k \rightarrow f$ and $f_k \rightharpoonup f$, respectively. Next, further basic facts regarding weak convergence from [Zei85, Prop. 38.2] and [ABM14, Prop. 2.4.6] are listed.

Proposition 4.2.2. *The following assertions hold in a Banach space X .*

- (1) *A closed convex subset $C \subset X$ is weakly closed, i.e. a sequence $(f_k)_{k \in \mathbb{N}} \subset C$ that weakly converges to f implies $f \in C$.*
- (2) *If X is reflexive (in particular, if X is a Hilbert space), then every bounded sequence in X has a weakly convergent subsequence.*
- (3) *If f_k weakly converges to f , then $(f_k)_{k \in \mathbb{N}}$ is bounded and*

$$\|f\|_X \leq \liminf_{k \rightarrow \infty} \|f_k\|_X. \quad (4.36)$$

The following theorem states conditions for minimizers of the functional to satisfy a corresponding variational inequality.

Theorem 4.2.3 ([Zei85, Thm. 46.A(a)]). *Let $F: C \rightarrow \mathbb{R}$ be a functional on the convex nonempty set C of a real locally convex space X , and let $b \in X'$ be a given element. Suppose the Gateaux-derivative F' exists on C . Then any solution f of*

$$\min_{f \in C} \{F(f) - \langle b, f \rangle_{X' \times X}\}, \quad (4.37)$$

satisfies the variational inequality

$$\langle F'(f) - b, h - f \rangle_{X' \times X} \geq 0, \quad \text{for all } h \in C. \quad (4.38)$$

4.2.2. Well-Posedness

Based on (2.8), the closed convex set

$$\mathcal{D}^1(\mathcal{M}) = \{S \in H^1(\mathcal{M}; \mathbb{R}^n) : S(x) \in \Delta \text{ a.e. in } \mathcal{M}\} \quad (4.39)$$

is defined and the focus is on the variational problem

$$\inf_{S \in \mathcal{D}^1(\mathcal{M})} J_\alpha(S), \quad (4.40)$$

with nonconvex J_α given by (4.33). The set of minimizers for (4.40) is specified below.

Proposition 4.2.4. *The functional $J_\alpha : \mathcal{D}^1(\mathcal{M}) \rightarrow \mathbb{R}$ given by (4.33) is lower bounded,*

$$J_\alpha(S) \geq -\alpha \text{Vol}(\mathcal{M}) > -\infty, \quad \forall S \in \mathcal{D}^1(\mathcal{M}). \quad (4.41)$$

This lower bound is attained at some point in

$$\arg \min_{S \in \mathcal{D}^1(\mathcal{M})} J_\alpha(S) = \begin{cases} \{S_{e_1}, \dots, S_{e_n}\}, & \text{if } \alpha > 0, \\ \{S_p : \mathcal{M} \rightarrow \Delta : p \in \Delta\}, & \text{if } \alpha = 0, \end{cases} \quad (4.42)$$

where, for any $p \in \Delta$, S_p denotes the constant map $x \mapsto S_p(x) = p$.

Proof. Let $S \in \mathcal{D}^1(\mathcal{M})$ be arbitrary. Since $S(x) \in \Delta$ for a.e. $x \in \mathcal{M}$, it follows $\|S(x)\|^2 \leq \|S(x)\|_1 = 1$ and therefore also

$$J_\alpha(S) \geq -\alpha \|S\|_{\mathcal{M}}^2 \geq -\alpha \|1\|_{\mathcal{M}} = -\alpha \text{Vol}(\mathcal{M}), \quad (4.43)$$

which is (4.41).

Next, it is shown that the right-hand side of (4.42) specifies minimizers of J_α . For any $p \in \Delta$, the constant map S_p is contained in $\mathcal{D}^1(\mathcal{M})$. Consider specifically S_{e_i} for all basis vectors $e_i \in \mathcal{B}_n, i \in [n]$. Since $\|S_{e_i}(x)\| = \|e_i\| = 1$ and $DS_{e_i} \equiv 0$, the lower bound is attained, $J_\alpha(S_{e_i}) = -\alpha \text{Vol}(\mathcal{M})$, and the functions $\{S_{e_1}, \dots, S_{e_n}\}$ minimize J_α , for every $\alpha \geq 0$. If $\alpha = 0$, then the constant functions S_p are minimizers as well, for any $p \in \Delta$, since then

$$J_\alpha(S_p) = \|DS_p\|_{\mathcal{M}}^2 = 0 = -0 \cdot \text{Vol}(\mathcal{M}). \quad (4.44)$$

The proof is conclude by showing that no minimizers other than (4.42) exist. Let $S_* \in \mathcal{D}^1(\mathcal{M})$ be another minimizer of J_α with $J_\alpha(S_*) = -\alpha \text{Vol}(\mathcal{M})$. The two cases $\alpha = 0$ and $\alpha > 0$ are distinguished in the following.

If $\alpha = 0$, then S_* satisfies (4.44) and $\|DS_*\|_{\mathcal{M}}^2 = 0$. Since $\|DS_{*;i}\|_{\mathcal{M}} \leq \|DS_*\|_{\mathcal{M}} = 0$ for every $i \in [n]$, S_* is constant by Lemma 4.2.1, i.e. a $p \in \Delta$ exists such that a.e. $S_* = S_p$ holds.

If $\alpha > 0$, then using the equation $J_\alpha(S_*) = -\alpha \text{Vol}(\mathcal{M})$ and $\|S_*(x)\|^2 \leq 1$ gives

$$\begin{aligned} \alpha \text{Vol}(\mathcal{M}) &\leq \|DS_*\|_{\mathcal{M}}^2 + \alpha \text{Vol}(\mathcal{M}) = \|DS_*\|_{1;\mathcal{M}}^2 - J_\alpha(S_*) = \alpha \|S_*\|_{\mathcal{M}}^2 \\ &\leq \alpha \|1\|_{\mathcal{M}} = \alpha \text{Vol}(\mathcal{M}), \end{aligned}$$

which shows $\|DS_*\|_{\mathcal{M}} = 0$ and hence by Lemma 4.2.1 again $S_* = S_p$ for some $p \in \Delta$. The preceding inequalities also imply $\text{Vol}(\mathcal{M}) = \|S_*\|_{\mathcal{M}}^2$, i.e. $\|S_*(x)\| = 1$ for a.e. $x \in \mathcal{M}$. By Lemma 4.1.7, the equality $S_* = S_p$ with $p \in \mathcal{B}_c$ can be concluded, that is $S_* \in \{S_{e_1}, \dots, S_{e_n}\}$. \square

Proposition 4.2.4 highlights the effect of the concave term in the objective J_α (4.33): labelings are enforced in the absence of data. Below, the latter are taken into account (i) by imposing non-zero boundary conditions and (ii) by initializing a corresponding gradient flow (see Section 4.2.4).

4.2.3. Fixed Boundary Conditions

In this section, the case where boundary conditions are imposed by restricting the feasible set of problem (4.40) to

$$\mathcal{A}_G^1(\mathcal{M}) = \{S \in \mathcal{D}^1(\mathcal{M}) : S - G \in H_0^1(\mathcal{M}; \mathbb{R}^n)\} = (G + H_0^1(\mathcal{M}; \mathbb{R}^n)) \cap \mathcal{D}^1(\mathcal{M}) \quad (4.45)$$

is considered, where G is some fixed map that prescribes simplex-valued boundary values (in the trace sense). As intersection of a closed affine subspace and a closed convex set, $\mathcal{A}_G^1(\mathcal{M})$ is closed convex.

Weak lower semicontinuity is a key property for proving the existence of minimizers. In the case of J_α (4.33) this is not immediate, due to the lack of convexity.

Proposition 4.2.5. *The functional J_α given by (4.33) is weak sequentially lower semicontinuous on $\mathcal{A}_G^1(\mathcal{M})$, i.e. for any sequence $(S_k)_{k \in \mathbb{N}} \subset \mathcal{A}_G^1(\mathcal{M})$ weakly converging to $S \in \mathcal{A}_G^1(\mathcal{M})$, the inequality*

$$J_\alpha(S) \leq \liminf_{k \rightarrow \infty} J_\alpha(S_k) \quad (4.46)$$

holds.

Proof. Let $S_k \rightharpoonup S$ converge weakly in $\mathcal{A}_G^1(\mathcal{M}) \subset H_0^1(\mathcal{M}; \mathbb{R}^n)$. Then, by Prop. 4.2.2 (3),

$$\|S\|_{1;\mathcal{M}} \leq \liminf_{k \rightarrow \infty} \|S_k\|_{1;\mathcal{M}}. \quad (4.47)$$

Since $S, S_k \in \mathcal{A}_G^1(\mathcal{M})$, it also follows $(S_k - G) \rightharpoonup (S - G)$ in $H_0^1(\mathcal{M}; \mathbb{R}^n)$ by (4.45) and consequently $S_k \rightarrow S$ strongly in $L^2(\mathcal{M}; \mathbb{R}^n)$ due to (4.35). Taking into account (4.47) and $\liminf_{k \rightarrow \infty} \|S_k\|_{\mathcal{M}} = \lim_{k \rightarrow \infty} \|S_k\|_{\mathcal{M}} = \|S\|_{\mathcal{M}}$ results in

$$\begin{aligned} J_\alpha(S) &= \|S\|_{1;\mathcal{M}}^2 - (1 + \alpha)\|S\|_{\mathcal{M}}^2 \leq \liminf_{k \rightarrow \infty} \|S_k\|_{1;\mathcal{M}}^2 + \liminf_{k \rightarrow \infty} (-(1 + \alpha)\|S_k\|_{\mathcal{M}}^2) \\ &\leq \liminf_{k \rightarrow \infty} J_\alpha(S_k). \end{aligned} \quad \square$$

After these preparations, it is now shown that J_α attains its minimal value on $\mathcal{A}_G^1(\mathcal{M})$, following the basic proof pattern of [Zei85, Ch. 38].

Theorem 4.2.6. *Let J_α be given by (4.33). There exists a $S_* \in \mathcal{A}_G^1(\mathcal{M})$ such that*

$$J_\alpha^* := J_\alpha(S_*) = \inf_{S \in \mathcal{A}_G^1(\mathcal{M})} J_\alpha(S). \quad (4.48)$$

Proof. Let $(S_k)_{k \in \mathbb{N}} \subset \mathcal{A}_G^1(\mathcal{M})$ be a minimizing sequence such that

$$\lim_{k \rightarrow \infty} J_\alpha(S_k) = J_\alpha^*. \quad (4.49)$$

Then there exists some sufficiently large $k_0 \in \mathbb{N}$ such that

$$1 + J_\alpha^* \geq J_\alpha(S_k) = \|S_k\|_{1;\mathcal{M}}^2 - (1 + \alpha)\|S_k\|_{\mathcal{M}}^2, \quad \forall k \geq k_0.$$

Since $S_k(x) \in \Delta$ for a.e. $x \in \mathcal{M}$, the inequality $\|S_k\|_{\mathcal{M}}^2 \leq \text{Vol}(\mathcal{M})$ follows and results in

$$\|S_k\|_{1;\mathcal{M}}^2 \leq 1 + J_\alpha^* + (1 + \alpha)\|S_k\|_{\mathcal{M}}^2 \leq 1 + J_\alpha^* + (1 + \alpha)\text{Vol}(\mathcal{M}), \quad \forall k \geq k_0.$$

Thus the sequence $(S_k)_{k \in \mathbb{N}} \subset H^1(\mathcal{M}; \mathbb{R}^n)$ is bounded and, by Prop. 4.2.2 (2), a weakly converging subsequence $S_{k_j} \rightharpoonup S_* \in H^1(\mathcal{M}; \mathbb{R}^n)$ may be extracted. Since the subset $\mathcal{A}_G^1(\mathcal{M}) \subset H^1(\mathcal{M}; \mathbb{R}^n)$ is closed convex, Prop. 4.2.2 (1) implies $S_* \in \mathcal{A}_G^1(\mathcal{M})$. Consequently, by Prop. 4.2.5 and (4.49),

$$J_\alpha(S_*) \leq \liminf_{j \rightarrow \infty} J_\alpha(S_{k_j}) = \lim_{j \rightarrow \infty} J_\alpha(S_{k_j}) = J_\alpha^* \quad (4.50)$$

which implies $J_\alpha(S_*) = J_\alpha^*$, i.e. $S_* \in \mathcal{A}_G^1(\mathcal{M})$ minimizes J_α . \square

4.2.4. Numerical Algorithm and Example

Subsequently, the variational problem (4.48)

$$\inf_{S \in \mathcal{A}_G^1(\mathcal{M})} \int_{\mathcal{M}} \|DS\|^2 - \alpha\|S\|^2 dx, \quad (4.51)$$

for some fixed G specifying the boundary values $S|_{\partial\mathcal{M}} = G|_{\partial\mathcal{M}}$, and the problem to compute a local minimum numerically using an optimization scheme that mimics the S -flow of Proposition 4.1.3 is considered.

Based on (4.45), the problem (4.51) is rewritten in the form

$$\begin{aligned} & \inf_{F \in H_0^1(\mathcal{M}; \mathbb{R}^n)} \left\{ \|D(G + F)\|_{\mathcal{M}}^2 - \alpha\|G + F\|_{\mathcal{M}}^2 + \delta_{\mathcal{D}^1(\mathcal{M})}(G + F) \right\} = \\ & \inf_{F \in H_0^1(\mathcal{M}; \mathbb{R}^n)} \left\{ \|DF\|_{\mathcal{M}}^2 + 2\langle DG, DF \rangle_{\mathcal{M}} - \alpha(\|F\|_{\mathcal{M}}^2 + 2\langle G, F \rangle_{\mathcal{M}}) + \delta_{\mathcal{D}^1(\mathcal{M})}(G + F) \right\} + c, \end{aligned}$$

where $\delta_{\mathcal{D}^1(\mathcal{M})}$ is the convex indicator function (B.2) of the convex set $\mathcal{D}^1(\mathcal{M})$ and the last constant c collects terms not depending on F . Discretization of the problem is done as follows, where the symbols F, G are kept for simplicity. F becomes a vector $F \in \mathbb{R}^{nm}$ with $m = |\mathcal{V}|$ subvectors $F_i \in \mathbb{R}^n, i \in [m]$ or alternatively with $n = |\mathcal{X}|$ subvectors $F^j, j \in [n]$. The inner product $\langle G, F \rangle_{\mathcal{M}}$ is replaced by

$$\langle G, F \rangle = \sum_{i \in [m]} \langle G_i, F_i \rangle = \sum_{j \in [n]} \langle G^j, F^j \rangle = \sum_{i \in [m]} \sum_{j \in [n]} G_i^j F_i^j.$$

In the following, the discretized setting is indicated by the subscript d as introduced next. D becomes a gradient matrix D_d that estimates the gradient of each subvector F^j separately, such that

$$L_d F := D_d^\top D_d F$$

is the basic discrete 5-point stencil Laplacian applied to each subvector F^j . The feasible set $\mathcal{D}^1(\mathcal{M})$ (4.39) is replaced by the closed convex set

$$\mathcal{D}_d := \{F \geq 0: \langle \mathbb{1}_n, F_i \rangle = 1, \forall i \in \mathcal{V}\}. \quad (4.52)$$

Thus the discretized problem reads

$$\inf_F \left\{ \|D_d F\|^2 + 2\langle L_d G - \alpha G, F \rangle - \alpha \|F\|^2 + \delta_{\mathcal{D}_d}(G + F) \right\}, \quad (4.53)$$

where $\delta_{\mathcal{D}_d}$ again denotes the convex indicator function (B.2) of the convex set \mathcal{D}_d . Having computed a local minimum F_* , the corresponding local minimum of (4.51) is of the form $S_* = G + F_*$.

In order to compute F_* , the proximal forward-backward scheme

$$F^{(k+1)} = \arg \min_F \left\{ \|D_d F\|^2 + 2\langle L_d G - \alpha(G + F^{(k)}), F \rangle + \frac{1}{2h_k} \|F - F^{(k)}\|^2 + \delta_{\mathcal{D}_d}(G + F) \right\} \quad (4.54)$$

is applied, with proximal parameters h_k , $k \in \mathbb{N}$ and initialization $F_i^{(0)}$, $i \in \mathcal{V}$ specified further below. The iterative scheme (4.54) is a special case of the PALM (Proximal Alternating Linearized Minimization) algorithm [BST14, Sec. 3.7]. Ignoring the proximal term, each problem (4.54) amounts to solve n (discretized) Dirichlet problems with the boundary values of G^j , $j \in [n]$ imposed, and with right-hand sides that change during the iteration since they depend on $F^{(k)}$. The solutions $(F^{(k)})^j$, $j \in \mathcal{X}$ to these Dirichlet problems depend on each other, however, through the feasible set (4.52). At each iteration k , problem (4.54) can be solved by convex programming. The proximal parameters h_k act as step-sizes such that the sequence $F^{(k)}$ does not approach a local minimum too rapidly. Then the interplay between the linear form that adapts during the iteration and the regularizing effect of the Laplacian can find a labeling (partition) corresponding to a good local optimum.

As for G , the value $G_i = L_i(\mathbb{1}_S)$ for boundary vertices $i \in \mathcal{V}$ is chosen and $G_i = 0$ for every interior vertex i , where L_i are the likelihood vectors (2.55) containing data information via the distance matrix. Consequently, with the initialization $F_i^{(0)} = L_i(\mathbb{1}_S)$, $i \in \mathcal{V}$ at interior vertices (the boundary values of F are zero), the sequence $S^{(k)} = G + F^{(k)}$ mimics the S -flow of Proposition 4.1.3 where the given data also show up in the initialization $\bar{S}(0)$ only.

Figure 4.5 provides an illustration using the experiment from Section 4.1.3 for evaluating the performance of geometric regularization in an unbiased way. Parameter values are specified in the caption. The result confirms that the continuous-domain formulations discussed above represent the assignment flow at the smallest spatial scale.

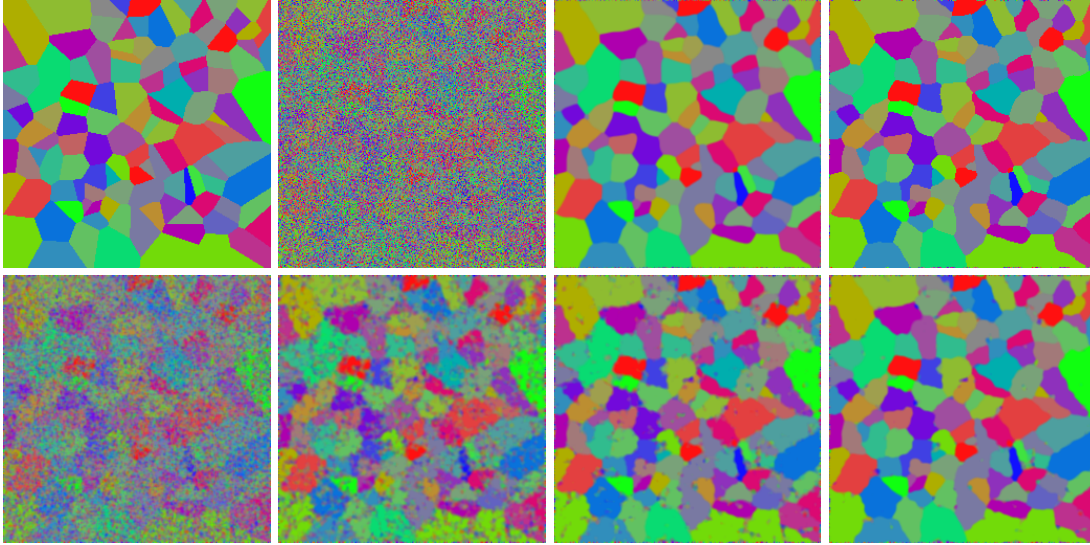


Figure 4.5.: Evaluation of the numerical scheme (4.54) that mimics the S -flow of Proposition 4.1.3. Parameter values: $\alpha = 1, h_k = \tau = 10, \forall k$. **Top**, from left to right: Ground truth, noisy input data $F^{(0)}$, iterate $F^{(100)}$ and F_* resulting from $F^{(100)}$ by a trivial rounding step. $S^{(k)} = F^{(k)} + G$ differs from $F^{(k)}$ by the boundary values corresponding to the noisy input data. Inspecting the values of $F^{(100)}$ close to the boundary shows that the influence of boundary noise is minimal. **Bottom**, from left to right: The iterates $F^{(10)}, F^{(20)}, F^{(30)}, F^{(40)}$. Taking into account rounding as post-processing step, the sequence $F^{(k)}$ quickly converges after rounding to a reasonable partition. About 50 more iterations are required to fix the values at merely few hundred remaining pixels. Slight rounding of the geometry of the components of the partition, in comparison to ground truth, corresponds to using uniform weights (2.26) for the assignment flow.

4.2.5. A PDE Characterizing Optimal Assignment Flows

This chapter is concluded by deriving a PDE corresponding to (4.56), that a minimizer S_* is supposed to satisfy in the weak sense. The derivation is *formal* in the sense that the unrealistic regularity assumption

$$S_* \in \mathcal{A}_G^2(\mathcal{M}) \quad (4.55)$$

adopt, with $\mathcal{A}_G^2(\mathcal{M})$ defined analogous to (4.45). Since S_* is expected (and wished) to become discontinuous, this would violate the regularity assumption (4.55) and the continuity implied by the Sobolev embedding theorem for $\mathcal{M} \subset \mathbb{R}^d$ with $d = 2$. Nevertheless, since the PDE provides another interpretation of the assignment flow, it is stated – see (4.59) below – and hoped to stimulate further research.

Proposition 4.2.7. *Let S_* solve the variational problem (4.51). Then S_* satisfies the variational inequality*

$$\langle DS_*, DS - DS_* \rangle_{\mathcal{M}} - \alpha \langle S_*, S - S_* \rangle_{\mathcal{M}} \geq 0, \quad \forall S \in \mathcal{A}_G^1(\mathcal{M}). \quad (4.56)$$

Proof. Functional J_α given by (4.51) is Gateaux-differentiable with derivative

$$\langle J'_\alpha(S_*) , S \rangle_{H^{-1}(\mathcal{M}; \mathbb{R}^n) \times H_0^1(\mathcal{M}; \mathbb{R}^n)} = 2(\langle DS_*, S \rangle_{\mathcal{M}} - \alpha \langle S_*, S \rangle_{\mathcal{M}}).$$

The assertion follows from applying Theorem 4.2.3. \square

In view of assumption (4.55), inserting S_* and an arbitrary $S \in \mathcal{A}_G^1(\mathcal{M})$ into (4.56) together with partial integration results in

$$\langle -\Delta S_* - \alpha S_*, S - S_* \rangle_{\mathcal{M}} \geq 0, \quad (4.57)$$

where $\Delta S_* = \Delta S_*^i e_i$ applies componentwise for $S_* = S_*^i e_i$. Using the shorthands

$$\begin{aligned} \nu_\alpha(S_*) &:= -\Delta S_* - \alpha S_*, \\ \mu_\alpha(S_*) &:= \nu_\alpha(S_*) - \langle \nu_\alpha(S_*), S_* \rangle_{\mathbb{R}^2} \mathbb{1}_n, \end{aligned}$$

with $\langle \nu_\alpha(S_*), S_* \rangle_{\mathbb{R}^2}$ denoting the function $x \mapsto \langle \nu_\alpha(S_*)(x), S_*(x) \rangle$, $x \in \mathcal{M}$, it follows

$$\langle \mu_\alpha(S_*), S_* \rangle_{\mathcal{M}} = 0 \quad (4.58a)$$

since $\langle \mathbb{1}_n, S_*(x) \rangle = 1$ for a.e. $x \in \mathcal{M}$, and

$$\langle \mu_\alpha(S_*), S \rangle_{\mathcal{M}} = \langle \nu_\alpha(S_*), S - S_* \rangle_{\mathcal{M}} \geq 0, \quad (4.58b)$$

which is (4.57). Since the components $S^i(x)$ of $S(x)$ are nonnegative a.e. in \mathcal{M} and may have arbitrary support, it can be deduce from the inequality $\langle \mu_\alpha(S_*), S \rangle_{\mathcal{M}} \geq 0$ and from the self-duality of the nonnegative orthant $\mathbb{R}_{\geq 0}^d$, i.e.

$$\mathbb{R}_{\geq 0}^d = \{y \in \mathbb{R}^d \mid \forall z \in \mathbb{R}_{\geq 0}^d, \langle y, z \rangle \geq 0\},$$

that $\mu_\alpha(S_*) \geq 0$ a.e. in \mathcal{M} . Since also $S_* \geq 0$ a.e., this implies that equation (4.58a) holds pointwise a.e. in \mathcal{M} :

$$\mu_\alpha(S_*)(x) S_*(x) = \nu_\alpha(S_*)(x) S_*(x) - \langle \nu_\alpha(S_*)(x), S_*(x) \rangle S_*(x) = 0 \quad \text{a.e. in } \mathcal{M}.$$

Substituting $\nu_\alpha(S_*)$ shows that a minimizer S_* as characterized by the variational inequality (4.56) weakly satisfies the PDE

$$R_{S_*}(-\Delta S_* - \alpha S_*) = 0, \quad (4.59)$$

where R_{S_*} defined by (2.32) applies $R_{S_*(x)}$ to the vector $(-\Delta S_* - \alpha S_*)(x)$ at every $x \in \mathcal{M}$.

Remark 4.2.1. Note, that computing a vector field S_* satisfying (4.56) is difficult in practice, due to the nonconvexity of problem (4.51). On the other hand, the algorithm proposed in Section 4.2.4 and the result illustrated by Figure 4.5 shows that good suboptima can be computed by merely solving a sequence of simple problems.

Chapter 5

A Variational Approach Based on Graphical Models

In the following, a classical discrete formulation of the image labeling problem on a graph $\mathcal{G} = (\mathcal{V}, \mathcal{E})$ with label set \mathcal{X} is considered. In this discrete setting, a random variable with values in the set of labels

$$x_i \in \mathcal{X} = \{\ell_1, \dots, \ell_n\}$$

is associated to each vertex $i \in \mathcal{V}$. The image labeling problem then refers to the task of assigning to each x_i a label such that the *discrete objective function*

$$\min_{x \in \mathcal{X}^m} J(x), \quad J(x) = \sum_{i \in \mathcal{V}} J_i(x_i) + \sum_{ij \in \mathcal{E}} J_{ij}(x_i, x_j) \quad (5.1)$$

is minimized. This function contains for each pixel $i \in \mathcal{V}$ local energy terms $J_i(x_i)$ that evaluate local label predictions for each possible value of $x_i \in \mathcal{X}$. In addition, $J(x)$ also contains for each edge $ij \in \mathcal{E}$ local energy functions $J_{ij}(x_i, x_j)$ that evaluate the joint assignment of labels to x_i and x_j . If the local energy functions $J_{ij}(x_i, x_j) = d(x_i, x_j)$ are defined by a metric $d: \mathcal{X} \times \mathcal{X} \rightarrow \mathbb{R}$, then (5.1) is called the *metric labeling problem* [KT02]. In general, the presence of these latter terms J_{ij} makes the discrete image labeling formulation (5.1) a combinatorially hard task. The function $J(x)$ has the common format of an objective function for image analysis consisting of a data term and a regularizer. From a Bayesian perspective, therefore, minimizing J corresponds to *maximum a-posteriori (MAP)* inference with respect to the associated probability distribution

$$p(x) = \frac{1}{Z} \exp(-J(x)), \quad (5.2)$$

also called *discrete probabilistic graphical model*, with the the underlying graph \mathcal{G} expressing the conditional dependence between the individual random variables x_i , $i \in \mathcal{V}$. The reader is referred to [KAH⁺15] for a recent survey on the image labeling problem and on algorithms for solving either approximately or exactly problem (5.1).

A major class of algorithms for approximately solving (5.1) is based on the *local polytope relaxation* [Wer07], a special linear programming (LP) relaxation for adequately representing the specific structure of the MAP inference problem of the form (see Section 5.1 for details)

$$\min_{\mu \in \mathcal{L}_{\mathcal{G}}} \langle \vartheta, \mu \rangle, \quad (5.3)$$

where $\mathcal{L}_{\mathcal{G}}$ is a convex set representing certain constraints of the relaxed indicator vector μ with components in $[0, 1]$. If the globally optimal solution $\bar{\mu}$ is a binary vector, i.e. with components either 0 or 1, then it corresponds to a solution of problem (5.1). In realistic applications, however, this is not the case and the relaxed solution $\bar{\mu}$ has to be rounded to an integral solution in a post-processing step. The local polytope relaxation can also be tightened by adding additional facet-defining inequalities, see [WJ08] and references therein.

The *goal* of this chapter is to derive a relaxed smooth variational model on the assignment manifold which represents problem (5.1) in a suitable geometric way and simultaneously incorporates a smooth rounding mechanism towards integral assignments. The starting point for this derivation is the above mentioned LP relaxation (5.3) and a smoothed version of it, introduced in more detail in Section 5.1, which results in the well known belief propagation algorithm [YFW05, WJ08]. The variational model is defined in Section 5.2 based on a reformulation of the smoothed LP relaxation using entropy regularized Wasserstein distances. These distances allow to properly take into account the regularization terms J_{ij} coupling the assignments W_i and W_j along edges $ij \in \mathcal{E}$. Subsequently an expression for the gradient of the entropy regularized Wasserstein distance is derived, making it possible to calculate these gradients using an iterative matrix scaling algorithm, called *Sinkhorn's algorithm* [Sin64, Sch90], made popular in the field of machine learning by [Cut13]. Finally, basic properties of the presented variational model are evaluated with two academical experiments in Section 5.3. The first one illustrates the effect of the rounding mechanism for enforcing integral assignments. The second one compares the accuracy and discrete energy level $J(x)$ for a specific binary image denoising problem to sequential tree-reweighted message passing (TRWS) [Kol06] (which is regarded as state of the art) and to loopy belief propagation (BP) based on the OpenGM package [ABK12].

This chapter is based on joint work which has already published in [HSÅS18].

5.1. Background on Graphical Models for Image Labeling

In the following, the necessary basic notation and definitions of the common linear programming (LP) relaxation (5.3) for the discrete labeling problem (5.1) is given in Section 5.1.1. Subsequently, in Section 5.1.2, a smoothed version of the LP relaxation is introduced whose optimality condition results in the belief propagation by ‘message passing’ algorithm. The reader is referred to [Wer07] for more information about the LP relaxation of labeling problems, to [WJ08] for connections to discrete probabilistic graphical models from the variational viewpoint and to [YFW05, WJ08] for more details on belief propagation.

It remains to address a minor technical point concerning the pairwise discrete energies $J_{ij}(x_i, x_j)$ in (5.1), for $ij \in \mathcal{E}$. So far, the functions J_{ij} are not assumed to be symmetric, allowing for $J_{ij}(x_i, x_j) \neq J_{ij}(x_j, x_i)$. However, if the graph \mathcal{G} is undirected, there is no distinction between ij and ji , leading to the problem that the assignment of edges ij to energy values $J_{ij}(x_i, x_j)$ might not be well defined due to asymmetry. One way to

overcome this, is to choose an arbitrary orientation of the edges, resulting in a well defined map $ij \mapsto J_{ij}(x_i, x_j)$ and allowing for asymmetric pairwise energies. It is important to note, that the orientation itself plays no essential role in the model, it is merely a technical assumption. If the pairwise energies are all symmetric, no orientation is necessary.

Assumption 5.1.1. Unless otherwise stated, the edge set \mathcal{E} of the graph \mathcal{G} is assumed to be (randomly) oriented throughout this chapter. By abuse of notation an oriented edges $(i, j) \in \mathcal{E}$ is often again denoted by $ij = (i, j)$, i.e. $ij \in \mathcal{E}$ then implies $ji \notin \mathcal{E}$.

5.1.1. Local Polytope Relaxation of Graphical Models

In the following, the transition from the discrete energy minimization problem (5.1) to the local polytope relaxation (5.3) is sketched. Thereby, additional notation needed in subsequent sections is introduced.

The linear map of simultaneously extracting the row and column sums of a square matrix $M \in \mathbb{R}^{n \times n}$ is defined by

$$\mathcal{A}: \mathbb{R}^{n \times n} \rightarrow \mathbb{R}^{2n}, \quad M \mapsto \mathcal{A}[M] := \begin{pmatrix} M \mathbb{1}_n \\ M^\top \mathbb{1}_n \end{pmatrix}. \quad (5.4a)$$

Its adjoint with respect to the corresponding Euclidean inner products is given by

$$\mathcal{A}^\top: \mathbb{R}^{2n} \rightarrow \mathbb{R}^{n \times n}, \quad z = \begin{pmatrix} x \\ y \end{pmatrix} \mapsto \mathcal{A}^\top[z] = x \mathbb{1}_n^\top + \mathbb{1}_n y^\top, \quad \text{with } x, y \in \mathbb{R}^n. \quad (5.4b)$$

For future reference, the following characterization for the kernel of \mathcal{A} is stated next.

Lemma 5.1.1. *The kernel of \mathcal{A}^\top and its orthogonal complement are given by*

$$\ker(\mathcal{A}^\top) = \left\{ a \begin{pmatrix} \mathbb{1}_n \\ -\mathbb{1}_n \end{pmatrix} \in \mathbb{R}^{2n} : a \in \mathbb{R} \right\} \quad (5.5a)$$

$$\ker(\mathcal{A}^\top)^\perp = \left\{ z \in \mathbb{R}^{2n} : \left\langle z, \begin{pmatrix} \mathbb{1}_n \\ -\mathbb{1}_n \end{pmatrix} \right\rangle = 0 \right\}. \quad (5.5b)$$

Proof. Let $z = \begin{pmatrix} x \\ y \end{pmatrix} \in \mathbb{R}^{2n}$, with $x, y \in \mathbb{R}^n$ and assume $0 = \mathcal{A}^\top[z] = x \mathbb{1}_n^\top + \mathbb{1}_n y^\top$. Applying \mathcal{A} results in

$$0 = \mathcal{A}[x \mathbb{1}_n^\top + \mathbb{1}_n y^\top] = \begin{pmatrix} nx + \langle y, \mathbb{1}_n \rangle \mathbb{1}_n \\ \langle x, \mathbb{1}_n \rangle \mathbb{1}_n + ny \end{pmatrix} \Leftrightarrow z = \begin{pmatrix} x \\ y \end{pmatrix} = -\frac{1}{n} \begin{pmatrix} \langle y, \mathbb{1}_n \rangle \mathbb{1}_n \\ \langle x, \mathbb{1}_n \rangle \mathbb{1}_n \end{pmatrix}.$$

Substituting the right-hand side back into $0 = \mathcal{A}^\top[z]$ directly gives $\langle x, \mathbb{1}_n \rangle = -\langle y, \mathbb{1}_n \rangle$. Thus, setting $a = \frac{1}{n} \langle x, \mathbb{1}_n \rangle \in \mathbb{R}$ shows that z has the form (5.5a). Conversely, in view of (5.4b), it is clear that any vector from the set (5.5a) is in $\ker(\mathcal{A}^\top)$. The characterization of the orthogonal complement $\ker(\mathcal{A}^\top)^\perp$ directly follows from the definitions. \square

Let $p, q \in \Delta$, representing two discrete probability distributions on the set of labels \mathcal{X} . Using the map \mathcal{A} , the set of joint probability distributions on $\mathcal{X} \times \mathcal{X}$ with marginals p and q , also called the set of *coupling measures*, is defined by

$$\Pi(p, q) := \left\{ M \in \mathbb{R}^{n \times n} \mid M \geq 0 \text{ and } \mathcal{A}[M] = \begin{pmatrix} p \\ q \end{pmatrix} \right\} \quad (5.6)$$

The first step towards the LP relaxation is the definition of *local model parameter vectors* and *matrices* associated to each vertex $i \in \mathcal{V}$ and edge $ij \in \mathcal{E}$, encoding the values of the corresponding discrete energy values J_i and J_{ij} in the objective function (5.1). For each $i \in \mathcal{V}$ and $ij \in \mathcal{E}$, these associated vectors and matrices are defined by

$$\vartheta_i \in \mathbb{R}^n \quad \text{with components} \quad (\vartheta_i)^k := J_i(\ell_k), \quad \forall k \in [n], \quad (5.7a)$$

$$\vartheta_{ij} \in \mathbb{R}^{n \times n} \quad \text{with components} \quad (\vartheta_{ij})_k^l := J_{ij}(\ell_k, \ell_l), \quad \forall k, l \in [n], \quad (5.7b)$$

where $\ell_k, \ell_l \in \mathcal{X}$. These local terms are commonly called *unary* and *pairwise terms* in the literature. Recall from the discussion of (5.1) that the unary terms represent the data and the pairwise terms specify a regularizer. All these local terms, indexed by the vertices $i \in \mathcal{V}$ and edges $ij \in \mathcal{E}$ of the underlying graph $\mathcal{G} = (\mathcal{V}, \mathcal{E})$, are stacked into the vector

$$\vartheta := \begin{pmatrix} \vartheta_{\mathcal{V}} \\ \vartheta_{\mathcal{E}} \end{pmatrix}, \quad \text{with} \quad \vartheta_{\mathcal{V}} := (\vartheta_i)_{i \in \mathcal{V}} \in \mathbb{R}^{|\mathcal{V}|n} \quad \text{and} \quad \vartheta_{\mathcal{E}} := (\vartheta_{ij})_{ij \in \mathcal{E}} \in \mathbb{R}^{|\mathcal{E}|n^2}, \quad (5.8)$$

where ϑ_{ij} is conveniently regard either as a vector in \mathbb{R}^{n^2} or as a matrix $\mathbb{R}^{n \times n}$, depending on the context.

Next, *local indicator vectors* and *matrices* are used to represent label choices $x \in \mathcal{X}^m$. For each vertex $i \in \mathcal{V}$ and edge $ij \in \mathcal{E}$, the associated indicator vector and matrix with respect to the choices $x_i, x_j \in \mathcal{X}$ are given by

$$\mu_i \in \{0, 1\}^n \quad \text{and} \quad \mu_{ij} \in \{0, 1\}^{n \times n}, \quad (5.9)$$

where $\mu_i = e_k$ and $\mu_{ij} = e_k e_l^\top$, if $x_i = \ell_k$ and $x_j = \ell_l$, with the standard basis vectors $e_k, e_l \in \mathcal{B}_n$. In the same way as (5.8), all local terms are stacked into the vector

$$\mu := \begin{pmatrix} \mu_{\mathcal{V}} \\ \mu_{\mathcal{E}} \end{pmatrix}, \quad \text{with} \quad \mu_{\mathcal{V}} := (\mu_i)_{i \in \mathcal{V}} \quad \text{and} \quad \mu_{\mathcal{E}} := (\mu_{ij})_{ij \in \mathcal{E}}. \quad (5.10)$$

This encoding establishes a one-to-one correspondence between label choices $x \in \mathcal{X}^m$ and discrete indicator vectors in the set

$$\mathcal{D}_{\mathcal{G}} := \left\{ \mu \in \{0, 1\}^{|\mathcal{V}|n + |\mathcal{E}|n^2} \mid \forall i \in \mathcal{V}, \mu_i \in \Delta \text{ and } \forall ij \in \mathcal{E}, \mu_{ij} \in \Pi(\mu_i, \mu_j) \right\}, \quad (5.11)$$

where \mathcal{A} is the linear map from (5.4a).

Combining the indicator vector μ and the model parameter ϑ , the energy values J_i and J_{ij} for vertex $i \in \mathcal{V}$ and edge $ij \in \mathcal{E}$ can now be written as inner products

$$J_i(x_i) = \langle \vartheta_i, \mu_i \rangle \quad \text{and} \quad J_{ij}(x_i, x_j) = \langle \vartheta_{ij}, \mu_{ij} \rangle.$$

5.1. Background on Graphical Models for Image Labeling

Therefore, the overall combinatorial optimization problem (5.1) now reads

$$\min_{x \in \mathcal{X}^m} \{J(x)\} = \min_{\mu \in \mathcal{D}_G} \{\langle \vartheta, \mu \rangle\}.$$

The corresponding linear programming relaxation consists in replacing the constraint of the indicator vectors in (5.11) from taking values in the discrete set $\{0, 1\}$ to taking values in the interval $[0, 1] \subset \mathbb{R}$, resulting in the so-called *local polytope* \mathcal{L}_G , defined by

$$\mathcal{L}_G := \left\{ \mu \in \mathbb{R}^{|\mathcal{V}|n + |\mathcal{E}|n^2} \mid \forall i \in \mathcal{V}, \mu_i \in \Delta \text{ and } \forall ij \in \mathcal{E}, \mu_{ij} \in \Pi(\mu_i, \mu_j) \right\}, \quad (5.12)$$

where the adjective ‘local’ refers to the local marginalization constraints $\Pi(\mu_i, \mu_j)$ (5.6). As a consequence of this, the LP relaxation (5.3) of (5.1) reads more explicitly

$$\min_{\mu \in \mathcal{L}_G} \{\langle \vartheta, \mu \rangle\} = \min_{\mu \in \mathcal{L}_G} \{\langle \vartheta_{\mathcal{V}}, \mu_{\mathcal{V}} \rangle + \langle \vartheta_{\mathcal{E}}, \mu_{\mathcal{E}} \rangle\}, \quad (5.13)$$

5.1.2. Smoothed LP Relaxation and Belief Propagation

Next, the smoothed LP relaxation is introduced and belief propagation is sketched together with the origin of the corresponding *messages*.

Starting point is the primal LP (5.3) written in the form

$$\min_{\mu} \langle \vartheta, \mu \rangle \quad \text{subject to} \quad A\mu = b, \quad \mu \geq 0, \quad (5.14)$$

with a suitably chosen matrix A and vector b for representing the constraints of the entire feasible set \mathcal{L}_G explicitly given by (5.12). The corresponding dual LP (B.24) reads

$$\max_{\nu} \{\langle b, \nu \rangle\}, \quad A^{\top} \nu \leq \vartheta,$$

with dual (multiplier) variable ν corresponding to the affine primal equality constraints $A\mu = b$. Due to the specific structure of these constraints, for each $i \in \mathcal{V}$ and $ij \in \mathcal{E}$ the vector ν contains local dual variables

$$\nu_i \in \mathbb{R} \quad \text{and} \quad \nu_{ij} = \begin{pmatrix} \nu_{ij;i} \\ \nu_{ij;j} \end{pmatrix} \in \mathbb{R}^{2n}, \quad \text{with} \quad \nu_{ij;i}, \nu_{ij;j} \in \mathbb{R}^n,$$

where ν_i corresponds to the constraint $\langle \mu_i, \mathbb{1}_n \rangle = 1$ and ν_{ij} to the marginal constraints on μ_{ij} , with $\nu_{ij;i}$ being associated to $\mu_{ij} \mathbb{1}_n = \mu_i$ and $\nu_{ij;j}$ to $\mu_{ij}^{\top} \mathbb{1}_n = \mu_j$. With this, ν can be viewed as resulting from stacking all local dual vectors

$$\nu = \begin{pmatrix} \nu_{\mathcal{V}} \\ \nu_{\mathcal{E}} \end{pmatrix}, \quad \text{with} \quad \nu_{\mathcal{V}} := (\nu_i)_{i \in \mathcal{V}} \quad \text{and} \quad \nu_{\mathcal{E}} := (\nu_{ij})_{ij \in \mathcal{E}}.$$

In order to obtain a condition that relates optimal vectors μ and ν without subdifferentials that are caused by the non-smoothness of these LPs, one considers the *smoothed* primal convex problem

$$\min_{\mu \in \mathcal{L}_G} \{\langle \vartheta, \mu \rangle - \tau H_B(\mu)\}, \quad (5.15)$$

with smoothing parameter $\tau > 0$ and the *Bethe entropy* H_B . This entropy constitutes an approximation of the underlying (usually) intractable true entropy of the associated probability distribution (5.2), defined by

$$H_B(\mu) := \sum_{ij \in \mathcal{E}} H(\mu_{ij}) - \sum_{i \in \mathcal{V}} (d(i) - 1)H(\mu_i), \quad (5.16)$$

with degree $d(i) := |\mathcal{N}_i \setminus \{i\}|$ of vertex $i \in \mathcal{V}$ (number of neighboring vertices) and the local entropy functions

$$H(\mu_i) = -\langle \mu_i, \log \mu_i \rangle \quad H(\mu_{ij}) = -\langle \mu_{ij}, \log \mu_{ij} \rangle. \quad (5.17)$$

As a consequence of this specific approximation, $-H_B$ is *not* convex. Setting temporarily $\tau = 1$ and evaluating the optimality condition $\partial_\mu L(\mu, \lambda, \nu) = 0$ based on the corresponding Lagrangian (B.15) for the primal LP (5.14)

$$L(\mu, \lambda, \nu) = \langle \vartheta, \mu \rangle - H_B(\mu) - \langle \lambda, \mu \rangle + \langle \nu, A\mu - b \rangle, \quad (5.18)$$

yields $\lambda = 0$ and the following relations connecting μ and ν ,

$$\mu_i^l = e^{\nu_i} e^{-\vartheta_i^l} \prod_{j \in \mathcal{N}_i} e^{\nu_{ij}^l}, \quad \forall l \in [n] \quad \forall i \in \mathcal{V}, \quad (5.19a)$$

$$(\mu_{ij})_l^r = e^{\nu_i + \nu_j} e^{-(\vartheta_{ij})_l^r - \vartheta_i^l - \vartheta_j^r} \prod_{k \in \mathcal{N}_i \setminus \{j\}} e^{\nu_{ik}^l} \prod_{k \in \mathcal{N}_j \setminus \{i\}} e^{\nu_{jk}^r}, \quad \forall l, r \in [n] \quad \forall ij \in \mathcal{E}. \quad (5.19b)$$

The terms $e^{\nu_i}, e^{\nu_i + \nu_j} \in \mathbb{R}$ normalize the expressions on the right-hand side, whereas the so-called *messages* $e^{\nu_{ij}^l} \in \mathbb{R}^n$ enforce the local marginalization constraints of the joint distributions $\mu_{ij} \in \Pi(\mu_i, \mu_j)$. Utilizing these latter constraints allows, after some algebra, to eliminate the left-hand side of (5.19) to obtain the fixed point equations

$$e^{\nu_{ij}^l} = e^{\nu_j} \sum_{r \in [n]} \left(e^{-(\vartheta_{ij})_l^r - \vartheta_j^r} \prod_{k \in \mathcal{N}_j \setminus \{i\}} e^{\nu_{jk}^r} \right), \quad \forall l \in [n], \quad \forall ij \in \mathcal{E}, \quad (5.20)$$

solely in terms of the *dual* variables, commonly called *sum-product algorithm* or *loopy belief propagation* by *message passing*. Repeating this derivation with the general smoothing parameter $\tau > 0$ of (5.15), it can be shown that taking the limit $\lim_{\tau \searrow 0}$ results in the fixed point equations

$$\nu_{ij}^l = \nu_j + \max_{r \in [n]} \left\{ e^{-(\vartheta_{ij})_l^r - \vartheta_j^r} \prod_{k \in \mathcal{N}_j \setminus \{i\}} e^{\nu_{jk}^r} \right\}, \quad \forall l \in [n], \quad \forall ij \in \mathcal{E},$$

called *max-product algorithm* in the literature, solving the original primal LP (5.14).

Using a smooth approximation with $0 < \varepsilon \ll 1$ for loopy belief propagation (5.20) to avoid the inherently non-smooth max-operation in the max-product algorithm, necessitates to choose ε very small so as to stay close to the original primal LP (5.14). Also, local

marginalization constraints are only satisfied *after* convergence of the iteration. Furthermore, the feasible set of the relaxation (5.13) is a superset of the original feasible set of (5.1). Therefore, a globally optimal solution $\bar{\mu}$ of (5.13) generally does *not* correspond to a valid labeling, but rather contains *non-integral* components $\mu_i^l \in (0, 1)$, $l \in [n]$ $i \in \mathcal{V}$. One way to overcome this are randomized rounding schemes as post-processing step for converting a relaxed solution vector $\bar{\mu}$ to a valid labeling $x \in \mathcal{X}^m$ [KT02, CKNZ05].

5.2. Variational Formulation of Graphical Models via local Wasserstein Distances

Optimal transport and the *Wasserstein distance* have become a major tool of signal modeling and analysis [KPT⁺17]. In connection with the metric labeling problem, using the Wasserstein distance (aka. optimal transport costs, earthmover metrics) was proposed before by [AFH⁺04] and [CKNZ05] in a non-smooth setting. However, the focus of the presented approach is on a *smooth geometric* problem reformulation on the assignment manifold which *simultaneously* performs rounding and that scales well with both the problem size and the number of labels.

Towards this goal, the smoothed LP relaxation (5.15) is reformulated in Section 5.2.1 using local entropy regularized Wasserstein distances, which will be the basis for the variational model on the assignment flow. In Section 5.2.2, the dual of the underlying convex optimization problem for general regularized Wasserstein distances is considered and optimality conditions are given. Furthermore, differentiability and analyticity is investigated and an expression for the corresponding gradient is derived. Subsequently, these results are applied in Section 5.2.3 in the case of the entropy regularized Wasserstein distance and a matrix scaling algorithm for computing the corresponding gradients, called Sinkhorn’s algorithm [Sin64], will be derived based on [Cut13]. Finally, in Section 5.2.4, the definition of the variational model is given, the effect of its components on the Riemannian gradient descent flow is identified and the Euclidean gradient is calculated. From the viewpoint of belief propagation, the Wasserstein gradients contained in the Riemannian gradient of the model can be considered as ‘Wasserstein messages’. At the end, some beneficial properties of the Riemannian gradient flow compared to loopy belief propagation are discussed and the influence of the rounding mechanism in the initial phase of the Riemannian gradient flow is investigated.

5.2.1. A Reformulation of the Smoothed LP Relaxation

Regarding the linear objective function of the LP relaxation (5.13) of the form

$$\langle \vartheta, \mu \rangle = \langle \vartheta_{\mathcal{V}}, \mu_{\mathcal{V}} \rangle + \langle \vartheta_{\mathcal{E}}, \mu_{\mathcal{E}} \rangle, \quad \mu \in \mathcal{L}_{\mathcal{G}}, \quad (5.21)$$

the parameters $\mu_i \in \Delta$, with $i \in \mathcal{V}$, can be interpreted as assignment vectors W_i on \mathcal{S} and thus, $\mu_{\mathcal{V}}$ can be viewed as an assignment matrix $W \in \mathcal{W}$. It is therefore natural to consider the LP relaxation as a starting point for deriving a variational formulation

of the underlying discrete objective (5.1) on the assignment manifold \mathcal{W} . With this identification of $\mu_{\mathcal{V}}$ and W in mind, the unary data terms ϑ_i can simply be represented on \mathcal{W} through the inner product $\langle \vartheta_{\mathcal{V}}, W \rangle$. However, it is not obvious how a variational formulation solely based on the assignment vectors W_i (i.e. μ_i) should properly incorporate the pairwise regularization parameters ϑ_{ij} for the edges $ij \in \mathcal{E}$, without referring to the coupling measures $\mu_{ij} \in \Pi(\mu_i, \mu_j)$.

The key observation for ‘eliminating’ the edge-based variables μ_{ij} in the LP relaxation (5.13), is the fact that the linear function $\langle \vartheta_{\mathcal{E}}, \mu_{\mathcal{E}} \rangle$ as well as the corresponding constraints for $\mu_{\mathcal{E}}$ separate over the edges $ij \in \mathcal{E}$. This allows to split and encapsulate the minimization with respect to the coupling measures μ_{ij} as subproblems inside the LP minimization itself, resulting in individual *local Wasserstein distances* only depending on the corresponding marginal distributions μ_i and μ_j for any edge $ij \in \mathcal{E}$.

Lemma 5.2.1. *The local polytope relaxation (5.13) given by*

$$\min_{\mu \in \mathcal{L}_{\mathcal{G}}} \{ \langle \vartheta, \mu \rangle \},$$

with $\mathcal{L}_{\mathcal{G}}$ from (5.12) is equivalent to the problem

$$\min_{\mu_{\mathcal{V}} \in \Delta^m} \left\{ \sum_{i \in \mathcal{V}} \langle \vartheta_i, \mu_i \rangle + \sum_{ij \in \mathcal{E}} d_{\vartheta_{ij}}(\mu_i, \mu_j) \right\} \quad (5.22)$$

involving the local Wasserstein distances

$$d_{\vartheta_{ij}}(\mu_i, \mu_j) := \min_{\mu_{ij} \in \Pi(\mu_i, \mu_j)} \{ \langle \vartheta_{ij}, \mu_{ij} \rangle \}, \quad (5.23)$$

with the set of coupling measures $\Pi(\mu_i, \mu_j)$ given by (5.6).

Proof. The claim follows from reformulating the LP-relaxation based on the local polytope constraints (5.12) with the indicator functions $\delta_{\Pi(\mu_i, \mu_j)}$ from (B.2) as follows.

$$\begin{aligned} \min_{\mu \in \mathcal{L}_{\mathcal{G}}} \{ \langle \vartheta, \mu \rangle \} &= \min_{\mu \in \mathcal{L}_{\mathcal{G}}} \{ \langle \vartheta_{\mathcal{V}}, \mu_{\mathcal{V}} \rangle + \langle \vartheta_{\mathcal{E}}, \mu_{\mathcal{E}} \rangle \} \\ &= \min_{\mu_{\mathcal{V}} \in \Delta^m} \left\{ \langle \vartheta_{\mathcal{V}}, \mu_{\mathcal{V}} \rangle + \min_{\mu_{\mathcal{E}}} \sum_{ij \in \mathcal{E}} \left(\langle \vartheta_{ij}, \mu_{ij} \rangle + \delta_{\Pi(\mu_i, \mu_j)}(\mu_{ij}) \right) \right\} \\ &= \min_{\mu_{\mathcal{V}} \in \Delta^m} \left\{ \sum_{i \in \mathcal{V}} \langle \vartheta_i, \mu_i \rangle + \sum_{ij \in \mathcal{E}} \min_{\mu_{ij} \in \Pi(\mu_i, \mu_j)} \{ \langle \vartheta_{ij}, \mu_{ij} \rangle \} \right\} \\ &= \min_{\mu_{\mathcal{V}} \in \Delta^m} \left\{ \sum_{i \in \mathcal{V}} \langle \vartheta_i, \mu_i \rangle + \sum_{ij \in \mathcal{E}} d_{\vartheta_{ij}}(\mu_i, \mu_j) \right\}. \quad \square \end{aligned}$$

This way, the edge-based variables μ_{ij} are hidden in the optimization subproblems for the local Wasserstein distances, where ‘local’ refers to the fact that the Wasserstein distances itself only depend on the local marginal distributions μ_i, μ_j for $ij \in \mathcal{E}$.

As only unary variables μ_i with simplex constraints occur in the reformulated problem (5.24), this objective function is a suitable candidate for a variational model on the

5.2. Variational Formulation of Graphical Models using local Wasserstein Distances

assignment manifold which properly takes into account the regularization parameters ϑ_{ij} . However, due to the convex but non-smooth (piecewise-linear (cf. [RW09, Def. 2.47])) local Wasserstein distances (5.23), the reformulated problem (5.22), as the original LP relaxation, is non-smooth.

To overcome this deficit and derive a smoothed version of (5.22), the reformulation from the proof of Lemma 5.2.1 is applied to the smoothed primal LP relaxation (5.16).

Lemma 5.2.2. *The smoothed LP relaxation (5.15) given by*

$$\min_{\mu \in \mathcal{L}_{\mathcal{G}}} \{ \langle \vartheta, \mu \rangle - \tau H_{\text{B}}(\mu) \},$$

with the local polytope $\mathcal{L}_{\mathcal{G}}$ (5.12), Bethe entropy H_{B} (5.16) and smoothing parameter $\tau > 0$ is equivalent to the problem

$$\min_{\mu_{\mathcal{V}} \in \Delta^m} \left\{ \langle \vartheta_{\mathcal{V}}, \mu_{\mathcal{V}} \rangle + \sum_{ij \in \mathcal{E}} d_{\vartheta_{ij}, \tau}(\mu_i, \mu_j) + \tau \sum_{i \in \mathcal{V}} (d(i) - 1) H(\mu_i) \right\}, \quad (5.24)$$

where the smoothed entropy regularized local Wasserstein distances $d_{\vartheta_{ij}, \tau}(\mu_i, \mu_j)$ are obtained by entropy regularization

$$d_{\vartheta_{ij}, \tau}(\mu_i, \mu_j) := \min_{\mu_{ij} \in \Pi(\mu_i, \mu_j)} \{ \langle \vartheta_{ij}, \mu_{ij} \rangle - \tau H(\mu_{ij}) \}, \quad (5.25)$$

for all $ij \in \mathcal{E}$, with entropy $H(\mu_{ij}) = -\langle \mu_{ij}, \log \mu_{ij} \rangle$ and smoothing parameter $\tau > 0$.

Proof. Keeping in mind the specific form of the Bethe entropy H_{B} and reformulating the smoothed LP relaxation as in the proof of Lemma 5.2.1, results in

$$\begin{aligned} & \min_{\mu \in \mathcal{L}_{\mathcal{G}}} \{ \langle \vartheta, \mu \rangle - \tau H_{\text{B}}(\mu) \} \\ &= \min_{\mu \in \mathcal{L}_{\mathcal{G}}} \left\{ \langle \vartheta_{\mathcal{V}}, \mu_{\mathcal{V}} \rangle + \langle \vartheta_{\mathcal{E}}, \mu_{\mathcal{E}} \rangle - \tau \sum_{ij \in \mathcal{E}} H(\mu_{ij}) + \tau \sum_{i \in \mathcal{V}} (d(i) - 1) H(\mu_i) \right\} \\ &= \min_{\mu_{\mathcal{V}} \in \Delta^m} \left\{ \langle \vartheta_{\mathcal{V}}, \mu_{\mathcal{V}} \rangle + \sum_{ij \in \mathcal{E}} \min_{\mu_{ij} \in \Pi(\mu_i, \mu_j)} \{ \langle \vartheta_{ij}, \mu_{ij} \rangle - \tau H(\mu_{ij}) \} + \tau \sum_{i \in \mathcal{V}} (d(i) - 1) H(\mu_i) \right\} \square \end{aligned}$$

Using the entropy regularized local Wasserstein distances (5.25) implies that the local marginalization constraints $\Pi(\mu_i, \mu_j)$ of the underlying ‘hidden’ edge variables μ_{ij} are *always* satisfied by definition. This is in sharp contrast to inference for the smoothed LP relaxation (5.15) by loopy belief propagation (5.20), where these constraints are only gradually enforced during the iteration and are guaranteed to hold only *after* convergence of the entire iteration process. Therefore, the reformulation (5.24) has two key properties that distinguishes it from established work:

- (I) inherent smoothness and
- (II) validity of the local polytope constraints at anytime.

Since the edge variables are only contained in the subproblems (5.25), this approach does not suffer from the enormous memory requirements that would arise from directly solving the smoothed LP (5.15) in the primal domain and thus allows to work with graphs having higher connectivity.

Thus, (5.25) will be the basis for the variational model in Section 5.2.4 below. However, first some basic properties of general regularized Wasserstein distances are investigated.

5.2.2. General Smoothed Wasserstein Distances

In this section, properties of a general regularized Wasserstein distance are considered. First, the dual optimization problem and corresponding optimality conditions are derived. Subsequently, differentiability as well as analyticity are investigated and an expression for the gradient is given. To this end, it will be convenient to temporarily simplify notation.

Suppose $p = (p_1, p_2) \in \Delta \times \Delta \subset \mathbb{R}^{2n}$ are two discrete probability distributions on the set of labels \mathcal{X} and $\Theta \in \mathbb{R}^{n \times n}$ is an associated nonnegative cost matrix. The (non-smooth) Wasserstein distance then reads

$$d_{\Theta}(p_1, p_2) = \min_{M \in \Pi(p_1, p_2)} \{ \langle \Theta, M \rangle \}. \quad (5.26)$$

Explicitly expressing the constraints $\Pi(p_1, p_2)$ from (5.6) using the linear map \mathcal{A} defined by (5.4a), the linear optimization problem (5.26) may be written as

$$d_{\Theta}(p_1, p_2) = \min_{M \in \mathbb{R}^{n \times n}} \langle \Theta, M \rangle \quad \text{s.t.} \quad \mathcal{A}[M] = \begin{pmatrix} p_1 \\ p_2 \end{pmatrix} = p, \quad M \geq 0. \quad (5.27)$$

The corresponding dual LP of (5.27) is given by (B.24) and takes the form

$$\max_{\mu, \nu \in \mathbb{R}^{2n}} \langle \mu, \nu \rangle \quad \text{s.t.} \quad \mathcal{A}^{\top}[\nu] \leq \Theta. \quad (5.28)$$

Using a general convex, lower-semicontinuous *smoothing function* $F_{\tau}: \mathbb{R}^{n \times n} \rightarrow \overline{\mathbb{R}}$, with $\overline{\mathbb{R}} = \mathbb{R} \cup \{\infty\}$, results in the *smoothed* local Wasserstein distance

$$d_{\Theta, \tau}(p_1, p_2) := \min_{M \in \Pi(p_1, p_2)} \{ \langle \Theta, M \rangle + F_{\tau}(M) \}, \quad (5.29)$$

with smoothing parameter $\tau > 0$. If the nonnegative cost matrix Θ is symmetric, then, under an additional assumption on the smoothing function, this property also translates to the smoothed Wasserstein distances.

Lemma 5.2.3. *Suppose the cost matrix is symmetric $\Theta^{\top} = \Theta$ and the convex smoothing function F_{τ} in (5.29) satisfies $F_{\tau}(M) = F_{\tau}(M^{\top})$ for all $M \in [0, 1]^{n \times n}$. Then, for any points $p_1, p_2 \in \Delta$, the smoothed Wasserstein distance is symmetric, that is*

$$d_{\Theta, \tau}(p_1, p_2) = d_{\Theta^{\top}, \tau}(p_2, p_1). \quad (5.30)$$

5.2. Variational Formulation of Graphical Models using local Wasserstein Distances

Proof. Assume $\bar{M} \in \Pi(p_1, p_2)$ is a minimizer of (5.31). Then, due to the assumption on F_τ , it follows

$$d_{\Theta, \tau}(p_1, p_2) = \langle \Theta, \bar{M} \rangle + F_\tau(\bar{M}) = \langle \Theta^\top, \bar{M}^\top \rangle + F_\tau(\bar{M}^\top).$$

Let $M \in \Pi(p_2, p_1)$ be arbitrary. Then $M^\top \in \Pi(p_1, p_2)$ and

$$\langle \Theta^\top, M \rangle + F_\tau(M) = \langle \Theta, M^\top \rangle + F_\tau(M^\top) \geq \langle \Theta, \bar{M} \rangle + F_\tau(\bar{M}) = \langle \Theta^\top, \bar{M}^\top \rangle + F_\tau(\bar{M}^\top).$$

This shows that $\bar{M}^\top \in \Pi(p_2, p_1)$ is a minimizer of $d_{\Theta^\top, \tau}(p_2, p_1)$, establishing (5.30). \square

It will be advantageous to slightly rewrite problem (5.29) with explicit expressions for the constraints in the form

$$d_{\Theta, \tau}(p_1, p_2) = \min_{M \in \mathbb{R}^{n \times n}} \{ \langle \Theta, M \rangle + F_\tau(M) \} \quad \text{s.t.} \quad \mathcal{A}[M] = p, \quad M \geq 0, \quad (5.31a)$$

$$= \min_{M \in \mathbb{R}^{n \times n}} \{ \langle \Theta, M \rangle + G_\tau(M) \} \quad \text{s.t.} \quad \mathcal{A}[M] = p, \quad (5.31b)$$

where $G_\tau: \mathbb{R}^{n \times n} \rightarrow \bar{\mathbb{R}}$ is defined as

$$G_\tau(M) := F_\tau(M) + \delta_{\mathbb{R}_{\geq 0}^{n \times n}}(M), \quad (5.32)$$

with the convex indicator function $\delta_{\mathbb{R}_{\geq 0}^{n \times n}}$ of (B.2) expressing the nonnegativity constraints for M . As $\mathbb{R}_{\geq 0}^{n \times n}$ is a closed convex set, $\delta_{\mathbb{R}_{\geq 0}^{n \times n}}$ and therefore also G_τ is convex and lower semicontinuous.

Next, the dual problem of (5.31b) is derived and, under the additional assumptions of strong duality and differentiability of the conjugate G_τ^* , an optimality condition relating the primal and dual solution is given.

Lemma 5.2.4. *The dual problem of (5.31b) is given by*

$$\max_{\nu \in \mathbb{R}^{2n}} \{ \langle p, \nu \rangle - G_\tau^*(\mathcal{A}^\top[\nu] - \Theta) \}, \quad (5.33)$$

where G_τ^* is the conjugate function (B.3). Additionally, suppose strong duality holds. Then, if G_τ^* is defined and continuously differentiable on all of $\mathbb{R}^{n \times n}$, the condition for optimal primal \bar{M} and dual $\bar{\nu} = (\bar{\nu}_1, \bar{\nu}_2)$ solutions is

$$\bar{M} = \partial G_\tau^*(\mathcal{A}^\top[\bar{\nu}] - \Theta), \quad \text{with} \quad \mathcal{A}[\bar{M}] = p \quad \text{and} \quad \bar{M} \geq 0. \quad (5.34)$$

Proof. Since the primal optimization problem (5.31b) has no inequality constraints, the associated Lagrangian (B.15), depending on $p = (p_1, p_2)$, is given by

$$L_p(M, \nu) = \langle \Theta, M \rangle + G_\tau(M) + \langle \nu, p - \mathcal{A}[M] \rangle = \langle \nu, p \rangle + \langle \Theta - \mathcal{A}^\top[\nu], M \rangle + G_\tau(M),$$

with $(M, \nu) \in \mathbb{R}^{n \times n} \times \mathbb{R}^{2n}$. The corresponding dual function then reads

$$\begin{aligned} h_p(\nu) &= \inf_M \{ L_p(M, \nu) \} = \langle \nu, p \rangle + \inf_M \{ \langle \Theta - \mathcal{A}^\top[\nu], M \rangle + G_\tau(M) \} \\ &= \langle \nu, p \rangle - \sup_M \{ \langle \mathcal{A}^\top[\nu] - \Theta, M \rangle - G_\tau(M) \} = \langle \nu, p \rangle - G_\tau^*(\mathcal{A}^\top[\nu] - \Theta), \end{aligned}$$

where the last equality directly follows from the definition (B.3) of conjugate functions.

Next, suppose strong duality holds and G_τ^* is continuously differentiable on all of $\mathbb{R}^{n \times n}$. For the optimal primal \bar{M} and dual $\bar{\nu} = (\bar{\nu}_1, \bar{\nu}_2)$ solutions, strong duality then implies

$$\langle \nu, p \rangle - G_\tau^*(\mathcal{A}^\top[\bar{\nu}] - \Theta) = h_p(\bar{\nu}) = d_{\Theta, \tau}(p_1, p_2) = \langle \Theta, \bar{M} \rangle + G_\tau(\bar{M}). \quad (5.35)$$

As a consequence of the constraint $\mathcal{A}[\bar{M}] = p$, the reformulation

$$\langle \bar{\nu}, p \rangle = \langle \bar{\nu}, \mathcal{A}[\bar{M}] \rangle = \langle \mathcal{A}^\top[\bar{\nu}], \bar{M} \rangle \quad (5.36)$$

follows. Furthermore, $G_\tau^{**} = G_\tau$ as a consequence of G_τ being convex and lower semi-continuous. Thus, rearranging (5.35) and applying the reformulation of (5.36) gives

$$\langle \mathcal{A}^\top[\bar{\nu}] - \Theta, \bar{M} \rangle - G_\tau^*(\mathcal{A}^\top[\bar{\nu}] - \Theta) = G_\tau(\bar{M}) = G_\tau^{**}(\bar{M}) = \sup_Z \{ \langle Z, \bar{M} \rangle - G_\tau^*(Z) \}.$$

Therefore, $\mathcal{A}^\top[\bar{\nu}] - \Theta$ is a maximizer of $H(Z) := \langle Z, \bar{M} \rangle - G_\tau^*(Z)$ and fulfills the first order optimality condition

$$0 = \partial H(\mathcal{A}^\top[\bar{\nu}] - \Theta) \Leftrightarrow \bar{M} = \partial G_\tau^*(\mathcal{A}^\top[\bar{\nu}] - \Theta). \quad (5.37)$$

The other two constraints in (5.34) directly follow from the primal optimality of \bar{M} . \square

Remark 5.2.1. The condition of strong duality (cf. Section B.4) made by Lemma 5.2.4 is crucial for what follows. This condition will be satisfied later on when working with the entropy regularization in a *geometric* setting with local coupling measures M , and $p_1, p_2 \in \mathcal{S}$ with *full* support.

In order to get a better intuition for suitable candidates F_τ in (5.29) for smoothing the original problem (5.26), rewrite the constraints of (5.28), using the indicator function (B.2) of the set $\mathbb{R}_{\leq 0}^{n \times n}$, in the form of

$$\delta_{\mathbb{R}_{\leq 0}^{n \times n}}(\mathcal{A}^\top \nu - \Theta). \quad (5.38)$$

Comparing this with the dual problem (5.33) shows that G_τ^* should be a smooth approximation of the indicator function for the set $\mathbb{R}_{\leq 0}^{n \times n}$. This point is revisited.

In the remainder of this section, it will be shown that, depending on the function G_τ^* , the smoothed Wasserstein distance $d_{\Theta, \tau}$ is differentiable or even analytic. Based on the dual problem (5.33), an expression for the gradient is given, allowing to numerically compute it in practice.

Theorem 5.2.5 (Wasserstein distance gradient). *Suppose for every $p = (p_1, p_2) \in \mathcal{S} \times \mathcal{S}$ strong duality holds for the problem (5.31b) and the conjugate function G_τ^* is C^2 on $\mathbb{R}^{n \times n}$ with positive definite Hessian everywhere. Then the smoothed Wasserstein distance $d_{\Theta, \tau}: \mathcal{S} \times \mathcal{S} \rightarrow \mathbb{R}$ is differentiable, and the Riemannian gradient of $d_{\Theta, \tau}$ at p with respect to the induced Euclidean metric is given by*

$$\text{grad}_E d_{\Theta, \tau}(p) = \begin{pmatrix} \text{grad}_{E,1} d_{\Theta, \tau}(p_1, p_2) \\ \text{grad}_{E,2} d_{\Theta, \tau}(p_1, p_2) \end{pmatrix} = \begin{pmatrix} P_{T_S} \bar{\nu}_1 \\ P_{T_S} \bar{\nu}_2 \end{pmatrix} = P_{T_S \times T_S}[\bar{\nu}], \quad (5.39)$$

5.2. Variational Formulation of Graphical Models using local Wasserstein Distances

where $\text{grad}_{E,i} d_{\Theta,\tau}$ denotes the gradient with respect to the argument p_i , $i \in \{1, 2\}$, and

$$\bar{\nu} = \begin{pmatrix} \bar{\nu}_1 \\ \bar{\nu}_2 \end{pmatrix} \in \operatorname{argmax}_{\nu \in \mathbb{R}^{2n}} \{ \langle p, \nu \rangle - G_\tau^*(\mathcal{A}^\top \nu - \Theta) \}.$$

Additionally, if G_τ^* is analytic, then so is $d_{\Theta,\tau}: \mathcal{S} \times \mathcal{S} \rightarrow \mathbb{R}$.

Corollary 5.2.6. *Suppose the assumptions of Theorem 5.2.5 are fulfilled. Furthermore, assume the cost matrix Θ is symmetric and $F_\tau(M) = F_\tau(M^\top)$ for all $M \in [0, 1]^{n \times n}$ holds. Then the Euclidean gradient of $d_{\Theta,\tau}: \mathcal{S} \times \mathcal{S} \rightarrow \mathbb{R}$, with $\tau > 0$, satisfies*

$$\text{grad}_{E,2} d_{\Theta,\tau}(q, p) = \text{grad}_{E,1} d_{\Theta,\tau}(p, q), \quad \forall p, q \in \mathcal{S}. \quad (5.40)$$

Proof. By Theorem 5.2.5, the Wasserstein distance $d_{\Theta,\tau}$ is differentiable. The equality (5.40) is verified by a direct calculation based on the symmetry of $d_{\Theta,\tau}$ due to Lemma 5.2.3. For this, let $\gamma: (-r, r) \rightarrow \mathcal{S}$, for $r > 0$, be a smooth curve with $\gamma(0) = p$ and $\dot{\gamma}(0) = v \in T_{\mathcal{S}}$. Then

$$\begin{aligned} \langle \text{grad}_{E,2} d_{\Theta,\tau}(q, p), v \rangle &= \frac{d}{dt} d_{\Theta,\tau}(q, \gamma(t)) \Big|_{t=0} \stackrel{(5.30)}{=} \frac{d}{dt} d_{\Theta,\tau}(\gamma(t), q) \Big|_{t=0} \\ &= \langle \text{grad}_{E,1} d_{\Theta,\tau}(p, q), v \rangle. \end{aligned}$$

Since this holds for any $v \in T_{\mathcal{S}}$, the equality in (5.40) follows. \square

A proof of Theorem 5.2.5 is given below after some preparatory lemmas. For this, it will be convenient to refer to the dual function (5.33) with the shorthand notation

$$h_p(\nu) := \langle p, \nu \rangle - G_\tau^*(\mathcal{A}^\top [\nu] - \Theta) \quad (5.41)$$

and view $p \in \Delta^2$ and $\nu \in \mathbb{R}^{2n}$ as stacked vectors of the form

$$p = \begin{pmatrix} p_1 \\ p_2 \end{pmatrix}, \quad p_1, p_2 \in \Delta, \quad \text{and} \quad \nu = \begin{pmatrix} \nu_1 \\ \nu_2 \end{pmatrix}, \quad \nu_1, \nu_2 \in \mathbb{R}^n.$$

The next lemma characterizes the set of optimal dual solutions to problem (5.33).

Lemma 5.2.7. *Assume strong duality holds and the function G_τ^* of the dual objective function (5.33), respectively (5.41), is defined, strictly convex and continuously differentiable on $\mathbb{R}^{n \times n}$. Let $p \in \Delta^2$. If $\bar{\nu}$ minimizes the dual function h_p , then the set of all optimal dual solutions has the form*

$$\operatorname{argmax}_{\nu \in \mathbb{R}^{2n}} \{ h_p(\nu) \} = \bar{\nu} + \ker(\mathcal{A}^\top). \quad (5.42)$$

Proof. Let $\bar{\nu}$ be an optimal dual solution. First, the inclusion from left to right is shown. For this, suppose $\bar{\nu}'$ is another optimal dual solution, that is $h_p(\bar{\nu}') = h_p(\bar{\nu})$. Using the shorthands $\bar{w} := \mathcal{A}^\top [\bar{\nu}] - \Theta$ and $\bar{w}' := \mathcal{A}^\top [\bar{\nu}'] - \Theta$ in the following gives

$$\bar{w} - \bar{w}' = \mathcal{A}^\top [\bar{\nu} - \bar{\nu}']. \quad (5.43)$$

Due to (5.41), the equality $h_p(\bar{\nu}') = h_p(\bar{\nu})$ can be reformulated as

$$G_\tau^*(\bar{w}) - G_\tau^*(\bar{w}') = \langle p, \bar{\nu} - \bar{\nu}' \rangle. \quad (5.44)$$

Since the requirements of Lemma 5.2.4 are satisfied, $\bar{\nu}'$ fulfills the optimality condition

$$\bar{M}' = \nabla G_\tau^*(\bar{w}'), \quad \mathcal{A}[\bar{M}'] = p, \quad (5.45)$$

with a corresponding primal optimal solution \bar{M}' . Hence

$$\langle p, \bar{\nu} - \bar{\nu}' \rangle = \langle \mathcal{A}[\bar{M}'], \bar{\nu} - \bar{\nu}' \rangle \stackrel{(5.43)}{=} \langle \bar{M}', \bar{w} - \bar{w}' \rangle \stackrel{(5.45)}{=} \langle \nabla G_\tau^*(\bar{w}'), \bar{w} - \bar{w}' \rangle. \quad (5.46)$$

Overall, the equality

$$G_\tau^*(\bar{w}) - G_\tau^*(\bar{w}') \stackrel{(5.44)}{=} \langle p, \bar{\nu} - \bar{\nu}' \rangle \stackrel{(5.46)}{=} \langle \nabla G_\tau^*(\bar{w}'), \bar{w} - \bar{w}' \rangle \quad (5.47)$$

follows. As a consequence of G_τ^* being strictly convex, the corresponding first order condition (B.4) is a strict inequality for $\bar{w}' \neq \bar{w}$. Thus, (5.47) can only hold if

$$0 = \bar{w}' - \bar{w} \stackrel{(5.43)}{=} \mathcal{A}^\top [\bar{\nu}' - \bar{\nu}],$$

showing that $\bar{\nu}$ and $\bar{\nu}'$ only differ by a vector in $\ker(\mathcal{A}^\top)$, i.e. $\bar{\nu}' \in \bar{\nu} + \ker(\mathcal{A}^\top)$.

It remains to prove the reverse inclusion, that is vectors characterized by the right-hand side of (5.42) maximize the dual objective function h_p . Let $\bar{\nu}'$ be an arbitrary vector in $\bar{\nu} + \ker(\mathcal{A}^\top)$. Lemma 5.1.1 implies that $\bar{\nu}'$ takes the form

$$\bar{\nu}' = \bar{\nu} + a \begin{pmatrix} \mathbb{1}_n \\ -\mathbb{1}_n \end{pmatrix}, \quad \text{with } a \in \mathbb{R}.$$

The fact that $\mathcal{A}^\top [\bar{\nu}'] = \mathcal{A}^\top [\bar{\nu}]$ and $\langle p, \begin{pmatrix} \mathbb{1}_n \\ -\mathbb{1}_n \end{pmatrix} \rangle = \langle p_1, \mathbb{1}_n \rangle - \langle p_2, \mathbb{1}_n \rangle = 1 - 1 = 0$, as a consequence of $p \in \Delta^2$, implies

$$\begin{aligned} h_p(\bar{\nu}') &= \langle p, \bar{\nu} + a \begin{pmatrix} \mathbb{1}_n \\ -\mathbb{1}_n \end{pmatrix} \rangle - G_\tau^*(\mathcal{A}^\top [\bar{\nu} + a \begin{pmatrix} \mathbb{1}_n \\ -\mathbb{1}_n \end{pmatrix}]) - \Theta \\ &= \langle p, \bar{\nu} \rangle - G_\tau^*(\mathcal{A}^\top [\bar{\nu}] - \Theta) = h_p(\bar{\nu}), \end{aligned}$$

showing that $\bar{\nu}' \in \operatorname{argmax}_{\nu \in \mathbb{R}^{2n}} h_p(\nu)$. \square

Using the characterization $\ker(\mathcal{A}^\top)^\perp = \operatorname{Im}(\mathcal{A})$, the space \mathbb{R}^{2n} is orthogonally decomposed for the subsequent considerations into

$$\mathbb{R}^{2n} = \ker(\mathcal{A}^\top) \oplus \operatorname{Im}(\mathcal{A}).$$

Denoting the orthogonal projections of a vector $\nu \in \mathbb{R}^{2n}$ by

$$\nu_k := P_{\ker(\mathcal{A}^\top)} \nu \quad \text{and} \quad \nu_l := P_{\operatorname{Im}(\mathcal{A})} \nu, \quad (5.48)$$

any vector $\nu \in \mathbb{R}^{2n}$ can be decomposed as

$$\nu = \nu_k + \nu_l. \quad (5.49)$$

With this, the *attainment* of optimal dual solutions on the subspace $\operatorname{Im}(\mathcal{A})$ can now be clarified.

Lemma 5.2.8. *Suppose the assumptions of Lemma 5.2.7 are fulfilled and let $p \in \Delta^2$. Then, for any $\bar{\nu} \in \operatorname{argmax}_{\nu \in \mathbb{R}^{2n}} \{h_p(\nu)\}$ with the decomposition $\bar{\nu} = \bar{\nu}_k + \bar{\nu}_l$ from (5.49), it follows*

$$h_p(\bar{\nu}) = h_p(\bar{\nu}_l) = \max_{z \in \operatorname{Im}(\mathcal{A})} \{h_p(z)\} \quad \text{and} \quad \operatorname{argmax}_{z \in \operatorname{Im}(\mathcal{A})} \{h_p(z)\} = \{\bar{\nu}_l\}, \quad (5.50)$$

that is a unique dual maximizer exists in the subspace $\operatorname{Im}(\mathcal{A})$.

Proof. First, the equality on the left-hand side of (5.50) is shown. Lemma 5.2.7 yields

$$\operatorname{argmax}_{\nu \in \mathbb{R}^{2n}} \{h_p(\nu)\} = \bar{\nu} + \ker(\mathcal{A}^\top). \quad (5.51)$$

The decomposition $\bar{\nu} = \bar{\nu}_l + \bar{\nu}_k$ shows that $\bar{\nu}_l$ is contained in $\bar{\nu} + \ker(\mathcal{A}^\top)$ and therefore also maximizes h_p over both sets, \mathbb{R}^{2n} and $\operatorname{Im}(\mathcal{A})$.

For the characterization of the minimizers of h_p over $\operatorname{Im}(\mathcal{A})$ on the right-hand side of (5.50), let $\bar{z} \in \operatorname{Im}(\mathcal{A})$ be another maximizer. As a consequence of the already established equality, $h_p(\bar{z}) = \max_{z \in \operatorname{Im}(\mathcal{A})} \{h_p(z)\} = h_p(\bar{\nu})$ follows and therefore implies $\bar{z} = \bar{\nu} + y$ with $y \in \ker(\mathcal{A}^\top)$ by (5.51). Applying the orthogonal projection onto $\operatorname{Im}(\mathcal{A})$ from (5.48) results in

$$\bar{z} = P_{\operatorname{Im}(\mathcal{A})}\bar{z} = P_{\operatorname{Im}(\mathcal{A})}[\bar{\nu} + y] = P_{\operatorname{Im}(\mathcal{A})}\bar{\nu} = \bar{\nu}_l. \quad \square$$

After these preparations, the main result Theorem 5.2.5 of this section can now be proven.

Proof of Theorem 5.2.5. The proof consists of two parts. First, the orthogonal decomposition $\mathbb{R}^{2n} = \ker(\mathcal{A}^\top) \oplus \operatorname{Im}(\mathcal{A})$ is related to the tangent space $T_{\mathcal{S} \times \mathcal{S}} = T_{\mathcal{S}} \times T_{\mathcal{S}} \subset \mathbb{R}^{2n}$. Second, this relation together with the implicit function theorem is used to show differentiability and derive the relation (5.39).

The first part begins by establishing the inclusion

$$T_{\mathcal{S}} \times T_{\mathcal{S}} \subseteq \operatorname{Im}(\mathcal{A}) = \ker(\mathcal{A}^\top)^\perp. \quad (5.52)$$

For this, let $v = \begin{pmatrix} v_1 \\ v_2 \end{pmatrix} \in T_{\mathcal{S}} \times T_{\mathcal{S}}$ be arbitrary. By definition of $T_{\mathcal{S}}$ in (2.10), the equality $\langle \mathbb{1}_n, v_1 \rangle = \langle \mathbb{1}_n, v_2 \rangle = 0$ and thus $\langle v, \begin{pmatrix} \mathbb{1}_n \\ -\mathbb{1}_n \end{pmatrix} \rangle = 0$ follows, which according to Lemma 5.1.1 means $v \in \ker(\mathcal{A}^\top)^\perp = \operatorname{Im}(\mathcal{A})$ and therefore establishes the inclusion. Next, consider the unique orthogonal decomposition $\nu = \nu_k + \nu_l \in \ker(\mathcal{A}^\top) \oplus \operatorname{Im}(\mathcal{A})$ from (5.49) for any vector $\nu \in \mathbb{R}^{2n}$. As a consequence of (5.52), $P_{T_{\mathcal{S}} \times T_{\mathcal{S}}}[\nu_k] = 0$ holds and implies

$$P_{T_{\mathcal{S}} \times T_{\mathcal{S}}}[\nu_l] = P_{T_{\mathcal{S}} \times T_{\mathcal{S}}}[\nu]. \quad (5.53)$$

For the second part, let C be a $2n \times (2n - 1)$ matrix with the columns C^j forming an orthonormal basis of $\operatorname{Im}(\mathcal{A}) \subset \mathbb{R}^{2n}$. Denote the coordinates of $u \in \operatorname{Im}(\mathcal{A})$ by $x = C^\top u$ and define the linear map

$$\mathcal{C}: \mathbb{R}^{2n-1} \rightarrow \mathbb{R}^{n \times n}, \quad x \mapsto \mathcal{C}[x] := \mathcal{A}^\top[Cx]. \quad (5.54)$$

Furthermore, let $\eta: \mathcal{S}^2 \rightarrow U^2$ denote the stacked m -affine coordinates from (3.20), i.e. for $p = (p_1, p_2) \in \mathcal{S}^2$ let

$$\eta(p) = \begin{pmatrix} \eta_1(p_1) \\ \eta_2(p_2) \end{pmatrix}, \quad \text{with } \eta_i: \mathcal{S} \rightarrow U \quad \text{for } i \in \{1, 2\}.$$

With this, the coordinate expression of $h_p(u)$, with $Cx = u \in \text{Im}(\mathcal{A})$, is given by

$$\hat{h}_\eta(x) = h_{p(\eta)}(Cx) = \langle p(\eta), Cx \rangle - G_\tau^*(\mathcal{C}[x] - \Theta).$$

The gradient of $\hat{h}_\eta(x)$ with respect to x can be viewed as a map

$$\Phi: \mathbb{R}^{2(n-1)} \times \mathbb{R}^{2n-1} \rightarrow \mathbb{R}^{2n-1}, \quad \Phi(\eta, x) := \partial \hat{h}_{p(\eta)}(x) = C^\top p(\eta) - \mathcal{C}^\top [\partial G_\tau^*(\mathcal{C}[x] - \Theta)].$$

Since G_τ^* is assumed to be C^2 , the map Φ is C^1 and the Jacobian of Φ with respect to x takes the form

$$J_{\Phi, x}(\eta, x) = -\mathcal{C}^\top \circ \text{Hess } G_\tau^*(\mathcal{C}[x] - \Theta) \circ \mathcal{C}.$$

If $0 \neq z \in \mathbb{R}^{2n-1}$ then $0 \neq Cz \in \text{Im}(\mathcal{A}) = \ker(\mathcal{A}^\top)^\perp$ and thus also $0 \neq \mathcal{A}^\top[Cz] = \mathcal{C}[z]$. As a consequence of $\text{Hess } G_\tau^*$ being positive definite everywhere, $0 \neq z \in \mathbb{R}^{2n-1}$ implies

$$\langle z, J_{\Phi, x}(\eta, x)[z] \rangle = -\langle \mathcal{C}[z], \text{Hess } G_\tau^*(\mathcal{C}[x] - \Theta)\mathcal{C}[z] \rangle < 0,$$

showing that $J_{\Phi, x}(\eta, x)$ is negative definite and therefore invertible for every η and x .

Now let $p \in \mathcal{S}^2$ be arbitrary and suppose \bar{M} as well as \bar{v} are primal and dual solutions. Because the Hessian of G_τ^* is positive definite, G_τ^* is strictly convex and the assumptions of Lemma 5.2.8 are fulfilled, resulting in the unique dual maximizer $\bar{v}_I = P_{\text{Im}(\mathcal{A})}\bar{v}$ of h_p in the subspace $\text{Im}(\mathcal{A})$ with coordinates \bar{x} , i.e. $C\bar{x} = \bar{v}_I$. Since strong duality is assumed to hold, Lemma 5.2.4 gives the corresponding optimality condition

$$\bar{M} = \partial G_\tau^*(\mathcal{A}^\top[\bar{v}_I] - \Theta) \stackrel{(5.54)}{=} \partial G_\tau^*(\mathcal{C}[\bar{x}] - \Theta) \quad \text{and} \quad \mathcal{A}[\bar{M}] = p. \quad (5.55)$$

Using these conditions in the evaluation of Φ at (η, \bar{x}) gives

$$\Phi(\eta, \bar{x}) = C^\top (p(\eta) - \mathcal{A}[\bar{M}]) = 0.$$

As $J_{\Phi, \bar{x}}(\eta, \bar{x})$ is invertible, the implicit function theorem yields that the maximizer can be parameterized by a unique C^1 function $\bar{x} = \bar{x}(\eta)$ in a small neighborhood of η . Since this holds for all $\eta \in U^2$, the maximizer \bar{x} is a global C^1 function of η , resulting in the differentiable map

$$\bar{v}_I: \mathcal{S}^2 \rightarrow \text{Im}(\mathcal{A}), \quad p \mapsto \bar{v}_I(p) := C\bar{x}(\eta(p)) \quad (5.56)$$

Due to strong duality, the Wasserstein distance is then given by the expression

$$d_{\Theta, \tau}(p) = h_p(\bar{v}_I(p)) = \langle p, \bar{v}_I(p) \rangle - G_\tau^*(\mathcal{A}^\top[\bar{v}_I(p)] - \Theta),$$

proving differentiability. Because of

$$\partial h_p(\bar{v}_I) = p - \mathcal{A}[\partial G_\tau^*(\mathcal{A}^\top[\bar{v}_I] - \Theta)] \stackrel{(5.55)}{=} p - \mathcal{A}[\bar{M}] \stackrel{(5.55)}{=} 0,$$

the gradient of the Wasserstein distance is given by

$$\text{grad}_E d_{\Theta, \tau}(p) = P_{T_S \times T_S} \left[\bar{\nu}_I(p) + d\bar{\nu}_I(p)^\top [\partial h_p(\bar{\nu}_I(p))] \right] = P_{T_S \times T_S} [\bar{\nu}_I(p)].$$

Finally, for an arbitrary $\bar{\nu}' \in \text{argmax}_{\nu \in \mathbb{R}^{2n}} \{h_p(\nu)\}$, the uniqueness of $\bar{\nu}_I(p)$ according to Lemma 5.2.8 implies $\bar{\nu}'_I = \bar{\nu}_I(p)$ and therefore by (5.53)

$$\text{grad}_E d_{\Theta, \tau}(p) = P_{T_S \times T_S} [\bar{\nu}_I(p)] = P_{T_S \times T_S} [\bar{\nu}'],$$

establishing (5.39).

Now, suppose G_τ^* is additionally analytic. Since all involved charts are analytic, so is the above defined map Φ . Then, the real analytic implicit function theorem [KP02, Thm. 2.5.3] implies that the parameterization $\bar{x}(\eta)$, and therefore also $\bar{\nu}_I(p)$ from (5.56), is analytic. Hence, this property also holds for $d_{\Theta, \tau}(p) = h_p(\bar{\nu}_I(p))$ as the composition of two analytic functions. \square

5.2.3. Entropy Regularized Wasserstein Distance

In the following, the results from the previous section are applied to the smoothed entropy regularized local Wasserstein distance (5.25). Based on [Cut13], an iterative matrix scaling algorithm, called Sinkhorn's algorithm [Sin64], will be derived for computing gradients of the entropy regularized Wasserstein distance and numerical aspects with respect to the smoothing parameter τ are examined. For clarity, the simplified notation from the previous section is kept in the following.

The *smooth* entropy regularized Wasserstein distance (5.25) corresponds to the choice $F_\tau(M) = -\tau H(M)$. For $p_1, p_2 \in \Delta$ and nonnegative cost matrix $\Theta \in \mathbb{R}^{n \times n}$, the optimization problem reads

$$d_{\Theta, \tau}(p_1, p_2) = \min_{M \in \Pi(p_1, p_2)} \{ \langle \Theta, M \rangle - \tau H(M) \}, \quad (5.57)$$

with the entropy function

$$H(M) = -\langle M, \log M \rangle = - \sum_{i,j \in [n]} M_i^j \log M_i^j.$$

Since the set of coupling measures $\Pi(p_1, p_2)$ (5.6) is compact as well as $\langle \Theta, M \rangle - \tau H(M)$ continuous and strictly convex, a unique minimizer \bar{M} of (5.57) always exists.

Lemma 5.2.9. *For every $p_1, p_2 \in \mathcal{S}$ and smoothing parameter $\tau > 0$, the optimization problem (5.57) defining $d_{\Theta, \tau}(p_1, p_2)$ satisfies strong duality.*

Proof. Problem (5.57) is a convex optimization problem with affine equality and inequality constraints. For $p_1, p_2 \in \mathcal{S}$ and $\tau > 0$, the matrix $p_1 p_2^\top \in \mathbb{R}^{n \times n}$ fulfills

$$p_1 p_2^\top > 0, \quad \text{and} \quad \mathcal{A}[p_1 p_2^\top] \stackrel{(5.4a)}{=} \begin{pmatrix} p_1 p_2^\top \mathbb{1}_n \\ p_2 p_1^\top \mathbb{1}_n \end{pmatrix} = \begin{pmatrix} p_1 \\ p_2 \end{pmatrix}.$$

Because of $\text{dom}(\langle \Theta, \cdot \rangle - \tau H) = \text{dom}(-H) = \mathbb{R}_{\geq 0}^{n \times n}$, the matrix $p_1 p_2^\top$ is contained in the relative interior $\text{rint}(\text{dom}(-H)) = \mathbb{R}_{> 0}^{n \times n}$. Thus, $p_1 p_2^\top$ satisfies Slater's condition (B.21), implying strong duality. \square

In order to state the dual problem (5.33) for this choice of F_τ , the conjugate function of G_τ from (5.32) is calculated next.

Lemma 5.2.10. *For the choice $F_\tau(M) = -\tau H(M)$, the conjugate of $G_\tau(M)$ from (5.32) is an analytic function $G_\tau^*: \mathbb{R}^{n \times n} \rightarrow \mathbb{R}$ given by*

$$G_\tau^*(X) = e^{-1} \tau \left\langle e^{\frac{1}{\tau} X}, \mathbb{1}_n \mathbb{1}_n^\top \right\rangle = e^{-1} \tau \sum_{k,l \in [n]} e^{\frac{1}{\tau} X_k^l}, \quad \forall X \in \mathbb{R}^{n \times n}, \quad (5.58)$$

where e^X is the componentwise application of the exponential map.

Remark 5.2.2. Because strong duality holds according to Lemma 5.2.9, the constant e^{-1} can be absorbed into the cost matrix Θ . Thus, the factor is dropped in the following considerations.

Proof. The optimization problem defining the conjugate G_τ^* separates as

$$G_\tau^*(X) = \sup_{M \geq 0} \{ \langle X, M \rangle + \tau H(M) \} = \sum_{k,l \in [n]} \sup_{M_k^l \geq 0} \left\{ M_k^l X_k^l - \tau M_k^l \log M_k^l \right\}. \quad (5.59)$$

Thus, consider the maximization of the real valued function

$$h_x: [0, \infty) \rightarrow \mathbb{R}, \quad y \mapsto h_x(y) := yx - \tau y \log y,$$

for fixed $x \in \mathbb{R}$. $\lim_{y \rightarrow \infty} h_x(y) = -\infty$ and $h_x(0) := \lim_{y \rightarrow 0^+} h_x(y) = 0$ directly follow. Due to $h_x''(y) = -\tau/y < 0$, the function is strictly concave, with unique minimizer \bar{y}

$$h_x'(\bar{y}) = x - \tau \log \bar{y} - \tau = 0 \quad \Leftrightarrow \quad e^{\frac{1}{\tau} x - 1} = \bar{y} > 0$$

and corresponding maximum value $\sup_{y \geq 0} \{ h_x(y) \} = h_x(\bar{y}) = \tau e^{\frac{1}{\tau} x - 1}$. Using this in (5.59) and extracting the common factor $e^{-1} \tau$ establishes (5.58). \square

By Lemma 5.2.4 and with the expression of G_τ^* from Lemma 5.2.10, keeping in mind Remark 5.2.2, the dual problem of (5.57) reads

$$\max_{\nu \in \mathbb{R}^{2n}} \langle p, \nu \rangle - \tau \left\langle e^{\frac{1}{\tau} (\mathcal{A}^\top \nu - \Theta)}, \mathbb{1}_n \mathbb{1}_n^\top \right\rangle. \quad (5.60)$$

Regarding the role of G_τ^* in the dual problem, the indicator function (5.38) is smoothly approximated by the function $\tau e^{\frac{1}{\tau} x}$. Figure 5.1 compares this approximation with the classical logarithmic barrier $-\tau \log(-x)$ function for approximating the indicator function $\delta_{\mathbb{R}_{\leq 0}}$ of the nonpositive orthant. Log-barrier penalty functions are the method of choice for interior point methods (see Section 3.1) which *strictly* rule out violations of the constraints. While this is essential for many applications where constraints represent physical properties that cannot be violated, it is *not* essential in the present case for calculating the Wasserstein distance. Moreover, the bias towards interior points by log-barrier functions, as Figure 5.1 clearly shows, is unfavorable in the present context and thus formulation (5.60) is preferred.

5.2. Variational Formulation of Graphical Models using local Wasserstein Distances

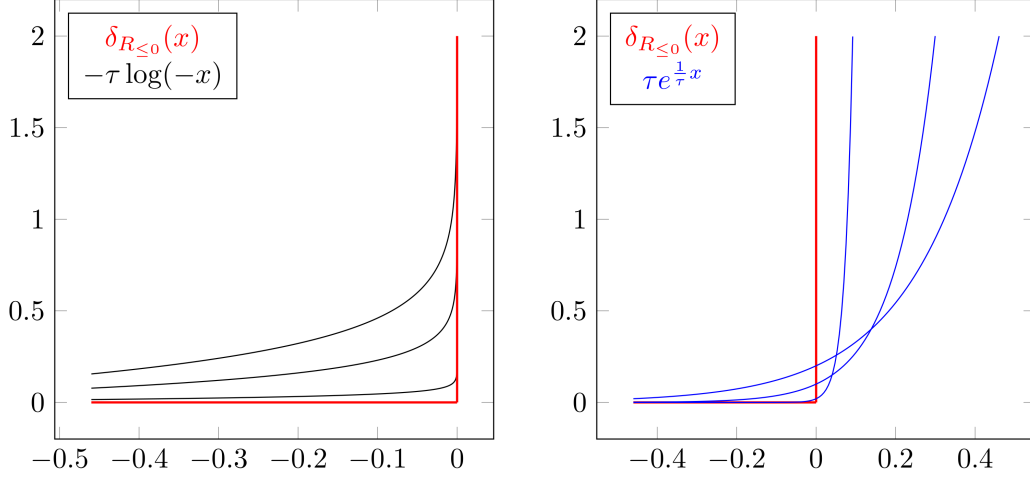


Figure 5.1.: Approximations of the indicator function $\delta_{\mathbb{R}_{\leq 0}}$ (red curves). **Left:** The log-barrier function (black curves) strictly rules out violations of the constraints but induce a bias towards interior points. **Right:** The entropy based formulation (blue curves) is less biased and approximates the δ -function (red curve) reasonably well depending on the smoothing parameter τ . Displayed are the approximations of $\delta_{\mathbb{R}_{\leq 0}}$ for $\tau = \frac{1}{5}, \frac{1}{10}, \frac{1}{50}$.

By Lemma 5.2.10 and Remark 5.2.2, the gradient and Hessian of G_τ^* are given by

$$\partial G_\tau^*(X) = e^{\frac{1}{\tau}X} \quad \text{and} \quad \text{Hess } G_\tau^*(X)[U] = \frac{1}{\tau} e^{\frac{1}{\tau}X} \bullet U, \quad \forall U \in \mathbb{R}^{n \times n}. \quad (5.61)$$

Because of

$$\langle U, \text{Hess } G_\tau^*(X)[U] \rangle = \frac{1}{\tau} \langle U \bullet U, e^{\frac{1}{\tau}X} \rangle = \frac{1}{\tau} \sum_{k,l \in [n]} (U_k^l)^2 e^{\frac{1}{\tau}X_k^l} > 0 \quad (5.62)$$

for all $X, U \in \mathbb{R}^{n \times n}$ with $U \neq 0$, the Hessian is positive definite everywhere, showing that G_τ^* is strictly convex. Therefore, all assumptions of Theorem 5.2.5, including analyticity, are fulfilled, directly implying the following statement.

Corollary 5.2.11. *For any cost matrix $\Theta \geq 0$ and smoothing parameter $\tau > 0$, the entropy regularized Wasserstein distance $d_{\Theta, \tau}: \mathcal{S} \times \mathcal{S} \rightarrow \mathbb{R}$ is analytic and the Euclidean gradient at $p = (p_1, p_2)$ is given by*

$$\text{grad}_E d_{\Theta, \tau}(p) = \begin{pmatrix} \text{grad}_{E,1} d_{\Theta, \tau}(p_1, p_2) \\ \text{grad}_{E,2} d_{\Theta, \tau}(p_1, p_2) \end{pmatrix} = \begin{pmatrix} P_{T_S} \bar{v}_1 \\ P_{T_S} \bar{v}_2 \end{pmatrix} = P_{T_S \times T_S} [\bar{v}], \quad (5.63)$$

where \bar{v} is any maximizer of the dual problem (5.60) and $\text{grad}_{E,i} d_{\Theta, \tau}$ denotes the gradient with respect to the argument p_i , for $i = 1, 2$. Moreover, if Θ is additionally symmetric, then so is $d_{\Theta, \tau}$ and the gradients satisfy

$$\text{grad}_{E,1} d_{\Theta, \tau}(p_1, p_2) = \text{grad}_{E,2} d_{\Theta, \tau}(p_2, p_1), \quad \forall p_1, p_2 \in \mathcal{S}. \quad (5.64)$$

Proof. The first part directly follows from Theorem 5.2.5. Since $H(M) = H(M^\top)$ for all matrices $M \in \mathbb{R}^{n \times n}$, the second part follows from Lemma 5.2.3 and Corollary 5.2.6. \square

Next, it will be derived how the local Wasserstein gradients (5.39) are computed based on the formulation (5.57) and numerical aspects depending on the smoothing parameter τ are examined. It is well known that doubly stochastic matrices as solutions of convex programs like (5.57) can be computed by iterative matrix scaling [Sin64, Sch90], [Bru06, ch. 9]. This has been made popular in the field of machine learning by [Cut13].

Because strong duality holds by Lemma 5.2.9 and G_τ^* is differentiable, the optimality condition (5.34) from Lemma 5.2.4 for optimal primal \bar{M} and dual $\bar{\nu}$ solutions holds and takes the form

$$\bar{M} = \partial G_\tau^*(\mathcal{A}^\top[\bar{\nu}] - \Theta) \stackrel{(5.61)}{=} e^{\frac{1}{\tau}(\mathcal{A}^\top\bar{\nu} - \Theta)}.$$

Rearranging this condition yields the connection to matrix scaling:

$$\begin{aligned} \bar{M} &= e^{\frac{1}{\tau}(\mathcal{A}^\top\bar{\nu} - \Theta)} \stackrel{(5.4b)}{=} e^{\frac{1}{\tau}(\bar{\nu}_1 \mathbf{1}_n^\top + \mathbf{1}_n \bar{\nu}_2^\top - \Theta)} \\ &= \left(e^{\frac{1}{\tau}\bar{\nu}_1} \mathbf{1}_n^\top \right) \bullet e^{-\frac{1}{\tau}\Theta} \bullet \left(e^{\frac{1}{\tau}\bar{\nu}_2} \mathbf{1}_n \right)^\top \\ &= \text{Diag} \left(e^{\frac{1}{\tau}\bar{\nu}_1} \right) e^{-\frac{1}{\tau}\Theta} \text{Diag} \left(e^{\frac{1}{\tau}\bar{\nu}_2} \right), \end{aligned}$$

where $\text{Diag}(\cdot)$ denotes the diagonal matrix with the argument vector as entries and results in a row-wise (left diagonal matrix) and column-wise (right diagonal matrix) scaling of the matrix

$$K := \exp \left(-\frac{1}{\tau}\Theta \right).$$

For given marginals $p = (p_1, p_2) \in \mathcal{S} \times \mathcal{S}$, the optimal dual variables $\bar{\nu} = (\bar{\nu}_1, \bar{\nu}_2) \in \mathbb{R}^{2n}$ can be determined by the Sinkhorn's iterative algorithm [Sin64], up to a common multiplicative constant.

Lemma 5.2.12 ([Cut13, Lemma 2]). *For $\tau > 0$, the solution \bar{M} of (5.57) is unique and has the form $\bar{M} = \text{Diag}(u_1)K \text{Diag}(u_2)$, where the two vectors $u_1, u_2 \in \mathbb{R}^n$ are uniquely defined up to a common multiplicative factor.*

Accordingly, by setting

$$u_1 := e^{\frac{1}{\tau}\bar{\nu}_1}, \quad u_2 := e^{\frac{1}{\tau}\bar{\nu}_2}, \tag{5.65}$$

the corresponding fixed point iterations of Sinkhorn's algorithm read

$$u_1^{(k+1)} = \frac{\mu_1}{K \left(\frac{\mu_2}{K^\top u_1^{(k)}} \right)}, \quad u_2^{(k+1)} = \frac{\mu_2}{K^\top \left(\frac{\mu_1}{K u_2^{(k)}} \right)}, \tag{5.66}$$

which are iterated until the change between consecutive iterates is small enough. Denoting the iterates after convergence by \bar{u}_1, \bar{u}_2 , resubstitution into (5.65) determines the optimal dual variables

$$\bar{\nu}_1 = \tau \log \bar{u}_1, \quad \bar{\nu}_2 = \tau \log \bar{u}_2. \tag{5.67}$$

5.2. Variational Formulation of Graphical Models using local Wasserstein Distances

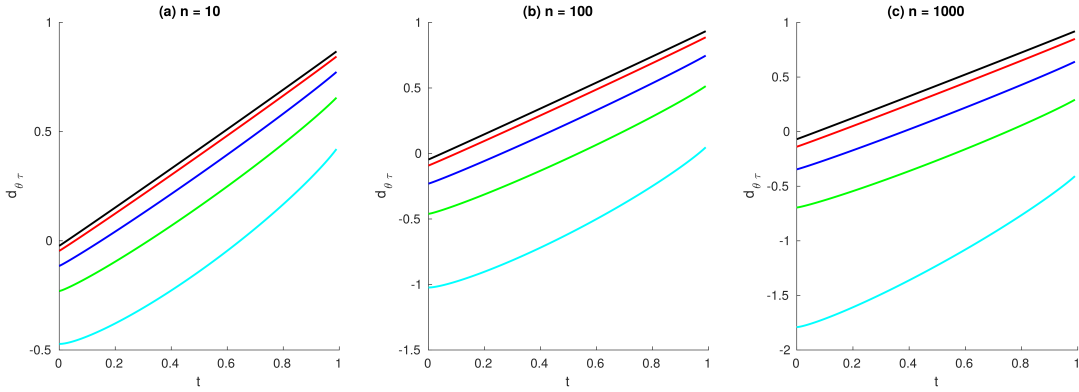


Figure 5.2.: The plots show the entropy-regularized Wasserstein distance $d_{\Theta, \tau}(\mathbb{1}_{\mathcal{S}}, \gamma(t))$ for varying τ and increasing numbers of labels n . Here, $\gamma(t) = t(e_1 - \mathbb{1}_{\mathcal{S}}) + \mathbb{1}_{\mathcal{S}} \in \Delta$, with $t \in [0, 1]$, is the line segment connecting the barycenter $\mathbb{1}_{\mathcal{S}}$ (2.34) to the vertex e_1 on the simplex Δ . The cost matrix Θ is given by the Potts prior (see (5.86)). In all three plots the parameter τ has been chosen as $\tau = \frac{1}{5}$ (cyan), $\tau = \frac{1}{10}$ (green), $\tau = \frac{1}{20}$ (blue), $\tau = \frac{1}{50}$ (red) and $\tau = \frac{1}{100}$ (black). Even though the values of the entropy regularized Wasserstein distance $d_{\Theta, \tau}$ differ considerably, the *slope* of the distance, is already approximated quite well for larger values of τ , uniformly for small up to large numbers n of labels.

Due to Corollary 5.2.11, the local Wasserstein gradients then finally are given by

$$\text{grad}_E d_{\Theta, \tau}(p_1, p_2) = \begin{pmatrix} P_{T_{\mathcal{S}}} \bar{v}_1 \\ P_{T_{\mathcal{S}}} \bar{v}_2 \end{pmatrix},$$

where the orthogonal projection $P_{T_{\mathcal{S}}}$ (2.35), due to $\ker(P_{T_{\mathcal{S}}}) = \mathbb{R}\mathbb{1}_n$, removes the common multiplicative constant resulting from Sinkhorn's algorithm.

While the linear convergence rate of Sinkhorn's algorithm is known theoretically [Kni08], the numbers of iterations required in practice significantly depends on the smoothing parameter τ . In addition, for smaller values of τ , an entry of the matrix $K = \exp\left(-\frac{1}{\tau}\Theta\right)$ might be too small to be represented on a computer, due to machine precision. As a consequence, the matrix K might have entries which are numerically treated as zeros and Sinkhorn's algorithm does not necessarily converge to the true optimal solution. Fortunately, the role of the smoothing parameter τ of the variational approach presented in the next section does allow larger values.

Fortunately, the variational approach presented in the next section does allow larger values of τ because merely a sufficiently accurate approximation of the *gradient* of the Wasserstein distance is required to obtain valid *descent* directions for the Riemannian

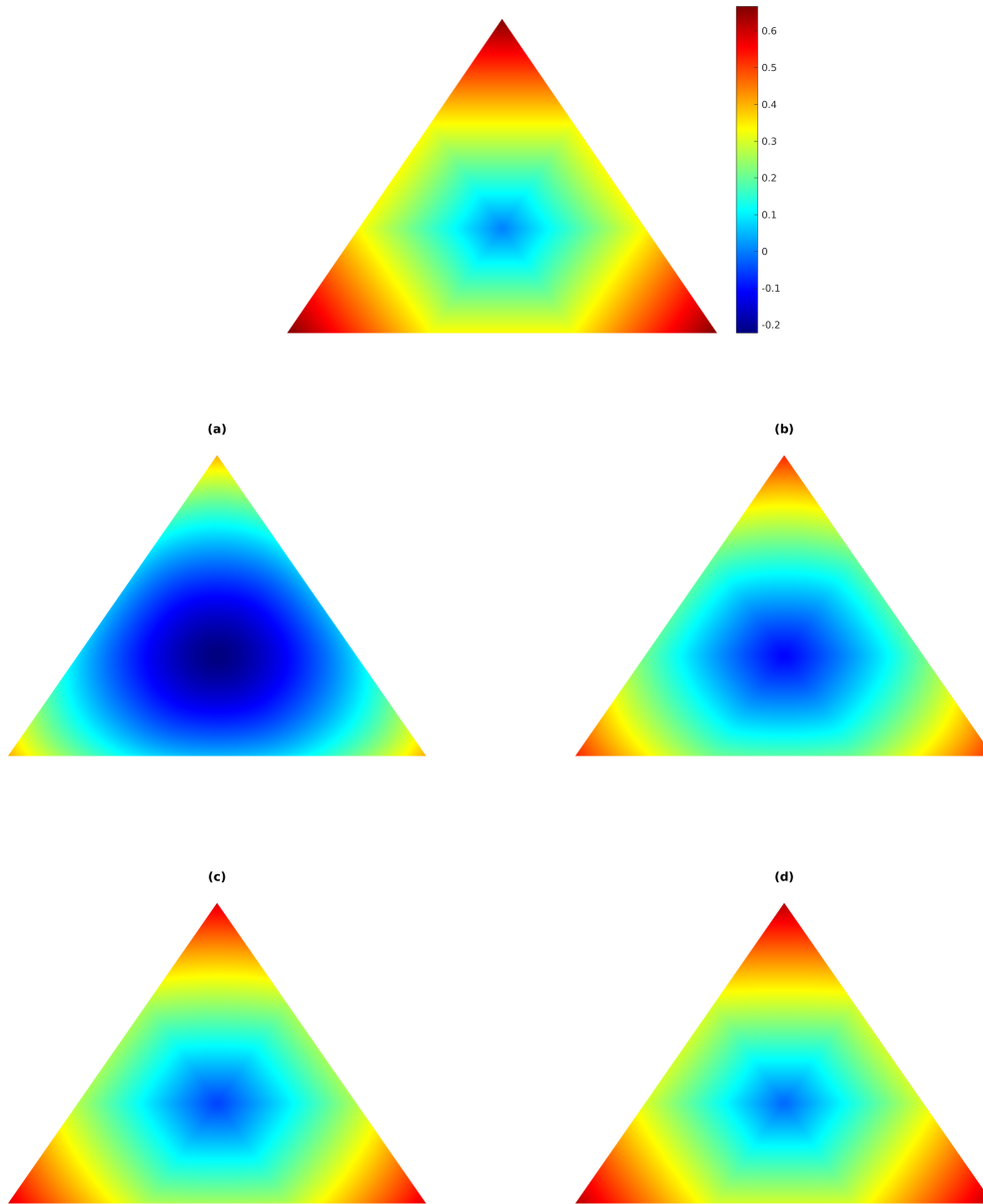


Figure 5.3.: The plot shows the exact Wasserstein distance (top) compared to the entropy regularized Wasserstein distance with the Potts prior (5.86) as a function $d_{\Theta, \tau}(\cdot, \mathbb{1}_{\mathcal{S}})$ from the barycenter to every point on Δ for $n = 3$ labels. Different values of τ are compared: (a) $\tau = \frac{1}{5}$, (b) $\tau = \frac{1}{10}$, (c) $\tau = \frac{1}{20}$ and (d) $\tau = \frac{1}{50}$. These plots confirm that even for relatively large values of τ , e.g. $\frac{1}{10}$ and $\frac{1}{20}$, the *gradient* of the Wasserstein distance is sufficiently accurate approximated so as to obtain valid descent directions for distance minimization through the Riemannian gradient descent flow.

gradient descent flow. Figures 5.2 and 5.3 demonstrate that this indeed holds for relatively large values of τ , e.g. $\tau \in \{\frac{1}{5}, \frac{1}{10}, \frac{1}{15}\}$, no matter if the number of labels is $n = 10$ or $n = 1000$.

5.2.4. Variational Formulation on the Assignment Manifold

In this section, the variational model on the assignment flow is defined based on the reformulation in Lemma 5.2.2. The resulting model consists of a data and regularization component plus an extra integrality enforcing term responsible for rounding to integral assignments, analog to the S -flow. Due to the results from the previous section, the model is analytic and an expression for the gradient can be given. Similar to message passing in belief propagation, the local gradients of the entropy regularized Wasserstein distances in the resulting Riemannian gradient descent flow can be seen as ‘Wasserstein messages’ that are ‘passed along edges’. Finally, the influence of the integrality enforcing term in the initial phase of the gradient flow is investigated.

Throughout this section $d_{\theta,\tau}$ always refers to the entropy regularized Wasserstein distance.

Variational Model

Motivated by the reformulation of the smoothed LP relaxation (5.24) in Lemma 5.2.2, the following variation model on the assignment manifold is defined by replacing $\mu_{\mathcal{V}}$ with W and absorbing the nonnegative factors $\tau(d(i) - 1)$ weighting the entropy term into a second parameter α .

Definition 5.2.1 (variational model). Suppose a discrete objective $J: \mathcal{X}^m \rightarrow \mathbb{R}$ of the form (5.1) is given. Then the associated variational model on the assignment manifold \mathcal{W} with smoothing and integrality enforcing parameter $\tau, \alpha > 0$, is defined by

$$J_{\tau,\alpha}: \mathcal{W} \rightarrow \mathbb{R}, \quad W \mapsto J_{\tau,\alpha}(W) := \langle \vartheta_{\mathcal{V}}, W \rangle + \sum_{ij \in \mathcal{E}} d_{\vartheta_{ij},\tau}(W_i, W_j) + \alpha H_{\mathcal{W}}(W), \quad (5.68)$$

where $H_{\mathcal{W}}(W) = \sum_{i \in \mathcal{V}} H(W_i)$ is the global entropy on \mathcal{W} .

The variational model $J_{\alpha,\tau}$ consists of three terms, each representing different ‘forces’ in the associated dynamics of the Riemannian gradient descent flow which drives inference. The *data term*,

$$J_{\text{data}}(W) := \langle \vartheta_{\mathcal{V}}, W \rangle = \sum_{i \in \mathcal{V}} \langle \vartheta_i, W_i \rangle$$

is responsible for selecting the best fitting label at each individual vertex based on the given unary values ϑ_i alone, irrespective of the spatial context. Regularization is induced by the *regularization term*,

$$J_{\text{reg},\tau}(W) := \sum_{ij \in \mathcal{E}} d_{\vartheta_{ij},\tau}(W_i, W_j) \quad (5.69)$$

taking into account the spatial context and punishing neighboring deviations in the assignments according to the pairwise cost matrices ϑ_{ij} , $ij \in \mathcal{E}$. Since the smoothed Wasserstein distances $d_{\vartheta_{ij},\tau}$ converge to the underlying non-smooth distances $d_{\vartheta_{ij}}$ in the limit $\tau \rightarrow 0$, the data and regularization term together,

$$J_\tau(W) := J_{\text{data}}(W) + J_{\text{reg},\tau}(W) = \langle \vartheta_{\mathcal{V}}, W \rangle + \sum_{ij \in \mathcal{E}} d_{\vartheta_{ij},\tau}(W_i, W_j) \quad (5.70)$$

constitute an approximation of the reformulated non-smooth local polytope relaxation (5.22). Finally, the smooth rounding mechanism of the model is represented by the *integrality enforcing term*, given by the entropy

$$J_{\text{int}}(W) := H_W(W) = \sum_{i \in \mathcal{V}} H(W_i) = \langle W, \log W \rangle. \quad (5.71)$$

Since $H(W_i) \geq 0$ with $H(W_i) = 0$ if and only if W_i is one of the standard basis vectors, this term pushes the flow towards integral assignments. As will be demonstrated in Section 5.3, the additional introduced integrality parameter $\alpha > 0$ enables to control precisely the trade-off between accuracy of labelings in terms of the given function J_τ , approximating the local polytope relaxation (5.22), and the speed of convergence to an integral assignment, independent of the choice for $\tau > 0$. This shows that the rounding mechanism to integral assignments is a *different one* compared to the local polytope relaxation (5.22), where the values τ have to be chosen close to zero and an additional post-processing step is needed.

Calculating the Euclidean Gradient of $J_{\tau,\alpha}$

In order to compute the Euclidean gradient $\text{grad}_E J_{\tau,\alpha}$ of the variational model, the regularization term J_{reg} (5.69) is slightly rewritten. As \mathcal{E} is assumed to be oriented according to Assumption 5.1.1, an edge $ij = (i, j) \in \mathcal{E}$ is interpreted as starting in i and ending in j . The corresponding sets of *outgoing* and *incoming* edges at vertex $i \in \mathcal{V}$ are defined as

$$O(i) := \{(i, j) \in \mathcal{E} \mid j \in \mathcal{V}\} \quad \text{and} \quad I(i) := \{(j, i) \in \mathcal{E} \mid j \in \mathcal{V}\}. \quad (5.72)$$

Since $\mathcal{E} \subset \mathcal{V}^2$, the indicator function $\chi_{\mathcal{E}}: \mathcal{V}^2 \rightarrow \{0, 1\}$ from (2.1) is given by

$$\chi_{\mathcal{E}}(ij) = \begin{cases} 1 & , \text{for } ij \in \mathcal{E} \\ 0 & , \text{for } ij \notin \mathcal{E}. \end{cases} \quad (5.73)$$

With this, the regularization term (5.69) can equivalently be expressed as

$$J_{\text{reg},\tau}(W) = \sum_{i \in \mathcal{V}} \sum_{j \in \mathcal{V}} \chi_{\mathcal{E}}(ij) d_{\vartheta_{ij},\tau}(W_i, W_j) = \sum_{i \in \mathcal{V}} \sum_{ij \in O(i)} d_{\vartheta_{ij},\tau}(W_i, W_j). \quad (5.74)$$

5.2. Variational Formulation of Graphical Models using local Wasserstein Distances

Proposition 5.2.13 (gradient of $J_{\tau,\alpha}$). *The objective function $J_{\alpha,\tau}: \mathcal{W} \rightarrow \mathbb{R}$ is analytic and the i -th row of the Euclidean gradient $\text{grad}_E J_{\tau,\alpha}(W) \in \mathcal{T}_{\mathcal{W}}$ at $W \in \mathcal{W}$ has the form*

$$\text{grad}_{E,i} J_{\tau,\alpha}(W) = P_{T_S} \vartheta_i + \text{grad}_{E,i} J_{\text{reg},\tau}(W) - \alpha \exp_{\mathbb{1}_S}^{-1}(W_i), \quad (5.75)$$

with the gradient of $J_{\text{reg},\tau}$ being given by

$$\text{grad}_{E,i} J_{\text{reg},\tau} = \sum_{ij \in \mathcal{O}(i)} \text{grad}_{E,1} d_{\theta_{ij},\tau}(W_i, W_j) + \sum_{ji \in \mathcal{I}(i)} \text{grad}_{E,2} d_{\theta_{ji},\tau}(W_j, W_i),$$

where $\text{grad}_{E,k} d_{\theta_{ij},\tau}(W_i, W_j) \in T_S$ denotes the gradient with respect to the k -th argument, for $k \in \{1, 2\}$, and $\mathcal{O}(i)$ as well as $\mathcal{I}(i)$ are the sets from (5.72).

Proof. As a consequence of Corollary 2.3.4, the gradients of $J_{\text{data}}(W) = \langle \vartheta_{\mathcal{V}}, W \rangle$ and $J_{\text{int}}(W) = -\langle W, \log W \rangle$ are directly given by

$$\begin{aligned} \text{grad}_E J_{\text{data}}(W) &= P_{\mathcal{T}_{\mathcal{W}}} [\partial J_{\text{data}}(W)] = P_{\mathcal{T}_{\mathcal{W}}} [\vartheta_{\mathcal{V}}] \\ \text{grad}_E J_{\text{int}}(W) &= P_{\mathcal{T}_{\mathcal{W}}} [\partial J_{\text{int}}(W)] = -P_{\mathcal{T}_{\mathcal{W}}} [\log W] \stackrel{(2.39)}{=} -\exp_{\mathbb{1}_{\mathcal{W}}}^{-1}(W). \end{aligned}$$

To determine the gradient of $J_{\text{reg},\tau}$, let $\gamma: (-r, r) \rightarrow \mathcal{W}$, for $r > 0$, be a smooth curve with $\gamma(0) = W$ and $\dot{\gamma}(0) = V \in \mathcal{T}_{\mathcal{W}}$. The i -th row of the assignment matrix $\gamma(t) \in \mathcal{W} \subset \mathbb{R}^{m \times n}$ is denoted by $\gamma_i(t)$. With this, the global gradient of $J_{\text{reg},\tau}$ is expressed as

$$\begin{aligned} \langle \text{grad}_E J_{\text{reg},\tau}(W), V \rangle &= \left. \frac{d}{dt} J_{\text{reg},\tau}(\gamma(t)) \right|_{t=0} \stackrel{(5.74)}{=} \sum_{i \in \mathcal{V}} \sum_{ij \in \mathcal{O}(i)} \left. \frac{d}{dt} d_{\theta_{ij},\tau}(\gamma_i(t), \gamma_j(t)) \right|_{t=0} \\ &= \sum_{i \in \mathcal{V}} \sum_{ij \in \mathcal{O}(i)} \left(\langle \text{grad}_{E,1} d_{\theta_{ij},\tau}(W_i, W_j), V_i \rangle + \langle \text{grad}_{E,2} d_{\theta_{ij},\tau}(W_i, W_j), V_j \rangle \right). \quad (5.76) \end{aligned}$$

Using the indicator function $\chi_{\mathcal{E}}$ (5.73), the sum over the expressions

$$\langle \text{grad}_{E,2} d_{\theta_{ij},\tau}(W_i, W_j), V_j \rangle =: a_{ij}(W_i, W_j, V_j)$$

in (5.76) can be rewritten as

$$\begin{aligned} \sum_{i \in \mathcal{V}} \sum_{ij \in \mathcal{O}(i)} a_{ij}(W_i, W_j, V_j) &= \sum_{i \in \mathcal{V}} \sum_{j \in \mathcal{V}} \chi_{\mathcal{E}}(ij) a_{ij}(W_i, W_j, V_j) = \sum_{j \in \mathcal{V}} \sum_{i \in \mathcal{V}} \chi_{\mathcal{E}}(ij) a_{ij}(W_i, W_j, V_j) \\ &= \sum_{j \in \mathcal{V}} \sum_{ji \in \mathcal{I}(j)} a_{ij}(W_i, W_j, V_j) = \sum_{i \in \mathcal{V}} \sum_{ji \in \mathcal{I}(i)} a_{ji}(W_j, W_i, V_i), \end{aligned}$$

where the last equation follows by renaming the indices of summation. Substitution into (5.76) results in

$$\begin{aligned} \sum_{i \in \mathcal{V}} \langle \text{grad}_{E,i} J_{\text{reg},\tau}(W), V_i \rangle &= \langle \text{grad}_E J_{\text{reg},\tau}(W), V \rangle \\ &= \sum_{i \in \mathcal{V}} \left\langle \sum_{ij \in \mathcal{O}(i)} \text{grad}_{E,1} d_{\theta_{ij},\tau}(W_i, W_j) + \sum_{ji \in \mathcal{I}(i)} \text{grad}_{E,2} d_{\theta_{ji},\tau}(W_j, W_i), V_i \right\rangle \end{aligned}$$

which proves (5.75). As the local entropy regularized Wasserstein distances are all analytic due to Corollary 5.2.11, the objective function $J_{\tau,\alpha}$ itself is analytic. \square

Subsequently, the specific case that all pairwise discrete energies $J_{ij}(x_i, x_j)$ in (5.1) are symmetric is considered. This assumption translates to the condition that all pairwise model parameters (5.7) are symmetric matrices $\vartheta_{ij} = \vartheta_{ij}^\top$, which in turn leads to symmetric Wasserstein distances $d_{\vartheta_{ij}, \tau}$ by Corollary 5.2.11. As a consequence of this, and also in light of the discussion leading up to Assumption 5.1.1, there is no need to choose an orientation for the edges in this situation, as the mapping of edges ij to $J_{ij}(x_i, x_j)$, respectively $d_{\vartheta_{ij}, \tau}$, is well defined. In this case, the regularization term can alternatively be expressed as

$$J_{\text{reg}, \tau}(W) = \frac{1}{2} \sum_{i \in \mathcal{V}} \sum_{j \in \mathcal{N}_i} d_{\vartheta_{ij}, \tau}(W_i, W_j), \quad (5.77)$$

where the additional factor $1/2$ enters because every edge occurs twice on the right-hand side. With this, Proposition 5.2.13 is now reformulated accordingly.

Proposition 5.2.14 (gradient of $J_{\tau, \alpha}$: symmetric case). *Suppose all edges $ij \in \mathcal{E}$ are undirected and the corresponding pairwise parameter matrices ϑ_{ij} are symmetric. Then $J_{\tau, \alpha}: \mathcal{W} \rightarrow \mathbb{R}$ is analytic and the i -th row of the Euclidean gradient $\text{grad}_E J_{\tau, \alpha}(W) \in \mathcal{T}_{\mathcal{W}}$ is given by*

$$\text{grad}_{E, i} J_{\tau, \alpha}(W) = P_{T_{\mathcal{S}}} \vartheta_i + \sum_{j \in \mathcal{N}_i} \text{grad}_{E, 1} d_{\vartheta_{ij}, \tau}(W_i, W_j) - \alpha \exp_{\mathbb{1}_{\mathcal{S}}}^{-1}(W_i), \quad (5.78)$$

where $\text{grad}_{E, 1} d_{\vartheta_{ij}, \tau}(W_i, W_j) \in T_{\mathcal{S}}$ denotes the gradient with respect to the first argument.

Proof. The expressions for the gradients of J_{data} and J_{int} as well as the analyticity of $J_{\tau, \alpha}$ follow from Proposition 5.2.13. Thus, only the gradient of the regularization term has to be calculated. The differential of $J_{\text{reg}, \tau}$ for the alternative expression (5.77) is given by

$$dJ_{\text{reg}, \tau}(W)[V] = \frac{1}{2} \sum_{i \in \mathcal{V}} \sum_{j \in \mathcal{N}_i} \left(\langle \text{grad}_{E, 1} d_{\vartheta_{ij}, \tau}(W_i, W_j), V_i \rangle + \langle \text{grad}_{E, 2} d_{\vartheta_{ij}, \tau}(W_i, W_j), V_j \rangle \right),$$

with $V \in \mathcal{T}_{\mathcal{W}}$ arbitrary. Using the indicator functions $\chi_{\mathcal{N}_i}: \mathcal{V} \rightarrow \{0, 1\}$ of the neighborhoods \mathcal{N}_i and following the analog calculation as in the proof of Theorem 5.2.13 after (5.76) shows

$$\sum_{i \in \mathcal{V}} \sum_{j \in \mathcal{N}_i} \langle \text{grad}_{E, 2} d_{\vartheta_{ij}, \tau}(W_i, W_j), V_j \rangle = \sum_{i \in \mathcal{V}} \sum_{j \in \mathcal{N}_i} \langle \text{grad}_{E, 2} d_{\vartheta_{ij}, \tau}(W_j, W_i), V_i \rangle. \quad (5.79)$$

As a consequence of the costs ϑ_{ij} being symmetric for all $ij \in \mathcal{E}$, the equality

$$\text{grad}_{E, 2} d_{\vartheta_{ij}, \tau}(W_j, W_i) \stackrel{(5.64)}{=} \text{grad}_{E, 1} d_{\vartheta_{ij}, \tau}(W_i, W_j)$$

can be applied to (5.79), overall resulting in

$$\begin{aligned} \sum_{i \in \mathcal{V}} \langle \text{grad}_{E, i} J_{\text{reg}, \tau}(W), V_i \rangle &= \langle \text{grad}_E J_{\text{reg}, \tau}(W), V \rangle = dJ_{\text{reg}, \tau}(W)[V] \\ &= \sum_{i \in \mathcal{V}} \left\langle \sum_{j \in \mathcal{N}_i} \text{grad}_{E, 1} d_{\vartheta_{ij}, \tau}(W_i, W_j), V_i \right\rangle. \end{aligned}$$

Since this equation holds for all $V \in \mathcal{T}_{\mathcal{W}}$, the desired expression in (5.78) for the regularization term follows. \square

The Riemannian Gradient Descent Flow

The resulting Riemannian gradient descent flow for W_i , $i \in \mathcal{V}$, on the assignment manifold \mathcal{W} has the form

$$\dot{W}_i = -\text{grad}_{g,i} J_{\tau,\alpha}(W) \stackrel{(5.75)}{=} R_{W_i}[-\vartheta_i - \text{grad}_{E,i} J_{\text{reg},\tau}(W) + \alpha \exp_{\mathbb{1}_S}^{-1}(W_i)], \quad (5.80)$$

with initial condition given by the unbiased uniform label distribution $W_i(0) = \mathbb{1}_S$.

With respect to loopy belief propagation (5.20), *message passing* for vertex $i \in \mathcal{V}$ in this approach is defined by evaluating the local Wasserstein gradients in the expression of $\text{grad}_{E,i} J_{\text{reg},\tau}$ for all edges incident to i . Therefore these local gradients are called *Wasserstein messages* which are ‘passed along edges’. Similarly to loopy belief propagation, each such message is given by *dual* variables through (5.63), that solve the regularized *local* dual LPs (5.60).

In addition, the following *observations* in correspondence to the smoothed local polytope relaxation (5.15) and loopy belief propagation (5.20) can be made:

- (1) **Local convexity and valid constraints.** Wasserstein messages of (5.75) are defined by local *convex* programs (5.60). As a consequence, all local marginalization constraints for the ‘hidden’ coupling measures of W_i and W_j are *always* satisfied *throughout* the inference process. This is in sharp contrast to belief propagation where this generally only holds after convergence.
- (2) **Smooth global rounding.** Rounding to integral solutions is *gradually* enforced by the Riemannian flow induced through J_{int} (5.71) depending on the integrality parameter α . In particular, repeated ‘aggressive’ local max operations of the max-product algorithm are replaced by a *smooth* flow.
- (3) **Smoothness and weak nonlinearity.** The role of the smoothing parameter τ in the variational model $J_{\tau,\alpha}$ (5.68) *differs* from the role of the smoothing parameter in the smoothed LP relaxation (5.15). While in the latter case, τ has to be chosen quite close to 0 so as to achieve rounding at all, the smoothing parameter of the variational model $J_{\tau,\alpha}$ merely mollifies the dual local problems (5.33) and hence should be chosen small, but may be considerably larger than for the smoothed local polytope relaxation. The *decoupling* of smoothing and rounding in $J_{\tau,\alpha}$ therefore enables to numerically compute labelings more efficiently. The results reported in the experiment section below demonstrate this fact.

In the remaining part of this section, the influence of the integrality enforcing term J_{int} in the initial phase of the Riemannian gradient flow (5.80) is investigated. For this, suppose that for all $ij \in \mathcal{E}$ the pairwise parameters ϑ_{ij} are symmetric and such that

$d_{\vartheta_{ij},\tau}(W_i, W_j) = 0$ if and only if $W_i = W_j$. Under this assumption, W_j is the global minimum of $d_{\vartheta_{ij},\tau}(\cdot, W_j)$, resulting in

$$\text{grad}_{E,1} d_{\vartheta_{ij},\tau}(W_j, W_j) = 0. \quad (5.81)$$

Because of the initial condition $W_i(0) = \mathbb{1}_{\mathcal{S}}$, for all $i \in \mathcal{V}$, all assignments $W_j(t)$ in the neighborhood of $i \in \mathcal{V}$ are almost the same on the initial time interval $[0, T)$ for sufficiently small $0 < T \ll 1$. Therefore, the initial dynamics of the Riemannian gradient flow is essentially governed by

$$\dot{W}_i = R_{W_i}[-\vartheta_i + \alpha \exp_{\mathbb{1}_{\mathcal{S}}}^{-1}(W_i)], \quad V_i(0) = \mathbb{1}_{\mathcal{S}} \quad \text{for } t \in [0, T),$$

depending only on the local unary costs ϑ_i and the parameter $\alpha \geq 0$. Applying the transformation $W_i(t) = \exp_{\mathbb{1}_{\mathcal{S}}}(V_i(t))$ from (2.64), with $V_i(t) \in T_{\mathcal{S}}$, the equivalent dynamical system on $T_{\mathcal{S}}$ reads

$$\dot{V}_i = -P_{T_{\mathcal{S}}}\vartheta_i + \alpha V_i, \quad \text{with } V_i(0) = 0 \quad \forall i \in \mathcal{V}.$$

Thus, for $\alpha = 0$, the solution of this linear ODE is given by

$$V_i(t) = -tP_{T_{\mathcal{S}}}\vartheta_i$$

while for $\alpha > 0$, the solution has the form

$$V_i(t) = \frac{1}{\alpha}(1 - e^{-\alpha t})P_{T_{\mathcal{S}}}\vartheta_i.$$

Since $\exp_{\mathbb{1}_{\mathcal{S}}}$ implicitly projects onto the tangent space by (2.38), the corresponding curves on \mathcal{S} in terms of W_i are given by

$$W_i(t) = \exp_{\mathbb{1}_{\mathcal{S}}}(-t\vartheta_i) \quad \text{and} \quad W_i(t) = \exp_{\mathbb{1}_{\mathcal{S}}}\left(\frac{1}{\alpha}(1 - e^{-\alpha t})\vartheta_i\right) \quad (5.82)$$

The limit behavior for t towards infinity is clarified in the next statement.

Lemma 5.2.15. *Let $x, y \in \mathbb{R}^n$ and suppose x has a unique maximum entry, i.e. there is an $r \in [n]$ with $x^r > x^j$ for all $j \neq r$. If $h: \mathbb{R} \rightarrow \mathbb{R}$ is continuous and satisfies $\lim_{t \rightarrow \infty} h(t) = \infty$, then $\exp_{\mathbb{1}_{\mathcal{S}}}(h(t)x + y) = e_r \in \mathcal{B}_n$.*

Proof. Define $a(t) := h(t)x + y$. By assumption $x^j - x^r < 0$ for every $j \neq r$, resulting in the limit

$$\lim_{t \rightarrow \infty} e^{a^j(t) - a^r(t)} = \lim_{t \rightarrow \infty} e^{h(t)(x^j - x^r) + y^j - y^r} = \delta_{jr},$$

where δ_{jr} is the Kronecker delta. Therefore, subtracting $a^r(t)$ in every component results in $\lim_{t \rightarrow \infty} e^{a(t) - a^r(t)\mathbb{1}_n} = e_r$. Because $\exp_{\mathbb{1}_{\mathcal{S}}}$ implicitly projects onto the tangent space according to (2.38), it finally follows

$$\lim_{t \rightarrow \infty} \exp_{\mathbb{1}_{\mathcal{S}}}(a(t)) \stackrel{(2.38)}{=} \lim_{t \rightarrow \infty} \exp_{\mathbb{1}_{\mathcal{S}}}(a(t) - a^r(t)\mathbb{1}_n) = \lim_{t \rightarrow \infty} \frac{e^{a(t) - a^r(t)\mathbb{1}_n}}{\langle e^{a(t) - a^r(t)\mathbb{1}_n}, \mathbb{1}_n \rangle} = e_r. \quad \square$$

Suppose ϑ_i has a unique minimum in the r -th component. Applying Lemma 5.2.15 implies that in both cases, $\alpha = 0$ and $\alpha > 0$, the solutions $W_i(t)$ from (5.82) converge towards the integral assignment e_r . However, in the latter case, the solution approaches e_r exponentially faster, showing that an increase in α leads to a more aggressive push of the assignments toward integral solutions in the initial phase of the flow.

5.3. Experiments

In this section, the main properties of the presented variational approach $J_{\tau,\alpha}$ (5.68) are assessed by two selected academical experiments. The dependency of label assignment on the integrality parameter α is illustrated in Section 5.3.1. A competitive evaluation of the variational approach with two established and widely applied methods, sequential tree-reweighted message passing (TRWS) [Kol06] and loopy belief propagation (5.20) based on the OpenGM package [ABK12], is made in Section 5.3.2.

The approach from Chapter 3 of GEA-sequences for numerical integration of the perturbed Riemannian gradient flow is used for optimization.

Perturbed model and flow. The perturbed variational model of $J_{\tau,\alpha}$ (5.68) reads

$$J_{\tau,\alpha;\varepsilon}(W) := J_{\tau,\alpha}(W) - \varepsilon \langle \log, \mathbb{1}_{\mathcal{W}} \rangle, \quad W \in \mathcal{W}, \quad (5.83)$$

with $0 < \varepsilon \ll 1$. By Lemma 3.1.2, the i -th row of the Euclidean gradient has the form

$$\text{grad}_{E,i} J_{\alpha;\varepsilon}(W) = P_{T_S} \vartheta_i + \text{grad}_{E,i} J_{\text{reg},\tau}(W) - \alpha \exp_{\mathbb{1}_S}^{-1}(W_i) - \varepsilon P_{T_S} \frac{\mathbb{1}_S}{W_i}, \quad (5.84)$$

for $W \in \mathcal{W}$. Due to $J_{\tau,\alpha;\varepsilon}: \mathcal{W} \rightarrow \mathbb{R}$ being analytic as a consequence of Proposition 5.2.13, the convergence and stability results for the corresponding Riemannian gradient descent flow from Section 3.3.3 apply.

Numerical integration. For given descent parameter $\tilde{\tau}$ and diminishing factor s , with $\tilde{\tau}, s \in (0, 1)$ as well as the maximal step-size $h_{\max} > 0$, the general GEA-sequence update scheme (3.89) is of the form

$$W^{(k+1)} = \text{GE}^A(W^{(k)}) = \exp_{W^{(k)}} \left(-h_k \text{grad}_E J_{\tau,\alpha;\varepsilon}(W^{(k)}) \right), \quad W^{(0)} = \mathbb{1}_{\mathcal{W}} \in \mathcal{W}, \quad (5.85)$$

where the step-size $h_k = h(W^{(k)}) > 0$ is the Armijo step-size (3.86), depending on the choices for $\tilde{\tau}$, s and h_{\max} . As a result of $J_{\tau,\alpha;\varepsilon}: \mathcal{W} \rightarrow \mathbb{R}$ being analytic according to Proposition 5.2.13, the convergence and stability results for the discrete-time case from Section 3.4 are valid.

Termination criterion. In all experiments, the normalized relative change (nrc) of $J_{\tau,\alpha;\varepsilon}$ from (4.30) is used as part of the convergence criterion.

Wasserstein gradients. In all experiments the iterative Sinkhorn's algorithm (5.66) is used to simultaneously compute the local Wasserstein gradients for all edges. The k -th (global) iteration of Sinkhorn's algorithm then results in an approximation $V_{\text{reg},\tau}^{(k)}$ for the gradient of the regularization term $\text{grad}_E J_{\text{reg},\tau}$. The iteration is terminated if the relative change with respect to the Euclidean metric

$$\frac{\|V_{\text{reg},\tau}^{(k)} - V_{\text{reg},\tau}^{(k-1)}\|}{\|V_{\text{reg},\tau}^{(k)}\|}$$

drops below the threshold of 10^{-5} .

5.3.1. Influence of the Integrality Parameter

The influence of the integrality parameter $\alpha \geq 0$ on the variational model $J_{\tau,\alpha}$ (5.68) is assessed through the second labeling problem of Section 4.1.3. Figure 5.4 again shows the noisy RGB-image $f: \mathcal{V} \rightarrow [0, 1]^3$ on the grid graph $\mathcal{G}_g = (\mathcal{V}_g, \mathcal{E}_g)$ (see Section 2.3.1) with minimal neighborhood size $|\mathcal{N}_i| = 3 \times 3$, $i \in \mathcal{V}$, together with the eight prototypical colors $\mathcal{X} = \{\ell_1, \dots, \ell_8\} \subset [0, 1]^3$ used as labels. Similar to the distance matrix (2.54) of the assignment flow, the unary (or data) term is defined using the $\|\cdot\|_1$ distance and a scaling factor $\rho > 0$ by

$$\vartheta_i := \frac{1}{\rho} (\|f(i) - \ell_1\|_1, \dots, \|f(i) - \ell_8\|_1), \quad \forall i \in \mathcal{V}_g,$$

and *Potts regularization* is used for defining the pairwise parameters of the model

$$(\vartheta_{ij})_k^r = 1 - \delta_{k,r}, \quad \forall ij \in \mathcal{E}_g, \quad (5.86)$$

where $\delta_{k,r}$ is the Kronecker delta. This way, the penalty costs of any two different discrete label choices is uniform.

For this experiment, the feature scaling factor is chosen as $\rho = 0.3$, the smoothing parameter as $\tau = 0.12$ and the perturbation parameter as $\varepsilon = 10^{-10}$. The GEA update scheme (5.85) uses the parameters $\tilde{\tau} = 0.01$, $s = 0.5$ and $h_{\max} = 0.05$. The iteration is terminated if either the normalized relative change of $J_{\tau,\alpha;\varepsilon}$ (4.30) drops below the threshold of 10^{-5} or the maximum number of 500 iterations is reached.

Figure 5.4 shows the influence of the integrality parameter α for the parameter choices $\alpha \in \{0, 0.5, 2, 4, 8, 16\}$. The color values of the individual results are the expected color label $\mathbb{E}_{W_i}[\mathcal{X}] = \sum_{j \in [8]} W_i^j \ell_j$ given the assignment W_i at every pixel i after reaching the termination criterion. For $\alpha = 0$ and $\alpha = 0.5$ the maximum number of 500 iterations was reached, while in all other cases the nrc of $J_{\tau,\alpha;\varepsilon}$ (4.30) drop below 10^{-5} first. If either no rounding is performed ($\alpha = 0$) or if the influence of rounding is too small compared to the smoothing of the Wasserstein distances ($\alpha = 0.5$), the Riemannian gradient flow does not converge to an integral solution, even though the assignments show a clear tendency. Increasing the strength of rounding (i.e. larger α) leads to a faster decrease in the integrality enforcing term $J_{\text{int}}(W) = H_{\mathcal{W}}(W)$ (cf. Figure 5.5) and therefore to an earlier convergence of the process to a specific labeling. Thus, a more aggressive rounding scheme yields a less regularized result due to the rapid decision for a labeling at an early stage of the algorithm (see also the discussion at the end of Section 5.2.4).

Figure 5.5 shows the interplay between minimizing the approximation of the LP relaxation J_τ (5.70) (middle) and the values of the integrality term J_{int} given by the entropy $H_{\mathcal{W}}$ (top) for the first 100 iterations dependent on the different choices for α . Less aggressive rounding in terms of smaller values for α results in a more regularized assignment as the flows spends more time minimizing J_τ . For too small values of α , the entropy is not sufficiently minimized leading to non-integral assignments, as discussed in the preceding paragraph. The effect of α on the speed of convergences can also be seen by the nrc values of $J_{\tau,\alpha;\varepsilon}$ (bottom) for the first 100 iterations.

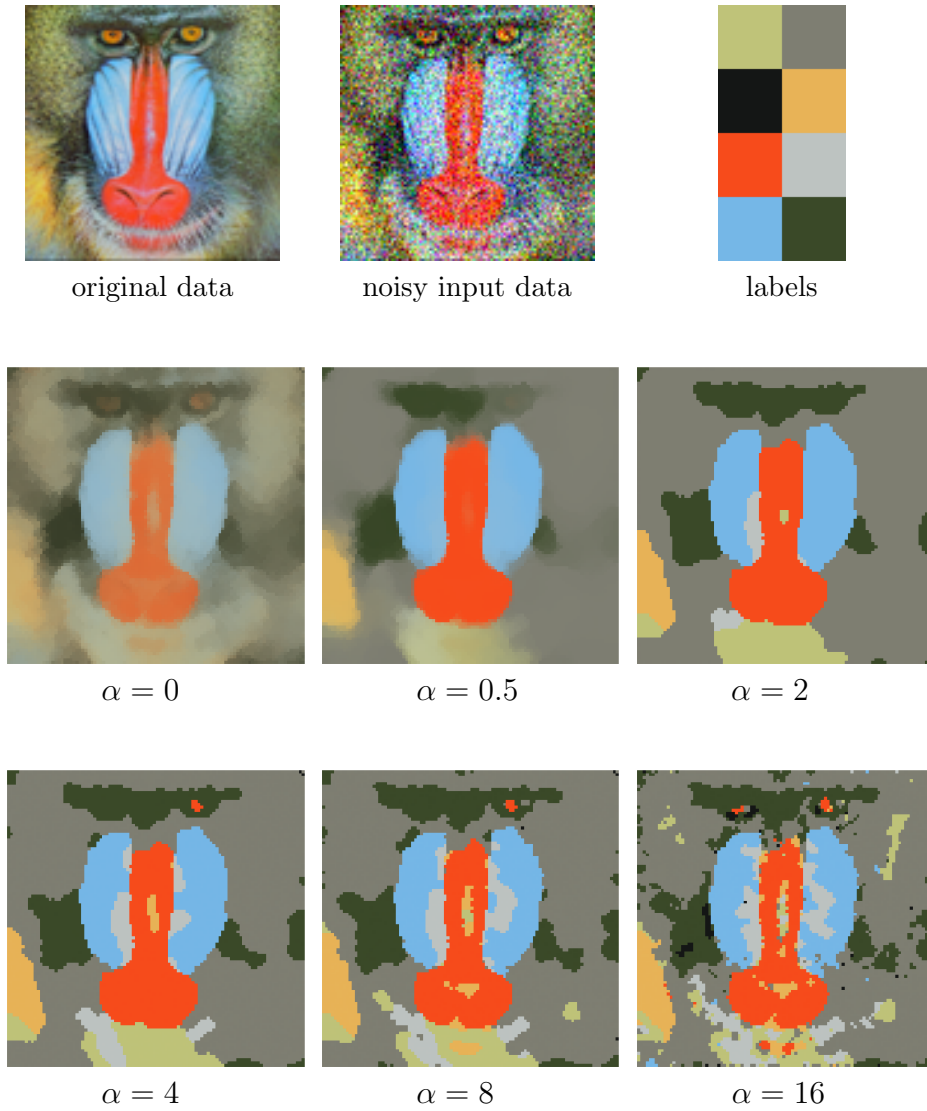


Figure 5.4.: Influence of the integrality parameter α on the model $J_{\tau,\alpha;\varepsilon}$ (5.83) with smoothing parameter $\tau = 0.12$ and perturbation parameter $\varepsilon = 10^{-10}$. **Top row:** The underlying original RGB-image together with a noisy input version of the model and 8 prototypical colors used as labels. **Middle and bottom row:** Results for increasing values of α after reaching the termination criterion. The images show the expected color label $\mathbb{E}_{W_i}[\mathcal{X}] = \sum_{j \in [8]} W_i^j \ell_j$ given the assignment W_i at every pixel i . For small values of α (0 and 0.5) the integrality term is too weak, resulting in non-integral assignments. For larger α , the rounding mechanism is becoming more dominant, leading to less regularized results.

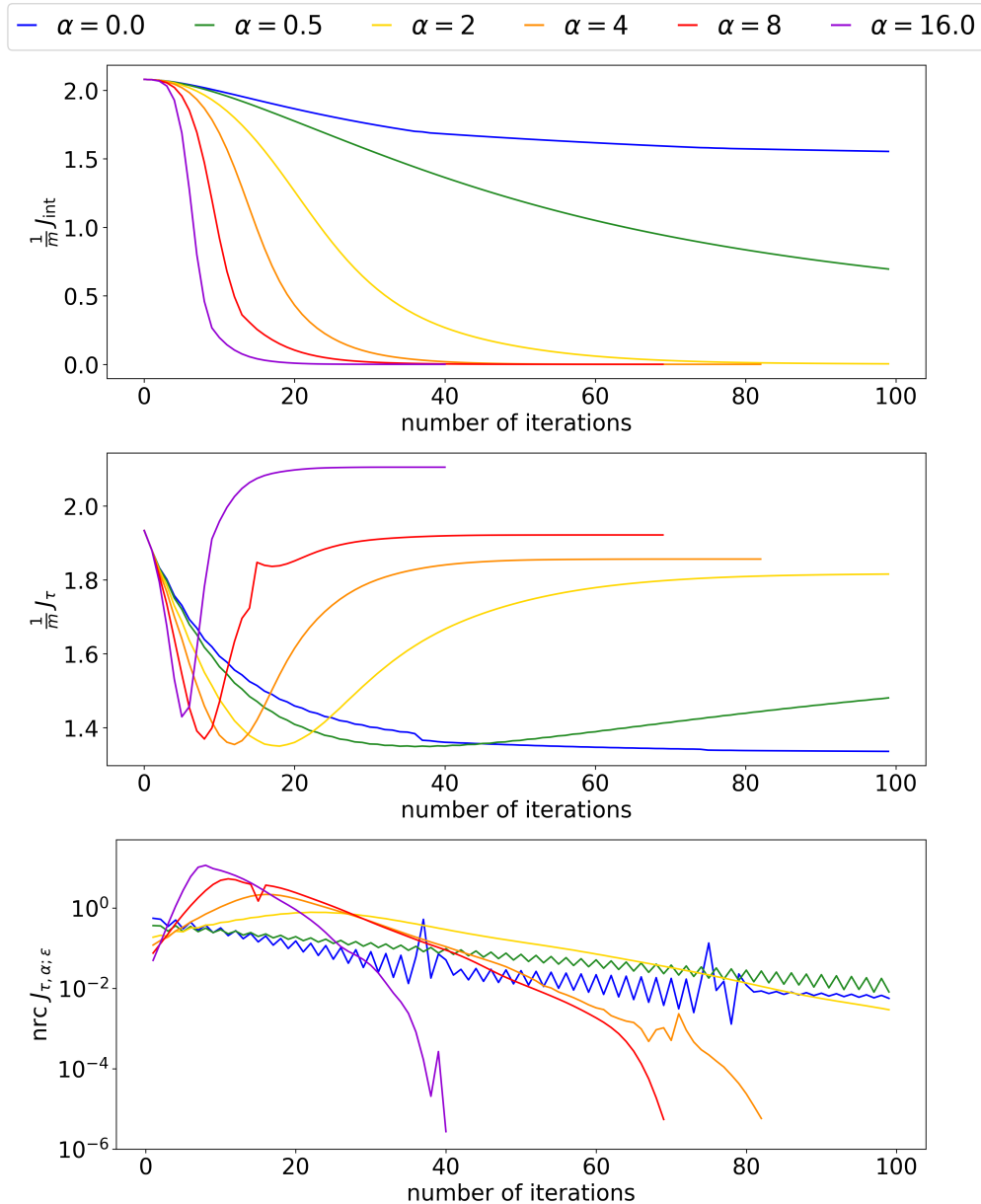


Figure 5.5.: The average values of the integrality term $J_{\text{int}} = H_{\mathcal{W}}$ (5.71) (top), approximation of the LP relaxation J_{τ} (5.70) (middle) and the nrc of $J_{\tau, \alpha; \epsilon}$ (4.30) in the first 100 iterations are shown for $\tau = 0.12$, $\epsilon = 10^{-10}$ and varying parameter $\alpha \in \{0, 0.5, 2, 4, 8, 16\}$ (see color code on top). **Top:** With increasing values of the rounding parameter α , the entropy $J_{\text{int}} = H_{\mathcal{W}}$ drops more rapidly and hence the iterates converge faster to an integral assignment. **Middle:** Two phases of the algorithm depending on α are visible. In the first phase, J_{τ} is minimized up to the point where rounding takes over in the second phase. For smaller values of α , the flow spends more time on minimizing J_{τ} leading to more regularized assignments. **Bottom:** Normalized relative change of $J_{\tau, \alpha; \epsilon}$ (4.30). For $\alpha = 0, 0.5$ the nrc did not drop below 10^{-5} within the allowed 500 iterations.

5.3.2. Comparison to Other Methods

The geometric variational approach is compared to sequential tree-reweighted message passing (TRWS) [Kol06] and loopy belief propagation [Wei01] (Loopy-BP) based on the OpenGM package [ABK12].

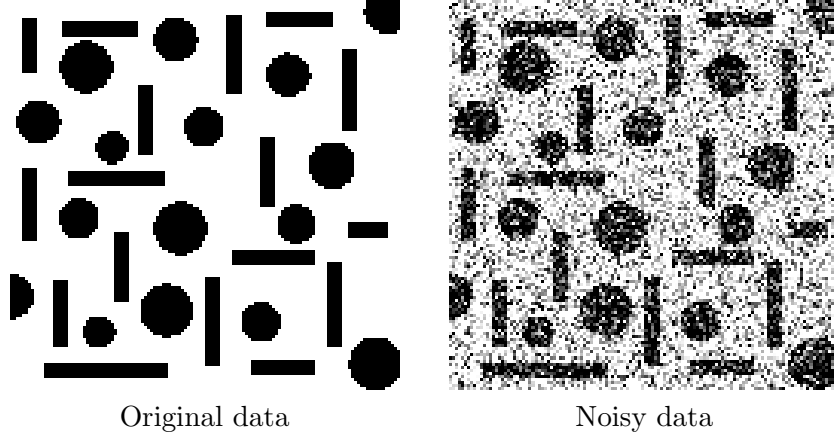


Figure 5.6.: Noisy image labeling problem: A binary ground truth image (left) with various rectangles and circles to be recovered from noisy input data (right).

For this comparison, the performance of the methods is evaluated with a noisy binary labeling scenario on a 128×128 image depicted by Figure 5.6. The spatial structure of the data is given by a slightly modified version of the grid graph $\mathcal{G}_g = (\mathcal{V}_g, \mathcal{E}_g)$ from Section 2.3.1, where instead of the $\|\cdot\|_{\max}$ the $\|\cdot\|_1$ norm is used for determining the neighborhood structure of the graph. In the following, the minimal nontrivial neighborhoods given by the $\|\cdot\|_1$ balls of radius 1 are used, also simply called 4-neighborhoods. Let $f: \mathcal{V}_g \rightarrow [0, 1]$ be the noisy image data and $\mathcal{X} = \{0, 1\}$ the binary set of labels. A standard (unary) data term together with the Potts prior (5.86) is used

$$\vartheta_i = \begin{pmatrix} f(i) \\ 1 - f(i) \end{pmatrix} \quad \text{for } i \in \mathcal{V} \quad \text{and} \quad \vartheta_{ij} = \begin{pmatrix} 0 & 1 \\ 1 & 0 \end{pmatrix} \quad \text{for } ij \in \mathcal{E}. \quad (5.87)$$

For this experiment, the smoothing parameter is chosen as $\tau = 0.1$ and the perturbation parameter again as $\varepsilon = 10^{-10}$. The GEA iteration (5.85) uses the parameters $\tilde{\tau} = 0.01$, $s = 0.5$ and $h_{\max} = 0.1$. The iteration is terminated if the normalized relative change of $J_{\tau, \alpha; \varepsilon}$ (4.30) drops below the threshold of 10^{-5} .

Figure 5.7 shows the resulting visual reconstruction as well as the corresponding values of the underlying discrete objective function J (5.1) and percentage of correct labels for all three methods. The variational model $J_{\tau, \alpha; \varepsilon}$ achieves similar accuracy and discrete function value than TRWS and Loopy-BP.

Figure 5.8 shows the nrc of $J_{\tau, \alpha; \varepsilon}$ (4.30) (bottom) and the interplay between the two terms in $J_{\tau, \alpha} = J_{\tau} + \alpha J_{\text{int}}$ (top, yellow), with relaxed LP approximation J_{τ} (5.70) (orange) and integrality term J_{int} (5.71) (blue). These curves illustrate again the smooth combination of optimization and rounding into a single two stage process.

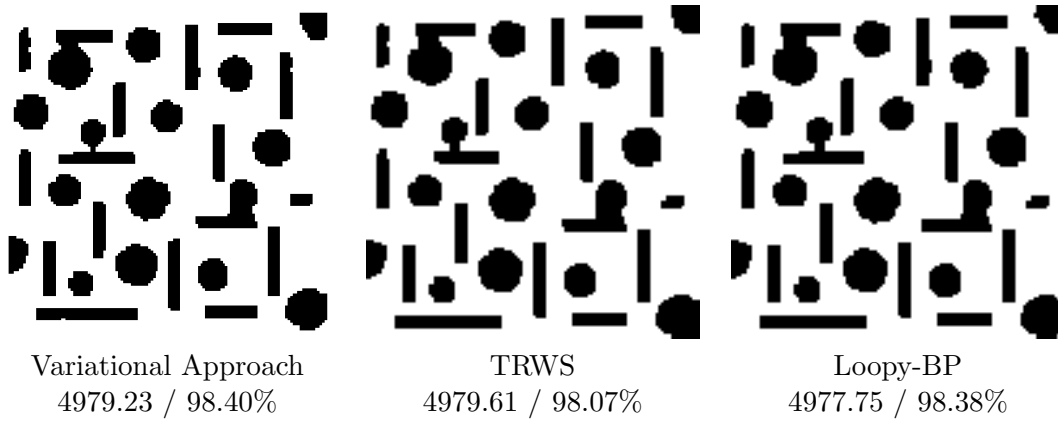


Figure 5.7.: Integral labeling results for the noisy labeling problem from Figure 5.6 for all three methods, using a standard data term with Potts prior. The presented numbers are in the formal discrete energy / accuracy. All methods show similar performance.

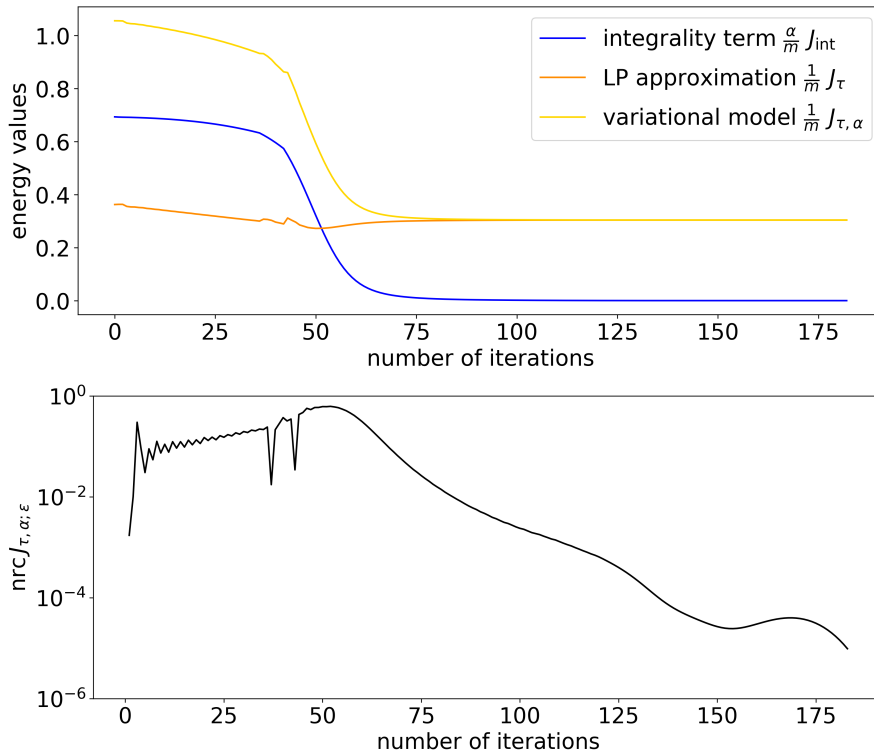


Figure 5.8.: **Top:** Decomposition of the variational model $J_{\tau, \alpha} = J_{\tau} + \alpha J_{\text{int}}$ (5.68) into the approximation of the LP relaxation J_{τ} (5.70) and the integrality enforcing term $J_{\text{int}} = H_{\mathcal{W}}$ (5.71) during iteration of the GEA sequence. The two stages of the algorithm are weakly visible. In the first 50 iterations J_{τ} is minimized until J_{int} takes over and drives the flow towards an integral assignment. **Bottom:** The corresponding normalized relative change of $J_{\tau, \alpha; \epsilon}$ (4.30).

Chapter 6

Conclusion and Outlook

Summary. The assignment flow is a dynamic selection process on the assignment manifold for image labeling. It is given by a spatially coupled replicator dynamic, driven by *spatial regularization* and gradual *enforcement* of unambiguous label decisions. Combining this dynamical process with the more classical viewpoint of image labeling results in a variational approach on the assignment manifold where label assignments are inferred through the induced Riemannian gradient descent flow with respect to the underlying information geometry.

This provided the motivation to consider general variational models in Chapter 3. To avoid any boundary issues, arbitrarily precise label decisions were avoided by slightly perturbing the model through the log-barrier function, introducing a minimum amount of uncertainty in the assignments. This made it possible to transfer already established convergence and stability results as well as convergence rates for the Euclidean setting to the assignment manifold for the Riemannian gradient flow and its discretization through the geometric Euler update with Armijo step-size selection.

The natural question whether there exists a potential, such that the assignment flow is a Riemannian gradient descent flow on the assignment manifold, was negatively answered in Chapter 4. However, alternatively parameterizing the assignment flow by its dominant component revealed a ‘hidden’ Riemannian gradient flow whose potential consists of a graph Laplacian and an integrality term, clearly identifying the two competing processes governing the flow: regularization of assignments in a spatial context and gradually enforcing unambiguous label decisions. Based on this potential, a continuous-domain variational formulation was introduced and well-posedness of the resulting optimization problem could be established.

Finally, in Chapter 5, relaxed variational models of discrete objective functions corresponding to discrete probabilistic graphical models were derived on the assignment manifold. For this, the associated smoothed local polytope relaxation was rewritten using entropy regularized local Wasserstein distances. Following the Riemannian gradient descent flow for inference resulted in an alternative optimization approach of discrete graphical models using parallel ‘Wasserstein messages’ along edges. In contrast to established methods, the local marginalization constraints are always satisfied and a smooth rounding mechanism towards integral assignments is incorporated in the inference process.

Future work. Subsequently, several research directions and open problems for further research are pointed out:

- Besides analyticity, compactness of level sets for the perturbed objective function was a vital property for transferring the presented general convergence and stability results from the Euclidean setting onto the assignment manifold in Chapter 3. To which extend these results also hold for the underlying unperturbed function remains an open question.
- In [ÅPSS17], the similarity matrix of the assignment flow was originally defined to be the weighted Riemannian mean of the likelihood vectors. In order to arrive at explicit formulas for efficient numerical updates, the Riemannian mean with respect to the Fisher-Rao metric was approximated by the geometric mean. Regarding the potential in the S -flow formulation in Section 4.1.2, the squared Euclidean differences between neighboring assignments may be replaced by the squared Riemannian distances as an alternative measure for similarity in spatial neighborhoods. This way, a relation to Riemannian means re-enters the assignment flow via the S -flow formulation through the objective function that defines the Riemannian mean. The corresponding Riemannian gradient S -flow pushes the assignments towards the Riemannian means of the likelihood vectors depending on the current assignment state. Since explicit expressions for the Riemannian distance and its gradient are available, there is no need for approximations. Initial work in this direction using an explicit data term and the entropy for integrality enforcement was presented in [SS19a].
- The derived numerical discrete-time algorithm for optimizing the continuous domain formulation of the assignment flow in Section 4.2 consists of a sequence of linear discretized elliptic PDE problems together with a convex simplex constraint. However, the limit case has not been considered so far and provides an opportunity for further investigation.
- In this thesis, uniform weights for controlling the spatial averages of the assignment flow were chosen. Depending on the application, however, it might be advantageous to allow label-dependent weights which adapt to the specific task at hand using methods from optimal control. A first step in this direction was presented in preliminary work on learning the weight parameter for a *linearized* version of the assignment flow in [HSPS19]. This might also be an interesting approach for parameter learning of discrete graphical models using the relaxed variational formulation in Chapter 5, as the relation between approximations for the learning problem and approximations of the inference problem for this class of models is less well understood [Wai06].

Appendix A

Differential Geometry

In the following, some basic definitions and facts from Riemannian geometry relevant for this work are briefly summarized. For proofs of the presented results and a more detailed exposition, the reader is referred to introductory material such as [Lee12], [Lee18] or [Jos17] and references therein. A treatment from the viewpoint of optimization on Riemannian manifolds can be found in [AMS08]. As in the latter reference, most of the considered manifolds are viewed as embedded submanifolds in \mathbb{R}^d .

In the context of pure geometric considerations in this work, the *Einstein summation convention* is used. That is, if the same index appears twice in an expression, once as an upper and once as a lower index, then it is implicitly assumed to be summed over, e.g.

$$a^i b_i = \sum_{i=1}^n a^i b_i. \quad (\text{A.1})$$

A.1. General Manifolds and Submanifolds of \mathbb{R}^d

Let M be smooth manifold of dimension m with associated tangent and cotangent bundle TM and T^*M . The set of all smooth vector and covector fields of M is denoted by $\mathfrak{X}(M)$ and $\mathfrak{X}^*(M)$ respectively. Using local coordinates x around a point $p \in M$, a vector field $X \in \mathfrak{X}(M)$ and covector field $\omega \in \mathfrak{X}^*(M)$ can be expressed in local coordinates around p through the induced basis $\frac{\partial}{\partial x^i}$ and dual basis dx^i as

$$X = X^i \frac{\partial}{\partial x^i} \quad \text{and} \quad \omega = \omega_i dx^i.$$

Suppose N is another smooth manifold of dimension n . The differential of a smooth function $F: M \rightarrow N$ at $p \in M$ is denoted by

$$dF(p): T_p M \rightarrow T_{F(p)} N, \quad X \mapsto dF(p)[X].$$

The map F in local coordinates is denoted by \hat{F} . That is, let $\phi: U_M \rightarrow \hat{U}_M$ be a chart around p with open sets $U_M \subset M$ and $\hat{U}_M \subset \mathbb{R}^m$ as well as $\eta: U_N \rightarrow \hat{U}_N$ a chart around $F(p)$ with open sets $U_N \subset N$ and $\hat{U}_N \subset \mathbb{R}^n$ with $F(U_M) \subset U_N$. Then

$$\hat{F} := \eta^{-1} \circ F \circ \phi: \hat{U}_M \rightarrow \hat{U}_N. \quad (\text{A.2})$$

Appendix A. Differential Geometry

If there is an embedding of the manifold M into \mathbb{R}^d , then M is identified as a submanifold $M \subset \mathbb{R}^d$. In this case, the tangent space at any $p \in M$ can be identified with a characterization using smooth curves on M by

$$T_p M = \{v \in \mathbb{R}^d \mid \exists \text{ curve } \gamma \text{ on } M, \gamma(0) = p, \dot{\gamma}(0) = v\}.$$

Let $N \subset \mathbb{R}^d$ be another submanifold and $F: M \rightarrow N$ a smooth map. With the above identification of the tangent space, the differential of F applied to $v \in T_p M$ can be expressed using any smooth curve $\gamma: (-\varepsilon, \varepsilon) \rightarrow M$, $\varepsilon > 0$, with $\gamma(0) = p$ and $\dot{\gamma}(0) = v$ as

$$dF(p)[v] = \left. \frac{d}{dt} F(\gamma(t)) \right|_{t=0}. \quad (\text{A.3})$$

Often, this equality provides a useful way of efficiently calculating $dF(p)[v]$, avoiding local coordinates.

Let $K \in \mathbb{N}$ and assume M_i is a smooth manifold for every $i \in [K]$. The tangent space of the product manifold $M := \prod_{i \in [K]} M_i$ at $p = (p_i)_{i \in [K]} \in M$ can naturally be identified (see e.g. [Lee12, Prop. 3.14]) with the product of the tangent spaces, i.e.

$$T_p M = \prod_{i \in [K]} T_{p_i} M_i. \quad (\text{A.4})$$

If N_i with $i \in [K]$ is another family of smooth manifolds together with smooth maps $F_i: M_i \rightarrow N_i$ for every $i \in [K]$, then there is a canonical *product map* F between M and $N := \prod_{i \in [K]} N_i$, defined by

$$F: M \rightarrow N, \quad p = (p_i)_{i \in [K]} \mapsto F(p) := (F_i(p_i))_{i \in [K]}. \quad (\text{A.5})$$

Due to the above identification of the tangent spaces $T_p M$ and $T_{F(p)} N$ with the product of the corresponding tangent spaces $T_{p_i} M_i$ and $T_{F_i(p_i)} N_i$, the differential of F at point $p = (p_i)_{i \in [K]} \in M$ factorizes and has the form

$$dF(p): T_p M \rightarrow T_p N, \quad V = (V_i)_{i \in [K]} \mapsto dF(p)[V] = (dF_i(p_i)[V_i])_{i \in [K]}. \quad (\text{A.6})$$

A.2. Flows on Manifolds

Let M be a manifold and $I \subset \mathbb{R}$ an open interval. A smooth curve $\gamma: I \rightarrow M$ determines a tangent vector, also called *velocity*, $\dot{\gamma}(t) = \left. \frac{d}{ds} \gamma(s) \right|_{s=t} = d\gamma(t) \left[\frac{\partial}{\partial t} \right] \in T_{\gamma(t)} M$ at every point along its trajectory. For $X \in \mathfrak{X}(M)$, a smooth curve $\gamma: I \rightarrow M$ is an *integral curve of X* , if

$$\dot{\gamma}(t) = X(\gamma(t)) \quad \text{for all } t \in I.$$

Collecting all integral curves into one mathematical object leads to the concept of a "flow". For this, a *flow domain* on M is an open subset $\mathcal{D} \subset \mathbb{R} \times M$ such that for every

$p \in M$ the set $\mathcal{D}^{(p)} := \{t \in \mathbb{R} \mid (t, p) \in \mathcal{D}\}$ is an open interval containing 0. A *smooth flow* on M is a smooth map $\theta: \mathcal{D} \rightarrow M$, with \mathcal{D} being a flow domain and θ satisfying

$$\theta(0, p) = p \quad \text{and} \quad \theta(t, \theta(s, p)) = \theta(t + s, p),$$

whenever the latter expressions are defined. The *infinitesimal generator* of θ is the vector field $X \in \mathfrak{X}(M)$ defined by $X(p) := \left. \frac{d}{dt} \theta(t, p) \right|_{t=0}$.

The following fundamental result shows that smooth flows induced by vector fields are unique if they are required to be maximal.

Theorem A.2.1 (Fundamental Theorem on Flows). *[Lee12, Thm. 9.12] For every vector field $X \in \mathfrak{X}(M)$ there is a unique maximal smooth flow $\theta: \mathcal{D} \rightarrow M$ whose infinitesimal generator is X , where maximal means θ cannot be extended to a flow on a larger flow domain. For every $p \in M$, the curve $\theta^{(p)}: \mathcal{D}^{(p)} \rightarrow M$, defined by $\theta^{(p)}(t) := \theta(t, p)$, is the unique maximal integral curve of X starting at p , i.e. $\theta^{(p)}(0) = p$.*

Even so, in general, integral curves only exist locally on a short time scale, the next lemma can often be used to prove global existence.

Lemma A.2.2 (Escape Lemma). *[Lee12, Lem. 9.19] Let $X \in \mathfrak{X}(M)$. If $\gamma: I \rightarrow M$ is a maximal integral curve of X such that the interval $I \subset \mathbb{R}$ has a finite least upper bound $b = \sup\{s \in I\}$, then for every $t \in I$, the image $\gamma([t, b))$ is not contained in any compact subset of M .*

A.3. Connections

Connections generalizing the notion of directional derivatives of vector fields on smooth manifolds in a coordinate independent way. A *covariant derivative* or *affine connection* on a smooth manifold M of dimension m is a map

$$\nabla: \mathfrak{X}(M) \times \mathfrak{X}(M) \rightarrow \mathfrak{X}(M), \quad (X, Y) \mapsto \nabla_X Y,$$

fulfilling the following three properties:

(I) $\nabla_X Y$ is tensorial in X . That is, for $f_1, f_2 \in C^\infty(M)$ and $X_1, X_2 \in \mathfrak{X}(M)$

$$\nabla_{f_1 X_1 + f_2 X_2} Y = f_1 \nabla_{X_1} Y + f_2 \nabla_{X_2} Y.$$

(II) $\nabla_X Y$ is \mathbb{R} -linear in Y , i.e. for $a_1, a_2 \in \mathbb{R}$ and $Y_1, Y_2 \in \mathfrak{X}(M)$

$$\nabla_X (a_1 Y_1 + a_2 Y_2) = a_1 \nabla_X Y_1 + a_2 \nabla_X Y_2.$$

(III) ∇ satisfies the product rule

$$\nabla_X (fY) = f \nabla_X Y + (Xf)Y \quad \text{for all } f \in C^\infty(M).$$

Appendix A. Differential Geometry

The expression $\nabla_X Y$ is termed the covariant derivative of Y in the direction X . Using local coordinates, the *Christoffel symbols* of the connection ∇ are defined by

$$\nabla_{\frac{\partial}{\partial x^i}} \frac{\partial}{\partial x^j} = \Gamma_{ij}^k \frac{\partial}{\partial x^k}.$$

For general vector fields $X, Y \in \mathfrak{X}(M)$, the covariant derivative $\nabla_X Y$ then has the coordinate expression

$$\nabla_X Y = (XY^k + \Gamma_{ij}^k X^i Y^j)^k \frac{\partial}{\partial x^k},$$

showing that the m^3 Christoffel symbols completely determine the affine connection. The *torsion tensor* for a connection ∇ is defined as

$$T(X, Y) := \nabla_X Y - \nabla_Y X - [X, Y]$$

for $X, Y \in \mathfrak{X}(M)$, where $[X, Y] = XY - YX$ is the *Lie bracket* of two vector fields. Using the local coordinate vector fields $\frac{\partial}{\partial x^i}$, the components of T are given by

$$T_{ij} = T\left(\frac{\partial}{\partial x^i}, \frac{\partial}{\partial x^j}\right) = \left(\Gamma_{ij}^k - \Gamma_{ji}^k\right) \frac{\partial}{\partial x^k}.$$

A connection ∇ is called *torsion-free* or *symmetric*, if the torsion vanishes $T \equiv 0$, which is equivalent to the Christoffel symbols being symmetric

$$\Gamma_{ij}^k = \Gamma_{ji}^k \quad \text{for all } i, j, k \in [m].$$

The *curvature tensor* corresponding to ∇ is defined as

$$R(X, Y)Z := \nabla_X \nabla_Y Z - \nabla_Y \nabla_X Z - \nabla_{[X, Y]} Z$$

for $X, Y, Z \in \mathfrak{X}(M)$.

A.3.1. Parallel Transport

Let $\gamma: I \rightarrow M$ be a smooth curve, with $I \subset \mathbb{R}$ an open interval. A *smooth vector field X along γ* is a smooth map $X: I \rightarrow TM$ such that $X(t) \in T_{\gamma(t)}M$ for every $t \in I$. Any connection ∇ on M induces a *covariant derivative along γ* , denoted by $\nabla_{\dot{\gamma}(t)} X$. In local coordinates, this covariant derivative has the form

$$\nabla_{\dot{\gamma}(t)} X(t) = \left(\dot{X}^k(t) + \dot{\gamma}^i(t) X^j(t) \Gamma_{ij}^k(\gamma(t)) \right) \frac{\partial}{\partial x^k}(\gamma(t)). \quad (\text{A.7})$$

A smooth vector field X along γ is *parallel along γ* if $\nabla_{\dot{\gamma}} X \equiv 0$. Since (A.7) is a system of linear first-order ODEs, for any given initial value $V \in T_{\gamma(0)}M$ there exists a unique parallel vector field X along γ with the initial condition $X(0) = V$. The *parallel transport* Π_{pq}^γ between $p = \gamma(t_0)$ and $q = \gamma(t_1)$ along γ is a linear isomorphism defined by

$$\Pi_{pq}^\gamma: T_p M \rightarrow T_q M, \quad V \mapsto X^V(t_1),$$

where $X^V(t_1)$ is the parallel vector field along γ with $X^V(t_0) = V$. For $X, Y \in \mathfrak{X}(M)$, the covariant derivative $\nabla_X Y$ can be recovered through parallel transport along any smooth curve $\gamma: I \rightarrow M$ with $\gamma(0) = p$ and $\dot{\gamma}(0) = X(p)$ by

$$\nabla_X Y(p) = \lim_{t \rightarrow 0} \frac{1}{t} (\Pi_{p\gamma(t)}^\gamma Y(\gamma(t)) - Y(p)). \quad (\text{A.8})$$

A vector field $X \in \mathfrak{X}(M)$ is said to be *parallel* if $X(\gamma(t))$ is a parallel vector field along γ for every smooth curve γ in M . This is equivalent to the condition $\nabla X \equiv 0$.

A.3.2. Geodesics and Exponential Maps

A *geodesic* is a smooth curve $\gamma: I \rightarrow M$ with zero acceleration $\nabla_{\dot{\gamma}(t)} \dot{\gamma}$ along γ . In local coordinates $\gamma = (\gamma^i)$ this is expressed as

$$0 = \nabla_{\dot{\gamma}(t)} \dot{\gamma}(t) = \ddot{\gamma}^k(t) + \dot{\gamma}^i(t) \dot{\gamma}^j(t) \Gamma_{ij}^k(\gamma(t)), \quad (\text{A.9})$$

which is a system of linear second-order ODEs. For every $p \in M$ and $V \in T_p M$ there is a unique maximal open interval $I_V \subset \mathbb{R}$ with $0 \in I_V$ and a geodesic $\gamma_V: I_V \rightarrow M$ with $\gamma_V(0) = p$ and $\dot{\gamma}_V(0) = V$. A connection is called *complete* if every maximal geodesic exists for all time, i.e. $\gamma_V: \mathbb{R} \rightarrow M$.

Viewing geodesics as a map depending on the initial conditions leads to the concept of the *exponential map* induced by a connection ∇

$$\text{Exp}: \mathcal{E} \rightarrow M, \quad V \mapsto \text{Exp}(V) := \gamma_V(1), \quad (\text{A.10})$$

with domain $\mathcal{E} := \{V \in TM \mid 1 \in I_V\} \subset TM$. The exponential map at a specific point $p \in M$ is denoted by $\text{Exp}_p: \mathcal{E}_p \rightarrow M$ and has a star-shaped domain $\mathcal{E}_p := \mathcal{E} \cap T_p M$. For every $V \in T_p M$ the geodesic γ_V can then be expressed as

$$\gamma_V(t) = \text{Exp}_p(tV)$$

for all t such that either side is defined. Furthermore, the differential of Exp_p at $0 \in T_p M$ is the identity $d\text{Exp}_p(0) = \text{id}_{T_p M}$, under the identification $T_0(T_p M) = T_p M$.

A.3.3. Flat Connections

A connection ∇ on a m dimensional manifold M is called *flat* if for each point $p \in M$ there exists local coordinates $x = (x^i)$ on a neighborhood U , for which all coordinate vector fields $\frac{\partial}{\partial x^i}$ are parallel, i.e. $\nabla \frac{\partial}{\partial x^i} \equiv 0$. Such coordinates are said to be an *∇ -affine coordinate system*. Flat connections can equivalently be characterized by their torsion and curvature tensor.

Theorem A.3.1. [Jos17, Thm. 4.1.3]. *A connection ∇ on M is flat if and only if its curvature and torsion tensor vanish identically, i.e. $T \equiv 0$ and $R \equiv 0$.*

Appendix A. Differential Geometry

A necessary and sufficient condition for a coordinate system $y = (y^i)$ to be another affine coordinate system on U is that the transition map $y \circ x^{-1}$ between the coordinate systems is a regular affine transformation (cf. [AN07, Ch. 1.7]), i.e. there exists a matrix $A \in \text{GL}_m(\mathbb{R})$ and a vector $b \in \mathbb{R}^m$ such that

$$y = Ax + b. \quad (\text{A.11})$$

Therefore, if a flat connection ∇ exists on M , then M is an *affine manifold*, i.e. M is covered by coordinate charts with affine coordinate changes.

A.4. Riemannian Manifolds

Denote the bundle of *covariant k -tensors* of a smooth manifold M by $T^k M = \bigotimes_{i \in [k]} T^* M$. A *Riemannian metric* g on M is a symmetric 2-tensor field $g: M \rightarrow T^2 M$ which is positive definite at each point, that is, g_p is an inner product on the tangent space,

$$g_p: T_p M \times T_p M \rightarrow \mathbb{R}, \quad (X, Y) \mapsto g_p(X, Y),$$

smoothly varying in $p \in M$. A *Riemannian manifold* is a manifold M together with a choice of a Riemannian metric g , sometimes denoted by (M, g) . The induced *Riemannian norm* on $T_p M$ at $p \in M$ is denoted by

$$\|X\|_{g,p} := \sqrt{g_p(X, X)}, \quad \forall X \in T_p M.$$

In any smooth local coordinates $x = (x^i)$, a Riemannian metric g can be written as

$$g = g_{ij} dx^i \otimes dx^j \quad \text{with} \quad g_{ij} = g\left(\frac{\partial}{\partial x^i}, \frac{\partial}{\partial x^j}\right).$$

The matrix (g_{ij}) is symmetric and positive definite with smooth component functions. Its inverse is given by (g^{ij}) , i.e. $g_{ik} g^{kj} = \delta_i^j$, where δ_i^j is the Kronecker delta.

Suppose (M, g) and (N, h) are Riemannian manifolds. An *Isometry* from (M, g) to (N, h) is a diffeomorphism $F: M \rightarrow N$ such that $F^* h = g$, i.e.

$$g_x(u, v) = h_{F(x)}(dF(x)[u], dF(x)[v]), \quad \forall x \in M \text{ and } \forall u, v \in T_x M.$$

Two Riemannian manifolds (M, g) and (N, h) are *isometric*, if there exists an isometry between them.

Suppose (M_i, g_i) is a Riemannian manifold for every $i \in [K]$, $K \in \mathbb{N}$. Using the identification (A.4), the product manifold, $M = \prod_{i \in [K]} M_i$ has a natural Riemannian metric g , called *product metric*, defined by

$$g_p(V, U) := \sum_{i \in [K]} g_i|_{p_i}(V_i, U_i) \quad (\text{A.12})$$

for all $p = (p_i) \in M$ and $V = (V_i), U = (U_i) \in T_p M$.

A.4.1. Riemannian Gradients

A Riemannian metric also induces a natural identification between the tangent space $T_p M$ and cotangent space $T_p^* M$. Every $X \in T_p M$ defines a covector $\omega_X \in T_p^* M$ by setting $\omega_X(Y) := g_p(X, Y)\mathbb{R}$ for all $Y \in T_p M$. The induced map

$$T_p M \rightarrow T_p^* M, \quad X \mapsto \omega_X \quad (\text{A.13})$$

is a linear isomorphism. Thus, for every $\eta \in T_p M^*$ there is a unique $X_\eta \in T_p M$ such that $\eta = \omega_{X_\eta}$. The identification between a vector $X = X^i \frac{\partial}{\partial x^i}$ and covector $\omega = \omega_j dx^j$ in local coordinates is given by

$$X^i = g^{ij} \omega_j \quad \text{and} \quad \omega_i = g_{ij} X^j.$$

In particular, for a smooth function $f: M \rightarrow \mathbb{R}$, the above identification (A.13) between vectors and covectors is used to define the *Riemannian gradient* $\text{grad}_g f$ of f as the tangent vector uniquely determined by the 1-form df via the identity

$$g_p(\text{grad}_g f(p), X) = df(p)[X] \quad \text{for all } p \in M, X \in T_p M.$$

In local coordinates, the Riemannian gradient is expressed by

$$(\text{grad}_g f)^i = g^{ij} \frac{\partial f}{\partial x^j}$$

It is important to note, that whether a vector field X has a *potential*, i.e. a function f with $\text{grad}_g f = X$, not only depends on X but also on the Riemannian metric. Also, for a fixed metric g , not every vector field has a potential in general.

If two Riemannian manifolds are isometric, then their Riemannian gradients are related

Lemma A.4.1. *Let $F: (M, g) \rightarrow (N, h)$ be an isometry between two Riemannian manifolds and $f: N \rightarrow \mathbb{R}$ and $\bar{f}: M \rightarrow \mathbb{R}$ a smooth function with $\bar{f} = f \circ F$. Then the Riemannian gradients of f and \bar{f} are related by*

$$\text{grad}_h f(F(p)) = dF(p)[\text{grad}_g \bar{f}(p)] \quad \forall p \in M \quad (\text{A.14})$$

and their norms by

$$\|\text{grad}_h f(F(p))\|_{h, F(p)} = \|\text{grad}_g \bar{f}(p)\|_{g, p} \quad \forall p \in M. \quad (\text{A.15})$$

Proof. Since $\bar{f} = f \circ F$, it follows for the 1-form $d\bar{f} = d(f \circ F) = F^* df$. Let $q \in N$ and $u \in T_q N$ be arbitrary and set $p := F^{-1}(q) \in M$ as well as $v := dF(p)^{-1}[u] \in T_p M$. The definition of the Riemannian gradient and $g = F^* h$ yields

$$\begin{aligned} df(q)[u] &= df(F(p))[dF_p[v]] = (F^* df)(p)[v] = d\bar{f}(p)[v] = g_p(\text{grad}_g \bar{f}(p), v) \\ &= h_{F(p)}(dF(p)[\text{grad}_g \bar{f}(p)], dF(p)[v]) = h_q(dF(p)[\text{grad}_g \bar{f}(p)], u). \end{aligned}$$

Because this equality holds for every $u \in T_q N$ and the Riemannian gradient is uniquely determined by the property $df(q)[u] = h_q(\text{grad}_h f(q), u)$, the relation (A.14) is established. With this characterization of gradients and $g = F^* h$, the norm equality in (A.15) directly follows. \square

A.4.2. Levi-Civita Connection

A connection ∇ on a Riemannian manifold (M, g) is a *metric connection* or *compatible with g* , if it fulfills the product rule

$$\nabla_Z g(X, Y) = g(\nabla_Z X, Y) + g(X, \nabla_Z Y)$$

for all $X, Y, Z \in \mathfrak{X}(M)$. For every Riemannian structure g on M , there exists a unique torsion free metric connection ∇^g , called the *Levi-Civita connection of g* . In local coordinates, the Christoffel symbols of the Levi-Civita connection are given by

$$\Gamma_{ij}^{(g)k} = \frac{1}{2} g^{kl} \left(\frac{\partial}{\partial x^i} g_{jl} + \frac{\partial}{\partial x^j} g_{il} - \frac{\partial}{\partial x^l} g_{ij} \right).$$

The geodesics and exponential map corresponding the Levi-Civita are called *Riemannian geodesics and Riemannian exponential map*, where the latter will be denoted by Exp^g to avoid confusion when multiple connections and their corresponding Exponential maps are considered.

A.4.3. Riemannian Distance and Mean

For a Riemannian manifold (M, g) , the length of a smooth curve $\gamma: [a, b] \rightarrow M$ depends on the metric and is defined by

$$L_g(\gamma) := \int_a^b \sqrt{g_{\gamma(t)}(\dot{\gamma}(t), \dot{\gamma}(t))} dt.$$

If M is connected, the *Riemannian distance* between two points $x, y \in M$ is defined as

$$d_g(x, y) := \inf \{ L_g(\gamma) \mid \gamma: [a, b] \rightarrow M \text{ piecewise smooth, } \gamma(a) = x, \gamma(b) = y \}$$

and turns (M, d_g) into a metric space. If (N, h) is another connected Riemannian manifold and $F: M \rightarrow N$ an isometry, then F is also an isometry between the metric spaces (M, d_g) and (N, d_h) , i.e.

$$d_g(x, y) = d_h(F(x), F(y)) \quad \forall x, y \in M.$$

Viewing the squared distance as a smooth function $x \mapsto \frac{1}{2} d_g^2(x, y) := \zeta(x)$ on M , for fixed $y \in M$, the Riemannian gradient is given by

$$\text{grad } \zeta(x) = -(\text{Exp}_x^g)^{-1}(y)$$

Let $x_1, \dots, x_N \in M$ be some points with associated weights $\omega_1, \dots, \omega_N \in \mathbb{R}$, satisfying $\sum_{k \in [N]} \omega_k = 1$ and $\omega_k > 0$ for $k \in [N]$. The *Riemannian center of mass*, in the following just called *Riemannian mean*, is a point $x_* \in M$ minimizing the function

$$x \mapsto c(x) := \frac{1}{2} \sum_{k \in [N]} \omega_k d_g^2(x, x_k)$$

on M , i.e. x_* fulfills the optimality condition (see [Jos17, Lem. 6.9.5])

$$0 = \text{grad } c(x_*) = \sum_{k \in [N]} \omega_k (\text{Exp}_{x_*}^g)^{-1}(x_k). \quad (\text{A.16})$$

A.4.4. Riemannian Hessian

Suppose (M, g) is a Riemannian manifold and $f: M \rightarrow \mathbb{R}$ a smooth function. Using the definition from [AMS08], the *Riemannian Hessian of f* at $p \in M$ is the linear map

$$\text{Hess}_g f(p): T_p M \rightarrow T_p M, \quad X \mapsto \text{Hess}_g f(p)[X] := \nabla_X^g \text{grad}_g f(p). \quad (\text{A.17})$$

Due to [AMS08, Prop. 5.5.3], $\text{Hess}_g f$ is symmetric with respect to the Riemannian metric g , i.e. at $p \in M$

$$g_p(\text{Hess}_g f(p)[X], Y) = g_p(X, \text{Hess}_g f(p)[Y]) \quad (\text{A.18})$$

holds for all $X, Y \in T_p M$.

Appendix B

Convex Analysis

The basic definitions and results from convex analysis necessary for this work are briefly summarized in the following, based on [BV04], [Roc70] and [RW09].

B.1. Affine and Convex Sets

A subset $A \subset \mathbb{R}^n$ is called an *affine set*, if $rx + (1 - r)y \in A$ holds for all $x, y \in A$ and $r \in \mathbb{R}$. For any subset $S \subset \mathbb{R}^n$ the *affine hull* of S , denoted by $\text{aff}(S)$, is the smallest affine set $A \subset \mathbb{R}^n$ containing S . A subset $C \subset \mathbb{R}^n$ is *convex*, if for all $x, y \in C$ the line segment $rx + (1 - r)y$, with $r \in [0, 1]$, is contained in C . Similar to the affine hull, the *convex hull* $\text{conv}(S)$ of a subset $S \subset \mathbb{R}^n$ is the smallest convex set $C \subset \mathbb{R}^n$ containing the set S .

Lemma B.1.1. *For any compact set $K \subset \mathbb{R}^d$, the convex hull $\text{conv}(K)$ is compact.*

Proof. See e.g. [RW09, Corollary 2.30]. □

Let (\mathbb{R}^n, d) be a metric space. The *relative interior* of a convex set $C \subset \mathbb{R}^n$ is denoted by $\text{rint}(C)$ and defined to be the interior when C is regarded as a subset of its affine hull $\text{aff}(C)$ in the subspace topology. Since the topology of \mathbb{R}^n is induced by the metric d , the relative interior of C can equivalently be described as

$$\text{rint}(C) = \{x \in \text{aff}(C) \mid \exists \varepsilon > 0: B_\varepsilon(x) \cap \text{aff}(C) \subset C\}, \quad (\text{B.1})$$

where $B_r(x) = \{y \in \mathbb{R}^n \mid d(x, y) < r\}$ is the open ball in \mathbb{R}^n of radius $r > 0$ around x .

B.2. Convex Functions

Let $C \subset \mathbb{R}^n$ be a convex set. A function $f: C \rightarrow \mathbb{R}$ is *convex* if

$$f(rx + (1 - r)y) \leq rf(x) + (1 - r)f(y) \quad \forall x, y \in C \text{ and } \forall r \in [0, 1].$$

The function f is called *strictly convex*, if the above inequality is strict for $x \neq y$ and $r \in (0, 1)$. Furthermore, for a constant $\sigma > 0$, the function f is σ -*strongly convex* with respect to the norm $\|\cdot\|_p$, if

$$f(rx + (1 - r)y) \leq rf(x) + (1 - r)f(y) - \frac{\sigma}{2}r(1 - r)\|x - y\|_p^2$$

Appendix B. Convex Analysis

holds for all $x, y \in C$ and $r \in (0, 1)$. If $\|\cdot\|_p = \|\cdot\|$, then f is just said to be σ -strongly convex, without referring to the norm.

Proposition B.2.1. [BT03, Prop. 5.1] *The negative entropy $-H$ is 1-strongly convex on $\text{rint}(\Delta)$ with respect to $\|\cdot\|_1$.*

In the following, it will be convenient to extend a convex function $f: C \rightarrow \mathbb{R}$ onto all of \mathbb{R}^n by allowing f to take the value infinity outside its domain, i.e. to be an *extended real-valued* function

$$f: \mathbb{R}^n \rightarrow \overline{\mathbb{R}} := \mathbb{R} \cup \{\infty\} \quad \text{with} \quad \text{dom}(f) := \{x \in \mathbb{R}^n \mid f(x) < \infty\}.$$

If f is convex then so is the set $\text{dom}(f)$. Thus, there is no need to refer to the convex set C when defining f , since it is implicitly given as $\text{dom}(f) = C$.

Let $C \subset \mathbb{R}^n$ be a subset and define the *indicator function of C* from an optimization point of view by

$$\delta_C: \mathbb{R}^n \rightarrow \overline{\mathbb{R}}, \quad x \mapsto \delta_C(x) = \begin{cases} 0 & , \text{for } x \in C \\ \infty & , \text{else.} \end{cases} \quad (\text{B.2})$$

If C is convex, then δ_C is an extended real-valued convex function. Moreover, if additionally C is closed, then δ_C is lower semicontinuous. With this, minimizing a function $f: \mathbb{R}^n \rightarrow \mathbb{R}$ restricted to a set $C \subset \mathbb{R}^n$ can now be viewed as minimizing $f + \delta_C$ over all of \mathbb{R}^n , i.e.

$$\min_{x \in C} \{f(x)\} = \min_{x \in \mathbb{R}^n} \{f(x) + \delta_C(x)\}.$$

For a function $f: \mathbb{R}^n \rightarrow \overline{\mathbb{R}}$, the *conjugate* function, denoted by f^* , is defined by

$$f^*(y) := \sup_{x \in \mathbb{R}^n} \{\langle y, x \rangle - f(x)\} = \sup_{x \in \text{dom}(f)} \{\langle y, x \rangle - f(x)\} \quad (\text{B.3})$$

and its domain consists of all $y \in \mathbb{R}^d$ for which the supremum is finite. The conjugate function is always convex. If f is convex and lower semicontinuous, then $f^{**} = f$.

Suppose the convex set $C \subset \mathbb{R}^n$ is open and f is continuously differentiable on C , then all these different forms of convexity can be characterized through first-order conditions. In this case, f is convex if and only if

$$f(y) \geq f(x) + \langle \partial f(x), y - x \rangle \quad \forall x, y \in C \quad (\text{B.4})$$

and strictly convex if and only if the above inequality is strict for $x \neq y$. Additionally, σ -strong convexity of f with respect to $\|\cdot\|_p$ is equivalent to the condition

$$f(y) \geq f(x) + \langle \partial f(x), y - x \rangle + \frac{\sigma}{2} \|y - x\|_p^2 \quad \forall x, y \in C. \quad (\text{B.5})$$

If f is even twice continuously differentiable, then second-order conditions are available. In this situation, the convexity of f is equivalent to the Hessian of f being positive semi-definite for all $x \in C$. For strict convexity, the condition of $\text{Hess } f(x)$ to be positive

definite for all $x \in C$ is only sufficient but not necessary. Furthermore, f is σ -strongly convex if and only if the smallest eigenvalue of $\text{Hess } f(x)$ is lower bounded by σ for all $x \in C$, i.e.

$$\langle u, \text{Hess } f(x)u \rangle \geq \sigma \|u\|^2, \quad \forall u \in \mathbb{R}^n. \quad (\text{B.6})$$

As a consequence, f is σ -strongly convex, if and only if $f - \frac{1}{2}\sigma \|\cdot\|^2$ is convex.

B.3. Bregman Divergences

Let the convex set $C \subset \mathbb{R}^n$ be open and $f: C \rightarrow \mathbb{R}$ continuously differentiable. Define the function $D_f: C \times C \rightarrow \mathbb{R}$ by

$$D_f(y, x) := f(y) - f(x) - \langle \partial f(x), y - x \rangle, \quad \forall x, y \in C. \quad (\text{B.7})$$

This function is linear in f , i.e. for another function $g: C \rightarrow \mathbb{R}$ and constants $\alpha, \beta \in \mathbb{R}$ it follows

$$D_{\alpha f + \beta g} = \alpha D_f + \beta D_g. \quad (\text{B.8})$$

Due to the definition of D_f and the first-order condition of convexity in (B.4), the characterization

$$f: C \rightarrow \mathbb{R} \text{ is convex} \quad \Leftrightarrow \quad D_f(y, x) \geq 0 \quad \forall x, y \in C \quad (\text{B.9})$$

follows as well the equivalence between f being strictly convex and $D_f(y, x) > 0$ for all $x \neq y$, by the corresponding first-order condition of strict convexity. Similarly, as a result of (B.5),

$$f \text{ is } \sigma\text{-strictly convex w.r.t. } \|\cdot\|_p \quad \Leftrightarrow \quad D_f(y, x) \geq \frac{\sigma}{2} \|y - x\|_p^2 \quad \forall x, y \in C. \quad (\text{B.10})$$

For a strictly convex function f , the expression D_f is called a *Bregman divergence* (see [Bre67]) and generalizes the concept of a distance. Examples of Bregman divergences are the Euclidean distance on \mathbb{R}^n , induced by the squared Euclidean norm

$$D_{\|\cdot\|^2}(y, x) = \|y - x\|^2, \quad \forall x, y \in \mathbb{R}^n \quad (\text{B.11})$$

and the *Kullback-Leibler (KL) divergence* on the probability simplex $\Delta \subset \mathbb{R}^n$ (see (2.8)), induced by the negative entropy $-H(p) = \langle p, \log p \rangle$, for $p \in \Delta$ and is given by

$$D_{-H}(p, q) = \left\langle p, \log \frac{p}{q} \right\rangle =: \text{KL}(p, q), \quad \forall p, q \in \Delta. \quad (\text{B.12})$$

Since the negative entropy can be extended onto the nonnegative orthant $\mathbb{R}_{\geq 0}^n$, the KL divergence can be generalized, again denoted by KL, as

$$\text{KL}(x, y) = D_{-H}(x, y) = \left\langle x, \log \frac{x}{y} \right\rangle - \langle x, \mathbf{1}_n \rangle + \langle y, \mathbf{1}_n \rangle, \quad \forall x, y \in \mathbb{R}_{\geq 0}^n. \quad (\text{B.13})$$

Bregman divergences are a useful concept with many applications in different fields, including information theory [CT12], optimization [BT03], information geometry [Ama16] and many more.

B.4. Lagrange Duality and KKT Conditions

Subsequently, a short summary of the necessary definitions and concepts from optimization theory for this work is given, based on [BV04].

Suppose a general minimization problem with equality and inequality constraints of the form

$$\min_{x \in \mathbb{R}^n} \{f(x)\} \quad \text{s.t.} \quad F(x) \leq 0 \quad \text{and} \quad H(x) = 0 \quad (\text{B.14})$$

is given, where the functions $f: \mathbb{R}^n \rightarrow \bar{\mathbb{R}}$, $F: \mathbb{R}^n \rightarrow \bar{\mathbb{R}}^m$ and $H: \mathbb{R}^n \rightarrow \bar{\mathbb{R}}^r$ are not necessarily convex and $\bar{\mathbb{R}} = \mathbb{R} \cup \{\infty\}$ as above. The *domain of the minimization problem* is defined by

$$\mathcal{D} := \{x \in \mathbb{R}^n \mid f(x) < \infty, H(x) < \infty \text{ and } F(x) < \infty\}$$

and the minimal value of the problem (B.14) is denoted by f_* . The associated *Lagrangian* to the optimization problem (B.14) is the function

$$L: \mathbb{R}^n \times \mathbb{R}^m \times \mathbb{R}^r \rightarrow \mathbb{R}, \quad L(x, \lambda, \nu) := f(x) + \langle \lambda, F(x) \rangle + \langle \nu, H(x) \rangle. \quad (\text{B.15})$$

The vectors λ and ν are called *Lagrange multipliers* or *dual variables*. The corresponding *Lagrange dual function*, or just *dual function*, is given by

$$h: \mathbb{R}^m \times \mathbb{R}^r \rightarrow \mathbb{R}, \quad h(\lambda, \nu) := \inf_{x \in \mathcal{D}} \{L(x, \lambda, \nu)\}, \quad (\text{B.16})$$

and is concave in (λ, ν) . In case the Lagrangian $L(x, \lambda, \nu)$ is unbounded below in x , the function $h(\lambda, \nu)$ takes the value $-\infty$.

If $\lambda \geq 0$ is assumed, then the dual function gives lower bounds on the optimal value f_* of problem (B.14), i.e. $h(\lambda, \nu) \leq f_*$ holds. The optimization problem of finding the best lower bound is called *Lagrange dual problem*, or just *dual problem*

$$\max_{\lambda, \nu} \{h(\lambda, \nu)\} \quad \text{s.t.} \quad \lambda \geq 0. \quad (\text{B.17})$$

In this context, the original minimization problem (B.14) is referred to as the *primal problem*. The optimal value of (B.17) is denoted by h^* and the corresponding pair of maximizers (λ^*, ν^*) is termed *dual optimal* or *optimal Lagrange multipliers*. Since h^* is the best lower bound of f_* , the inequality

$$h^* \leq f_*$$

is always fulfilled. This fact is called *weak duality* and the difference $0 \leq f_* - h^*$ is referred to as *duality gap*. The case in which the duality gap is zero and

$$h^* = f_*$$

holds is termed *strong duality*. In general, strong duality is not guaranteed to hold, however, there are various known sufficient conditions for it, named *constraint qualifications*.

If the functions f , F and H of the primal problem (B.14) are differentiable, then there is a set of optimality conditions, called KKT conditions, which hold under the assumption of strong duality.

Theorem B.4.1 (Karush-Kuhn-Tucker (KKT) conditions [BV04]). *Let $L(x, \lambda, \nu)$ be the Lagrangian (B.15) and suppose x^* is a primal optimal point of (B.14) and (λ^*, ν^*) a dual optimal point of (B.17). If strong duality is satisfied, then the following KKT conditions hold:*

$$\partial f(x^*) + dF(x^*)^\top \lambda^* + dH(x^*)^\top \nu^* = \partial_x L(x^*, \lambda^*, \nu^*) = 0, \quad (\text{B.18a})$$

$$F(x^*) \leq 0, \quad H(x^*) = 0, \quad 0 \leq \lambda^*, \quad \text{and} \quad \langle \lambda^*, F(x^*) \rangle = 0. \quad (\text{B.18b})$$

In the following, convex optimization problems

$$\min_{x \in \mathbb{R}^n} \{f(x)\} \quad \text{s.t.} \quad F(x) \leq 0 \quad \text{and} \quad Ax = b \quad (\text{B.19})$$

are considered, where A is a matrix, b a vector and $f: \mathbb{R}^n \rightarrow \bar{\mathbb{R}}$ as well as all components $F^i: \mathbb{R}^n \rightarrow \bar{\mathbb{R}}$, $i \in [m]$, are convex. In this case, the resulting domain of the problem

$$\mathcal{D} = \{x \in \mathbb{R}^n \mid f(x) < \infty, \text{ and } F(x) < \infty\} = \text{dom}(f) \cap \bigcap_{i \in [m]} \text{dom}(F^i) \quad (\text{B.20})$$

is a convex set. It is important to note, that if the primal problem (B.14) is convex, then the KKT conditions are also sufficient for optimality, i.e. if x^* , λ^* and ν^* are points satisfying the KKT conditions (B.18), then x^* and (λ^*, ν^*) are primal and dual optimal and the duality gap is zero.

A well known constraint qualification for convex problems is *Slater's condition*, requiring the existence of a *strictly feasible point*

$$\exists x \in \text{rint}(\mathcal{D}), \quad F(x) < 0 \quad \text{and} \quad Ax = b. \quad (\text{B.21})$$

If additionally, F is also affine, i.e. there is a matrix C and a vector d with $F(x) = Cx + d$, then the domain (B.20) of the convex problem reduces to $\mathcal{D} = \text{dom}(f)$ and the condition can be weakened to

$$\exists x \in \text{rint}(\text{dom}(f)), \quad Cx + d \leq 0 \quad \text{and} \quad Ax = b. \quad (\text{B.22})$$

As an example, consider a *linear program (LP) in standard form*

$$\min_{x \in \mathbb{R}^n} \langle c, x \rangle \quad \text{s.t.} \quad x \geq 0 \quad \text{and} \quad Ax = b, \quad (\text{B.23})$$

where $c \in \mathbb{R}^n$ is a given cost vector and the equality constraints are represented by a matrix $A \in \mathbb{R}^{m \times n}$ and a vector $b \in \mathbb{R}^m$. The Lagrangian (B.15) is given by

$$L(x, \lambda, \nu) = \langle c, x \rangle - \langle \lambda, x \rangle + \langle \nu, b - Ax \rangle = \langle b, \nu \rangle + \langle c - \lambda - A^\top \nu, x \rangle,$$

for $(x, \lambda, \nu) \in \mathbb{R}^n \times \mathbb{R}^n \times \mathbb{R}^m$ and the corresponding dual function (B.16) takes the form

$$h(\lambda, \nu) = \langle b, \nu \rangle + \inf_{x \in \mathbb{R}^n} \{ \langle c - \lambda - A^\top \nu, x \rangle \} = \begin{cases} \langle b, \nu \rangle & , \text{ for } 0 = c - \lambda - A^\top \nu \\ -\infty & , \text{ else.} \end{cases}$$

Appendix B. Convex Analysis

The resulting dual problem (B.17) is then given by

$$\begin{aligned} & \max_{\lambda \in \mathbb{R}^n, \nu \in \mathbb{R}^m} \{ \langle b, \nu \rangle \} \quad \text{s.t.} \quad \lambda \geq 0 \quad \text{and} \quad 0 = c - \lambda - A^\top \nu \\ & = \max_{\nu \in \mathbb{R}^m} \{ \langle b, \nu \rangle \} \quad \text{s.t.} \quad A^\top \nu \leq c, \end{aligned} \tag{B.24}$$

after eliminating the variable λ . Since the primal problem (B.23) is convex with affine equality and inequality constraints as well as $\text{rint}(\text{dom}(\langle c, \cdot \rangle)) = \mathbb{R}^n$, the weak Slater's condition (B.22) is fulfilled, proving that the LP satisfies strong duality.

Bibliography

- [AB09] Hedy Attouch and Jérôme Bolte, *On the convergence of the proximal algorithm for nonsmooth functions involving analytic features*, *Mathematical Programming* **116** (2009), no. 1-2, 5–16.
- [ABB04] Felipe Alvarez, Jérôme Bolte, and Olivier Brahic, *Hessian Riemannian Gradient Flows in Convex Programming*, *SIAM Journal on Control and Optimization* **43** (2004), no. 2, 477–501.
- [ABK12] B. Andres, T. Beier, and J.H. Kappes, *OpenGM: A C++ Library for Discrete Graphical Models*, *CoRR* [abs/1206.0111](#) (2012).
- [ABM14] H. Attouch, G. Buttazzo, and G. Michaille, *Variational Analysis in Sobolev and BV Spaces: Applications to PDEs and Optimization*, 2nd ed., SIAM, 2014.
- [AE05] Nihat Ay and Ionas Erb, *On a notion of linear replicator equations*, *Journal of Dynamics and Differential Equations* **17** (2005), no. 2, 427–451.
- [AFH⁺04] A. Aaron, J. Fakcharoenphol, C. Harrelson, R. Krauthgamer, K. Talwar, and E. Tardos, *Approximate Classification via Earthmover Metrics*, *Proc. SODA*, 2004, pp. 1079–1087.
- [AFMS18] L. Ambrosio, M. Fornasier, M. Morandotti, and G. Savaré, *Spatially Inhomogeneous Evolutionary Games*, *CoRR* [abs/1805.04027](#) (2018).
- [AJVLS17] Nihat Ay, Jürgen Jost, Hông Vân Lê, and Lorenz Schwachhöfer, *Information geometry*, vol. 64, Springer, 2017.
- [AK06] P-A Absil and K Kurdyka, *On the stable equilibrium points of gradient systems*, *Systems & control letters* **55** (2006), no. 7, 573–577.
- [Ama98] Shun-Ichi Amari, *Natural gradient works efficiently in learning*, *Neural computation* **10** (1998), no. 2, 251–276.
- [AMA05] P. Absil, R. Mahony, and B. Andrews, *Convergence of the Iterates of Descent Methods for Analytic Cost Functions*, *SIAM Journal on Optimization* **16** (2005), no. 2, 531–547.
- [Ama16] Shun-ichi Amari, *Information geometry and its applications*, vol. 194, Springer, 2016.

BIBLIOGRAPHY

- [AMS08] P-A Absil, Robert Mahony, and Rodolphe Sepulchre, *Optimization Algorithms on Matrix Manifolds*, Princeton University Press, 2008.
- [AN07] Shun-ichi Amari and Hiroshi Nagaoka, *Methods of information geometry*, vol. 191, American Mathematical Soc., 2007.
- [ÅPSS17] Freddie Åström, Stefania Petra, Bernhard Schmitzer, and Christoph Schnörr, *Image Labeling by Assignment*, Journal of Mathematical Imaging and Vision **58** (2017), no. 2, 211–238.
- [ARP⁺19] V. Antun, F. Renna, C. Poon, B. Adcock, and A. C. Hansen, *On Instabilities of Deep Learning in Image Reconstruction - Does AI Come at a Cost?*, CoRR abs/1902.05300 (2019).
- [BCM05] Antoni Buades, Bartomeu Coll, and Jean-Michel Morel, *A review of image denoising algorithms, with a new one*, Multiscale Modeling & Simulation **4** (2005), no. 2, 490–530.
- [BDL07] Jérôme Bolte, Aris Daniilidis, and Adrian Lewis, *The Lojasiewicz Inequality for Nonsmooth Subanalytic Functions with Applications to Subgradient Dynamical Systems*, SIAM Journal on Optimization **17** (2007), no. 4, 1205–1223.
- [BM88] Edward Bierstone and Pierre D Milman, *Semianalytic and subanalytic sets*, Publications Mathématiques de l’IHÉS **67** (1988), 5–42.
- [BPN14] A. S. Bratus, V. P. Posvyanskii, and A. S. Novozhilov, *Replicator equations and Space*, Math. Modelling Natural Phenomena **9** (2014), no. 3, 47–67.
- [Bre67] Lev M Bregman, *The relaxation method of finding the common point of convex sets and its application to the solution of problems in convex programming*, USSR computational mathematics and mathematical physics **7** (1967), no. 3, 200–217.
- [Bru06] R.A. Brualdi, *Combinatorial Matrix Classes*, Cambridge Univ. Press, 2006.
- [BST14] J. Bolte, S. Sabach, and M. Teboulle, *Proximal Alternating Linearized Minimization for Nonconvex and Nonsmooth Problems*, Math. Progr., Ser. A **146** (2014), no. 1-2, 459–494.
- [BSTV18] Jérôme Bolte, Shoham Sabach, Marc Teboulle, and Yakov Vaisbourd, *First Order Methods Beyond Convexity and Lipschitz Gradient Continuity with Applications to Quadratic Inverse Problems*, SIAM Journal on Optimization **28** (2018), no. 3, 2131–2151.
- [BT03] Amir Beck and Marc Teboulle, *Mirror descent and nonlinear projected subgradient methods for convex optimization*, Operations Research Letters **31** (2003), no. 3, 167–175.

- [BV04] Stephen Boyd and Lieven Vandenberghe, *Convex optimization*, Cambridge university press, 2004.
- [CCP12] Antonin Chambolle, Daniel Cremers, and Thomas Pock, *A Convex Approach to Minimal Partitions*, SIAM Journal on Imaging Sciences **5** (2012), no. 4, 1113–1158.
- [CEN06] Tony F Chan, Selim Esedoglu, and Mila Nikolova, *Algorithms for Finding Global Minimizers of Image Segmentation and Denoising Models*, SIAM journal on applied mathematics **66** (2006), no. 5, 1632–1648.
- [CKNZ05] C. Chekuri, S. Khanna, J. Naor, and L. Zosin, *Linear Programming Formulation and Approximation Algorithms for the Metric Labeling Problem*, SIAM J. Discr. Math. **18** (2005), no. 3, 608–625.
- [CT12] Thomas M Cover and Joy A Thomas, *Elements of information theory*, John Wiley & Sons, 2012.
- [Cut13] M. Cuturi, *Sinkhorn Distances: Lightspeed Computation of Optimal Transport*, Advances in Neural Information Processing Systems **26**, Curran Associates, Inc., 2013, pp. 2292–2300.
- [dB13] Russ deForest and A. Belmonte, *Spatial Pattern Dynamics due to the Fitness Gradient Flux in Evolutionary Games*, Physical Review E **87** (2013), no. 6, 062138.
- [E17] Weinan E, *A Proposal on Machine Learning via Dynamical Systems*, Comm. Math. Statistics **5** (2017), no. 1, 1–11.
- [GG84] S. Geman and D. Geman, *Stochastic Relaxation, Gibbs Distributions, and the Bayesian Restoration of Images*, IEEE Trans. Patt. Anal. Mach. Intell. **6** (1984), no. 6, 721–741.
- [HPW93] Ernst Hairer, Nørsett Syvert P., and Gerhard Wanner, *Solving Ordinary Differential Equations I*, Springer Berlin Heidelberg, 1993.
- [HR17] E. Haber and L. Ruthotto, *Stable Architectures for Deep Neural Networks*, Inverse Problems **34** (2017), no. 1, 014004.
- [HS03] Josef Hofbauer and Karl Sigmund, *Evolutionary Game Dynamics*, Bulletin of the American Mathematical Society **40** (2003), no. 4, 479–519.
- [HSÅS18] R. Hühnerbein, F. Savarino, F. Åström, and C. Schnörr, *Image Labeling Based on Graphical Models Using Wasserstein Messages and Geometric Assignment*, SIAM Journal on Imaging Sciences **11** (2018), no. 2, 1317–1362.
- [HSPS19] R. Hühnerbein, F. Savarino, S. Petra, and C. Schnörr, *Learning Adaptive Regularization for Image Labeling Using Geometric Assignment*, Proc. SSVM, Springer, 2019.

BIBLIOGRAPHY

- [HZ83] R. A. Hummel and S. W. Zucker, *On the Foundations of the Relaxation Labeling Processes*, IEEE Trans. Patt. Anal. Mach. Intell. **5** (1983), no. 3, 267–287.
- [HZRS16] K. He, X. Zhang, S. Ren, and J. Sun, *Deep Residual Learning for Image Recognition*, Proc. CVPR, 2016.
- [Jos17] Jürgen Jost, *Riemannian Geometry and Geometric Analysis*, 7th ed., Springer, 2017.
- [KAH⁺15] J.H. Kappes, B. Andres, F.A. Hamprecht, C. Schnörr, S. Nowozin, D. Batra, S. Kim, B.X. Kausler, T. Kröger, J. Lellmann, N. Komodakis, B. Savchynskyy, and C. Rother, *A Comparative Study of Modern Inference Techniques for Structured Discrete Energy Minimization Problems*, Int. J. Comp. Vision **115** (2015), no. 2, 155–184.
- [Kha02] H.K. Khalil, *Nonlinear systems*, Pearson Education, vol. 3, Prentice Hall, 2002.
- [KMS00] R. Kimmel, R. Malladi, and N. Sochen, *Images as Embedded Maps and Minimal Surfaces: Movies, Color, Texture, and Volumetric Images*, Int. J. Comp. Vision **39** (2000), no. 2, 111–129.
- [Kni08] P.A. Knight, *The Sinkhorn-Knopp Algorithm: Convergence and Applications*, SIAM J. Matrix Anal. Appl. **30** (2008), no. 1, 261–275.
- [Kol06] V. Kolmogorov, *Convergent Tree-Reweighted Message Passing for Energy Minimization*, IEEE Trans. Patt. Anal. Mach. Intell. **28** (2006), no. 10, 1568–1583.
- [KP02] Steven G Krantz and Harold R Parks, *A primer of real analytic functions*, 2nd ed., Springer Science & Business Media, 2002.
- [KPT⁺17] S. Kolouri, S. Park, M. Thorpe, D. Slepcev, and G.K. Rohde, *Optimal mass transport: Signal processing and machine-learning applications*, IEEE Signal Proc. Mag. **34** (2017), no. 4, 43–59.
- [KSH12] Alex Krizhevsky, Ilya Sutskever, and Geoffrey E Hinton, *Imagenet classification with deep convolutional neural networks*, Advances in neural information processing systems, 2012, pp. 1097–1105.
- [KT02] J. Kleinberg and E. Tardos, *Approximation Algorithms for Classification Problems with Pairwise Relationships: Metric Labeling and Markov Random Fields*, Journal of the ACM **49** (2002), no. 5, 616–639.
- [KZ04] Vladimir Kolmogorov and Ramin Zabini, *What energy functions can be minimized via graph cuts?*, IEEE transactions on pattern analysis and machine intelligence **26** (2004), no. 2, 147–159.

- [Lag02] Christian Lageman, *Konvergenz reell-analytischer gradientenähnlicher Systeme*, Diplomarbeit, Universität Würzburg, 2002.
- [Lag07] ———, *Pointwise convergence of gradient-like systems*, *Mathematische Nachrichten* **280** (2007), no. 13-14, 1543–1558.
- [Lau96] S. L. Lauritzen, *Graphical Models*, Clarendon Press, Oxford, 1996.
- [Lee12] John M Lee, *Introduction to Smooth Manifolds*, Springer, 2nd ed., 2012.
- [Lee18] ———, *Introduction to Riemannian Manifolds*, Springer, 2018.
- [IL65] Stanis law Lojasiewicz, *Ensembles semi-analytiques*, IHES notes (1965).
- [Loj82] S Lojasiewicz, *Sur les trajectoires du gradient d'une fonction analytique*, *Seminari di geometria* **1983** (1982), 115–117.
- [LS11] J. Lellmann and C. Schnörr, *Continuous Multiclass Labeling Approaches and Algorithms*, *SIAM J. Imag. Sci.* **4** (2011), no. 4, 1049–1096.
- [MK99] Hans Munthe-Kaas, *High order Runge-Kutta methods on manifolds*, *Applied Numerical Mathematics* **29** (1999), no. 1, 115–127.
- [NN87] Y. Nesterov and A. Nemirovskii, *Interior Point Polynomial Algorithms in Convex Programming*, *Studies in Applied Mathematics*, Society for Industrial and Applied Mathematics, 1987.
- [NPB11] A. Novozhilov, V. P. PosvNovozh, and A. S. Bratus, *On the Reaction–Diffusion Replicator Systems: Spatial Patterns and Asymptotic Behaviour*, *Russ. J. Numer. Anal. Math. Modelling* **26** (2011), no. 6, 555–564.
- [NW06] Jorge Nocedal and Stephen Wright, *Numerical optimization*, Springer Science & Business Media, 2006.
- [NY83] Arkadii Semenovich Nemirovsky and David Borisovich Yudin, *Problem Complexity and Method Efficiency in Optimization*.
- [PDM12] J Jr Palis and Welington De Melo, *Geometric theory of dynamical systems: an introduction*, Springer Science & Business Media, 2012.
- [Pel99] Marcello Pelillo, *Replicator equations, maximal cliques, and graph isomorphism*, *Advances in Neural Information Processing Systems*, 1999, pp. 550–556.
- [RHZ76] A. Rosenfeld, R. A. Hummel, and S. W. Zucker, *Scene Labeling by Relaxation Operations*, *IEEE Trans. Systems, Man, and Cyb.* **6** (1976), 420–433.
- [RM15] Garvesh Raskutti and Sayan Mukherjee, *The information geometry of mirror descent*, *IEEE Transactions on Information Theory* **61** (2015), no. 3, 1451–1457.

BIBLIOGRAPHY

- [Roc70] R Tyrrell Rockafellar, *Convex analysis*, vol. 28, Princeton university press, 1970.
- [RW09] R Tyrrell Rockafellar and Roger J-B Wets, *Variational Analysis*, vol. 317, Springer Science & Business Media, 2009.
- [San10] W. H. Sandholm, *Population Games and Evolutionary Dynamics*, MIT Press, 2010.
- [SC03] Yuzuru Sato and James P Crutchfield, *Coupled replicator equations for the dynamics of learning in multiagent systems*, Physical Review E **67** (2003), no. 1, 015206.
- [Sch90] M.H. Schneider, *Matrix Scaling, Entropy Minimization, and Conjugate Duality (II): The Dual Problem*, Math. Progr. **48** (1990), 103–124.
- [Sch20] C. Schnörr, *Assignment Flows*, Variational Methods for Nonlinear Geometric Data and Applications (P. Grohs, M. Holler, and A. Weinmann, eds.), Springer (in press), 2020.
- [Sin64] R. Sinkhorn, *A Relationship Between Arbitrary Positive Matrices and Doubly Stochastic Matrices*, Ann. Math. Statist. **35** (1964), no. 2, 876–879.
- [SS19a] F. Savarino and C. Schnörr, *A Variational Perspective on the Assignment Flow*, Proc. SSVM, Springer, 2019.
- [SS19b] ———, *Continuous-Domain Assignment Flows*, European J. of Applied Mathematics (2019), conditionally accepted subject to revisions. preprint: <https://arxiv.org/abs/1910.07287>.
- [TC04] A. Traulsen and J. C. Claussen, *Similarity-Based Cooperation and Spatial Segregation*, Phys. Rev. E **70** (2004), no. 4, 046128.
- [Ter96] T. Terlaky, *Interior Point Methods of Mathematical Programming*, Kluwer Acad. Publ., 1996.
- [Wai06] Martin J Wainwright, *Estimating the “Wrong” Graphical Model: Benefits in the Computation-Limited Setting*, Journal of Machine Learning Research **7** (2006), no. Sep, 1829–1859.
- [Wei98] Joachim Weickert, *Anisotropic diffusion in image processing*, vol. 1, Teubner Stuttgart, 1998.
- [Wei01] Y. Weiss, *Comparing the Mean Field Method and Belief Propagation for Approximate Inference in MRFs*, Advanced Mean Field Methods: Theory and Practice, MIT Press, 2001, pp. 229–240.
- [Wer07] T. Werner, *A Linear Programming Approach to Max-sum Problem: A Review*, IEEE Trans. Patt. Anal. Mach. Intell. **29** (2007), no. 7, 1165–1179.

- [WJ08] M.J. Wainwright and M.I. Jordan, *Graphical Models, Exponential Families, and Variational Inference*, Found. Trends Mach. Learning **1** (2008), no. 1-2, 1–305.
- [YFW05] J.S. Yedidia, W.T. Freeman, and Y. Weiss, *Constructing Free-Energy Approximations and Generalized Belief Propagation Algorithms*, IEEE Trans. Information Theory **51** (2005), no. 7, 2282–2312.
- [YMW06] C. Yanover, T. Meltzer, and Y. Weiss, *Linear Programming Relaxations and Belief Propagation - An Empirical Study*, J. Mach. Learning Res. **7** (2006), 1887–1907.
- [Zei85] E. Zeidler, *Nonlinear Functional Analysis and its Applications*, vol. 3, Springer, 1985.
- [Zie89] W. P. Ziemer, *Weakly Differentiable Functions*, Springer, 1989.
- [ZRS18] A. Zern, K. Rohr, and C. Schnörr, *Geometric Image Labeling with Global Convex Labeling Constraints*, EMMCVPR, LNCS, vol. 10746, 2018, pp. 533–547.
- [ZSPS20] A. Zeilmann, F. Savarino, S. Petra, and C. Schnörr, *Geometric Numerical Integration of the Assignment Flow*, Inverse Problems **36** (2020), 034004 (33pp).
- [ZZPS19] M. Zisler, A. Zern, S. Petra, and C. Schnörr, *Self-Assignment Flows for Unsupervised Data Labeling on Graphs*, CoRR abs/1911.03472 (2019).
- [ZZPS20] A. Zern, M. Zisler, S. Petra, and C. Schnörr, *Unsupervised Assignment Flow: Label Learning on Feature Manifolds by Spatially Regularized Geometric Assignment*, Journal of Mathematical Imaging and Vision (2020), (in press: <https://doi.org/10.1007/s10851-019-00935-7>).

